INSTITUT FÜR IMMUNOLOGIE

LEITER: PROF. DR. H.R. RODEWALD

TOWARDS THE IDENTIFICATION OF THE THYMUS SEEDING PROGENITOR: "FATE MAPPING" OF EARLY T-CELL STAGES USING GENE "KNOCK-IN" STRATEGIES

zur Erlangung des Doktorgrades

Humanbiologie

vorgelegt der Medizinischen Fakultät der Universität Ulm

Universitätsklinikum Ulm

von Hervé LUCHE

aus Saint-Just en Brie, France

Ulm 2007

Amtierender Dekan: Professor Dr. K.-M. DEBATIN

Berichterstatter 1: Professor Dr. H.J. FEHLING

Berichterstatter 2: Professor Dr. T. WIRTH

Tag der Promotion: 15/06/07

À Marie et Camille

CONTENTS

CONTENTS I

ABBREVIATIONS IV

INTRODUCTION 1

1. CURRENT VIEWS IN T-CELL DEVELOPMENT 2
1.1. T-CELL PRECURSORS ARE BONE MARROW-DERIVED AND MATURE IN THE THYMUS 2
1.2. FROM BONE MARROW TO BLOOD: THE THYMUS SEEDING PROGENITOR (TSP) 8
1.3. αβ-TCR THYMOCYTE DEVELOPMENT AND IMMATURE SUBSETS 9
1.4. HETEROGENEITY OF DN1 AND EARLY T-CELL PROGENITOR (ETP) 10
1.5. DEVELOPMENT OF γδ-TCR-EXPRESSING THYMOCYTES[34] 11
1.6. DEVELOPMENT OF THE NK-T CELL LINEAGE 12
2. PRE-TCR ALPHA-CHAIN: A GOOD MARKER FOR EARLY T-CELL DEVELOPMENT 12
2.1. THE pTα GENE AND PRE-TCR STRUCTURE 12
2.2. pTα EXPRESSION PATTERN 13
2.3. ROLE OF THE pTα CHAIN DURING αβ T-CELL DEVELOPMENT 15
2.4. LIMITATIONS TO THE DIRECT USE OF pTα AS A CONVENIENT MARKER FOR EARLY T LINEAGE CELLS 16
3. THE USE OF LINEAGE TRACING TECHNIQUES TO IDENTIFY DEVELOPMENTALLY INTERESTING CELL POPULATIONS 17
3.1. TRANSGENESIS 17
3.2. GENE TARGETING AND KNOCK-IN ANIMALS 18
3.3. CONDITIONAL GENETIC MODIFICATIONS USING THE CRE/LOXP SYSTEM 20
3.4. SUCCESFUL FATE MAPPING OF HEAMATOPOIETIC PROGENITORS USING "KNOCK-IN" MICE 22
4. CRE-ACTIVATED ROSA26 REPORTER MOUSE STRAINS 23
4.1. THE ROSA26 LOCUS 24
4.2. COMMONLY USED FLUORESCENT REPORTERS IN LIVE CELL IMAGING 24
4.3. DSRED, AN ALTERNATIVE TO EGFP AND EYFP 26
4.4. ENGINEERING OF DSRED FOR OPTIMAL EXPRESSION IN MICE 27

AIM OF THE PROJECT 29

MATERIALS 31

5. CHEMICALS, REAGENTS AND CONSUMABLE MATERIALS 31
6. KITS 32
7. PLASMID VECTORS 32
8. SYNTHETIC OLIGONUCLEOTIDES 33
8.1. PRIMERS FOR PCR AND SEQUENCING 33
8.2. LINKERS FOR CLONING 35
9. FREQUENTLY USED BUFFERS AND SOLUTIONS 36
10. CULTURE MEDIA 37
10.1. FOR BACTERIAL GROWTH 37
10.2. FOR MAMMALIAN CELL CULTURE 37
11. BACTERIAL STRAINS, CELL LINES AND ANIMALS 38
11.1. BACTERIAL STRAINS 38
11.2. MAMMALIAN CELL LINES 38
11.3. MOUSE STRAINS 38

12. ANTIBODIES 39
13. COMPUTER ANALYSIS 40

METHODS 42

14. MOLECULAR BIOLOGY METHODS 42
14.1. *ESCHERICHIA COLI* HEAT SHOCK TRANSFORMATION 42
14.2. POLYMERASE CHAIN REACTION (PCR) OF DNA FRAGMENTS 42
14.3. SEQUENCING 43
14.4. SEMI-QUANTITATIVE RT-PCR 44
14.5. SOUTHERN BLOT 45
15. MAMMALIAN CELL CULTURE 46
15.1. BHK-21 MAINTENANCE 46
15.2. NEOR MURINE EMBRYONIC FEEDER (MEF) PREPARATION AND MAINTENANCE 46
15.3. MAINTENANCE AND GENETIC MANIPULATION OF ES CELLS 47
16. GENERATION OF KNOCK-IN MOUSE LINES 49
16.1. CONSTRUCTS USED FOR GENE TARGETING 49
16.2. GENERATION OF PTα TARGETING CONSTRUCTS 53
16.3. PLASMID DNA PREPARATION FOR GENE TARGETING 56
16.4. SELECTION OF RECOMBINANT ES CLONES 56
16.5. PICKING AND GROWING ES COLONIES IN 96-WELL PLATE FORMAT 57
16.6. SINGLE ES CELL CLONE PROPAGATION 57
16.7. DNA EXTRACTION AND SCREENING OF TARGETED CLONES 57
16.8. CHARACTERIZATION OF TARGETED CLONES BY SOUTHERN 58
16.9. *IN VITRO* DELETION OF THE NEOR CASSETTE IN TARGETED CLONES 60
16.10. RECOMBINATION MEDITATED CASSETTE EXCHANGE (RMCE) IN ROSA26-RFP ES CELLS 61
16.11. GENERATION OF MOUSE MUTANTS FROM TARGETED ES CELLS 61
17. ANIMAL PROCEDURES 63
17.1. ANIMAL MAINTENANCE 63
17.2. MOUSE GENOTYPING 63
18. IMMUNOLOGICAL METHODS 65
18.1. HEMATOPOIETIC CELL ISOLATION FROM MOUSE TISSUES 65
18.2. IMMUNOSTAINING, FLOW CYTOMETRY AND CELL SORTING 67
18.3. 5-FLUOROURACYL (5-FU) INJECTION IN MOUSE 67
18.4. IMMUNO-HISTOCHEMISTRY (IHC) 68
19. IMAGING PROCEDURES 68
19.1. FLUORESCENCE STEREOMICROSCOPY 68
19.2. FLUORESCENCE STEREOSCOPY 69
19.3. WHOLE BODY FLUORESCENCE IMAGING 69
19.4. CONFOCAL MICROSCOPY 69

RESULTS 70

20. GENERATION OF A REPORTER MICE WITH CRE INDUCIBLE RFP EXPRESSION 70
20.1. DSRED2 "KNOCK-IN" IN THE ROSA26 LOCUS 70
20.2. USE OF HCRED1, A FAR-RED FLUORESCENT REPORTER 76
20.3. TDRFP, THE OPTIMAL RFP REPORTER FOR LINEAGE TRACING EXPERIMENT 78
21. GENERATION OF A T-CELL SPECIFIC DELETER LINE : THE PTα-ICRE KNOCK-IN MOUSE 86
21.1. HCRE TARGETING IN THE PTα LOCUS OF E14.1 ES CELLS 86
21.2. ICRE TARGETING INTO 5' UTR OF PTα GENE 87
21.3. ICRE TARGETING INTO THE FIRST EXON OF PTα 88
22. CRE-INDUCIBLE ROSA26-RFP MOUSE: ONE REPORTER FOR MULTIPLE APPLICATIONS 95
22.1. CHARACTERISTICS OF ROSA26-RFP MICE PRIOR CRE-ACTIVATION 95
22.2. GERMLINE ACTIVATION OF THE ROSA26-RFP REPORTER IN THE MOUSE 95
22.3. STRONG UBIQUITOUS EXPRESSION OF TDRFP IN ROSA26-RFP MICE 97
22.4. 100% OF CELLS ARE LABELED IN ROSA26-RFP MICE 99

22.5. Inducible activation of ROSA26-RFP in T-cell specific Cre deleter mice 101
22.6. Full compatibility of tdRFP with EGFP and EYFP fluorescent reporter 103
22.7. ROSA26-RFP cells are primed for Recombinase Mediated Cassette Exchange (RMCE) 103
23. The pTα-iCre deleter mouse: a reliable Cre knock-in strain for efficient genome manipulation in T-lineage cells 106
23.1. Non-toxicity of iCre-expression in pTα-iCre deleter mice 106
23.2. Specific labelling of lymphoid organs in pTα-iCre x ROSA26-RFP mice 106
23.3. Specific reporter activation in all T-related lineages of pTα-iCre x ROSA26-RFP mice 109
23.4. pTα-iCre marks dendritic epidermal T-cells (DETC) in the murine skin 113
23.5. pTα-iCre expression labels extrathymic T cell development 116
24. pTα-iCre Marks efficiently early stages of T-cell development 119
24.1. Onset of pTα-iCre–mediated reporter activation in the thymus 119
24.2. pTα-iCre: a superior tool for Cre-mediated genomic modifications in the T-cell lineage 122
24.3. Cells expressing tdRFP in the bone marrow of pTα-iCre x ROSA26-RFP mice 124

DISCUSSION 127

25. Cre-inducible ROSA26-RFP reporter strain 127
26. The pTα-iCre-deleter strain and T- lineage tracing 131

SUMMARY 139

REFERENCES 141

ACKNOWLEDGMENTS 150

CURRICULUM VITAE 151

ABBREVIATIONS

BAC Bacterial artificial chromosome
BM: Bone marrow
CLP: Common lymphoid progenitor
DC: Dentritic cell
DN: Double negative
DNA: Deoxyribonucleic acid
DP: Double positive
ECFP: Enhanced cyan fluorescent protein
EGFP: Enhanced green fluorescent protein
ELP: Early lymphoid progenitor
ES: Embryonic stem cell
ETP: Early T-cell progenitor
EYFP: Enhanced yellow fluorescent protein
MEF: Murine embryonic feeder cell
FACS: Fluorescence activated cell sorting
FITC: Fluorescein isothiocyanate
GvHD: Graft versus host disease
HSC: Hematopoietic stem cell
KI: Knock-in allele
KO: Knock-out allele
LIF: Leukemia inhibitory growth factor
LSK: Lineage marker$^-$, Sca-1$^+$, c-Kit-R$^+$ cell
MPP: Multipotent progenitor
NK: Natural Killer
NKT: Natural Killer T-cell
PB: Peripheral blood
PCR: Polymerase chain reaction
pTα: pre-TCR alpha chain
p(A)n: polyadenylation signal
RAG: Recombination activated gene
RMCE: Recombination mediated cassette exchange
RFP: Red fluorescent protein
ROSA: Reverse-Orientation-Splice-Acceptor
SCID: Severe combined immunodeficiency
Sca-1: Spino-cerebellar antigen-1
TCR: T-cell receptor
tdRFP: Tandem-dimer RFP
TR: Texas Red
TSP: Thymus seeding progenitor

INTRODUCTION

Although thymocyte development is one of the best studied paradigms of cellular differentiation in higher eukaryotes, the nature and developmental potential of the cells that seed the thymus throughout life is still elusive, despite more than 20 years of intense research. Shedding new light on the developmental steps linking hematopoietic stem cells (HSCs) to T cells is of therapeutic concern because it might help (i) to better understand the process of malignant transformation in T-lineage cells, (ii) to reduce patients susceptibility to infections after immunotherapy by accelerating the onset of T cell reconstitution, and (iii) to avoid ultimately graft *versus* (*vs*) host disease (GvHD) following allogenic bone marrow (BM) transplantation. Recent expansion of publications and reviews[1-8] addressing this question illustrates the increasing interest of the scientific community in the early steps of T-cell development. Two equally plausible scenarios are currently competing. On one side, the thymus is seeded by cells with unrestricted lineage capacity, or at least the capacity to generate multiple lineages. On the other side, commitment to the lymphoid lineage occurs in the BM before thymic entry. One of the main limitations which restricted this research was the need to study minute populations of cells encompassing the earliest precursor of T cells among very complex populations of hematopoietic cells.

Technical improvements, such as magnetic bead cell depletion or multicolor high speed cell sorting, make it now possible to extensively dissect these complex populations and determine the differentiation potential of very small subpopulations of cells in culture or transplantation experiments. However, success in this quest remains tightly bound to the correct combination of defined set of antigens found on the cell surface, which expression pattern would ideally suit solely the earliest T-cell precursor. Alternatively, engineering of recombinant markers *via* gene targeting could help better delineating progenitor populations in the bone marrow. I will first review the current "state of research" in early T-cell development to stress the need for new T-lineage markers, and then describe the fate mapping strategy we followed to mark early T-cells, which is based on the generation of two knock-in mouse lines *via* gene targeting.

1. CURRENT VIEWS IN T-CELL DEVELOPMENT

1.1. T-cell precursors are bone marrow-derived and mature in the thymus

The importance of the thymus in immunity was first discovered in mice through surgical removal of the thymus at birth (thymectomy), as it resulted in immunodeficient animals due to the lack of T-cell production[9]. The thymus is unable to support long-term self-renewal of T-cell progenitors. Hence, when thymocytes are transferred either intrathymically or intravenously, they only give rise to transient thymocyte production[10]. Parabiosis experiments, in which the blood circulation of two mice is connected, showed that cells residing in the thymus can only sustain thymocyte production for 6 to 8 weeks[11]. Only BM transplantation experiments following lethal or sub-lethal whole body irradiation could maintain stable thymopoiesis[12]. Among others, Zinkernagel *et al.*[13] illustrated the interdependence of thymus and BM using tissue graft experiments between two distinct mouse mutants lacking T-cells (Fig. 1).

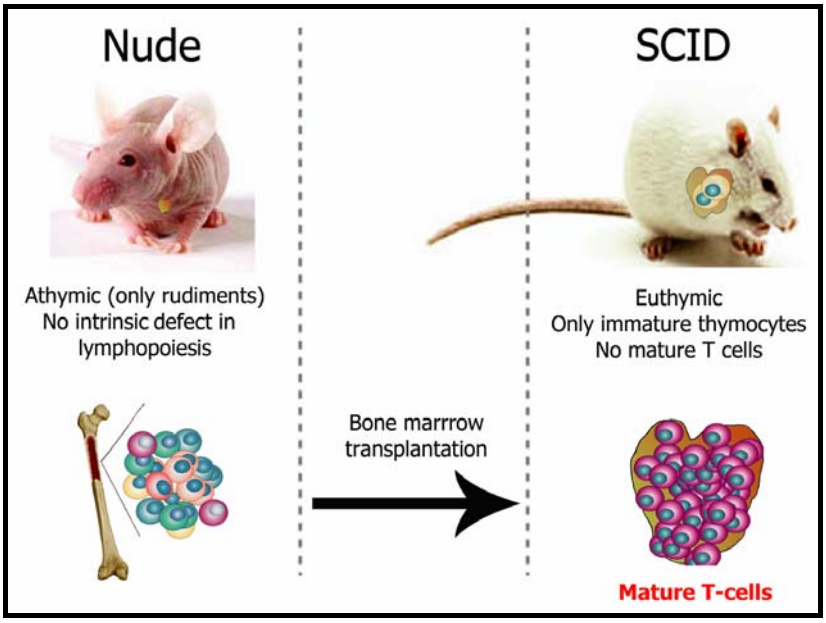

Figure 1: T cells develop in the thymus but derive from progenitor cells residing in the bone marrow.
Due to a defect in thymic epithelial cell development, nude mice lack a functional thymus impairing the development of mature T-cells. Upon intravenous injection of bone marrow cells from a nude mouse into a T-cell deficient recipient animal (such as SCID mice), bone marrow derived progenitors of nude mice can rescue long-term production of full mature T-cells. This result implies that the host thymus is required for mature T cell production and is seeded by progenitors residing in the bone marrow.

The athymic *nude* mouse presenting a defect in thymic epithelium development, and the severe combined immuno-deficiency or *scid* mouse deprived of mature B and T lymphocytes because of a defect in T-cell receptor gene

rearrangement. Transplantation of BM cells from *nude* mice could restore T-cell production in *scid* mice showing that the *nude* BM cells are intrinsically normal and capable of producing T-cells but need a functional thymus to fulfill complete T-cell development.

Most of the work performed over the last decades to improve our understanding of pre-thymic T-cell progenitors has been focused on the characterization of BM subsets that have T-cell potential. A perplexing diversity of potential lymphoid progenitors has surfaced. In adult mouse BM, cells with efficient T lineage precursor activity have been identified within the hematopoietic stem cell (HSC) population and in downstream progenitor populations (Table 1). Cells with T lineage precursor activity following adoptive intrathymic injection have been found within (i) the multipotent progenitors (MPP)[14, 15], (ii) subsets of these MPP cells called L-selectin progenitor (LSP)[16] and early lymphocyte progenitor (ELP)[17] , and (iii) common lymphoid progenitor (CLP)[18] (Fig. 2). It is unknown which of these cells if any seed the thymus physiologically. It remains equally possible that the thymus is seeded not only by one but various types of progenitors characterized by different lineage potential and efficiency to commit to the T-cell lineage[8].

Table 1: Early haematopoietic progenitors in the bone marrow and thymus

Progenitor	Cell-surface phenotype	Localisation ?	Additional information	References
Multipotent, self-renewing **HSC**	lin$^-$ Sca-1$^+$c-Kit^{hi} Flt-3$^-$	BM/PBL	CD34$^-$ (LT-HSC) CD34$^+$ (ST-HSC)	20, 15
MPP (also known as L-MPP)	lin$^-$ Sca-1$^+$c-Kit^{hi} Flt-3$^+$	BM/PBL		15, 16, 21
ELP	lin$^-$ Sca-1$^+$c-Kit^{hi} Flt-3$^+$	BM	Lymphoid-specified subsets of MPPs that are RAG$^+$CD44^{hi} and GFP$^+$ in RAG-EGFP mice	18
L-selectin expressing MPP (**LSP**)	lin$^-$ Sca-1$^+$c-Kit^{hi} L-selectin$^+$	BM		17
CLP	lin$^-$ Sca-1^{low}c-Kit^{int} IL-7Ra$^+$	BM		19
CLP-2	IL-7Rα^+ B220$^+$ CD19$^-$ c-Kit$^{-/int}$	BM		25
TSP	?	PBL	?	?
ETP	lin^{low} c-Kit^{hi} IL-7Rα^- CD25$^-$	T	CD24$^-$ (DN1a) and CD24$^+$ (DN1b)	34
DN2	lin^{low} c-Kit^{hi} CD25$^+$	T	IL-7Rα^+ CD4^{low} CD44^{hi}	30

HSC: hematopoietic stem cell, LT: long term, ST: short term, L-MPP: lymphoid-primed multipotent progenitor, ELP: early lymphocyte progenitor, CLP: common lymphoid progenitor, TSP: thymus seeding progenitor , ETP: early thymic progenitor.

1.1.1. Hematopoietic stem cells (HSC)

HSC were found in the population of cells that did not express lineage markers (Lin^-) of the bone marrow and were originally defined as Lin^- $Sca\text{-}1^+c\text{-}Kit^+$[19] (so-called LSK cells). This population is heterogeneous in capacity to produce long-term reconstitution of the hematopoietic system as well as in surface antigen expression (Table 1). The HSC population can be further separated into three subpopulations representing stages of differentiation according to a progressive loss of ability to self-renew. The most primitive long-term reconstituting cells (LT-HSC) constitute 0.005% – 0.01% of mouse bone marrow and can self-renew virtually for life; the short-term HSCs (ST-HSC) have a limited self-renewal capacity while multipotent (lympho-myeloid) progenitors (MPP) do not significantly self-renew.

1.1.2. Multipotent progenitors (MPP)

MPPs have been isolated from the HSC pool using the expression of the cytokine tyrosine kinase receptor Flt-3, as LT- and ST-HSCs lack Flt-3R expression[14]. These $Lin^-Sca\text{-}1^+c\text{-}Kit^+Flt3^+$ cells represent 50% of the LSK HSC compartment. Upon transplantation of the $Flt\text{-}3^+$ subset, faster (2 weeks) lymphoid reconstitution was achieved in comparison to LT- and ST-HSC[5, 14]. $Flt3^+$ cells have lost the ability to adopt erythroid and megakaryocytic lineage fates[20] but still retain the potential to generate lymphoid and myeloid cells.

1.1.3. Common lymphoid progenitor (CLP)

Because of the pivotal role of the IL-7R-mediated signals in lymphoid development, Kondo *et al.* searched for a more lymphoid committed progenitor using IL-7Rα expression as marker[18]. The IL-7Rα^+ fraction of Lin^- BM cells contained a population of $Sca\text{-}1^{lo}c\text{-}Kit^{lo}CD90.1^-$ cells that constituted up to 0.02% of total bone marrow cells. The $Lin^-Sca\text{-}1^{lo}c\text{-}Kit^{lo}CD90.1^-IL\text{-}7R\alpha^+$ population in the BM (Fig. 2) possesses rapid (10 days after adoptive transfer) and prominent short-term lymphoid-restricted (T, B, and NK cells) reconstitution activity.

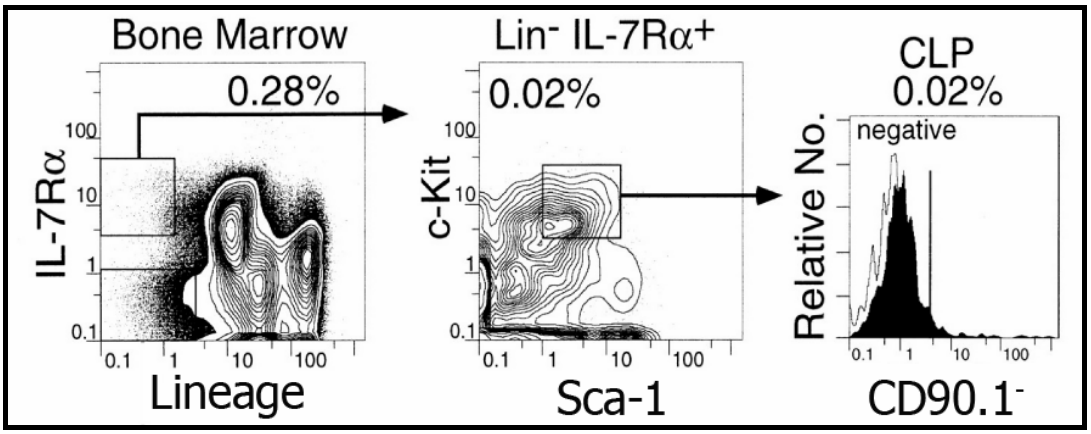

Figure 2: Identification of IL-7Rα$^+$ Common lymphoid progenitors (CLPs) in mouse bone marrow.
The cells that stained in the negative to low range for lineage markers (CD45R, CD4, CD8, CD3, Gr-1, CD11b, and TER119) were subdivided into IL-7Rα positive and negative fractions (left). Sca-1 and c-Kit profiles of IL-7Rα$^+$ fraction showed the presence of Lin$^-$IL-7Rα$^+$Sca-1^{lo}c-Kit^{lo} cells. 90% of these cells were CD90.1$^-$ and contained the CLP activity.

A clonogenic analysis of the cells revealed that single CLP could differentiate into both T and B cells. Phenotypic and functional analyses support that CLP derive directly from MPP cells[15].

1.1.4. L-selectin progenitor (LSP)

Separation of the MPP population based on L-selectin (CD62L) expression resolved two significant populations[16]. The smaller CD62L$^-$ fraction harbors a very high degree of B-lineage potential, along with high T-cell potential and notable myeloid potential. In contrast, the CD62L$^+$ fraction contains robust T-lineage progenitor activity, with minor B-lineage and myeloid potential similar to the thymic ETP. Furthermore, *in vivo* analysis showed that these L-selectin positive progenitors (LSP) colonize the thymus with wave-like kinetics reminiscent of normal thymic seeding[16].

1.1.5. Early lymphoid progenitor (ELP)

Cells with similar properties can be identified and sorted to high purity from knock-in mice with one GFP marked *rag-1* allele[21]. As Rag proteins are required for normal immunoglobulin gene rearrangement in B and T cell development, Igarashi *et al.* [17] have evaluated T/B-cell precursor potential of several Lin$^-$ BM sub-population fractions of Rag-EGFP knock-in mice. Over 90% of CLP (Lin$^-$ Sca-1^{lo}c-Kit^{lo}CD90.1$^-$IL-7Rα$^+$) cells in the bone marrow were expressing Rag-EGFP. However, 40% of the Lin$^-$c-Kit^{Lo}GFP$^+$ cells had no detectable levels of IL-7Rα which indicates heterogeneity of lymphoid primed precursors in the bone marrow.

GFP labeling was found in 3 to 5% of $Lin^-c\text{-}Kit^+Sca\text{-}1^+$ cells[17] together with $D_H\text{-}J_H$ re-arrangement products suggesting that the *rag-1* locus becomes active as early as the HSC stage. GFP/Rag expressing progenitor cells were shown to be $Flt\text{-}3R^+$ and to represent less than 0.002% of the nucleated cells in bone marrow of normal mice. This subset has been called early lymphoid progenitor (ELP). Although MPP and ELP can both give rise to myeloid and lymphoid progeny, ELPs are said "lymphoid-primed" as they express *rag-1* gene[17], a hallmark of the lymphoid genetic program. The degree of overlap of ELP with LSP has not yet been evaluated.

1.1.6. Physiological relevance of these BM lymphoid progenitors

It has been long inferred that CLP, the most lymphoid-committed progenitor population of the murine BM, were the physiologically relevant thymus seeding progenitor (TSP). Several experiments performed in other laboratories now question this finding[5]. Direct comparison of the T-cell potential of MPP and CLP showed that CLP could only briefly sustain the production of T cells upon intrathymic transplantation (2 weeks) in contrast to MPP (more than 4 weeks), inferring that CLP is not the most efficient BM progenitor population for thymocyte production. The fact that thymopoiesis was not affected in $Ikaros^{-/-}$ mice, which lack CLP cells in their BM[5] strongly suggests that CLP and TSP are not developmentally linked. It is thus tempting to think that the CLP might play only a marginal role in early T-cell development, if any at all. Alternatively, CLP may first differentiate in the BM into one or more phenotypically distinct subset(s) that will subsequently home to the thymus. The recent identification of a new subset of BM progenitors with T/B lineage potential that can efficiently enter the thymus and give rise to T cells support this view[22]. Using conventional transgenesis, Gounari *et al.*[22] engineered a mouse expressing the human CD25 (hCD25) marker as a reporter driven by the pre-T cell receptor α-chain ($pT\alpha$) promoter and enhancer sequences. In these transgenic mice, $Lin^-Sca\text{-}1^+c\text{-}Kit^-IL\text{-}7R\alpha^-B220^+CD19^-$ cells (later referred to as CLP-2) were labeled. Short-term culture assays proved that CLP-2 directly arise from a fraction of CLP expressing the hCD25 transgene at the cell-surface.

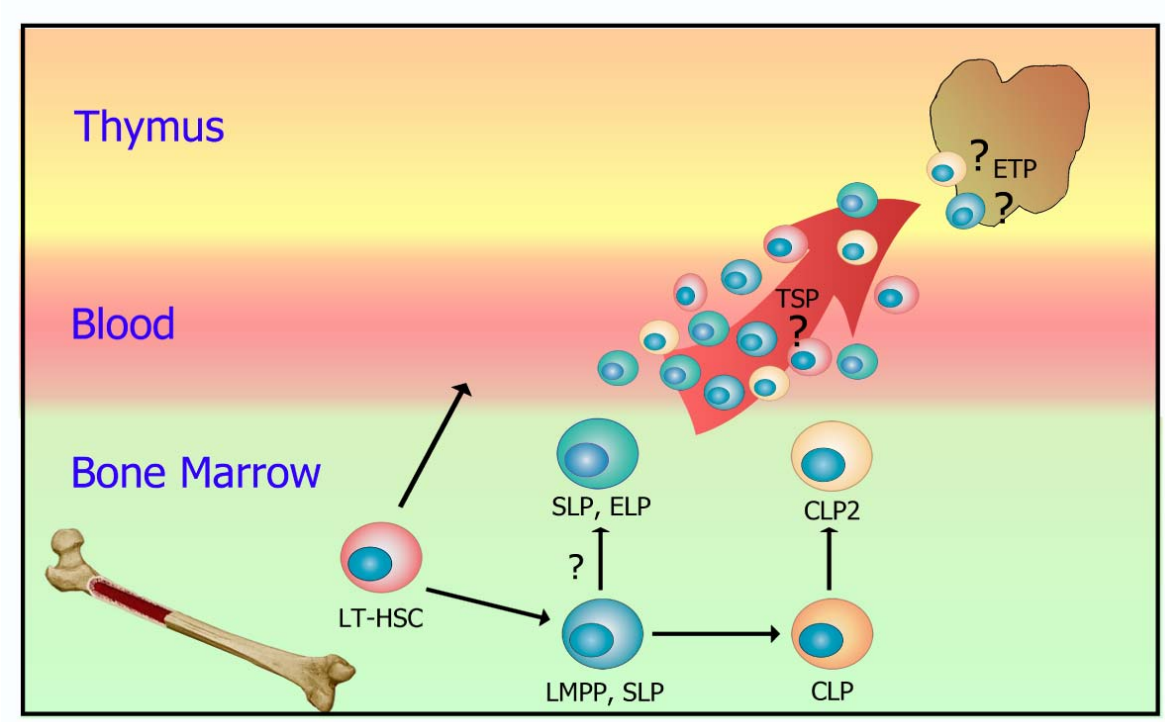

Figure 3: Tissue distribution of the bone marrow progenitor cells described so far with T-cell potential.
Many bone marrow progenitor cells are possible candidates for the putative thymus seeding progenitor. ST-HSC and LMPP are certainly present in peripheral blood whereas CLP and CLP2 have not yet been detected. However, CLP2 has been found to home really efficiently to the thymus, which could explain the virtual absence of this progenitor population in the peripheral blood. Thus, the identity of the TSP is still debated. It remains also fairly possible that more than one progenitor population seed the thymus under physiological conditions to give rise to ETP. Question-marks mark the current uncertainties about the developmental link and/or the identity of several T-cell precursor populations.

The labeled population contained clonogenic precursors for T and B cells but had no myeloid potential, at least in short-term assays[22]. Finally, Scimone *et al.* [23] reported that upon short-term adoptive transfer, CLP-2 were the most efficient cells to seed the thymus than any other BM-derived progenitors. However, Bhandoola *et al.*[2] mentioned that this result could be also explained by homing of plasmacytoid dendritic cells (pDC) which are also included in CLP-2 population[24]. This observation stresses the necessity to further refine the phenotype of CLP-2.

Altogether, these contradictory results emphasize that the identity of the main progenitor subset migrating from the BM to the thymus remains unclear (Fig. 3). If multiple pathways for T-lineage development exist, the degree to which each pathway contributes to the mature T-cell pool should be determined. Considerations for such an analysis must include thymic homing, intrathymic expansion, and degree of contribution to peripheral T-cell pools. A first step towards unravelling whether multipotent MPP, "lymphoid-primed" ELP and LSP

subsets, or lymphoid restricted CLP-2 subsets are responsible for the main T-cell production in the thymus would be to determine where T cell commitment takes place, in the bone marrow, blood or thymus.

1.2. From bone marrow to blood: the thymus seeding progenitor (TSP)

To maintain thymopoiesis throughout life, thymus seeding progenitors (TSP) must be mobilized from BM to peripheral blood (PB) and finally settle in the thymus. These TSPs are defined as BM derived circulating progenitor cells which are able to give rise to an efficient T-cell production sustained for 6 to 8 weeks upon entry in the thymus microenvironment. The precise identity of these progenitors settling the thymus from the blood is currently unknown, in part because of the rarity of such progenitors in adult mice[25]. As half-life of progenitors in the circulation seems very short[26] and the number of circulating progenitors very small[3], TSP identification has turned out to be extremely difficult. Schwarz *et al*[3] have recently reported that only a rare population of circulating LSKFlt-3^+ (200 per adult mouse) could efficiently generate T-cells. This estimation goes along with the finding that thymic niches seem to be very limited (~100 to 400 per mouse) and intermittently vacant (every 3 to 4 weeks)[27]. As Rag or CD62L expression has not been investigated in the latter study, it is not yet possible to tell which subset of MPP corresponds to these LSKFlt-3^+ cells. Interestingly, Schwarz *et al.* [3] have not been able to find CLPs circulating in blood suggesting that CLPs are unlikely to be the physiological TSP. However, they did not look for CLP-2, the subset downstream of CLP. Moreover, Scimone *et al.*[23] argued that CLP-2 was expressing potential adhesion molecules that would be required for efficient homing of TSPs to the thymus[23]. It is therefore still possible that CLP1 (or CLP2) is not detected in the blood stream as it migrates really rapidly to the thymus. Recently, Krueger *et al.*[28] identified in peripheral blood Sca-1^+IL7Rα^+Flt3^- c-Kit^{lo}CD90.1^{hi} circulating T cell progenitors (CTP) cells that were already T lineage restricted, suggesting that T lineage commitment can occur pre-thymically. Thus, similar to the situation in BM, the precise identity of the TSP in the circulation remains unclear (Fig. 3). New mouse mutants with specific defects in genes required for TSP generation or with artificial markers expressed in the TSP population should provide a new approach to re-address this question.

1.3. αβ-TCR thymocyte development and immature subsets

The development of T lymphocytes involves multiple steps of progressive cellular differentiation, selection and lineage commitment. These distinct phases are marked by changes in the status of T-cell receptor genes, expression of the T-cell receptor, and by changes in expression of cell-surface proteins such as the CD3 complex and the co-receptor proteins CD4 and CD8. These changes reflect the state of functional maturation of the cell[4] (Fig. 4).

The earliest thymocyte precursors do not yet express CD4 and CD8 and are therefore called double negative (DN) cells[29]. DN cells represent ~ 5% of total thymocytes in an adult mouse. Based on the differential expression of CD44, CD25 and CD117 (c-Kit receptor), DN cells can be further sub-divided into four consecutive developmental stages as reviewed by Fehling *et al.*[30]. The most immature thymocyte precursors reside in the DN1-cell subset ($CD4^-CD8^-CD25^-CD44^+$). DN2, the next developmental subset ($CD4^-CD8^-CD25^+CD44^+$) lacks B-cell potential but still has NK-cell and DC potential in addition to T-cell potential[31]. At the DN3 cell stage ($CD4^-CD8^-CD25^+CD44^-$), immature thymocytes are fully committed to the T-cell-lineage. Extensive rearrangement of the T-cell-receptor β (*tcr-β*), *tcr-γ*, and *tcr-δ* loci occurs. DN3 cells with productive TCR-β rearrangements express the pre-T Cell Receptor (pre-TCR) at their surface and start down-regulating CD25 surface expression. Resulting DN4-cells ($CD4^-CD8^-CD25^-CD44^-$) give rise to αβ-lineage $CD4^+CD8^+$ double positive (DP) cells that are short-lived and comprise the vast majority of T-lineage cells in the adult mouse thymus (~ 90%). These DP cells initiate rearrangement of the TCR-α locus followed by αβ TCR-dependent positive and negative selection to finally give rise to single positive (SP) CD4 helper or CD8 cytotoxic T-lymphocytes (Fig. 4).

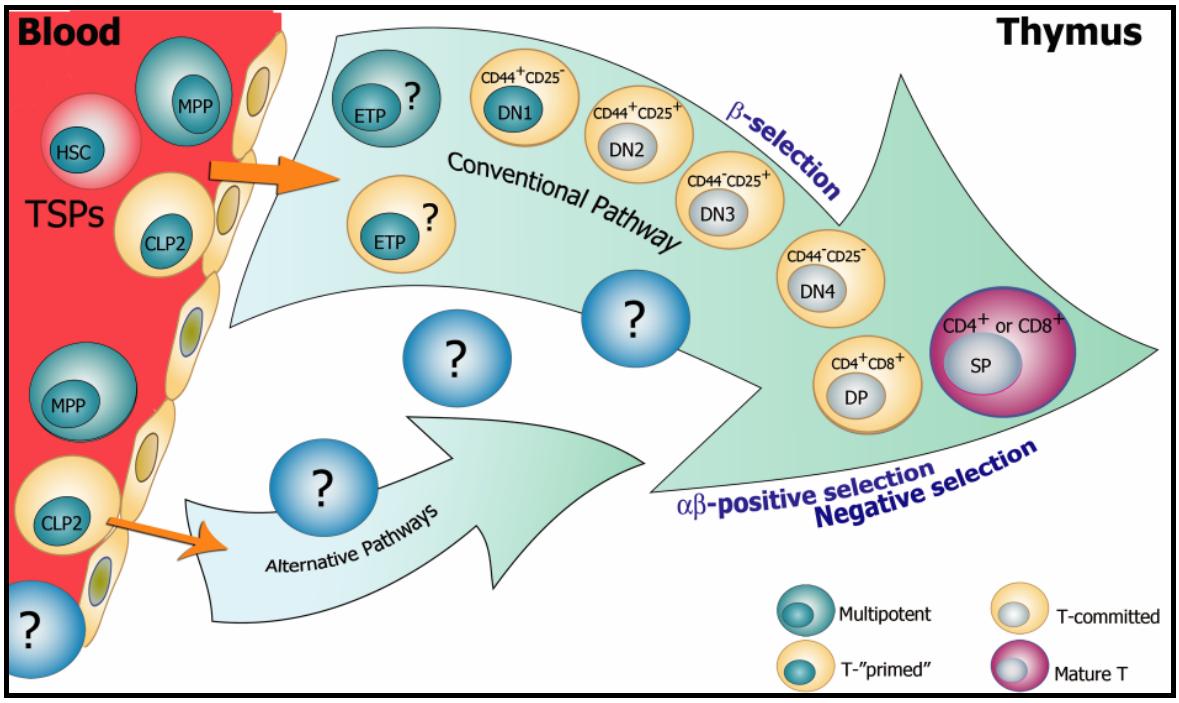

Figure 4: Successive developmental steps in the maturation of αβ-T-cells in the thymus.
Thymus seeding by the elusive thymus seeding progenitor (TSP) cell leads to the production of a primary thymocyte progenitor population called early thymic progenitor (ETP). Either T-lineage commitment is initiated prior/at the level of ETP (from a "T-primed" progenitor such as ELP) or ETPs remain multipotent for B, T and NK lineage.
The ETP population with the highest T-cell potential and proliferation capacity is defined as $CD44^+CD24^-c\text{-}Kit^+$. ETPs give rise to DN2 cells ($CD44^+CD25^+$) in which the first TCR γ-, δ- and β-chain rearrangements are detected. Next, DN3 cells ($CD44^-CD25^+$) undergo β-selection. Only the cells with a productive β-rearrangement can mature further thanks to a survival signal mediated through the pre-TCR. Resulting DN4 ($CD44^-CD25^-$) cells upregulate CD4 and CD8 TCR co-receptors to give rise to the DP stage in which the α-chain is rearranged. Most of the DP cells express a non-productive α-chain and "die by neglect" as they cannot receive the survival signal delivered from the TCR. Only DP cells engaging antigen/MHC complex to a low-affinity *via* their αβ-TCR will develop further (positive selection). Final maturation either to CD8 or CD4 single positive cells depends on the class of MHC molecule recognize by the TCR (MHC I and MHC II respectively). DP thymocytes with αβ-TCR recognizing antigen/MHC complexes to a high affinity are eliminated by "negative selection" to delete potential auto-reactive T-cells.
Beside this conventional pathway, it remains possible that other progenitor cells could contribute to the early steps of thymocyte development *via* alternative pathways which remain to be characterized.

1.4. Heterogeneity of DN1 and early T-cell progenitor (ETP)

DN1 cells are highly heterogeneous as they are essentially defined by the lack of any T-lineage marker expression[32]. Thus, $CD44^+$ non-hematopoietic cells would be found within DN1. Further fractionation of the DN1 subset according to CD117 (c-Kit) surface expression allowed the identification of cells capable of 10,000 fold population expansion in T-cell related lineages upon intrathymic injection[5]. These $Lin^{low}CD44^+CD25^-CD117^{hi}$ cells are commonly described as early T-cell progenitors (ETP) and comprise ~ 0.01% of total thymocytes in an adult mouse. Although the ETP population is considerably enriched for efficient lymphoid lineage progenitors, Porrit *et al.*[33] reported an additional level of phenotypic and functional heterogeneity. Based on CD24 expression levels, the ETP subset was separated in 3 further subsets[33]. $CD24^-$ TN1a and $CD24^{lo}$ TN1b

appear to form a precursor/progeny pair that give rise to DN2 and more mature thymocytes with conventional kinetics and proliferative expansion (Fig. 5). $Lin^{low}CD44^{+}CD25^{-}CD117^{int}CD24^{+}$ TN1c cells also give rise to T cells, but without appreciable levels of proliferation. According to Porrit *et al.*[33], this subset represents the only $CD117^{+}$ DN1 subset with a B lineage capacity. These findings seem to settle conflicting results from several other groups[5, 24] by showing that multiple progenitors with a DN1 phenotype can produce T cells, but possess different proliferative potentials and lineage capacities.

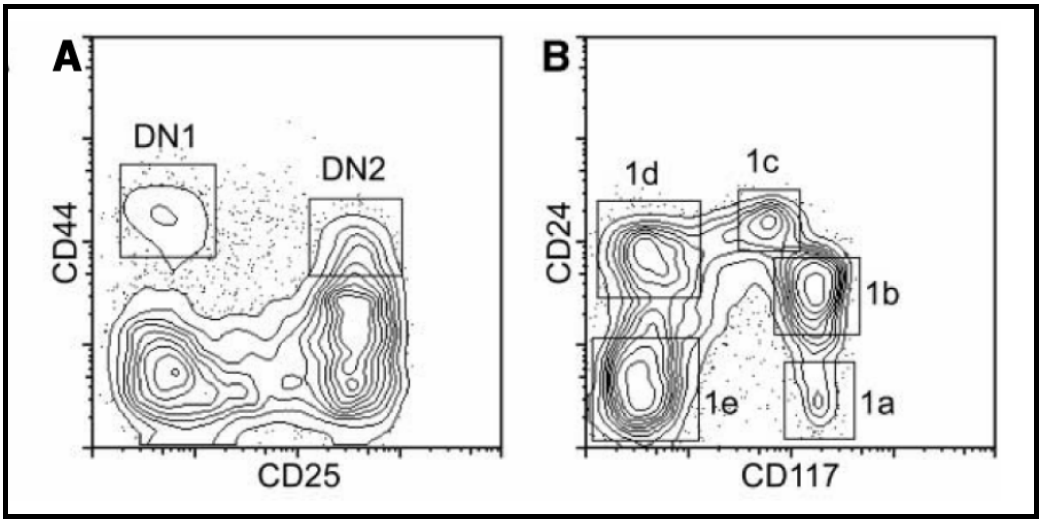

Figure 5: Characterization of DN1 subsets (taken from Porrit *et al.*[33])
A. Standard identification of DN subsets in thymocytes depleted of lineage-positive cells. Rectangular gates used to identify DN1 and DN2 cells are shown. **B.** Representative profile for CD24/CD117 staining in the DN1 subset. For clarity, these are subsequently defined as DN1 subsets a–e, as indicted.

1.5. Development of γδ-TCR-expressing thymocytes[34]

Knowledge of γδ-T cell development remains limited. Because there is no phenotypic marker other than the γδ-TCR itself for tracking thymocytes committed to the γδ lineage, delineation of γδ cell development has relied mainly on monitoring the expression of γδ-TCR heterodimer using antibodies that recognize epitopes generated by the association of TCRγ and TCRδ chains. Most γδ cells are DN and probably diverge from αβ-T cell progenitors before the up-regulation of CD4 and CD8 expression. In normal mice, expression of the γδ-TCR can be prevented in DP cells by silencing of *tcr-γ* expression, as well as by *tcr-α* rearrangement, which deletes the *tcr-δ* locus. As very few γδ–T cells seem to express productive *tcr-β* genes (~10%)[35] and αβ T cells are depleted of in-frame γ and δ rearrangements[36], αβ *vs* γδ lineage decision may be made by expression of

pre-TCR/γδ-TCR. At present, there are no compelling data to contradict either a receptor-instructed or a receptor-independent mechanism of commitment to the γδ *vs* αβ lineage.

1.6. Development of the NK-T cell lineage

NKT cells express markers of both NK and T cells and play an important role in the suppression of autoimmune reactions[37]. Unlike conventional αβ T cells which are selected by classical MHC I or MHC II molecules, NKT cells are restricted to a non-polymorphic class I-like molecule: CD1d. CD1d presents glycolipid-antigens rather than peptides. As the number of ligand for CD1d is not as diverse as for peptides, NKT cells exhibit a limited TCR repertoire: 80% express an invariant Vα14Jα18 α-chain and 50% the Vβ8 TCR-β-chain[37]. NKT cells also develop in the thymus and are thought to arise from DP cells expressing the Vα14Jα18 associated with an appropriate TCR β-chain[38]. The DP cells rapidly undergo positive selection mediated by the CD1d molecule. NKT cells become $CD4^+$ SP or DN (but never $CD8^+$ SP) and progressively acquire the expression of markers commonly associated to the NK lineage ($NK1.1^+$, $DX5^+$)[37].

2. PRE-TCR ALPHA-CHAIN: A GOOD MARKER FOR EARLY T-CELL DEVELOPMENT

2.1. The pTα gene and pre-TCR structure

The *ptcrα* gene is located on mouse chromosome 17, in a region syntenic to the human chromosome 6[39]. *ptcrα* spans over 8.4 kilobases (kb) and consists of four exons encoding a protein of 33 kDa, the pre-T cell receptor (pre-TCR) alpha-chain (pTα) (Fig. 6). Exon/intron structure of *ptcrα* is similar to both *tcr-α* and *tcr-δ* genes which encode the TCR-α and TCR-δ chains, respectively. Exon 1 bears the 5'-untranslated region, a leader peptide and the first three amino acids of the mature protein. Exon 2 encodes only a single extracellular immunoglobulin-like domain in strong contrast to other TCR chains (Fig. 6). Exon 3 assures the synthesis of a connecting peptide, which contains an important cystein residue required in the hinge region for the establishment of an intermolecular disulfide bond with the TCR-β chain. Exon 4 encodes a transmembrane region which allows pTα association with signal-transducing CD3 molecules. It also encodes a considerably longer cytoplasmic tail than any other

TCR or immunoglobulin proteins studied so far.

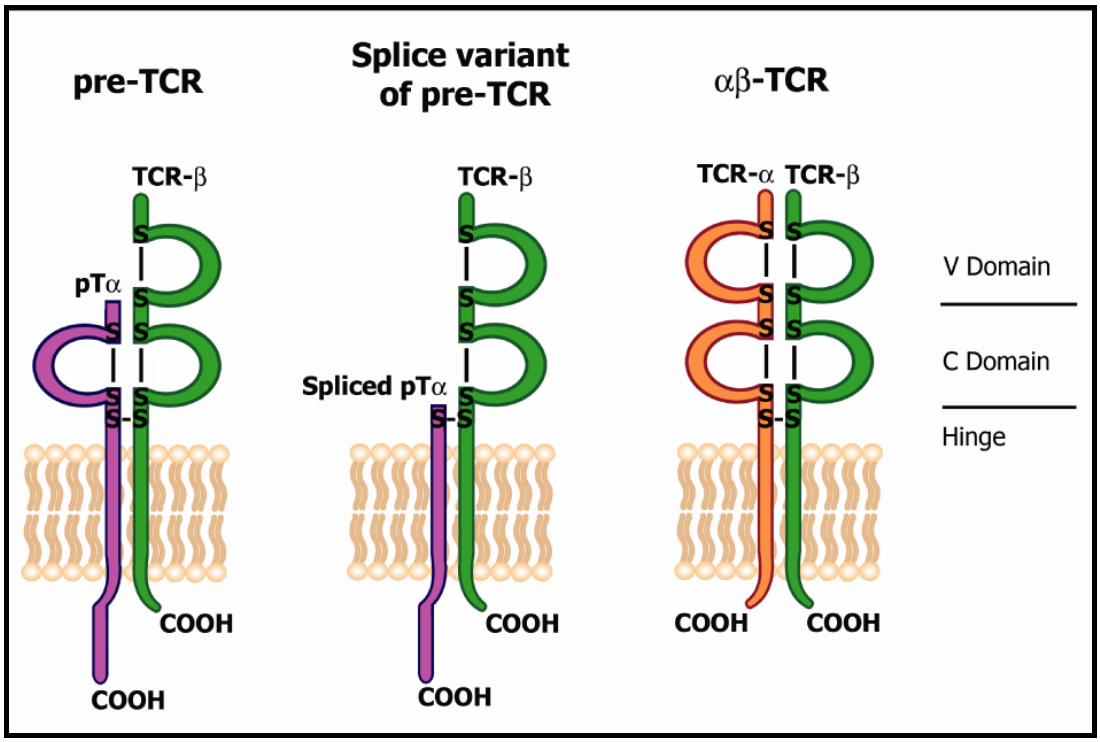

Figure 6: Comparison of the schematic structure of the pre-TCR (left) and the αβ-TCR (right). For clarity, CD3 components (γ,δ,ε,ζ) are omitted. In strong contrast to the α-chain, the invariant pre-TCR α-chain (pTα) has only one immunoglobulin domain, pairing less efficiently to the β-chain. The cytoplasmic tail of pTα is longer than the one of TCR-α chain. This tail itself plays a crucial role in promoting one characteristic of the pre-TCR, being its constitutive internalization and degradation once expressed at the cell surface[40, 41]. The receptor in the centre represents a possible heterodimer containing a spliced variant of pTα. There is no conclusive evidence that this heterodimer is ever expressed at the cell surface. It is rather thought to be degraded intracellularly[42].

2.2. pTα expression pattern

During ontogeny, pTα is detected first at day 14,5 in the fetal thymus and not at other site of early hematopoiesis[43] (Fig. 7A). In embryonic blood, pTα expression seems specific to cells with T- progenitor activity as pTα was only detected in circulating d16.5 fetal pro-thymocytes but not in multipotent progenitors (Fig. 7B). In adult mice, pTα transcripts are very abundant in the thymus but are not found in mature, peripheral T cells (Fig. 7C) indicating that pTα expression may provide a unique marker for immature T-cells. Expression of pTα is restricted to the T-cell lineage as pTα-expression has never been detected in cells committed to the myeloid, B lymphoid or NK cell lineage (see for example Fig. 7C, E). Also, T cells with surface γδ-TCR expression lack pTα-transcripts (Fig. 7D).

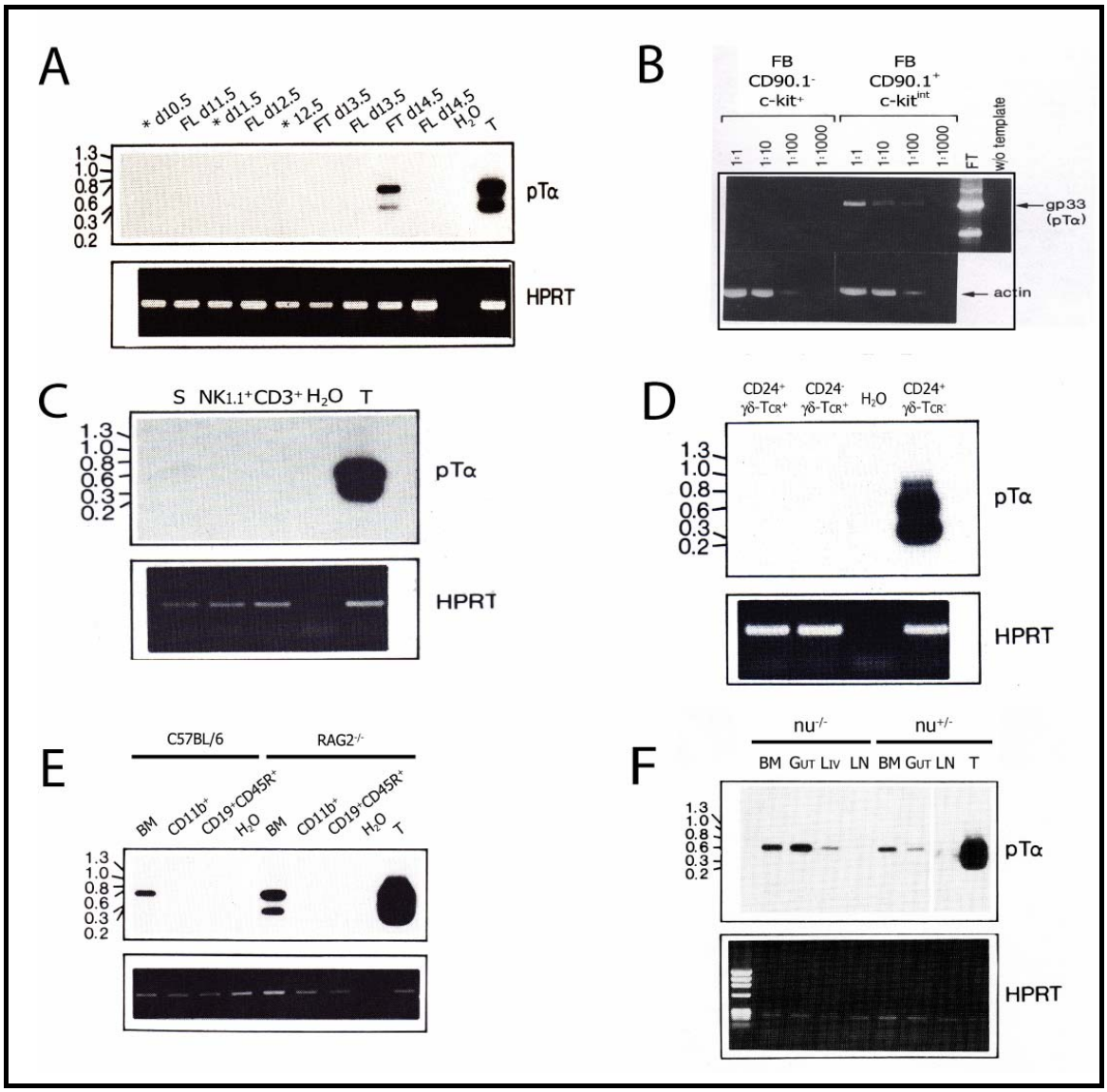

Figure 7: RT-PCR detection of pTα expression in various cell types and tissue.
A. pTα expression during ontogeny. pTα is first detected in the fetal thymus at day 14.5 of embryo development but not at sites of early fetal hematopoiesis such as the fetal liver.
B. pTα expression in progenitor cell subsets of d15.5 fetal blood. pTα is detected in circulating fetal pro-thymocytes ($CD90.1^+c\text{-}kit^{int}$) but not in hematopoietic multipotent progenitors ($CD90.1^-c\text{-}kit^+$).
C. In the adult mouse, pTα is expressed in the thymus but not in the periphery. Total splenocytes do not express pTα in contrast to thymocytes. More specifically, neither NK nor T-cells in the spleen express pTα.
D. Immature ($CD24^+\gamma\delta\text{-}TCR^+$) and more mature γδ-T cells ($CD24^-\gamma\delta\text{-}TCR^+$) of the $CD4^-CD8^-$ thymocyte subset do not express pTα in contrast to surface TCR-negative $CD24^+$ thymocytes.
E. pTα expression in bone marrow subsets. pTα is neither found in myeloid ($CD11b^+$) nor progenitor cells of the B-lymphoid lineage ($CD19^+CD45R^+$). However, pTα is detected in total BM of wild type and RAG-deficient mice. The lower band corresponds to the splice variant form of pTα.
F. pTα expression at putative sites of extrathymic T-cell development. pTα was detected in the bone marrow and the gut of wild type animals but not in their peripheric lymphoid organs (lymph nodes). In athymic mice homozygous for the nude mutation, pTα was also found in the bone marrow, gut and liver

(*: total embryo, FL: Fetal Liver, FT: Fetal Thymus, FB: Fetal Blood, T: Thymus, BM: Bone Marrow, Liv: Liver, LN: Lymph Nodes, S: Spleen). All data presented in this figure are taken from Bruno *et al.*[43]

In immature thymocytes, pTα transcripts are found expressed at increasing levels in DN1, DN2, DN3 and DN4 thymocyte populations to finally decline in DP thymocytes[44]. Actually, pTα gene expression is thought to be terminated by TCR signals that result in positive selection[44].

Most interestingly, Bruno *et al.* also reported pTα expression outside the murine thymus, particularly in the lineage marker negative (Lin^-) fraction of the bone marrow (Fig. 7E) which might indicate the presence of a T-lineage or at least lymphoid-committed progenitor population[43]. The source of bone marrow pTα transcripts were clearly not re-circulating thymocytes as pTα could also be detected in the bone marrow of nude animal, congenitally lacking a thymus (see results, section 23.5). Rigorous and careful analysis of pTα expression at putative sites for extrathymic development in wild type and nude animals (Fig 7F) further strengthened the hypothesis that pTα might be a reliable marker for early thymic, but also extrathymic T-cell development.

2.3. Role of the pTα chain during αβ T-cell development

In the absence of productive TCR β-chains such as in DN1 and the vast majority of DN2 cells, pTα is not expressed at the cell surface. In DN3 cells, the pairing of pTα to a TCR-β chain upon productive rearrangement forms – together with components of the CD3 complex - an asymmetrical transmembrane heterodimer, pre-TCR (Fig. 6). The pre-TCR is targeted to lipid rafts at the cell surface which appears to self-induce activation of signal transduction cascades in a ligand independent fashion[45, 46], cell survival and progression of the immature thymocyte to the DN4 stage. Then, DN4 and DP thymocytes undergo rearrangement of their *tcrα* gene loci. The higher affinity of the TCR-α chain to the TCR-β chain displaces pTα from the pre-TCR leading to a functional TCR.

To assess the physiological role of pTα, knock-out mouse mutants have been generated *via* gene targeting[47]. Homozygous pTα-deficient mice have about one-tenth the number of thymocytes of wild type littermates and show a developmental block at the DN3 stage of maturation[47]. The number of DP thymocytes is dramatically reduced, reflecting a severe block in αβ-T cell development. Importantly, γδ-T cell development is not impaired despite pTα deficiency. In fact, 20-fold more γδ-T cells are found in $pT\alpha^{-/-}$ animals[47]. This finding has led to the hypothesis that pTα expression might allow discrimination of αβ- *versus* γδ-committed T progenitors – a hypothesis that has been tested in this

thesis with conclusive results (see Results, section 23.3). In contrast to genetically unmanipulated mice, γδ T cells from pTα-deficient animals are rich of in-frame TCRβ rearrangements, which would hint at a role of pTα in normal αβ *vs* γδ lineage commitment. Importantly, NKT cells are absent in pTα knock out mice confirming that NKT cells are absolutely dependent on the pre-TCR for normal development[48].

2.4. Limitations to the direct use of pTα as a convenient marker for early T lineage cells

Surface expression of the pre-TCR is in general very low, possibly due to pTα-mediated rapid internalization and degradation[40, 41]. The constitutively low pre-TCR surface levels preclude quantitative separation of pre-TCR-positive from pre-TCR-negative cell populations by FACS. Moreover, during T cell maturation pTα-transcription precedes V>DJ rearrangements of the TCR-β locus, *i.e.* in some cell subsets - among them the developmentally most interesting populations - pTα is expressed in the absence of a functional TCR-β chain. Such cells synthesize pTα protein, but fail to transport it to the cell surface.

Although cells with cytoplasmic expression of pTα can be detected by intracellular staining methods, the need for fixation and permeabilization precludes subsequent functional studies. For instance, it is impossible to determine the developmental potential of sorted cells that have undergone fixation and permeabilization. A reporter mouse line, in which pTα transcription can be directly visualized, would overcome all these limitations and provide a unique tool for the unequivocal, non-invasive identification of pTα-expressing cells.

3. THE USE OF LINEAGE TRACING TECHNIQUES TO IDENTIFY DEVELOPMENTALLY INTERESTING CELL POPULATIONS

As described in section 1.2, the identity of the thymus seeding progenitor(s) has not yet been unambiguously elucidated[2, 5, 24]. Additional markers are required to better delineate candidate BM subsets or TSP. During lineage commitment and further differentiation into a certain lineage, unique regulatory programs are established that direct cell-type-specific patterns of gene expression. Any gene products, expressed specifically in early T-lineage cells such as transcription factors[49], could at least in theory be used to refine our current models of T-lymphopoiesis. However, assessment of the development potential of "candidate" progenitor populations implies the isolation of viable cells. This excludes the use of any gene products expressed in the cytoplasm or nucleus of the cells as permeabilization of the plasma membrane required for direct immunostainings of intracellular antigens impairs cell viability. This technical limitation excludes the direct use of transcription factors or soluble factors to mark BM subsets. Cell surface proteins expressed at low level can neither be considered because their weak immunostaining will not allow quantitative separation from other cells[22]. Specific insertion of a fluorescent or cell surface marker behind a well-characterized promoter should label all cells normally expressing this promoter. Together with more classical approaches, such genetic manipulation might help to understand the sequence of critical differentiation events required for multipotent HSCs to give rise to T-cells and significantly improve our current models of T-lymphopoiesis.

3.1. Transgenesis

The easiest way to introduce a genetic modification in the mouse genome is to inject a transgene fused with sequences for transcriptional regulation (promoter, enhancer and polyadenylation sites), into a fertilized mouse egg. For lineage tracing experiments, promoter of choice should ideally only be expressed in the cell-type of interest. Injected DNA usually integrates into one or more loci during the first cell divisions of pre-implantation. The risk of "collateral" gene disruption due to transgene integration is not negligible and could lead to an

unexpected mutation. In addition, the transgene may either insert into a locus that is subject to gene silencing, leading to the extinction of transgene expression. Third, the transgene might insert in the vicinity of an enhancer resulting in aberrant expression in cells irrelevant of the original promoter specificity. Finally, abnormal juxtaposition of a transgene with heterochromatin might cause gene silencing in some cells by position effect variegation (PEV)[50]. PEV has been linked to the establishment and maintenance of heterochromatin in *Drosophila*[51, 52] and could directly influence transcription rate of transgenes in mouse. Changes of histone epigenetic trends (acteylation, methylation) controlling higher-order structures in chromatin at neighboring genes[52] could result in variegated expression of transgene, considerably complicating lineage tracing analysis in transgenic animals[53].

To ensure that the resulting phenotype is not a transgenic artifact due to the site of transgene insertion, one could experimentally circumvent this problem by analyzing several independent transgenic lines[54] and selecting one with specific transgene expression pattern. However in some experiments, characterization of the cells expressing a given promoter is the main goal of investigation. To guarantee faithful expression of transgenes, the knock-in approach described in the next section, is the only possible approache for lineage tracing experiments.

3.2. Gene targeting and knock-in animals

Another approach consists in the single insertion of a marker into the coding sequence of a lineage-specific gene by homologous recombination. In contrast to other eukaryote organisms such as yeast, homologous recombination in mouse cells is only achievable at sufficently high frequencies in embryonic stem (ES) cells which makes them a excellent tool to specifically modify genes[55-57]. Derived from the epiblast of the mouse blastocyst stage, ES cells remain pluripotent and can give rise to all three germ layers of a mouse embryo. In the presence of leukemia inhibitory factor (LIF), ES cells self-renew and can be maintained in culture in an undifferentiated state for a virtually unlimited number of passages. Specific integration is achieved by flanking a targeting cassette by several kilobases of sequence homologous to a given locus. Stable integrants are

selected using positive selection cassettes conferring resistance to a selective agent such as neomycin. As random insertion is still more efficient than homologous recombination, clones with a correct insertion must be identified by PCR screening and further confirmed by Southern blotting on total genomic DNA. Following micro-injection into the cavity of a wild-type blastocyst, healthy ES cells contribute to the development of most of the resulting embryo, including germ cells which will allow stable transmission of the engineered genetic modification to the mouse offspring[58, 59].

To trace a particular lineage of cells, knock-in mice, in which part of the coding sequence of a lineage specific gene is replaced by a traceable marker, are favored over transgenic animals because the expression level of the introduced marker is expected to vary less or not at all between animals. Genetic environment surrounding the marker remains the same as for the original gene and thus ensures a better control over the expression of the recombinant transcript. Such a gene targeting strategy has been successfully applied by Fontenot *et al.*[49] to trace developing thymocytes expressing the transcription factor FoxP3. This marker for regulatory T-cells was fused with EGFP. As green fluorescent cells were first found at the DP stage, one could conclude that thymic FoxP3$^+$ cells were branching off at this stage.

Recently, Prinz *et al.*[60] also applied a lineage tracing method to better characterize γδ-T cell development. As no phenotypic marker other than γδ-TCR itself was available for tracking thymocytes committed to the γδ lineage, Prinz *et al.* generated mice expressing a reporter gene (fusion protein of histone 2β with EGFP)"knocked-in" the *tcr-δ* constant region gene. Using these mice, Prinz *et al.* have characterized γδ-T cell development from the point of opening of the *tcr-δ* locus in a subset of early T cell progenitors (TN1b) to the point of emergence of mature γδ-TCR$^+$ DN4 thymocytes.

Similarly, a cDNA encoding a truncated version of the human CD4 coreceptor (hCD4) has been "knocked-in" the pTα locus (Fehling *et al.*, unpublished) to trace T-cell progenitors but it resulted in an extremely weak cell

surface expression as revealed by immunostaining (Fig. 8). A better separation was observed in homozygous knock-in animals. However, the associated pTα knock-out phenotype of these mice prevented any analysis of normal T-cell development. The low level of cell surface expression of this hCD4 marker might reflect the rather weak expression of the pTα gene in normal immature thymocytes, but other explanations cannot be excluded (for instance, nonsense-mediated decay of the recombinant fusion transcript). A more sensitive knock-in approach using a combination of enzymatic marker and Cre-activated reporter is required to label pTα expressing cell lineages.

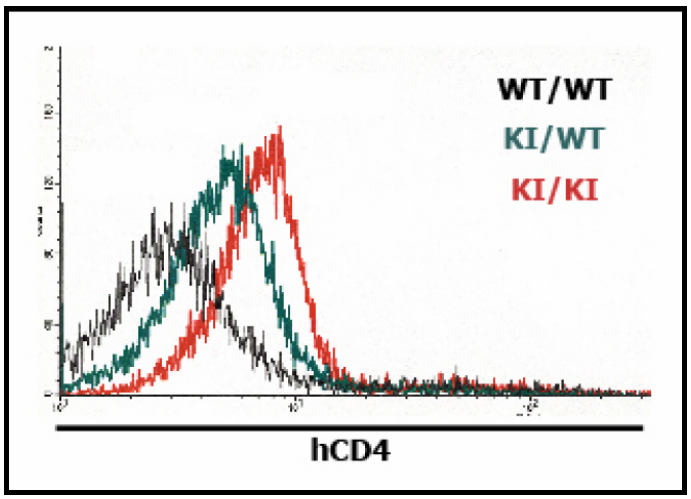

Figure 8: hCD4 expression on $CD4^{-}CD8^{-}$ immature thymocytes.
hCD4 was readily detected in DN thymocytes of $pT\alpha^{(hCD4/+)}$ (KI/WT) and $pT\alpha^{(hCD4/hCD4)}$ (KI/KI) mice as compared to wild type cells (WT/WT). The shift of hCD4 surface staining observed in heterozygous $pT\alpha^{(hCD4/+)}$ knock-in cells is not separated enough from the background of negative cells to allow the isolation of minute populations of precursor cells. A better, but still insufficient separation was obtained with the $pT\alpha^{(hCD4/hCD4)}$ cells.

3.3. Conditional genetic modifications using the Cre/loxP system

Cre recombinase, a site-specific integrase isolated from the bacteriophage P1, catalyzes the recombination between two loxP recognition sites without the need for any cofactor[61]. loxP sites are 34 base pairs long and consist of two 13 bp inverted repeats that flank a central spacer sequence of 8 bp which determines the orientation of the loxP site (Fig. 9A). Depending on the location and the orientation of these loxP sites, Cre recombinase can catalyze the invertion or deletion of DNA fragments (Fig. 9B). When loxP sites are placed in opposite orientation to each other on either side of a DNA sequence, the sequence will be inverted by the Cre recombinase. When two loxP sites are placed in the same orientation on a same DNA molecule, recombination results in the excision of the

sequence (Fig. 9B). The reverse reaction resulting in DNA integration can also be mediated by the Cre recombinase *via* intermolecular recombination (Fig. 9B). This property of the Cre/loxP system has already been used in transgenic experiments to drive reproducible expression of transgenes by specific integration of transfected DNA into a recipient loxP site in a target genome[62]. Unfortunately, integrative recombination is highly inefficient because the insert is flanked by loxP sites, which themselves become targets for Cre and lead to subsequent excision of the recombined product.

To promote efficient integrative reactions, mutant loxP sites have been developed. Araki *et al.*[63] achieved stable targeted integration using lox66 and lox71 sites in which 5-bp were mutated respectively in the right and left inverted repeat of the loxP site. Recombination between lox66 and lox71 results in a wild type loxP site and a mutant lox site that can no longer serve as substrate for the Cre recombinase. Other mutant loxP sites with one or more mutations in the spacer region have been described[64]. As recombination does not occur efficiently between two loxP sites differing in the spacer region[65], combination of heterospecific loxP sites has been used to develop an alternative integrative method: recombinase mediated cassette exchange or RMCE[66]. A genomic DNA segment flanked by lox511 and loxP was replaced with another cassette flanked by lox511 and loxP. Lee *et al.*[64] developed another heterospecific mutant site, lox2372 (Fig. 9A), which promotes efficient recombination but has completely lost the ability to recombine with original loxP sites. Alternatively, recombination-mediated Cre activation of the reporter locus could be achieved by combining loxP and lox2372 sites as described previously by Schnutgen *et al.*[67].

As loxP sites do not recombine in the absence of Cre recombinase, control over Cre expression is sufficient to regulate DNA recombination events and initiation of the genomic modifications. Therefore, the Cre/ loxP system has been used to generate conditional gene disruption or expression of a reporter in a given cell-type or lineage[68, 69]. Lineage-specific activation of a reporter can be achieved by crossing a "deleter" mouse line expressing Cre under the control of a specific promoter with a "indicator" line in which a genetic marker is separated from a

ubiquitous promoter by a loxP-flanked stopper region (Fig. 9C). Most frequently, a stopper consisting of three successive polyadenylation sites has been used to block any transcription initiated from the promoter[70-72]. It also prevents leaky marker expression in the absence of Cre by blocking any read-through the reporter gene. When Cre is expressed by the lineage specific promoter, the stopper is removed by Cre-mediated excision resulting in constitutive expression of the reporter gene. This method is called "fate mapping" as cells expressing the gene in which the Cre is "knocked in" as well as their progeny will thus be irreversibly labeled (Fig. 9C).

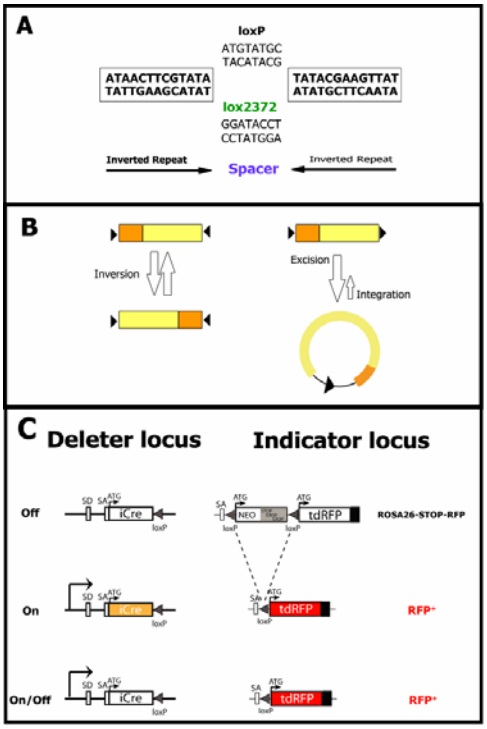

Figure 9: Conditional reporter activation using the Cre/loxP system.
A. The Cre recombinase recognizes specific sequences of 34 bp called loxP sites. These loxP sites consist of two 13 bp inverted repeats in opposite orientation flanking a 8 bp spacer sequence. As the spacer sequence does not form a palindrome, lox site are orientated. The Cre recombinase recognizes original loxP site as well as mutant sites with mutations in the spacer sequence. loxP and lox2372 depicted here are not compatible, preventing lox-heterospecific recombination reactions by the Cre recombinase.
B. Recombination reactions catalyzed by the site-specific Cre recombinase. When two loxP sites are found in opposite orientation, the Cre recombinase catalyzes the inversion of the lox-flanked DNA fragment. This inversion reaction is reversible (top and bottom left). When the two loxP site are found in the same orientation, the Cre recombinase will excise the loxP-flanked DNA fragment (top right). The product of excision is circular and retains a loxP site. This product can be reintegrated by a "trans" recombination reaction with another lox site when it is found in the same orientation. However, the excision reaction (top right) is favored over the integration (bottom right).
C. Example of Cre-activated reporter expression using the Cre/loxP system. To mark cells expressing a gene of interest (GOI) as well as their progeny, two transgenic lines are required. The enzymatic marker Cre recombinase is placed under the control of GOI promoter. At a second locus ideally constitutively expressed in the mouse such as the ROSA26 locus, a reporter preceded by a transcriptional "stopper" is integrated. Upon crossing of GOI-Cre deleter mouse strain with this Cre-activated reporter strain, only GOI expressing cells will express the Cre recombinase (middle panel). Cre will catalyze the irreversible excision of the stopper sequence, labeling the GOI expressing cell and its daughter cell even if GOI promoter is switch off (bottom panel). This strategy allowing the labeling of a specific cell lineage is called fate mapping.

3.4. Succesful fate mapping of heamatopoietic progenitors using "knock-in" mice

Cre-mediated cell fate mapping is a powerful tool for *in vivo* analysis of the development of specific cell lineages, especially because it avoids the use of invasive methods perturbing normal development such as the γ-irradiations preceding adoptive transfers that are currently used to study hematopoietic lineages. By crossing a RORγT-Cre transgenic line with a Cre-inducible ROSA26-STOP-**EGFP** fluorescent reporter strain (later referred to as ROSA26-**EGFP**), Egawa *et al.*[38] could mark all Vα14Jα18 iNKT cells in the thymus

supporting selection of the Vα14 iNKT cell lineage from double positive thymocyte precursors. The same fate mapping strategy allowed the conclusion that intestinal αβ-T cells were thymus-derived[73].

The success of such Cre-activated conditional reporter expression mostly relies on the selection of a promoter driving a strong enough, highly specific Cre recombinase expression in a given lineage. Most of the currently available Cre deleter mouse lines specific for the T-cell lineage are transgenics[54, 74-76] *ie* potentially subject to expression variegation of the transgene. Therefore, Cre expression is frequently not reliable, mosaic in the target tissue or cell type, and frequently associated with unexpected ectopic reporter expression. Leaky expression of Cre from a cell-type-specific promoter will result in unwanted recombination events in unrelated cell types and their labeling considerably complicates the analysis as observed when using Lck-Cre transgenic lines (for example reference[77, 78] and our own data, result section 24.2). This critical point is illustrated by the negative experience of Ye *et al.* who failed to mark exclusively myeloid lineage-committed cells using lysozyme-Cre knock-in mice, most likely because of a weak basal level of lysozyme expression in hematopoietic stem cells. As currently no deleter Cre line is available to potentially mark the TSPs, we decided to generate a pTα-Cre knock-in mouse to follow the fate of pTα expressing cells.

4. CRE-ACTIVATED ROSA26 REPORTER MOUSE STRAINS

Reporter mouse strains are important tools for monitoring Cre recombinase-expression *in vivo.* Ideally, upon Cre activation, they should ensure ubiquitous expression of the reporter from a single-copy transgene. The level of expression should be high enough to easily separate Cre activated from non-activated cells for successful lineage tracking experiments. The reporter locus should not be subject to gene silencing otherwise reporter expression might be down-regulated in some cell types. Reporter knock-in lines to the ROSA26 locus have been shown to present most of these advantageous features.

4.1. The ROSA26 locus

Initially, the ROSA26 locus has been identified in a gene trap experiment targeting actively-transcribed genes in ES cells[79]. Briefly, a promoter-less cassette consisting of a splice acceptor and β-geo (β-galactosidase fusion with neomycin resistance gene) was inserted in reverse orientation in a retroviral vector. After infection, the mutant lines referred to as **ROSA** (**R**everse-**O**rientation-**S**plice-**A**cceptor) showed single copy integration *per* locus in the 5' end of genes, often downstream of the initiation codon ATG. Upon injection into blastocysts, the ROSA26 strain exhibited ubiquitous β-galactosidase staining during embryogenesis and in adult tissues[80], with no obvious phenotype and deleterious effect on mouse development. Importantly, the ROSA26 locus appeared to be easily accessible for gene targeting in ES cells. It has been reported that 10 to 50% of the recombinant clones recovered in a gene targeting experiment have indeed correctly integrated the ROSA26 locus[81]. This exceptionally high targeting efficiency exceeds by far the less than 1% usually observed for most other loci. ROSA26 is thus a convenient locus for the site-specific integration of foreign genes into the mouse genome , such as those encoding fluorescent reporters.

4.2. Commonly used fluorescent reporters in live cell imaging

Over the last fifteen years, fluorescent proteins have been extensively engineered to generate a large palette of spectrally shifted mutants suitable for live specimen imaging. Most of the variants used for cell tagging studies are derived originally from a green fluorescent protein (GFP) isolated from the jellyfish *Aequorea victoria*[82] (Fig. 10). Of note are the enhanced green (EGFP)[83], yellow (EYFP)[84] and cyan (ECFP)[85] variants which have been successfully expressed in the mouse system. As revealed by crystallographic analysis, the structure of GFP[86] and its variants[87, 88] resembles a 11-stranded β-can wrapped around a single central helix, in the middle of which lays the chromophore.

The unique ability of these chromophores to emit fluorescence without the need for external substrates or co-factors apart from molecular oxygen[82], made them excellent *in vivo* markers of gene expression and protein localization. As their visualization is non-invasive, they can be monitored in real-time experiments

and exhibit the additional advantage that they can be quantified by flow cytometry, confocal microscopy, and fluorometric assays.

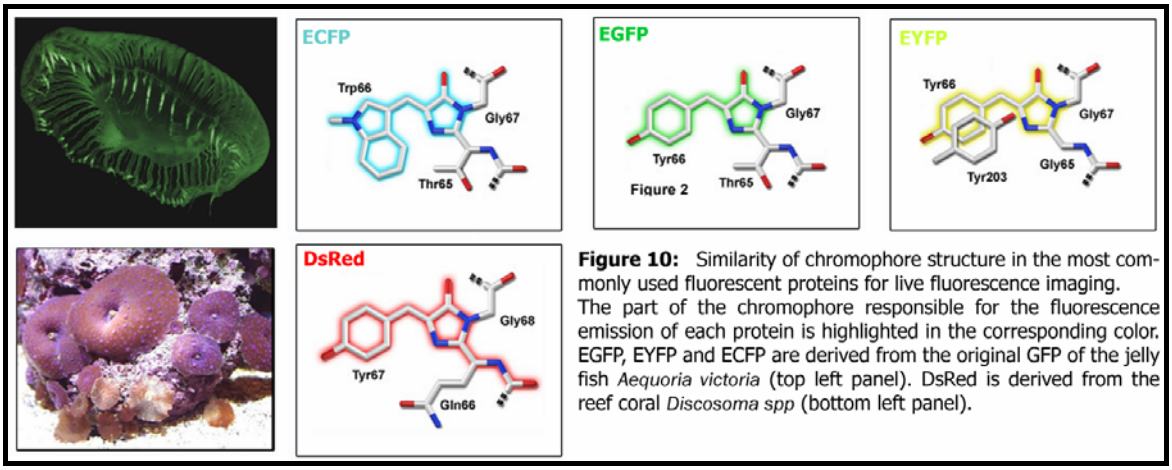

Figure 10: Similarity of chromophore structure in the most commonly used fluorescent proteins for live fluorescence imaging. The part of the chromophore responsible for the fluorescence emission of each protein is highlighted in the corresponding color. EGFP, EYFP and ECFP are derived from the original GFP of the jelly fish *Aequoria victoria* (top left panel). DsRed is derived from the reef coral *Discosoma spp* (bottom left panel).

Cre-inducible fluorescent reporter lines such as ROSA26-**EGFP**[71], ROSA26-**YFP**[85] and ROSA26-**CFP**[85] mice were successfully generated by gene targeting. Although the level of EGFP driven from ROSA26 appeared to be too weak for optimal cell labeling[71, 73], ROSA26-**YFP** has been used successfully in lineage tracing studies[73, 77, 78, 84]. However, simultaneous detection of EGFP and EYFP is problematic. The emissions maxima of the fluorochromes are relatively close (Table 2) complicating their simultaneous detection with standard cell imaging and flow cytometry systems. For instance, it is possible to separately analyze IL-4 or IFN-gamma expression using IL-4-IRES-EGFP and IFN-gamma-IRES-EYFP reporter mice[89, 90]. However, when the two reporter genes were combined in a single mouse to analyse Th1 vs Th2 fate determination, problems of fluorescence compensation occurred[89]. Moreover, EGFP and EYFP emission maxima are found within the range of cell autofluorescence[91]. Once excited with blue light (450-490 nm), intracellular riboflavin, flavin co-enzymes (NADPH) and flavoproteins of the mitochondria fluoresce in a green–yellow color (500–560 nm). This high background makes arduous the visualization of low-expressed fluorescent or dimly emitting fusion proteins. This major drawback limits the use of EYFP and EGFP *in vivo* and urged for the development of fluorescent markers with pronounced red emission near 600 nm.

Table 2: Biophysical properties of commonly used fluorescent proteins either derived from *Aequoria victoria* (EGFP, EYFP and ECFP) and *Discosoma spp* (DsRed and other red variants).

Protein (Acronym)	Excitation Maximum (nm)	Emission Maximum (nm)	Extinction Coefficient ($M^{-1}cm^{-1}$)	Quantum Yield	Oligomerisation State	Relative Brightness ($EC*QY*10^{-3}$)
EGFP#	488	507	56,000	0.6	Weak Dimer	34
EYFP#	514	527	84,000	0.6	Monomer	50.4
ECFP#	439	476	32,500	0.4	Monomer	13
DsRed#	558	583	75,000	0.79	Tetramer	59
DsRed1*	558	583	52,000	0.68	Tetramer	35.4
DsRed2*	563	582	43,800	0.55	Tetramer	24
DsRed.T3*	560	587	49,500	0.59	Tetramer	29
HcRed1	588	618	20,000	0.015	Dimer	1
mRFP1#	584	607	50,000	0.25	Monomer	12.5
mCherry#	587	610	72,000	0.22	Monomer	16
tdRFP(12) #	552	579	120,000	0.68	Dimer	81.6
tdTomato#	554	581	138,000	0.69	Dimer	95.22

The computed brightness values were derived from the product of the extinction coefficient per chain (CE) and the quantum yield (QY). (Data extracted from Bevis[92] (*) and Shaner[93] (#)).

4.3. DsRed, an alternative to EGFP and EYFP

Sequence shuffling of GFP never led to a red fluorescent variant with characteristics optimal for live cell imaging. A breakthrough was achieved with the isolation of drFP583 (later commonly referred to as DsRed) from *Discosoma*[94], a genus of non-bioluminescent *Anthozoa* coral (Fig. 10). DsRed has rapidly fascinated the scientific community because of its interesting spectral and biochemical properties. DsRed fluorescence is optimally excited at 558 nm but can also be excited by a standard 488 nm laser, allowing its use with laser-based confocal microscopes and flow cytometers[95]. DsRed has a much higher extinction coefficient and quantum yield than EGFP (Table 2) resulting in ~ 2 times brighter fluorescence emission. DsRed is more stable than GFP[96] and exhibits considerable resistance to extreme pH, denaturants and photobleaching[96, 97]. However, wild-type (WT) DsRed has at least two major drawbacks. First, maturation of the chromophore is slow ($t_{½}$ > 24h in *E. coli*)[97] and goes through a green intermediate[98-100]. Analyses of the WT DsRed crystal structure[101, 102] highlighted the strong chromophore similarities with GFP from *Aequorea victoria* (Fig 10). Red-shift of emission spectrum requires an additional oxidation step which is accompanied by a change in the configuration of the peptide bond preceding the chromophore from *trans* to *cis*[103, 104]. This rare isomerization event is slow,

explaining why DsRed requires a longer time to fully shift from green to red *in vitro* or *in vivo*. Resulting fluorescence bleed-through into the GFP channel is unacceptable for double-labeling experiments with EGFP. Slow emergence of red fluorescence limits the intensity of the DsRed signal, particularly with rapidly growing cells such as ES cells. Second, in contrast to EGFP, DsRed needs to form tetramers to emit fluorescence as demonstrated by *in vitro* and *in vivo* experiments[96, 97, 101]. This property considerably limited the use of DsRed in protein tagging since tetramerization of the DsRed domain could perturb the function and localization of the fused protein[105]. Furthermore, DsRed tetramers tend to form insoluble higher order aggregates leading to growth retardation and strong reduction of DsRed fluorescence lifetime in aging *E. coli* cultures[106]. In light of these known detrimental effects in bacteria, it is possible that constitutive expression of WT DsRed will also affect cell viability in eukaryotic cells[93].

4.4. Engineering of DsRed for optimal expression in mice

The first attempts to ameliorate DsRed were performed by Clontech[107]. DsRed1 (codon-optimized for expression in mammalian cells) and DsRed2 (twofold faster maturation) have provided only modest improvements of DsRed properties. Reports from Hadjantonakis[84] and Zwaka (Baylor College, Houston; personal communication) even suggested their potential toxicity, at least in ES cells. To solve the remaining problems restricting the use of DsRed in mouse transgenesis, two additional modifications were tested.

Bevis *et al*[92] improved maturation time ($t_{½}$ ~ 1 h) and solubility of DsRed by random mutagenesis and selection of appropriate mutants. Generation of a stable Cre-inducible transgenic line[108] demonstrated that widespread expression of the DsRed.T3 tetramer variant did not impair mouse development. However, high-resolution imaging of embryonic stem cells that exhibit constitutive expression of DsRed.T3 revealed the same perinuclear punctuate staining observed as with DsRed1 and DsRed2 variants[109]. This heterogeneous expression pattern within the cell, the obligate tetramerization and dimmer fluorescence (~ 2 times) compared to WT DsRed (Table 2) further disqualified DsRed.T3 as being the universal red fluorescent marker long awaited in mouse genetic manipulation.

Campbell *et al.* [110] tried to reduce the oligomerization state of DsRed by a stepwise evolution of its sequence. Fast maturing variants with mutations in the heavily charged N-terminal protein-interface were successfully generated. mRFP1, the first reported red fluorescent monomer, and tdimer2(12), an artificial tandem-dimer (further referred to as tdRFP), were the most promising variants. Although far less brighter (~ 6 times) than tdRFP (Table 2)[93], mRFP1 has been readily used to generate constitutively expressing transgenic mouse lines[109, 111]. Beside the maintenance of fluorescence intensity throughout development, transgenic lines were fertile and exhibited normal behavior. Fluorescence was homogeneous within the cells. These observations prove the neutrality of widespread stable mRFP1 expression in mice. Since tdRFP is a genetic fusion of two copies of mRFP1, it is likely that tdRFP will combine mRFP1 characteristics with a brighter fluorescence (nearly as bright as WT DsRed) which should make tdRFP a superior genetic marker especially for single-copy gene integrations.

AIM OF THE PROJECT

My Ph.D.-project had the following technical and scientific goals:

- To test whether Cre/loxP methodology can be applied in principle for *in vivo* lineage tracing of T cell development.

- To test whether pTα expression is of sufficient specificity for reliable visualization of T-cell lineage restriction in the mouse.

- To generate a new Cre-inducible reporter mouse for optimal detection of reporter expressing cells in live tissue and histological sections. To this end, an RFP variant had to be found that could be used in combination with GFP-based fluorescent proteins to allow multicolour lineage tracing experiments, also in combination with GFP-expressing transgenic/knock-in mouse strains already available. The RFP variant would need to be non-toxic during mouse embryogenesis and to be neutral with respect to cellular differentiation, in particular in the haematopoietic system. Moreover, the RFP variant should be of sufficient brightness to be clearly detectable, even when expressed from a single-copy integration site.

- To develop a Cre expression cassette that would ensure optimal levels of Cre protein in pTα-expressing cells of "knock-in" mice and exclude transgene silencing *via* epigenetic processes, e.g. DNA methylation. Introduction of this expression cassette into the pTα locus of the mouse genome should maintain the specificity of the pTα promoter and strictly correlate with endogenous pTα-expression.

- To reliably identify pTα-expressing cells and their progeny in the immune system using the two newly developed "knock-in" mouse strains, the pTα-iCre deleter line and the Cre-inducible RFP reporter line.

- To determine at which immature stage of thymocyte development a T-lineage

specific genetic program is initiated.

- To investigate whether pTα expression also marks extrathymic T-cell development.

- To isolate potential pTα-expressing cell populations in the bone marrow and characterize their cell surface phenotype.

- To improve current models of $\alpha\beta$ versus $\gamma\delta$ lineage commitment of thymopoiesis.

MATERIALS

5. CHEMICALS, REAGENTS AND CONSUMABLE MATERIALS

Chemicals were obtained from the companies Sigma (München), Roth (Karlsruhe), Merck (Darmstadt), Fluka (Neu-Ulm), Gibco BRL (Karlsruhe) and Pharmacia (Freiburg) if not stated otherwise. Restriction enzymes were from New England Biolabs (Bad Schwallbach) or Roche (Mannheim). Radioactive reagents were purchased from Amersham (Braunschweig).

Table 3: References of Chemicals used

Acetic acid	Merck	Darmstadt
Agar	Fluka	Neu-Ulm
Agarose	Gibco/BRL	Karlsruhe
Ammonium acetate	Fluka	Neu Ulm
Ampicillin	Sigma	München
Bacto-tryptone	Difco	Detroit, USA
Bacto-Yeast-Extract	Difco	Detroit, USA
Bromophenol blue	Sigma	München
BSA (Factor V)	Roche	Mannheim
Cell culture media (DMEM)	Gibco/BRL	Eggenstein
Chloroform	Baker	Deventer, Holland
DAPI	Burfingame	
Dextran sulfate	Pharmacia	Freiburg
Diethyl pyrocarbonate (DEPC)	Fluka	Neu Ulm
Dimethyl sulfoxide (DMSO)	Sigma	München
dNTPs	Pharmacia	Freiburg
D-PBS	Gibco/BRL	Karlsruhe
Ethanol	Merck	Darmstadt
Ethidium bromide	Roth	Karlshure
FCS	Gibco/BRL	Karlsruhe
Formamide	Sigma	München
Ficoll 400	Pharmacia	Freiburg
Fluoromount	Southern Biotech	USA
Glycerol	Gibco/BRL	Karlsruhe
Geneticin	Gibco/BRL	Karlsruhe
Gelatin	Sigma	München
Gancyclovir (Cymevene)	Sigma	München
HCl	Merck	Darmstadt
IPTG	Gibco/BRL	Karlsruhe
Isopropanol	Merck	Darmstadt
K Acetate	Sigma	München
LIF ESGRO	Chemicon	
Methanol	Merck	Darmstadt
MgCl2	Merck	Darmstadt
Monothioglycerol	Sigma	München
Na Acetate	Merck	Darmstadt
NaCl	Merck	Darmstadt
NaOH	Merck	Darmstadt
Na N-LauroylSarcosine	Sigma	München
Na Pyruvate	Gibco/BRL	Karlsruhe
Paraformaldehyde	Merck	Darmstadt
Pepton	Gibco/BRL	Karlsruhe
Phenol	Gibco/BRL	Karlsruhe
Polyethylene glycol (PEG) 6000	Serva	Heidelberg
Proteinase K	Pharmacia	Freiburg
RNase A	Sigma	München
Salmon sperm DNA	Sigma	München
Sodium Dodecylsulfate (SDS)	Serva	Heidelberg
Tris	Sigma	München
X-Gal	Gibco/BRL	Karlsruhe

6. KITS

Table 4: Kit references

Avidin/Biotin Blocking Kit	Vector Lab	# SP2001
Abi Prism BigDye Terminator Cycle Sequencing	Perkin-Elmer	#4337450
Expand long template PCR system	Roche Applied Science	#11 681 834 001
GC Rich PCR system	Roche Applied Science	#12 140 306 001
NICK™ Column	Pharmacia Biotech	#17-0855-01
Prime-It® Random Primer Labeling Kit	Stratagene	#300385
Qiafilter Plasmid midi kit	Qiagen	# 12243
Qiaquick PCR Purification kit	Qiagen	#28104
Qiaquick Gel Extraction kit	Qiagen	#28704
Superscript II Reverse transcriptase	Invitrogen	# 18064-022
TOPO-TA PCR Cloning Kit	Invitrogen	# K4660-40

7. PLASMID VECTORS

- pBSK, Bluescript SK (Stratagene, Heidelberg)

- pCRII-TOPO, pCR-BluntII-TOPO (Invitrogen, Karlsruhe)

- pMC-Neo-p(A)n (Stratagene, Heidelberg). The vector contains a loxP flanked NeoR cassette driven by the TK (Thymidine Kinase) promoter.

- pCAU8 containing an expression cassette for the thymidine kinase gene.

- pEGFP-C1, pDsRed1-C1, pDsRed2-C1, pHcRed1-C1 (BD Biosciences Clontech, Heidelberg)

- pCre-AC for bicistronic expression of an improved version of Cre (iCre) and EGFP *via* an IRES sequence (Fehling, unpublished) from the CMV promoter.

- pCAGGS-FlpE-V1 for bicistronic expression of an improved version of Flp (FlpE) and EGFP *via* IRES sequence from the CAGGS promoter[112].

- pDOI5 used for stable expression of iCre from the pTα locus[113]. This vector contains a splice donor sequence, intron and splice acceptor from rabit β-globin gene.

- pB-iCre for the iCre cDNA[114]

- pSAβgeo and pROSA26.1 kindly provided by Soriano *et al.*[81]

- pmRFP1 and ptdRFP(12) provided by Tsien *et al.*[110]

- pX2GFP provided by Irion *et al.*[115] consisting of a EGFP-p(A)n cassette flanked by a loxP and a lox2372 site.

8. SYNTHETIC OLIGONUCLEOTIDES

Most of the oligonucleotides used in this work were ordered from the company ThermoHybaid (Ulm). All primers were adjusted to 100 pmol/µL stock concentrations in ddH2O and stored at -20°C. Primer stocks were further diluted down to 10 pmol/µL for most molecular biology applications.

8.1. Primers for PCR and Sequencing

Table 5: PCR and Sequencing primers

Name	Sequences	Tm	Comments
HL5	agacaacttgttactaac	28.8	pHL-AA sequencing primer
HL14	aatcaagggtccccaaactcac	55.7	pTα KI screening (βglobuline III intron) Rev
HL15	aagaccgcgaagagtttgtcc	54.9	ROSA26 KI screening (in βgeo Splice acceptor site) Rev
HL16	cctaaagaagaggctgtgctttgg	57.5	Primers for ROSA26 KI screening (CA) Fwd
HL17	catcaaggaaaccctggactactg	55.7	Primers for ROSA26 KI screening (5' promoter region) Rev
HL23	aatagtcgacttaggcccaacgcggcgccac	74.9	*Xho* I/R26 CA/*Sal* I
HL24	atgtctcgagccgcccatccccgcaaacgca	80.7	*Xho* I/R26 CA/*Sal* I
HL25	caattcccctgcaggacaacg	58.9	Sequencing of 3' region after *Xba* I site in pROSA26.1
HL34	accaggtcgacactactgtgttggcggact	68.6	Sequencing of ROSA26 promoter region
HL35	cgttccttccatgcgaaccttt	57.8	Sequencing of DsRed ATG side
HL36	ggcttttcctctggttcttg	50.7	gDNA testing Fwd
HL37	caggaacattacgccagatg	49.6	gDNA testing Rev
HL48	aacccagtgagcccagttagc	54.8	pTα external probe (Southern) Fwd
HL49	gatggccttgaatttctgacactt	55.4	pTα external probe (Southern) Rev
HL50	agcacggctaactgggctcactgg	64.3	pTα KI screening (pTα control arm) Fwd
HL51	cctgaaaactttgccccctccata	61.1	pTα KI screening (β–globulin III intron) Rev
HL52	ctgccggggccgcctaaagaagag	59.1	R26 KI screening (5' promoter region)
HL53	ctggaaagaccgcgaagagtt	55.1	R26 KI screening (after βgeo SA site)
HL54	taagcctgcccagaagactcc	55	Sequencing of 3' region after *Xba* I site in pR26.1
HL55	tcaagtcggaaacgtgcttgc	57.6	Sequencing of ROSA26 SA 3' of *Not* I site
HL56	tgcgtttgcggggatgg	58.4	ROSA26 KI screening (5' promoter region) Fwd
HL59	gcaaaggcgcccgatagaataa	59.1	ROSA26 external probe (Southern) Fwd
HL60	ccgggggaaagaagggtcac	59.1	ROSA26 external probe (Southern) Rev
HL69	cggggccgtcggaggggaagt	68.5	Sequencing of DsRed2 5' region (381 from ATG)
HL70	tagggcgcagtagtccagggtttc	61.4	Confirm NeoR deletion in R26 targeted clone
HL71	ggagcaaagctgctattgg	50.1	Sequencing primer in PGK promoter
HL72	gtttcaggttcaggggaggtgtg	61.5	Sequencing primer in SV40 p(A)n
HL73	atacaaggaatcggcaacatca	53.7	Screening of IRES-Cre KI into pTα locus Fwd
HL74	agccagaccgatgtagcaagattc	57.6	Screening of IRES-Cre KI into pTα locus Rev
HL79	atcacactgctggtagatgga	49.4	*ptcra* RT-PCR Fwd
HL80	tcagaggggtgggtaagatc	50.3	*ptcra* RT-PCR Rev
HL85	gcagaaccacagaaacagagg	51.4	IRES-CRE KI pTα probe (Southern) Fwd
HL86	ttctcacttgaacctggagcg	54.4	IRES-CRE KI pTα probe (Southern) Rev
HL87	aaagatatcaacacaggcatgtcgggctggtg	70.5	SA for IRES-Cre KI into pTα
HL88	aaagcggccgctttccctggccaactcttcatttc	77.2	SA for IRES-Cre KI into pTα
HL91	ggtgatgctggacactactgc	52	Sequencing primer IRES-iCre in 3' UTR pTα
HL95	ctctagctcgaggaattccgatc	55.3	Sequencing primer for p(A)n-loxP junction
HL96	ggatccgcggttacaggcccttgc	68.6	*Eco* RI- pTα KI Ext Probe Fwd
HL97	ggatcccaacaacaaaagactacag	55	*Eco* RI- pTα KI Ext Probe Rev
HL98	tgagttggatagttgtggaaagag	52.1	Sequencing primer for tdRFP ATG

HL100	gcttgatctcgtcttccctg	51.3	*dppa5* RT-PCR
HL101	tccatttagcccgaatcttg	51.9	*dppa5* RT-PCR
HL102	gagcagtcgggtgttcctac	51.1	*pramel4* RT-PCR
HL103	gaaaacgctgctgcaacata	51.6	*pramel4* RT-PCR
HL104	ctttcccaagagaagggtcc	51.8	*dppa3* RT-PCR
HL105	tgcagagacatctgaatggc	50.8	*dppa3* RT-PCR
HL106	cctggctgtcagtcatcaga	50.6	*dppa2* RT-PCR
HL107	gttaaaatgcaacgggctgt	52	*dppa2* RT-PCR
HL108	ctccttctcccagcagtttg	51.4	*dppa1* RT-PCR
HL109	ggcaaattggaacacgctat	51.9	*dppa1* RT-PCR
HL110	agagaacccacatggctttg	51.5	*pramel7* RT-PCR
HL111	ggatttggcttggcatacat	51.6	*pramel7* RT-PCR
HL112	actttcttgggctgcctttt	52.4	*pramel6* RT-PCR
HL113	agattccagggctcatcctt	51.7	*pramel6* RT-PCR
HL114	tactggacctccccaagaaa	51.1	*pramel5* RT-PCR
HL115	gcattccagcactgtctgag	50.4	*pramel5* RT-PCR
HL116	gctctagacgccaacactgcccggactactc	65.9	iCRE KI into pTα B6 LA Fwd
HL117	ttggcgcgccccccgagaggctccggaaagcag	84.5	iCRE KI into pTα B6 LA Rev
HL118	acagaactgcttgctagccc	51.3	*tcf* 1 RT-PCR Fwd
HL119	gagacaggcagcctaacagc	51.6	*tcf* 1RT-PCR Rev
HL120	cctgggatgggagtgggacctg	63.2	pTα KI mouse typing Fwd
HL121	gaattcagggtcgctgcgtgggtcagc	71.2	pTα External Probe Fwd (Southern)
HL122	gaattcccgaaggcgccatattacacg	66.4	pTα External Probe Rev (Southern)
HL146	tggtgcagatgaacttcagg	51	EYFP internal primer Rev
HL147	gccagaggccacttgtgtag	52	PGK Promoter
HL152	aagggagctgcagtggagta	51	Universal Primer for EYFP Typing Fwd
HL154	atcataatcagccataccacat	48	SV40 p(A)n primer going outwards Rev
HL155	gcgaagagtttgtcctcaacc	53	ROSA26-YFP genotyping Fwd
HL156	ggagcgggagaaatggatatg	55	ROSA26-YFP genotyping Rev
HL157	aaagtcgctctgagttgttat	45.4	ROSA26-YFP genotyping Rev
HL158	ggcccagcaggcagcccaag	65.6	Nude genotyping Fwd
HL159	agggatctcctcaaaggcttc	53.1	Nude genotyping Rev
VM57	gtccaatttactgaccgtacaccaa	56	Bacteriophage Cre typing Fwd
VM58	ccatcgctcgaccagtttagttac	56.2	Bacteriophage Cre typing Rev
292	cttgtacagctcgtccatgccg	59.3	EGFP/EYFP internal primer Fwd
293	accatcttcttcaaggacgacgg	58.3	EGFP/EYFP internal primer Rev
13024	gagacctcattaagacagtagga	46.5	pTα KI screening Fwd
13025	gatccagcaccagaagcaagtgccta	63.4	pTα KI genotyping PCR Rev
13758	gtgagagccaaatagggaggcaaga	60.7	pTα WT genotyping PCR Rev
Oligonucleotides used for DsRed knock-in (KI) into ROSA26 (R26)			
Oligonucleotides used for iCre knock-in (KI) into pTα.			

KI: Knock-in, LA: long arm, SA: short arm, CA: Control arm, Fwd: Forward, Rev: Reverse, TC: targeting construct.

8.2. Linkers for cloning

Linkers were prepared by phosphorylation of complementary oligonucleotides and their subsequent progressive hybridizing in a boiling water bath cooled down to room temperature (RT).

Table 6: Linker characteristics

	Sequences	Tm	Comments
HL1	aattcggatcctgcagctcgaggcgcgccg	79.5	*Eco RI/Bam HI/Pst I/Xho I/Asc I/Sal I*
HL2	tcgacggcgcgcctcgagctgcaggatccg	82.6	*Eco RI/Bam HI/Pst I/Xho I/Asc I/Sal I*
HL3	aattctcgagtcgacggccga	60.5	*Eco RI/Xho I/Sal I/Eag I/(Eco RI)*
HL4	aatttcggccgtcgactcgag	60	*Eco RI/Xho I/Sal I/Eag I/(Eco RI)*
HL6	tatagtcgacggcgcgccatc	61.7	*(Xho I)/Sal I/Asc I/Xho I*
HL7	tcgagatggcgcgccgtcgac	68.9	*(Xho I)/Sal I/Asc I/Xho I*
HL8	ctagcgctggatccgaattcaagcttctcgagt	70.8	*NheI/Eco 47III/Bam HI/Eco RI/Hind III/Xho I/(Bam HI)*
HL9	gatcactcgagaagcttgaattcggatccagcg	71.8	*Nhe I/Eco 47III/Bam HI/Eco RI/Hind III/Xho I/(Bam HI)*
HL10	ggccagtcgacgctagctcgagcgctagatctgca	86.2	*(Not I)/Sal I/Nhe I/Xho I/Eco 47III/Bgl II/Pst I*
HL11	gatctagcgctcgagctagcgtcgac	69.2	*(Not I)/Sal I/Nhe I/Xho I/Eco 47III/Bgl II/Pst I*
HL12	gcggccggatcctgcagacgcgtctagaggtac	76.8	*Pst I/Eag I/Bam HI/Pst I/Mlu I/Xba I/Kpn I*
HL13	ctctagacgcgtctgcaggatccggccgctgca	79.9	*Pst I/Eag I/Bam HI/Pst I/Mlu I/Xba I/Kpn I*
HL18	ggccgaagctta	30.7	*Eag I/Hind III/Bgl II*
HL19	gatctaagcttc	10	*Eag I/Hind III/Bgl II*
HL21	ggccatttaggccgtcgacgc	64.2	*Sac II/Sfi I/Sal I/(Sac II)*
HL22	gtcgacggcctaaatggccgc	64.2	*Sac II/Sfi I/Sal I/(Sac II)*
HL26	tcgagaagttcctattctctagaaagtataggaacttcg	64.1	*Xho I/FRT/Sal I*
HL27	tcgacgaagttcctatactttctagagaataggaacttc	64.1	*Xho I/FRT/Sal I*
HL30	cgcggccgct	38	*Kpn I/Not I/Xba I*
HL31	ctagagcggccgcggtac	55.8	*Kpn I/Not I/Xba I*
HL32	tcgtgtcgacggcgcgcc	65.9	*(Xho I)/Sal I/Asc I/Xho I*
HL33	tcgaggcgcgccgtcgac	65	*(Xho I)/Sal I/Asc I/Xho I*
HL38	ctagagaattcgc	38	*Xba I/Eco RI/Not I*
HL39	ggccgcgaattct	42	*Xba I/Eco RI/Not I*
HL40	ggccgcactagttaattaac	46.5	*Not I/Spe I/Pac I/Xma I*
HL41	ccgggttaattaactagtgc	46.4	*Not I/Spe I/Pac I/Xma I*
HL42	cctaggcgcgccactagtggatc	62.7	*Kpn I/Avr II/Asc I/Spe I/(Kpn I)/Bam HI*
HL43	cactagtggcgcgcctagggtac	60.8	*Kpn I/Avr II/Asc I/Spe I/(Kpn I)/Bam HI*
HL44	catgcagatctaccggtgctagcc	60.8	*(Nco I)/Bgl II/Age I/Nhe I/(Eco RI)*
HL45	aattggctagcaccggtagatctg	57.6	*(Nco I)/Bgl II/Age I/Nhe I/(Eco RI)*
HL46	agcttaccggtc	38	*Hind III/Age I/Eag I*
HL47	ggccgaccggta	42	*Hind III/Age I/Eag I*
HL57	ggccgctatggccaccggtatgca	70.3	*Not I/Sfi I/Msc I/Age I/Nsi I*
HL58	ataccggtggccat	44	*Not I/Sfi I/Msc I/Age I/Nsi I*
HL61	cctggtagtagcat	42	*SexAI/(PacI)*
HL62	gctacta	20	*SexAI/(PacI)*
HL63	tcgagatatca	30	*(Sal I)/EcoRV/SexAI*
HL64	ccaggtgacatc	38	*(Sal I)/EcoRV/SexAI*
HL65	acctatgggccctctctggctccggacggcacc	79	*Apa I/BspEI/pTα exon II*
HL66	ccaagcttcatgtggttgctgggattgaactcagg	75.8	*Apa I/BspEI/pTα exon II*
HL67	catggtgaggctgctcgaggatggggactgaaactgag	78	*Nco I/end of iCRE/Sal I*
HL68	tcgactgagtttcagtccccatcctcgagcagcctcac	78	*Nco I/end of iCRE/Sal I*
HL75	tcgagatatcaccaggtc	41.5	*(Sal I)/EcoRV/SexAI/(Sal I)*
HL76	tcgagacctggtgatatc	41.5	*(Sal I)/EcoRV/SexAI/(Sal I)*
HL81	tagacgtcgctag	22.8	*(Pac I)/Nhe I/Sex AI Fwd*

HL82	cctggctagcgacgtctaat	51.4	*(Pac I)/Nhe I/Sex AI Rev*
Oligonucleotides used for DsRed knock-in (KI) into ROSA26			
Oligonucleotides used for iCre knock-in (KI) into pTα.			

9. FREQUENTLY USED BUFFERS AND SOLUTIONS

Solutions were prepared according to Sambrook *et al.*[116] with de-ionized dH_2O, unless otherwise stated.

Table 7: Composition of buffers and solutions

20x TAE buffer	455 mmol/L Tris 445 mmol/L boric acid 10 mmol/L EDTA
DNA loading buffer	10 mmol/L M Tris/HCl (pH 7.5) 10 mmol/L EDTA (pH 8) 0.025% (w/v) bromophenol blue 30% (v/v) glycerol 0.5% of N-lauroyl-Sarcosine sodium salt 1mg/mL proteinase K
PK Lysis buffer	10mmol/L Tris/HCl pH 7.5 10mmol/L EDTA 10mmol/L NaCl 0.5% of N-LauroylSarcosine sodium salt 100 μg/mL Proteinase K
Denaturation solution	1.5 mol/L NaCl 0.5 mol/L NaOH
Neutralisation solution	1.5 mol/L NaCl 1 mol/L tris/HCl (pH 7.0)
50x Denhardt´s Solution	1 % (v/v) Ficoll 1 % (w/v) Polyvinylpyrrolidone 1 % (w/v) BSA, pH 7.0 Filtered and stored at –20 °C.
DEPC-ddH_2O	0.1% (v/v) DEPC dissolved in ddH_2O, incubated 24 h at RT and autoclaved afterwards.
10x TE buffer	100 mmol/L Tris/HCl, (pH 8.0) 1 mmol/L EDTA
20X SSC	3 mol/L NaCl 0.3 mol/L NaHCO3,2 H_2O
Hybridization solution	5x SSC 5x Denhardt´s solution 40% (v/v) Formamide 0.5% (w/v) SDS
Washing Solution 1	2x SSC 0.1% (w/v) SDS
Washing Solution 2	0.2x SSC 0.1% (w/v) SDS
10x PBS buffer	1.3 mol/L NaCl 70 mmol/L Na2(HPO_4) 30 mmol/L NaH_2(HPO_4), pH 7.4
Erythrocyte Lysis Buffer	8.3 g/L NH_4Cl 1 g/L $KHCO_3$ EDTA-$Na_2$37,2 mg/L pH 7.2 to 7.4
FACS Wash	PBS/ 5% (v/v) FCS
Protease mix (volume required/sample)	20 µL of Collagenase D1 (10 mg/mL) 200 µL of Dispase I (10 mg/mL) 5 µL of DNAse I (1 mg/mL) 775 µL PBS
Paraformaldehyde (PFA) solution	4%(w/v) PFA dissolved in PBS Add 1 drop of 2 mol/L NaOH and heat at 60°C for complete dissolution. Adjust pH to 7.3

10. CULTURE MEDIA

10.1. For Bacterial Growth

All media for bacteria were prepared with ddH_2O, autoclaved and stored at 4°C.

Table 8: Bacterial culture media

LB-Medium	1% (w/v) peptone or bacto-tryptone 0.5% (w/v) yeast extract 0.5% (w/v) NaCl pH 7.0
2xYT	1.6% (w/v) Tryptone 1% (w/v) Yeast extract 0.5% (w/v) NaCl pH 7.0

Agar plates were prepared by addition of 1.5% (w/v) agar to these media and were stored at 4°C. For positive selection, antibiotics were added to a pre-cooled (~50°C) sterile media to a final concentration of 100 µg/ml for ampicillin and 25 µg/ml for kanamycin. For a blue/white color screen, α-complementation was revealed by spreading 40 µL XGal (40 g/L) and 40 µL IPTG (100 mol/L) before plating the bacteria.

10.2. For Mammalian Cell culture

All media were filtered using 0.22 μM (Nunc) and stored at 4°C.

Table 9: Cell culture media and solutions

Feeder (FD) medium	DMEM/Glutamax/high Glucose (Gibco) 10% (v/v) fetal calf serum (FCS) (Gibco) 1% (v/v) of penicillin (6 mg/mL)/streptomycin (5 mg/mL) solution (Gibco)
ES (embryonic stem cell) medium	DMEM/Glutamax/high Glucose (Gibco) 15% (v/v) Heat inactivated FCS (Gibco) 1mM Sodium Pyruvate (Gibco) 150 μM Monothioglycerol (MTG) 50 μg/mL Getamycin (Gibco) 1000 U/mL ESGRO LIF (Chemikon)
Freezing medium	40% (v/v) ES medium 50% (v/v) FCS (Gibco) 10% (v/v) DMSO (Sigma)
Gelatin solution	0.15% (w/v) gelatin dissolved in PBS.
Trypsin-EDTA (Gibco 25200-072)	0.25% (w/v) Trypsin (Gibco) 1 mmol/L EDTA•4Na
Geneticin (G418) stock solution	60 mg/mL G418 (Gibco) in ES-medium
Gancyclovir stock solution	2mM Gancyclovir in ES-Medium, prepared daily (purchased as a prescription from an M.D.).

For use in ES cell culture, FCS (Gibco) was thawed at 37°C and subsequently heat inactivated for 30 min at 56°C in a water bath. Heat inactivated ES-FCS was then stored at -20°C in 50-mL aliquots.

11. BACTERIAL STRAINS, CELL LINES AND ANIMALS

11.1. Bacterial Strains

The following *Escherichia coli* strains were used:

Table 10

XL1-Blue (for standard cloning)	*recA1 endA1 gyrA96 thi-1 hsdR17 supE44 relA1 lac [F´ proAB lacIqZΔM15 Tn10 (Tetr)].*
JM110 (to recover unmethylated DNA)	*F´ traD36 lacIqΔ(lacZ)M15 proA+B+/rpsL (Strr) thr leu thi lacY galK galT ara fhuA dam dcm glnV44 Δ(lac-proAB)*

11.2. Mammalian Cell Lines

Table 11

NeoR Feeder cells	Prepared as in 15.2, Methods section
BHK-21 (BHK)	Baby Hamster Kidney cancer cell line (fibroblast), ATCC #CCL-10
BRUCE4	Mouse ES cell, C57BL/6-derived
E14.1	Mouse ES cell, 129P2/OlaHsd-derived
AB2.2	Mouse ES cell, 129S7/SvEvBrd-Hprt1-derived

11.3. Mouse strains

Transgenic Lck-Cre[76] and KI ROSA26-**EGFP** mice[71] were purchased from Charles River Laboratories (Sulzfeld, Germany). ROSA26-**EYFP** mice[85] were provided by T. Boehm (Freiburg). A breeding pair of the ubiquitous deleter strain CMV-Cre (carrying a huCMV-Cre transgene on the X-chromosome[117]) was obtained from R. Schmid (University Clinics Ulm). These mice have subsequently been backcrossed onto C57BL/6 for five to seven generations. C57BL/6 FoxN1$^{(nu/nu)}$ were purchased from Taconics (Germantown, NY).

Inbred C57BL/6 ROSA26-**RFP** reporter mice were generated from targeted Bruce4 ES clone #11 following blastocyst injection. Upon F1 inter-cross, homozygous ROSA26-**RFP** reporter mice were obtained and maintained on a C57BL/6 background. To generate animals with one constitutively activated ROSA26-**RFP** allele, ROSA26-**RFP** reporter mice were inter-crossed with CMV-Cre deleter animals. Offspring typed positive for both the Cre recombinase transgene and the reporter allele were further backcrossed onto C57BL/6. Heterozygous progeny with the predicted, complete recombination event were identified by

FACS of peripheral blood (PB) cells. Homozygous ROSA26-**RFP** animals were obtained from inter-crosses of heterozygous parents.

pTα-iCre KI deleter line was derived from targeted E14.1 ES clone #44Δ[1]Neo2. Heterozygous pTα-iCre animal were backcrossed onto C57BL/6 for 5 generations and further inter-crossed to obtain homozygous pTα-iCre animals. These mice were used as stock to generate pTα$^{(iCre/WT)}$ ROSA26$^{(\mathbf{RFP}/WT)}$ animals by inter-cross with homozygous ROSA26-**RFP** reporter mice.

pTα-iCre deleter mice were inter-crossed with other fluorescent reporter lines (floxed ROSA26-**EYFP** and ROSA26-**EGFP**) to compare the efficiency of reporter activation.

For lineage tracing analysis in athymic mice, FoxN1$^{(nu/nu)}$ pTα$^{(iCre/WT)}$ ROSA26$^{(\mathbf{RFP}/WT)}$ were obtained by a first breeding round of homozygous ROSA26-**RFP** reporter and homozygous pTα-iCre deleter females with C57BL/6 FoxN1$^{(nu/nu)}$ males. Resulting FoxN1$^{(nu/WT)}$ pTα$^{(iCre/WT)}$ and FoxN1$^{(nu/WT)}$ ROSA26$^{(\mathbf{RFP}/WT)}$ were further crossed to generate FoxN1$^{(nu/WT)}$ pTα$^{(iCre/iCre)}$ and FoxN1$^{(nu/WT)}$ ROSA26$^{(\mathbf{RFP}/\mathbf{RFP})}$ offsprings. These animals were then used as stocks to generate FoxN1$^{(nu/nu)}$ pTα$^{(iCre/WT)}$ ROSA26$^{(\mathbf{RFP}/WT)}$ and FoxN1$^{(nu/WT)}$ pTα$^{(iCre/WT)}$ ROSA26$^{(\mathbf{RFP}/WT}$ euthymic mice.

12. ANTIBODIES

The optimal working concentrations were determined for each antibody on 10^6 cells of a relevant lineage. Dilutions given in table 12 were used for FACS staining and immuno-histochemistry (IHC) accordingly.

Table 12: Antibody descriptions and titers

Classification	Recognised Antigen	Dye Coupled	FACS 1/…	IHC 1/…	Clone	Isotype	Provider
CD3ε	ε chain of CD3 complex	Fluorescein	25	5 PFA	#17A2	Rat IgG-2b, k	P
CD3ε	ε chain of CD3 complex	PE-Cy7	25	ND	#2C11	Syrian Hamster IgG	eB
CD3ε	ε chain of CD3 complex	APC	25	10 PFA	#2C11	Syrian Hamster IgG	P
CD3ε	ε chain of CD3 complex	APC-Cy7	25	ND	#2C11	Syrian Hamster IgG	P
CD3ε	ε chain of CD3 complex	Biotine	200	ND	#500A2	Syrian Hamster IgG	P
CD4	L3T4	FITC	800	Not on PFA	#H129.19	Rat IgG-2a, k	P
CD4	L3T4	APC	400	Not on PFA	#RM4.5	Rat IgG2a, k	P
CD4	L3T4	Biotine	800	ND	#GK1.5	Rat IgG-2a, k	P
CD8α	Ly-2	FITC	200	ND	#53-6.7	Rat IgG-2a, k	P

CD8α	Ly-2	Biotine		ND	#53-6.7	Rat IgG-2a, k	P
CD11b	Mac-1	FITC	800	ND	#M1/70	Rat IgG-2b, k	P
CD11b	Mac-1	Biotine	500	ND	#M1/70	Rat IgG-2b, k	P
CD11c		PE-Cy7	50	ND	#HL3	Syrian Hamster IgG	P
CD16/CD32	FCg III/II, FC BLOCK			ND	#2.4G2	Rat IgG-2b, k	P
CD19	Glycoprotein	FITC	400	ND	#1D3	Rat IgG-2a, k	P
CD19	Glycoprotein	PE-Cy5.5	200	ND	#1D3	Rat IgG-2a, k	eB
CD19	Glycoprotein	Biotine	800	ND	#1D3	Rat IgG-2a, k	P
CD24	HSA	FITC	200	ND	#30-F1	Rat IgG-2b, k	eB
CD25	IL-2 R α-chain	PE-Cy7	1600	ND	#PC61	Rat IgG1, lambda	P
CD31	PECAM-1	APC	400	ND	#MEC13.3	Rat IgG-2b, k	P
CD34		FITC	25	ND	#RAM34	rat IgG2a, k	P
CD44	Pgp-1	FITC	500	ND	#IM7	Rat IgG-2b, k	P
CD44	Pgp-1	PE	400	ND	#IM7	Rat IgG-2b, k	P
CD44	Pgp-1	PE-Cy5.5	400	ND	#IM7	Rat IgG-2b, k	eB
CD45 Pan	Ly-5	APC-Cy7	400	ND	#30-F11	Rat IgG-2b, k	P
CD45 Pan	Ly-5	Biotine	400	ND	#30-F11	Rat IgG-2b, k	P
CD45R	B220	FITC	400	10 PFA	#RA3-6B2	Rat IgG-2a, k	P
CD45R	B220	APC	100	ND	#RA3-6B2	Rat IgG-2a, k	P
CD97	Gr-1, Ly-6G	FITC	200	ND	#RB6-8C5	Rat IgG-2b, k	P
CD97	Gr-1, Ly-6G	Biotine	500	ND	#RB6-8C5	Rat IgG-2b, k	eB
CD117	c-kit R	APC	200	20 PFA	#2B8	Rat IgG-2b, k	eB
CD127	IL7Rα chain	PE-Cy7	25	ND	#A7R34	Rat IgG2a,k	eB
CD135	Flk2/Flt-3R	Biotin	200	ND	#A2F10	Rat IgG-2a, k	eB
CD161	NK-1.1, NKR-P1C	APC	100	ND	#PK137	Mouse IgG-2a, k	eB
CD229.1	Ly9.1	Biotine	400	ND	#30C7	Rat IgG-2a, k	P
Ter119	Ly-76	FITC	100	ND	#Ter119	Rat IgG-2b, k	P
Ter119	Ly-76	Biotine	200	ND	#Ter119	Rat IgG-2b, k	eB
Sca-1	Stem Cell Antigen	PE-Cy5.5	400	HSC	#D7	Rat IgG-2a, k	P
αβ TCR		FITC	400	ND	#57-597	Syrian Hamster IgG	P
αβ TCR		Biotine	200	ND	#57-597	Syrian Hamster IgG	P
γδ TCR		FITC	800	ND	#GL3	Armenian Hamster IgG	P
γδ TCR		Biotine	1600	ND	#GL3	Armenian Hamster IgG	P
Vγ1		FITC	100	ND	#2.11		aliquot
Vγ4		FITC	100	ND	#UC3-10A6		aliquot
Vγ5		FITC	100	ND	#F536		aliquot
Vγ7		Biotine	100	10	#F2.67		P
SA-PE-Cy5.5		PE-Cy5.5	400	ND			eB
SA-PE-Cy7		PE-Cy7	800	ND			eB
SA-APC		APC	400	ND			MP
SA-APC-Cy7		APC-Cy7	200	ND			eB

ND: Not determined, SA: Streptavidin.

Antibodies and second step reagents used in this study were either purchased from Pharmingen (P), eBioscience (eB) or Molecular Probes (MP).

13. COMPUTER ANALYSIS

For the analysis of the nucleotide sequences, BLAST, BLAST2 and other programs from National Center for Biotechnology Information (NCBI) were used (www.ncbi.nlm.nih.gov) as well as Lasergene software package (DNAstar).

Information about mouse alleles, phenotypes and strains were taken from Jackson Laboratory (www.informatics.jax.org). Statistical analysis, cell distributions, and graphs were done using Prism 4.03 (Graphpad). Mouse genome sequences were downloaded from Ensembl (http://www.ensembl.org). Plasmid maps and restriction analysis were generated using Gene Construction Kit 2 (Textco) and/or Clone Manager 7 Pro (Scientific and Educational Software). Cell Quest, FACS DIVA (Becton Dickinson) and Flojo (Treestar) softwares were used to analyze flow cytometry data.

METHODS

14. MOLECULAR BIOLOGY METHODS

The general molecular biological methods, *E. coli* culture, competent cell preparation, agarose gel preparation and DNA electrophoresis, DNA extraction and precipitation, measurement of DNA/RNA concentration, DNA digestion were performed according to *Molecular Cloning: A Laboratory Manual* (Sambrook et al., 1989). For cloning, plasmid DNA was prepared using standard alkaline lysis protocol and digested with NEB restriction enzymes in corresponding NEB buffers, unless otherwise stated. DNA extraction from agarose gels were performed using Qiaquick gel extraction kit (Qiagen). DNA preparations were ligated in a volume of 10-µL using a 3x molar excess of insert and 1 unit of T4 DNA ligase (NEB) in ligase buffer in a PCR block set at 16° C overnight. PCR products were cloned using TOPO cloning kit (Invitrogen). Prior to ES cell electroporation, large amount of plasmid DNA was prepared using Qiafilter Midiprep kit (Qiagen).

14.1. *Escherichia coli* heat shock transformation

Competent cells were thawed on ice, 20-ng plasmid DNA in H_2O or 1-µL of ligation mix was added and gently mixed with a pipette tip. The suspension was left on ice for 30 min, then heat shocked in a 42°C water bath for 30 seconds, and placed on ice for 2 min. 500-µL LB medium were added and cells were incubated at 37°C, 200 rpm for 60 min before plating on 2xYT agarose plates.

14.2. Polymerase chain reaction (PCR) of DNA fragments

AmpliTaq polymerase (ROCHE, #58003456-02) was used for analytic PCR, Expand long template PCR system (ROCHE #11 681 834 001) was used for cloning PCR as it contains 3´to 5´exonuclease activity ("proof-reading") which recognizes and removes incorrectly incorporated deoxynucleotide. This polymerase mix was also used for the amplification of fragments larger than 2 kb which were generated for subcloning. GC Rich PCR system (ROCHE #12 140 306 001) was used to amplify complex templates such as the GC-rich promoter region encompassed in ROSA26 short arm.

Standard PCR conditions were:

		Volume (µL)
Template DNA	50-200 ng	1
Fwd Primer	10 pM/uL	1
Rev Primer	10 pM/uL	1
dNTPs	2,5 mM	2
$MgCl_2$	25 mM	2
ReadyLoad	10X	2.5
Buffer	10X	2.5
AmpliTaq	(20 U/µL)	0.1
H_2O		12.9
V final		up to 25

The individual profile for each PCR was determined experimentally on a T3 Thermocycler (Biometra). After an initial denaturation step at 94 °C (AmpliTaq and Long Expand: 2 min; GC-rich: 3 min) 30-35 cycles followed:

1. Denaturation at 94 °C for 30 sec
2. Annealing at 50-65 °C for 30 sec
3. Extension at 72 °C for 1 min/kb (AmpliTaq) and 2 min/kb (Long Expand, GC-rich), respectively. At the end of the run, a 10 min incubation at 72 °C followed to complete the ends of all amplicons.

14.3. Sequencing

Sequencing reactions were performed according to the chain termination method from Sanger *et al*. (1977) using 4 different fluorescently labeled ddNTPs (didesoxynucleosid-5´-triphosphate).

		Volume (µL)
Template DNA	500 ng	
Sequencing Primer	10 pmol/µL	0.5
ABI Prism BigDye Mix		4
ddH2O		up to 10

The following program was run in the T3 Thermocycler (Biometra):
After an initial denaturation step of 1 min at 95 °C, 25 cycles followed:

1. Denaturation at 95°C for 15 sec
2. Annealing at 50°C for 15 sec
3. Extension at 60°C for 4 min

Sequencing reaction was stopped by adding following mix to the sample

		Volume (µL)
Dextran Blue	5 mg/mL	5
Na acetate	3 mol/L	1
EDTA	125 mmol/L	1
Ethanol	100% (v/v)	30

After 10 min incubation at RT and protected from light, the sample was centrifuged for 10 min at 13000 rpm using 5417R centrifuge (Eppendorf) and washed with 200 µL of 75 % Ethanol. The air-dried pellet was resuspended in 25-µL sequencing ddH_2O (Roth, #A5112.), and applied to the ABI Prism 377 DNA Sequencer (Perkin- Elmer, Weiterstadt). Sequences were verified and aligned using Seqman module of Lasergene software (DNAstar).

14.4. Semi-quantitative RT-PCR

mRNAs were extracted from up to $5x10^4$ cells using RNAzol™ B (Cinna/BiotecX, #CS-101) according to suppliers protocol. cDNA was prepared with Superscript II RT kit (Invitrogen) as following:

Table 13: Standard Protocol for first strand cDNA synthesis

		Volume (µL)
mRNA Sample	1 to 5 µg total RNA	x
dNTPs Mix	10 mmol/L	1
Oligo d(T)	0.5 µg/µL	1
DEPC-H_2O		Up to 10
	65°C for 5 min 4°C for 5 min	
RT Buffer	10X	2
MgCl2	25 mmol/L	4
DTT	0.1 mol/L	2
RNAse OUT	40 U/µL	1
	42°C for 2 min	
Superscript II RT	50 U/µL	1
	42°C for 50 min 70°C for 15 min 4°C for 5 min and centrifugation	
RNAse H	2 U/µL	1
	37°C for 20 min	

The amount of cDNA was first quantified using HPRT amplification (JF47/JF48). Subsequent PCR amplification on normalised cDNA quantity was performed using gene specific primers (See material section 8.1).

14.5. Southern Blot

14.5.1. Southern transfer of DNA fragments onto membranes

10-µg of genomic DNA prepared by phenol/chloroform extraction was digested with appropriate restriction endonucleases in digestion buffer overnight; separated on a 0.8% agarose gel, denatured and transferred onto nylon membrane (Hybond N^+, Amersham) by diffusion of denaturation solution. The membrane was washed briefly in 6x SSC.

14.5.2. Radioactive random labeling of nucleic acids

To detect specific nucleic acid sequences on Southern blot filters, DNA probes (30 to 40-ng) were labeled with 50-µCie αdCT^{32}P using the "Prime it" (Stratagene) according to the suppliers protocol and purified using NICK^{TM} chromatography columns. The yield was determined by measuring the radioactivity of 1 µL using an LS3801 counter (Beckman, Palo Alto, USA). 2.10^6-cpm of labeled probe was denatured at 95°C for 10-min and placed on ice for 2-min.

14.5.3. Detection of genomic DNA fragments with radio-labeled probe

The blotted nylon filters containing either DNA were rolled and placed into a hybridization tube (nucleic acid facing inwards), which was filled with 2x SSC and freed from air bubbles. Once the filters on place, 2x SSC was poured out and replaced with 15-mL of pre-warmed (65°C) hybridization solution and 500-µL of denatured (95°C, 10 min) sonicated salmon sperm DNA (100 µg/mL). The tubes were pre-hybridized for 2 hrs in a rotation oven at 65°C. Denatured radioactive probe (see section 14.5.2) was added to the tube and the hybridization was carried out overnight under the same conditions as the pre-hybridization. The next day, the hybridization solution was poured out and the filters were washed at 65°C with the washing solution 1 for 5-20 min, depending on the activity shown by the filters. The radioactive signals were checked with a hand monitor (β-detector, LB 1210B, Berthold, Bad Wildbad). A more stringent wash with washing solution 2 was done for 5-10 min if the filter had an activity >10 desintegration *per* s^{-1}. Finally, the filters were wrapped into saran plastic, placed in an autoradiography cassette and exposed to a Kodak BioMax MS-1 Film (Sigma,

München) film for 2 to 3 days at -80°C.

15. MAMMALIAN CELL CULTURE

15.1. BHK-21 maintenance

BHK cells were used to assay expression of various fluorescent reporters in mammalian cells.

15.1.1. BHK growth and trypsinization

One vial of BHK-21 cells were grown in 10-mL FD-Medium in 7,5 cm^2 cell culture flasks (Nunc). BHK-21 cells were grown at 37°C in a humidified 5% CO_2 incubator and medium was changed every other day. At confluency, cells were trypsinized for 5 min at 37°C with 1-mL of 0.05% Trypsin EDTA (Gibco). Trypsinization reaction was stopped with 9-mL FD-Medium and cells were further propagated following a 1/5 to 1/6 sub-cultivation split.

15.1.2. Electroporation of BHK cells

After trypisinization, 5 x 10^6 BHK cells were distributed into a 0.4 cm electroporation cuvette (Biorad #165-2088) and electroporated with 20-µg of plasmid DNA at 220-KV, 960-µFd in 400 µL PBS/DNA solution, yielding a time constant of 5 to 8 ms. Circular plasmids were electroporated for transient expression. BHK cells were resuspended in 20-mL FD-medium and plated on two 10-cm plates. BHK cells were grown for 24 hrs at 5% CO_2 in a humidified incubator and analyzed the next day by FACS.

15.2. NeoR Murine Embryonic Feeder (MEF) preparation and maintenance

Pregnant NeoR transgenic females were sacrificed at 14 dpc (day *post coitum*) and their uteri were dissected out in MT-PBS. The embryos were then dissected away from the uterus, the placenta was subsequently removed to retain only the embryo proper. Head and fetal liver were cut out to remove most of the tissue not supporting ES cell growth. Remaining carcasses were cut into a slurry, and transferred into 10-mL of 0.05% (v/v) Trypsin/EDTA with sterile glass beads. After 30 min of digestion at 37°C under gentle stirring (~1-2 turns/second), cell debris were filtered out through a sterile silk filter (50-µm mesh opening). The cell

suspension was mixed with FD-medium (20-mL per digested embryo) and plated on 10-cm cell-culture dishes. After a day of incubation at 37°C in a humidified 10% CO_2 incubator, the medium was changed to remove dead cells and debris. 2-3 days later, the confluent monolayers of feeder cells were trypsinized and frozen to a density of 1 embryo equivalent into 1 mL of freezing medium. Cells were stored at -70°C for one day and transferred into liquid nitrogen for long time storage. One vial of this stock of feeder cells was thawed on six 10-cm dishes. Confluent dishes were reached within 3-4 days. MEFs could be further propagated in FD-medium for 3 more times on gelatinized plates following a 1/3 sub-cultivation split. Prior to ES cell experiments, feeder cell growth was inhibited by 33 rad of γ-irradiation.

15.3. Maintenance and genetic manipulation of ES cells

Similar protocols were applied to all ES cell lines used in this study.

15.3.1. Thawing, trypsinizing ES cells

1 vial of ES cells (containing a 10-cm dish equivalent) was thawed [ES cells were transferred to a 15-mL Falcon tube and "drop wise" resuspended in 9-mL of ES-medium] and plated on two 10-cm dishes with irradiated MEFs. ES cells were grown at 37°C in a humidified 10% CO_2 incubator and medium was changed every day. After 2-3 days, the cells were trypsinized with 2-mL of 0.25% (v/v) Trypsin/EDTA for 2 min at 37°C. To stop the trypsinization reaction, 8-mL ES-medium solution was added to the cell suspension. To prevent differentiation, colonies need to be broken up into single cells when passaged. Therefore, the suspension was pipetted slowly up and down about three times in ES-medium, avoiding the production of foam. Cells were left for 10 min at 4°C to sediment the remaining cell lumps. The supernatant (9-mL) was carefully collected, centrifuged at 1200 rpm for 5 min at 4°C (Heraus, Rotor #2250) and cells were split on 3 to 4 10-cm dishes with irradiated MEFs.

15.3.2. Electroporation of ES cells

ES cells were grown on three 10-cm cell culture dishes with irradiated MEFs until they were almost confluent; then split 1/4 on 12 new plates. Two days later, the cells were ready to be harvested for electroporation. Medium was changed 3 to 4 hrs before the electroporation to keep cells in a good shape. ES cells were trypsinized (see section 15.3.1), and collected by centrifugation at 1200 rpm for 5 min at 4°C (Heraus, Rotor #2250). Cells were resuspended altogether in 10 ml PBS, counted (using a 1/5 dilution) in a Neuhaus chamber. 2 x 10^7 ES cells were distributed into a 0.4 cm electroporation cuvette (Biorad #165-2088). Cells were electroporated with 20-40-µg DNA at 250-KV, 500-µFd in 800 µL PBS/DNA solution, yielding a time constant of 10 to 14 ms. For transient expression, circular plasmids were electroporated; for stable integration, plasmids were linearized with convenient restriction enzymes before electroporation. After electroporation, ES cells were kept on ice for 10 min and resuspended in 20-mL ES-medium/electroporation. Finally, cells were plated on two 10-cm plates with irradiated feeders and grown for 24 hrs at 10% CO_2 in a humidified incubator.

15.3.3. Freezing ES cells

The cells were allowed to grow to higher confluency (85%) and fed 4 hrs before freezing. To freeze, cells were trypsinized (see section 15.3.1) and washed into 4 volumes of ES-medium. The pellet of cells was promptly broken by flicking the side of the tube and cells were gently resuspended in 1-mL of 1x freezing medium (10.2) per trypsinized dish. The cell suspension was then distributed into 2-mL cryovials (Corning) on ice until all the cryovials were ready to freeze. The vials were then transferred to isopropanol (temperature controlled) freezing vessel. For long term storage, the vials were transferred to liquid nitrogen 48 hours later.

16. GENERATION OF KNOCK-IN MOUSE LINES

16.1. Constructs used for gene targeting

All the cloning steps required for the generation of targeting constructs are listed in this section.

16.1.1. Knock-in of Cre-inducible DsRed1/2 into the ROSA26 locus

Two different gene targeting strategies were tested. The use of TK-NeoR cassette for gene targeting yields to many recombinant clones irrelevantly of the expression status of the locus of integration. The resulting gene targeting efficiency is expected to be low and requires a labor intensive screening of recombinant colonies. In contrast, IRES (Internal Ribosome Entry Site)-NeoR cassette selects only for ES clones in which the recombinant DNA has inserted in an actively transcribed locus. This targeted "gene trap" strategy can be applied to target more efficiently the ROSA26 locus as it is expressed in ES cells[81]. The whole expression cassette was fused to the adenovirus splice acceptor taken from pSAβgeo[81] and cloned at the unique *Xba* I site of pROSA26.1 vector. pROSA26.1 provides the arms of homology required for the insertion of the expression cassette *via* homologous recombination within the first intron of the ROSA26 gene[81]. In both pHL-BP and BS targeting constructs, the longest arm of homology was fused to a negative selection cassette in order to eliminate recombinant ES clones with residual sequences of the plasmid backbone at the integration site[58]. The thymidine kinase (TK) or diphteria toxine a (DTa) genes were both tested. TK exerts its toxicity only in the presence of a nucleotide analogue, the gancyclovir (Cymeven, Roche) whereas DTa itself irreversibly inhibits the protein synthesis by ADP-ribosylation of elongation factor 2[118]. In the present work, pHL-BP-TK and BS-TK were not used for gene targeting.

Table 14: DsRed ROSA26 targeting construct generation

pHL-BA	Derived from pBSK after insertion into *Spe I*/*Eco RV* of a 1.3 kb *Spe I*/*Eco RV* fragment from pβGeo wich encodes for a βgal/Neo fusion protein. Construction checked using restriction digests.
pHL-BB	Derived from pHL-BA after deletion of 1.150 kb *Hind III* fragment in order to remove all βgeo gene sequence except its first exon and intron. Construction confirmed by restriction digests and sequencing using oligonucleotide 11102.
pHL-BC	Derived from pHL-BB insertion of a 1.265 kb *Xho I* fragment of pL2Neo coding for LoxP-NeoR cassette into *Sal I*/*Xho I* sites. Screening for insertion and orientation was achieved using *Sal I* and *Hind III*/*Xho I* respectively.
pHL-BC-inv	Same as for pHL-BC with the 1.265 kb *Xho I* fragment of pL2Neo coding for LoxP-NeoR cassette in the other orientation. Construct confirmed by sequencing.
pHL-BC-ΔXho I	Same as for pHL-BC with the 1.265 kb *Xho I* fragment of pL2Neo coding for LoxP-NeoR cassette only cloned in the *Xho I* of pHL-BB. Construct confirmed by sequencing and restriction digests.
pHL-BD	Oligonucleotides HL10/HL11/HL12/HL13 were inserted into the *Kpn I*/*Not I* sites of pBSK-. Purpose: create a new polylinker with restriction sites (*Not I*)/*Sal I/Nhe I/Xho I/Eco 47 III/Bgl II/Pst I/Eag I/Bam HI/Pst I/Mlu I/Xba I/Kpn I* in order to construct 3p(A)n-lox P-DsRed1-SV40 p(A)n.
pHL-BE	Derived from pHL-BD after insertion of a 284 bp *Xba* I fragment bearing the bGH polyadenylation site from pbGeo into its *Nhe* I site. Orientation of the fragment was confirmed by *Xho* I/*Sac* I restriction digest and sequencing.
pHL-BF	Insertion of a 284 bp *Sac* I/*Sal* I fragment bearing bGH polyadenylation site from pbGeo into *Sac* I/*Sal* I sites of pHL-BE. Insertion of the fragment was confirmed by *Xho* I/*Sal* I restriction digest and sequencing using 14013 primer.
pHL-BG	Insertion of a 284 bp *Sac* I/*Sal* I fragment bearing bGH polyadenylation site from pbGeo into *Sac* I/*Sal* I sites of pHL-BF. Insertion of the fragment was confirmed by *Xho* I/*Sal* I restriction digest.
pHL-BH	Insertion of a 695 bp *Eco* 47III/*Bgl* II fragment of pDsRed1-C1 into *Eco* 47III/*Bgl* II of pHL-BG.
pHL-BI	Insertion of a 251 bp *Bam* HI/*Mlu* I fragment of pEGFP.C1 into *Bam* HI/*Mlu* I of pHL-BH.
pHL-BJ	Insertion of a 121 bp *Xho* I/*Sal* I loxP site of pL2-Neo into *Xho* Isite of pHL-BI. Insertion of the fragment was confirmed by *Xho* I/*Age* I restriction digest.
pHL-BK OK	Insertion of a 1.96 kb *Sal* I/*Kpn* I fragment bearing 3*p(A)n-loxP-DsRed1-SV40 p(A)n from pHL-BJ into *Xho /Kpn* I sites of pHL-BC.
pHL-BK V(HL40/41)	Oligonucleotides HL40/HL41 were inserted into the *Not I/Xma I* sites of pHL-BK. Purpose: create a new polylinker with restriction sites (*Not I*)/*Spe I/Pac I/Xma I)* in order to transfer easily the cassette in pROSA26.1. Insertion was confirmed by sequencing and restriction digest using *Xba* I.
pHL-BL	Insertion of a 695 bp *Eco* 47III/*Xba* I fragment of pDsRed2-C1 into *Eco* 47III/*Xba* I of pHL-BK.V(HL40/HL41). Purpose: exchange DsRed1 with the newest version of DsRed from Clontech. Insertion checked with *Bam* HI/*Not* I.
pHL-BLΔ*Not* I	Disrupt *Not* I/*Xma* I of pHL-BL by exonuclease III treatment and re-ligation. Purpose: disrupt *Not* I site for the cloning of loxP-Ires. Complete disruption of *Not* I/*Eag* I site was confirmed by sequencing.
pHL-BM	Oligonucleotides HL42/HL43 were inserted into the *Kpn I* site of pHL-BL. Purpose: create a new polylinker with restriction sites on the 3' side of the cassette (*Kpn I/Avr II/Asc I/Spe I/(Kpn I))* in order to transfer easily the cassette in pROSA26.1. Insertion was confirmed by sequencing.
pHL-BP-DTa	Transfer of a 3.4 kb *Spe* I/*Avr* II fragment bearing SA-loxP-Neo-3*p(A)n-loxP-DsRed2-SV40 p(A)n from pHL-BM into *Xba* I site of pROSA26.1. Plasmid was confirmed using multiple restriction digests and linearized using *Sac* II digestion.
pHL-BP-TK	Transfer of a 3.4 kb *Spe* I/*Avr* II fragment bearing SA-loxP-Neo-3*p(A)n-loxP-DsRed2-SV40 p(A)n from pHL-BM into *Xba* I site of pROSA26-TK. Plasmid was confirmed using multiple restriction digests and linearized using *Sac* II digestion.

Table 15: IRES-Neo/DsRed ROSA26 targeting constructs generation

pHL-BQ	Transfer a 688 bp *Eag* I fragment from pCAGGS.V1.loxP bearing loxP-IRES into the *Hind* III/*Eag* I sites of pHL-BLΔ*Not* I using the linker HL47/HL46. Insertion checked by restriction digest and sequencing.
pHL-BR	Transfer a 2.5 kb *Bgl* II/*Xho* I fragment from HL-BQ bearing SA-loxP-IRES-Neo-3*p(A)n into the *Bgl* II/*Xho* I sites of pHL-BM. Insertion checked by restriction digest and sequencing. Purpose: sub-clone this fragment in previous construct to be able to use the 5' MCS for transfer into pROSA26.1 and pROSA26-TK.
pHL-BS-DTa	Transfer the 3.6 kb *Pac* I/Asc I cassette from pHL-BR into the *Pac* I/Asc I sites of pHL-BP-DTa (orientated cloning). This the final targeting construct of DsRed2 into ROSA26 locus using IRES-Neo and DTa. Plasmid was confirmed using multiple restriction digests and linearized using *Sac* II digestion.
pHL-BS-TK	Transfer the 3.6 kb *Pac* I/Asc I cassette from pHL-BR into the *Pac* I/Asc I sites of pHL-BP-TK (orientated cloning). This the final targeting construct of DsRed2 into ROSA26 locus using IRES-Neo and DTa. Plasmid was confirmed using multiple restriction digests and linearized using *Sac* II digestion.

For the establishment of a PCR screen of recombinant clones at the ROSA26 locus, pHL-BO control construct was cloned with a sequence prolonging the 5' end of the short homology arm of pROSA26.1 targeting vector.

Table 16: ROSA26 control arm construct generation

pTOPO(HL23/HL24)	Amplify a 552 bp fragment using GC rich Kit PCR system and clone it into TOPO vector. This results in the *Xho* I/*Sal* I flanked control arm for ROSA26 targeting. Amplified product was confirmed by sequencing.
pHL-BN	Transfer a *Kpn* I/*Xba* I fragment from pHL-BC bearing SA-loxP-Neo into the *Kpn* I/*Xba* I sites of pR26.1V(HL21/22). Construct confirmed by sequencing.
pHL-BO	Transfer a *Sal* I/*Xho* I fragment from TOPO(HL23/24) bearing CA-loxP-Neo into the *Sal* I site of pHL-BN. Orientation confirmed by restriction digest and sequencing. This is the control construct for ROSA26 targeting.

Table 17: ROSA26 variants generation

pR26.1V(HL21/22)	Linker HL21/HL22 was inserted into the *Sac* II site of pR26.1. It creates a new polylinker with restriction sites *Sfi* I/*Sal* I/(*Sac* II) in order to be able to make linear the constructs with *Sfi* I and insert the control arm. The correct orientation has been determined by sequencing using oligonucleotide 14013.
pR26∆Sal I	pROSA26.1 was digested with *Sal* I and filled in using Klenow polymerase. Disruption of *Sal* I site checked by restriction digest
pR26∆*Sal* IV(HL21/22)	Linker HL21/HL22 were inserted into the *Sac* II site of pR26.1∆*Sal* I. Purpose: create a new polylinker with restriction sites *Sfi* I/*Sal* I/(*Sac* II) in order to be able to linearize the constructs with *Sfi* I and insert the control arm. The correct orientation has been determined by sequencing using oligonucleotide 14013.

16.1.2. Knock-in of Cre-inducible HcRed1 into the ROSA26 locus

As expression of DsRed2 from the ROSA26 promoter was not yielding any red fluorescence in ES cells, HcRed1 (another commercially available RFP from another coral) was targeted into the ROSA26 locus using the "targeted trapping" approach with IRES-Neo positive selection cassette. Negative selection was performed with DTa gene. No control construct was generated as the PCR screen remained the same as in (see section 16.1.1)

Table 18: HcRed1 Targeting construct generation

pHL-DA	Insertion of a *Age I/Not I* 0.7 kb fragment bearing HcRed1 from pHcRed-N1 into the *Age I/Eag I* of pHL-BJ
pHL-DB	0.99 kb *Mlu* I/*Nhe* I fragment from pHL-DA cloned into *Mlu* I/*Nhe* I of pHL-BT.
pHL-DC	*Mlu* I/*Xma* I fragment from pHL-DB inserted into *Mlu* I/*Xma* I of pHL-BS-DTa. This is the final targeting construct of HcRed1 into the ROSA26 locus. Plasmid was linearized using a *Sfi* I digestion.
pHL-DD	*Mlu* I/*Spe* I fragment from pHL-DB inserted into *Mlu* I/*Xba* I of pCAGGS-Flpe.V2. This construct allows testing of HcRed1 expression upon Cre mediated stopper deletion.

16.1.3. Knock-in of Cre-inducible mRFP1/tdRFP into the ROSA26 locus

HcRed1 expression from the ROSA26 locus was too weak to be useful in lineage tracing. Another set of constructs were constructed to target mRFP1 and tdRFP[110]. These DsRed variants were targeted using the "targeted trapping" approach with IRES-Neo selection cassette. Negative selection was performed with DTa gene. No control construct was generated as the PCR screen remained the same as in (see section 16.1.1)

Table 19: mRFP and tdRFP targeting construct generation

pHL-FA	A 0.685 kb *Bam* HI/*Eco* RI fragment from pmRFP (Tsien *et al.*) inserted into *Bam* HI/*Eco* RI of linearized pEGFP.C1.V(HL8/HL9).
pHL-FB	A 1.4 kb *Bam* HI/*Eco* RI fragment from ptdRFP (Tsien *et al.*) inserted into *Bam* HI/*Eco* RI of linearized pEGFP.C1.V(HL8/HL9).
pHL-FG	0.96 kb fragment *Mlu* I/*Nhe* I of pHL-FA cloned into *Mlu* I/*Nhe* I (partial fragment of 11 kb) of pHL-DC. This final targeting vector for mRFP into the ROSA26 locus is linearized using *Eco* RV.
pHL-FH	1.7 kb fragment *Mlu* I/*Nhe* I of pHL-FB cloned into *Mlu* I/*Nhe* I (partial fragment of 11 kb) of pHL-DC. This final targeting vector for tdRFP into the ROSA26 locus is linearized using *Eco* RV.

16.1.4. Knock-in of Cre-inducible tdRFP in reverse orientation into the ROSA26 locus

Recombinant clones targeted with tdRFP exhibited fluorescence before the excision of the stopper sequence. A new generation of targeting constructs was cloned to target tdRFP to the ROSA26 locus. tdRFP was cloned in opposite orientation to the ROSA26 promoter to prevent reporter expression before Cre activation. As for previous gene targeting experiment, the ROSA26 locus was "gene trapped" with the marked difference that Neo was directly fused with the ROSA26 transcripts. Negative selection was performed with DTa gene. No control construct was generated as the PCR screen remained the same as in (see section 16.1.1).

Table 20: "tdRFP flip" targeting construct generation

pHL-HA	pHL-FH was digested with *Xho* I/*Nhe* I and the 6.5 kb band was purified. The linker JF77/JF78 ((*Xho I*)-*Nsi* I-lox2372-*Mlu* I-spacer-*Xho* I) was inserted into the *Xho* I site and the orientation checked using the *Nsi* I site next to the p(A)n. This step introduce lox2372 site next to the p(A)n stopper.
pHL-HB	pHL-FB was digested with *Xho* I, filled-in with Klenow and relegated creating a *Pvu* I site. Recombinant plasmids were screened using *Pvu* I.
pHL-HC	The linker JF79/JF80 (*Nhe* I-*Xho* I-spacer-*Eco* RI) was inserted into the *Nhe* I/*Eco* RI of pHL-HB. This step inserts a spacer next to the CMV promoter in pHL-HB.
pHL-HD	The *Eco* RI fragment of pHL-FH containing loxP-tdRFP (1.5 kb) was inserted into the *Eco* RI site of pHL-HC. This step inserts of loxP-tdimer RFP next to the spacer of pHL-HC
pHL-HE	The linker JF81/JF82 (*Xho* I-*Asc* I-lox2372-(*Xho* I)) was inserted into the *Xho* I site of pHL-HD. This step introduces a lox2372 site upstream of the conventional loxP site
pHL-HF	The NeoR-p(A)n cassette was extracted from pHL-GA with a *Xba* I/*Nco* I partial digestion and inserted into the *Eco* RI/*Xba* I sites of pHL-HA using the linker JF83/JF84 (*Eco* RI-Kozak-*Nco* I). This step inserts Kozak-Neo-pA into pHL-HA.
pHL-HG	The 1.8 Kb *Xho* I/*Mlu* I fragment (lox2372-spacer-loxP-tdRFP-SV40 p(A)n) from pHL-HE was inserted into the *Xho* I/*Mlu* I sites of pHL-HF.
pHL-HH	The *Pac* I/*Asc* I fragment (SA-loxP-Kozak-Neo-p(A)n-lox2372-tdRFPrev-loxPrev-spacer-lox2372rev) was inserted in the *Pac* I/*Asc* I sites of pHL-FH. This final targeting construct is linearized using *Xho* I.

16.2. Generation of pTα targeting constructs

All the cloning steps required for the generation of the pTα-Cre targeting constructs are listed in this section.

16.2.1. Constructs for targeting hCRE into the first exon of pTα

Constructs were designed to target a cDNA encoding a humanized version of Cre (hCre)[119] into the first exon of pTα, just downstream of the endogenous ATG start codon. Such a targeting event would disrupt the pTa gene. Several targeting constructs were generated: positive selection was always performed using a NeoR cassette driven by a TK promoter (from pMC-Neo-p(A)n). For negative selection either a TK (pHL-AI) or a DTa (pHL-AP) cassette was used.

Table 21: pTα-hCre targeting construct generation

pHL-AA	Linker HL03/HL04 was inserted into the *Eco* RI site of $pDOI_5$. The purpose is to create a new multiple cloning site with convenient restriction sites *Xho* I/*Sal* I/*Eag* I in order to fuse hCRE with rabit β-globin sequence bearing Splice Donor (SD)-intron-Splice Acceptor (SA)-Exon III. The correct orientation was determined with a *Bam* HI/*Eco* RI digest confirmed by sequencing using HL03.
pHL-AB	Derived from pHL-AA after deletion of the *Sma* I/*Sma* I fragment in order to remove native $pDOI_5$ *Sal I* site to allow an easier cloning of hCRE. Construct checked using *Xma* I digests.
pHL-AC	Results of the insertion of a *Eco* RI/*Xho* I fragment encoding hCRE from pCXN-hCRE *into Eco RI/Sal I* sites of pHL-AB. As hCRE cloning introduces a new *Xma* I site, *Xma* I was used for the screening of recombinant plasmids.
pKBAB.V1	Derived from pKBAB after disruption of the *Bam* HI site by *Bam* HI digest followed by a fill in reaction with Klenow. This step inserts hCRE construct from pHL-AC using a *Bam HI/Xho I* digests. Disruption of *Bam HI* site was confirmed by sequencing.
pHL-AE	Derived from pBSK.V(HL01/HL02) after insertion of a *Not* I/partial *Eco* RI fragment of pKBAB.V1 into its *Not* I/*Eco* RI sites. Recombinant plasmids were screened using *Not* I/*Eco* RI and *Eco* RV digests.
pHL-AF	Cloning of *Bam* HI/*Xho* I fragment of pHL-AC (E1-Intron-E2-hCRE-polyA) into *Bam* HI/*Xho* I sites of pHL-AE.
pHL-AG	Linker HL06/HL07 was inserted into the *Xho* I site of pHL-AF. It creates a new multiple cloning site with restriction sites *Xho* I/*Asc* I/*Sal* I/(*Xho* I) in order to clone the long arm of pTα KI. Insertion was checked using an *Asc I* digest as pHL-AF does not bear any *Asc* I site (clones #1, 2, 3, 4, 5, 7, 9, 11, 12). Integrity of inserted sequence and orientation of the insert were checked by sequencing
pHL-AN	As hCRE has been shown to be expressed in bacteria during cloning of the positive control construct, the floxed NeoR cassette has been to replaced by a flipped NeoR cassette extracted from plasmid FRT-neo-FRT. pHL-AN is derived from pHL-AG after insertion into its *Sal* I site of a *Xho* I/*Sal* I fragment from pFRT-Neo-FRT. Construction verified using a *Xba* I digest which release the NeoR gene (*Xba* I site present within both FRT sequences).
pHL-AI	Derived from pT-OA after insertion into its *Spe* I/*Sal* I sites of a *Spe* I/*Sal* I fragment from pHL-AN bearing intron-hCRE-p(A)n. This is the final targeting construct with TK as a negative selection marker. Construction (19kb) verified using multiple restriction digests. Linearization using *Spe* I.
Constructs to use diphteria toxin a as negative selection	
pHL-AO	Derived from pDTa after insertion of a *Eco* RI/*Eco* RI fragment (6,5 kb) from pHL-AH into its *Eco* RI sites. Orientation checked using a *Nhe* I/*Xho* I digest.
pHL-AP	Derived from pHL-AO after insertion into its *Spe* I/*Nhe* I sites of a *Spe* I/*Nhe* I fragment (8,3 kb) from pHL-AI. Orientation checked using a *Xho* I digest. This is the final targeting vector using DTa as a negative selection marker. Linearization with *Spe* I site.

To establish PCR conditions for the identification of targeted clones, plasmid pHL-ALinv was constructed, which carries an extended "short arm" of homology at the 5' end of pHL-AI SA:

Table 22: pTα-Cre KI control construct generation

pHL-AK-inv	Derived from pHL-AF-inv after cloning of a 1.4 Kb *Nhe* I/*Eco* RV fragment of pGL3-AF into its *Xba* I/*Eco* RV sites. It extends the short arm sequence. Confirmed by a fine restriction digest analysis and sequencing.
pHL-AL-inv	Derived from pHL-AK-inv after cloning of a 1.1 kb *Xho* I/*Sal* I fragment of pMC1-Neo into its *Xho I* site. Screening was performed using an *Eco* RI digestion and clones with both orientation of NeoR were isolated: pHL-AL-inv#2 and pHL-AL-inv#10. This is final control construct was linearized using *Spe* I.

16.2.2. Constructs for targeting IRES-iCRE into the 3' Untranslated Region (UTR) of pTα

An alternative strategy was designed to knock-in Cre in the pTα locus without disrupting the pTα gene. iCre was used instead of hCre as it was shown to be well expressed in mouse transgenic animals[114] and had become available meanwhile. iCre was fused with an IRES sequence and cloned into the 3' UTR of the pTα gene, *i.e.* between the stop codon and the polyadenylation signal. As the locus of insertion differs from the previous targeting strategy, an additional control construct needed to be generated to establish PCR conditions for screening of ES colonies. A TK (pHL-CI) or DTa (pHL-CJ) gene was included in the targeting constructs to allow negative selection.

Table 23: pTα-IRES-iCre Control construct generation

pHL-CA	Insertion of a 0,6 kb *Pac* I/*Nco* I fragment of pCAGGS.V1 into *Pac* I/*Nco* I site of pHL-BT.
pHL-CA V(HL68/HL69)	Insertion of a *Nco* I/*Sal* I linker bearing 3' end of iCRE into *Nco* I/*Sal* I of pHL-CA using linker HL68/HL69. Insertion confirmed by sequencing.
pHL-CB	Insertion of a *Nco* I/*Nco* I fragment bearing 5' coding sequence of iCRE into *Nco* I site of pHL-CA.V(HL68/HL69).
pHL-CC	Insertion of a 1,3 kb *Xho* I/*Sal* I fragment encoding the flipped NeoR cassette into *Sal I* site of pHL-CB. Required orientation was the following (*Xho* I)/FRT-NeoR-FRT/(*Sal* I)
pHL-CD	Insertion of *Spe* I/*Avr* II fragment from pHL-AO into the *Avr* II site of pHL-BT. Correct orientation was *Not* I/(*Spe* I)/*Avr* II. Insertion and orientation determined using a *Xho* I/*Not* I digest.
pHL-CE	Insertion of a *Nsi* I/*Sal* I fragment from pHL-AI into *Nsi* I/*Sal* I sites of pHL-CD. DNA from clone #12 kept and transformed into *dcm*⁻ JM1S10 strain to allow further digestion with *Sex* AI.
pHL-CF	Exchange of a *Apa* I/*Apa* I fragment from pHL-CE with *Apa* I/*Apa* I fragment from pT-KAN.V3 in order to introduce a *Bam* HI restriction site into the Exon III of pTα.
pHL-CG	Insertion of a 2.9 kb *Pac* I/*Sal* I fragment of pHL-CC into *Sex* AI site of pHL-CE using linkers HL61/HL62 and HL63/HL64. Wright orientation: *Sex* AI/(*Pac* I)/IRES-CRE/FRT-NeoR-FRT/(*Sal I*)/*Eco RV*/*Sex* AI. This is the control construct. Linearization using *Not* I.

Table 24: pTα-Ires-iCre Targeting construct generation

pHL-CH	Insertion of *Pac* I/*Kpn* I fragment from pHL-CE into *Pac* I/*Spe* I sites of pHL-CE using linker HL30/HL31 (*Kpn* I/*Not* I/*Xba* I).
pHL-CI	Insertion of a *Not* I/*Sal* I fragment from pHL-CG into *Not* I/*Sal* I sites of pDTa.V1. This is the final targeting vector with DTa as negative selection marker. Linearization with *Not* I
pHL-CJ	Insertion of a *Not* I/*Sal* I fragment from pHL-CG into *Not* I/*Xho* I sites of pCAU6. This is the final targeting vector with TK as negative selection marker. Linearization with *Not* I.

16.2.3. Constructs for targeting iCRE into the first exon of pTα

Constructs were designed to target a cDNA encoding an improved version of Cre (iCre) into the first exon of pTα, similar to pHL-AI except that the orientation of the NeoR cassette was inversed. Negative selection was performed using the TK gene (pHL-IE). No additional control construct was required as the PCR screen remained the same as for pHL-AI (see section 16.2.1.).

Table 25: pTα-iCre targeting construct generation

pHL-IA	Insertion of a *Bam* HI/*Sal* I 2.3 kb fragment from pHL-AG into *Bam* HI/*Sal* I of pBSK. Results in the subcloning of SD-intron-SA-hCRE-p(A)n
pHL-IB	1.12 kb *Eco* RI/*Bam* HI fragment of pD-BAC cloned into *Eco* RI/*Bgl* II of pHL-IA. Exchange iCre against hCRE.
pHL-IC	1.4 kb *Not* I/*Bam* HI fragment of pHL-AE.V2 inserted into *Not* I/*Bam* HI of pHL-IB. This inserts the short arm.
pHL-IC.V2	Insertion of 13025 oligonucleotide annealing site inside *Bam* HI using oligonucleotide pair HL89/HL92. Allows the use of PCR screen developed by HJ Fehling for hCD4 targeting into the pTα locus.
pHL-ID	1.3 kb *Xho* I/*Spe* I fragment of FRT-Neo-FRT inserted into *Sal* I/*Spe* I sites of pHL-AI. Results in the Insertion of a flipped NeoR cassette.
pHL-IE	Transfer the 4.9 kb *Not* I/*Sal* I fragment of pHL-IC into pHL-CD digested with *Not* I/*Sal* I. This is the final targeting construct of iCRE into pTα. Vector linearized using *Not* I.

16.2.4. Constructs for targeting iCre into the first exon of pTα in BRUCE4 ES cells

The long arm (LA) of homology in pHL-IE was exchanged to a LA amplified from Bruce4 ES cell DNA by "long-range PCR". The use of isogenic DNA should improve the targeting efficiency in C57BL/6 derived ES cells. Positive and negative selection cassettes were as in pHL-IE.

Table 26: pTα-iCre Targeting construct generation for C57BL/6 ES cells

TOPO(HL115/ HL116)	Long arm was amplified from Bruce4 ES cells using HL115/HL116 and cloned into TOPO vector. Inserted fragment was checked by sequencing.
pHL-IF	Sub-cloning of a 6.3 kb *Asc* I/*Xba* I fragment from TOPO(HL115/HL116) into *Asc* I/*Xba* I sites of pCre-AC. Integration of C57BL/6 was confirmed using multiple restriction digest.
pHL-IG	Sub-cloning of a 7.7 kb *Avr* II/*Not* I fragment from pHL-IE into *Avr* II/*Not* I sites of pHL-IF. Integration of short arm-iCre-FRT-Neo-FRT 6 was confirmed using *Eco* RI restriction digest. This is the final targeting construct of iCRE into pTα. Vector linearized using *Not* I.

16.3. Plasmid DNA preparation for gene targeting

Homologous integration of a targeting vector into the mouse genome requires a linearized double stranded DNA intermediate. To prevent the disruption of any recombinant module at this stage, each targeting vector was linearized with an appropriate restriction enzyme before electroporation. For one electroporation, 40-µg of plasmid DNA [prepared using Qiafilter Midipreparation Kit (Qiagen)] was digested in 400-µL restriction reaction [10x Enzyme buffer, 50-100 U restriction endonuclease, sterile ddH_2O]. After 3 hrs to overnight digestions, a small aliquot of the digest was analysed on a 1% (w/v) agarose gel to verify complete digestion. The linearized plasmid DNA was extracted with an equal volume of PCI (Phenol/Chloroform/Isoamyl Alcohol) to remove protein contaminants. DNA in the aqueous phase was precipitated with Na-acetate and ethanol. Salts were removed by a final wash with 70% (v/v) ethanol and the DNA pellet was briefly air dried in the laminar flow hood. The DNA was finally dissolved in 100-µL of TE and stored at 4°C for at least 8 hours to resuspend the DNA. The linearized DNA was stored at 4°C until needed for electroporation.

16.4. Selection of recombinant ES clones

Twenty-four hours after electroporation of ES cells with the linearized targeting construct (see section 15.3.2), the old medium was removed and positive selection was initiated by adding fresh medium containing G418 at a concentrations of 220 µg/mL for IRES-Neo and other gene trap constructs and 250 µg/mL for TK-Neo-p(A)n-containing constructs, respectively. The next day, ES cells were fed with ES-medium containing G418 and 2 µmol/L Gancyclovir (Cymevene, Roche) in addition when the TK gene was used as negative selection marker. Massive death among G418-treated cells was apparent approximately 3 to 4 days later. After 7-10 days of selection, only cells expressing the neomycin marker gene survived and grew as colonies.

16.5. Picking and growing ES colonies in 96-well plate format

Resistant clones were picked 7-10 days after electroporation. The basic procedure is similar to what Bradley *et al.* described[120]. Briefly, selection medium was exchanged to PBS. Individual colonies were aspirated and separated with an elongated, pulled-out glass pipette and a mouth pipettor. Single clones were transferred into 25 μL of 0.25% Trypsin/EDTA solution. The trypsinization was stopped after 10 min with ES-medium. Cells of each clone were dissociated by pipetting up and down and the cell suspension was plated into one well of a 96-well cluster layered with irradiated feeders. 2 to 3 days later, ES cells which had reached 80% confluency were partly propagated, most of the cells being used for DNA preparation, followed by PCR analysis.

16.6. Single ES cell clone propagation

The goal is to achieve a nice even cell suspension so that the ES cell clones will spread out evenly. 96-wells were washed with PBS and layered with 50-μL of fresh trypsin. After 5-min incubation at 37°C, 96-well clusters were checked for completion of trypsinization. The reaction was stopped by addition of 180-μL fresh medium containing G418. Each well was then vigorously pipetted up and down 5-8 times to generate a single cell suspension. 2-3 drops of cells were plated on 24-well clusters containing fresh ES-medium + G418. Medium was changed daily thereafter until cells were confluent. The rest of cell suspension was kept on ice and pooled with up to 15 other clone cell suspensions for the preparation of genomic DNA. Clones of positive pools identified by PCR screen were further propagated on 6-well clusters, 80% of the cell suspension being saved for further genomic DNA preparation.

16.7. DNA Extraction and screening of targeted clones

Clones were washed in PBS and digested overnight at 37°C in 400-μL for pools, 200-μL for individual clones of PK lysis buffer (see section 9). DNA samples were purified by Phenol/Chloroform extraction followed by an ethanol precipitation. DNA was resuspended in TE at 37°C for 1-hr in a Thermomixer (Eppendorf) before UV quantification of the DNA concentrations. The quality of the DNA preparation was assessed by running a test PCR to amplify a 600 bp fragment using gp120 specific primers HL36 and HL37 (see section 8.1).

PCR conditions for the identification of homologous recombination events were dependent on the respective targeting construct and are summerized in table 25.

Table 27: PCR conditions used for the screening of targeted events

Targeting construct	pHL-AI, AP	pHL-IE, IG	pHL-CI, CJ	pHL-BP, BS, DC, FG, FH, HH
Primer pair	13024/HL14 HL50/HL51	HL13024/HL13025 HL50/HL51	HL8361/HL74	HL15/HL16
Fragment Size (kb)	1.4	1.3	1.6	1.3
PCR System	AmpliTaq	AmpliTaq	AmpliTaq	GC rich kit
$MgCl_2$ final	2 mmol/L	1.5 mmol/L	1.5 mmol/L	2 mmol/L
Amplification Cycles	1) 94°C, 2 min 2) 94°C, 30 sec 3) 65°C, 30 sec 4) 72°C, 2 min x 35 5) 72°C, 10 min	1) 94°C, 2 min 2) 94°C, 30 sec 3) 60°C, 30 sec 4) 72°C, 2 min x 35 5) 72°C, 10 min	1) 94°C, 2 min 2) 94°C, 30 sec 3) 58°C, 30 sec 4) 72°C, 2 min x 35 5) 72°C, 10 min	1) 94°C, 2 min 2) 94°C, 30 sec 3) 60°C, 30 sec 4) 68°C, 2 min 5) 68°C, 10 min x 35

16.8. Characterization of targeted clones by Southern

Each positive clone identified by PCR was verified by Southern blotting with probes external and/or internal to the targeting construct. Genomic DNA was prepared from ES cells propagated twice on gelatinized plates without feeder cells and digested with appropriate restriction enzymes. Sizes of expected fragments are indicated in table 28 (ND: Not determined):

Table 28: Southern strategies used to characerize targeted clones

	Targeting constuct	pHL-AI, AP	pHL-IE, IG	pHL-CI, CJ	pHL-BS	pHL-DC	pHL-FH	pHL-HH
External Probe	Probe	JF26/27	JF26/27	HL85/HL86	HL59/HL60	HL59/HL60	HL59/HL60	HL59/HL60
	Probe Size (bp)	381	381	786	821	821	821	821
	gDNA restriction	*Afl* III	*Afl* III	*Afl* III	*Bam* HI/*Eco* RI	*Bam* HI/*Eco* RI	*Bam* HI/*Eco* RI	*Bam* HI
	WT band (kb)	7.8	7.8	6.4	2.94	2.94	2.94	5.82
	KI band (kb)	4.8	4.6	6.7	5.82	5.82	5.82	5.15
	KIΔNeo band (kb)	ND	ND	ND	5.82	5.82	5.82	3.13
Internal Probe	Probe	iCre	iCre		DsRed2	Neo	Neo	
	Probe Size (bp)	1095	1095		732	526	526	
	gDNA restriction	*Hind* III	*Hind* III		*Hind* III	*Hind* III	*Eco* RI	
	KI band (kb)	5.4	5.4		3.96	2.94	4.1	
	KIΔNeo band (kb)	4.3	4.3		1.85	-	-	

(ND: Not determined, bp: base pair, kb: kilobase)

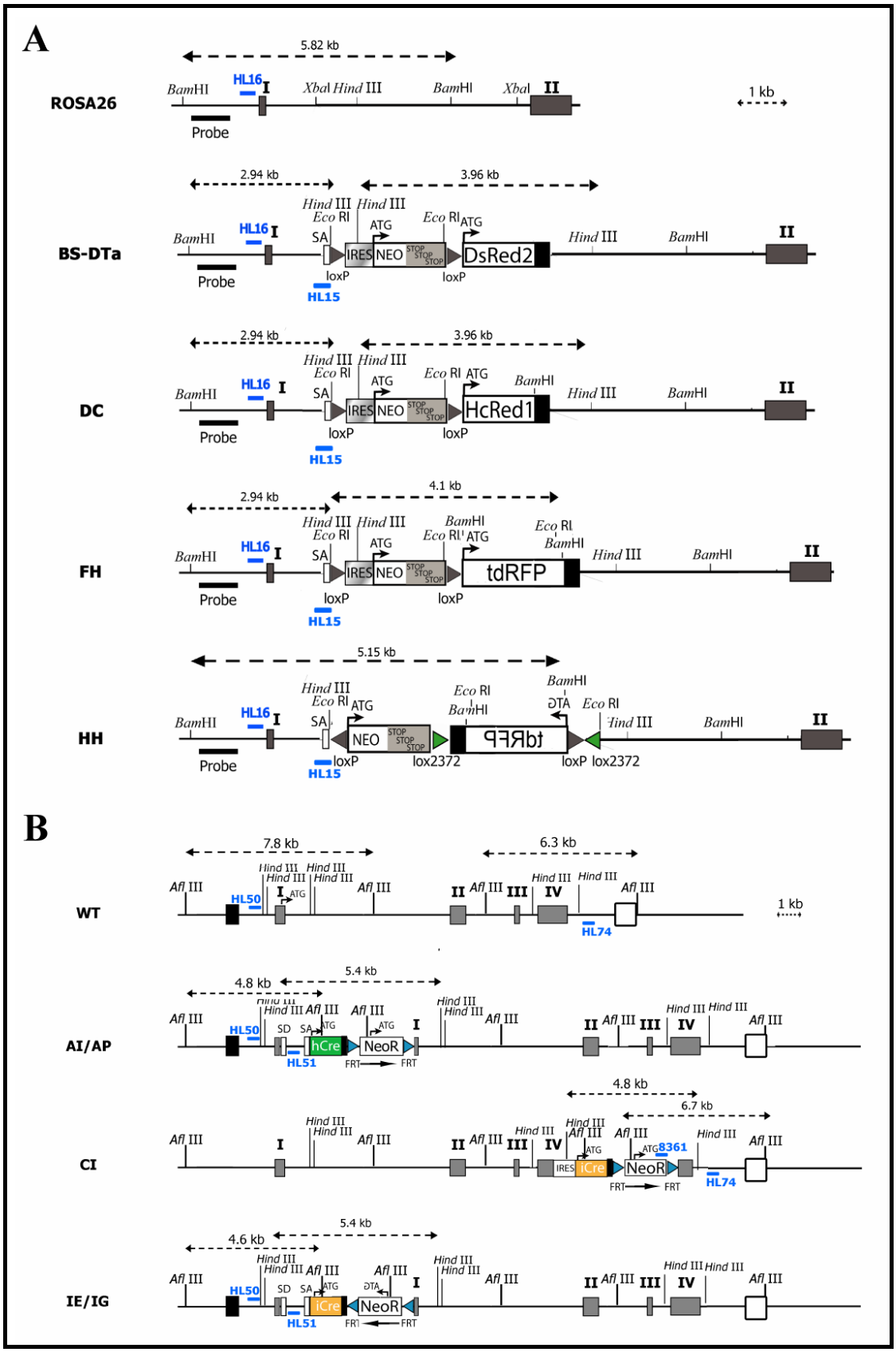

Figure 12: Detection of different recombinant KI alleles by Southern blotting at the *rosa26* (**A**) and the *ptcra* (**B**) locus. Exons are numbered using roman numerals. Size of relevant fragments are delineated using arrows. Oligonucleotides used for PCR screen are depicted in blue. Targeting constructs used for each gene targeting experiment are indicated with respective initials.

16.9. *In vitro* deletion of the NeoR cassette in targeted clones

In order to test the Cre-inducibility of our fluorescent reporters in ROSA26 knock-in ES clones or to prevent any unwanted effects of the NeoR cassette on the expression of neighboring genes[121-123] (such as in pTα-iCre knock-in ES cells), targeted clones were transiently transfected with pCre-AC or pCAGGS-FlpE-V1 for deletion of loxP or FRT-flanked sequences, respectively. These expression plasmids are bi-cistronic vectors in which a codon –improved site specific recombinase (iCre or FlpE respectively) are fused to an IRES-EGFP. At the peak of gene expression in transient transfection (18 hours after electroporation at 37°C), EGFP fluorescence should report iCre or FlpE expression.

Targeted ES cell clones were expanded to get enough material for 3 electroporations [usually 4 sub-confluent 10-cm dishes per electroporation]. Cells were trypsinized (see section 15.3.1), washed with ES-Media, and plated on 4 10-cm dishes (not gelatinized) to deplete MEFs. After 30 min incubation at 37°C, plates were observed under a phase contrast microscope to monitor feeder cell attachment. Unattached cells were then carefully collected, centrifuged at 1200 rpm for 5 min at 4°C (Heraus, Rotor #2250) and resuspended in 10-mL PBS for cell counting. $2x10^7$ ES cells were electroporated (see section 15.3.2) with 40-µg of circular plasmid, either pEGFP.C1 as control [CMV promoter fused to EGFP], pCre-AC, or pCAGGS-FlpE-V1. The day after electroporation, ES cells were trypsinized and resuspended in 1-mL sterile PBS/5% (v/v) FCS. Alternatively, the cells were stained with anti-mouse CD31-APC antibody (1/400) to discriminate $CD31^+$ ES cells from $CD31^-$ MEF cells. After 20 min incubation at 4°C, cells were washed with 9-mL of PBS PBS/5% (v/v) FCS and resuspended in 500-uL of ES-media containing 25 µg/mL DNAse I to digest DNA/cell clumps before the cell sort. Stained cells were filtered by gravity through a sterile sorter mesh to remove large cell aggregates. Cells electroporated with EGFP.C1 were used to setup the gates. At least 2000 ES cells expressing iCre or FlpE were sorted on a FACS sorter (see section 18.2) as GFP^+ in 5-mL Falcon tubes containing 3-mL of ES-media. No more than 1000 sorted cells were distributed onto one 10-cm dish layered with irradiated MEF, assuming a maximal plating efficiency of 30%. 6 to 7 days later,

50-100 individual colonies were picked and transferred onto 96-well clusters. After two days, clones were propagated (see section 16.6) on 2x 24-well clusters with 1/3 of the cell suspension being plated in ES-medium and the remaining 2/3 in ES medium + G418 (250 µg/mL). 3-4 days later, the number of dying clones in the presence of G418 was scored and their corresponding replicates were further propagated in ES-medium onto 6-well clusters. Deletion of the NeoR gene was then confirmed by Southern blotting (see section 16.8) or by flow cytometry for ROSA26 knock-in clones (see section 18.2).

16.10. Recombination Meditated Cassette Exchange (RMCE) in ROSA26-RFP ES cells

To exchange the tdRFP cassette to EGFP at the ROSA26 locus, ROSA26-**RFP** ES cells (after *in vitro* deletion of the neomycine/stopper cassette) were electroporated with 20-µg of both pCre-AC and pX2GFP[66, 115]. The next day, iCre-expressing cells ($EGFP^+$) were sorted on a FACS cell sorter (18.2) and deposited as single cell per well on a 96–well cluster layered with irradiated MEFs. 5 days later, colonies were observed on a fluorescence inverted microscope and scored for EGFP expression and loss of tdRFP. 2 $EGFP^+$ exchanged clones (1 in 75) were passaged further to allow for the charaterization of the recombination event.

16.11. Generation of mouse mutants from targeted ES cells

All ES cell lines used for gene targeting had been tested for their ability to colonize the germline. To this end, individual ES cells of the respective lines had been injected into host blastocysts which were implanted into pseudo-pregnant foster mothers using standard procedures[59].

16.11.1. ES cell preparation for injection into blastocysts

ES cell clones, in which the targeted gene locus had been extensively characterized, were thawed 2 days before microinjection on irradiated MEF monolayer and grown in ES-medium without antibiotics or selective agents, like G418. At the day of microinjection, these plates were carefully trypsinized (15.3.1) for approximately 6 to 10 min at RT to generate a single cell suspension. [A too short trypsinization would result in clumpy ES cells; a too long in sticky ES cells]. When trypsinization reactionwas complete, almost all ES cells within each colony

looked round. Trypsinized ES cell colonies were then resuspended, washed and plated onto a fresh gelatinized 10-cm dish for 30 min at 37°C to deplete MEF cells. The supernatant containing optimally dissociated ES cells was gently collected, transferred to a 15-mL tube on ice and delivered to the injection facility.

16.11.2. ES cell injection into blastocysts

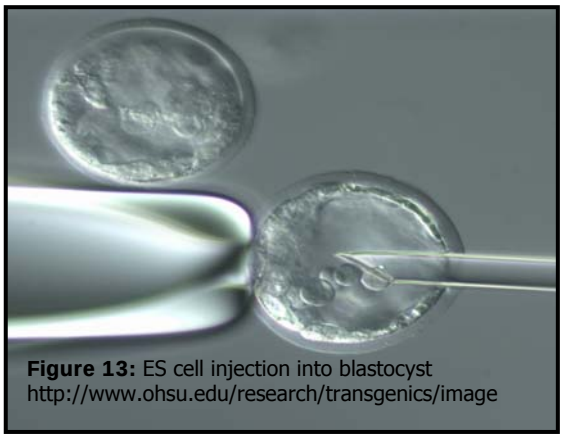

Figure 13: ES cell injection into blastocyst
http://www.ohsu.edu/research/transgenics/image

In order to allow easy estimation of the percentage of chimerism (i.e., contribution of the ES cell genome to the chimeric offspring), ES cell lines from mouse strains with colored coats (C57BL/6N) were injected in BALB/c blastocysts whereas ES cell lines from mice with cream-colored furs (129/SvEv, 129/OlaHsd) were chimerized with black C57BL/6 blastocysts.

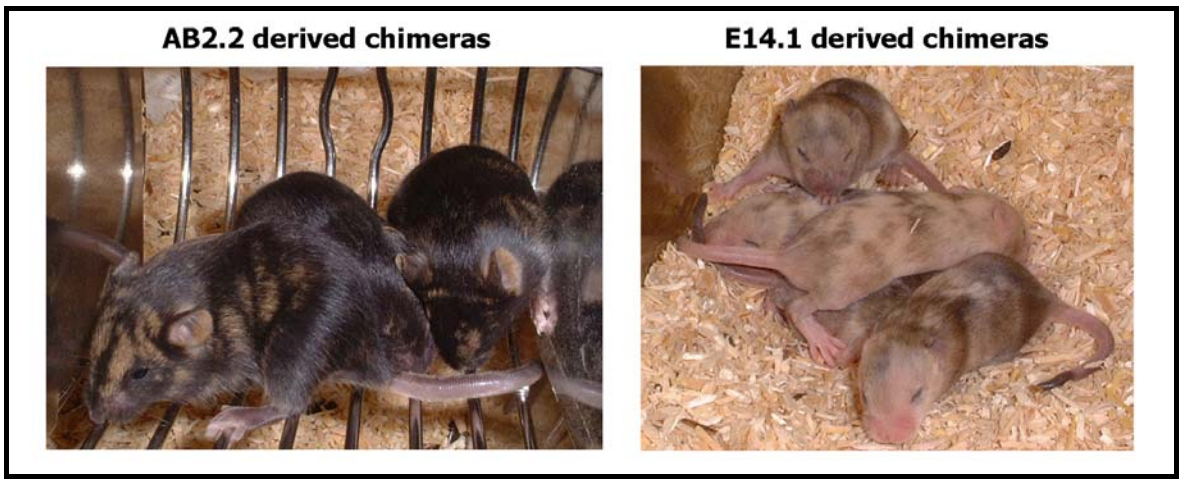

Figure 14: Coat color chimerism of mice generated upon injection of two 129-derived ES cell lines: AB2.2 (129S7/SvEvBrd-Hprt1) and E14.1 (129P2/OlaHsd) in C57BL/6 blastocysts.

Blastocyst injection was carried out using day-3.5 blastocysts collected from the uteri of female mice by flushing with M2 medium (Gibco). The collected blastocysts were washed with and cultivated in M16 medium (Gibco) under 5% CO_2 at 37°C. After injection of 10-15 genetically modified ES cells, 7-8 blastocysts were re-implanted into each horn of the uterus of 2.5-day pseudo-pregnant (C57BL/6xDBA) F1 foster mothers, previously mated to vasectomized males. The percentage of chimerism of the offspring was visually estimated from the extent of the coat color contributed by the ES genome.

16.11.3. Screening for germ line transmission of KI alleles

Germ line transmission of the ES cell genome was tested by crossing high-percentage male chimeras with female C57BL/6 mice, to establish the ES-cell-line-derived coat color in F1 offspring. As chimeric males derived from pTα-iCre KI ES cells did not give rise to germ line offspring, female chimeric mice were further crossed with C57BL/6 males. Coat color positive offspring was screened for transmission of the targeted allele by PCR, using genomic DNA from tail biopsies (see 17.2). PCR-positive samples were confirmed by Southern blotting.

17. ANIMAL PROCEDURES

17.1. Animal maintenance

Mice were handled in accordance with German and European directives. All mouse lines were kept under specific pathogen-free conditions in individually-ventilated cages (IVC) and were routinely screened for common mouse pathogens. At the age of 3-4 weeks, mice were weaned and genders were separated. At the same time, they were ear marked, and a 3-mm tail biopsy was cut off to prepare a sample of genomic DNA for PCR genotyping.

17.2. Mouse genotyping

All mice were genotyped by PCR.

17.2.1. Genomic DNA preparation from tail biopsies

Tail biopsies were digested with 350-μL PK lysis buffer for an hour at 56°C and strong shaking (1300 rpm) in a thermomixer (Eppendorf). After a short centrifugation at maximal speed (14000 rpm) in a Eppendorf centrifuge 5417R to clear the suspension from residual hair and tissue, tail DNA was precipitated with 300-μL isopropanol. DNA precipitates were fished out with a sterile pipetman tip and resuspended in 250-μL TE buffer. 2-μL of this preparation was used per 25-μL PCR reaction.

17.2.2. PCR genotyping of ROSA26-RFP mice

Heterozygosity and homozygosity for the ROSA26-**RFP** KI was determined by PCR on tail genomic DNA using one forward primer in ROSA26 intron (HL152) and two reverse primers, HL15 in the splice acceptor of the KI cassette and HL54 located 3' of the knock-in integration site (Fig. 24A). This multiplex PCR can yield two different PCR products depending on the genotype of the mouse being analyzed: a 301-bp band indicative of the KI allele and a 201-bp fragment for the ROSA26 WT allele (Fig. 15A).

17.2.3. PCR genotyping of pTα-iCre mice

The genotype of mice at the pTα locus was determined by multiplex PCR using a set of 3 primers: HL120 annealing 5' of pTα first exon, oligo 13758 annealing 3' of the pTα first exon and oligo 13025 annealing 3' of the rabbit β-globin splice donor. Presence of a WT and KI allele was detected after amplification of a 350-bp and a 288-bp fragment, respectively (Fig. 15B).

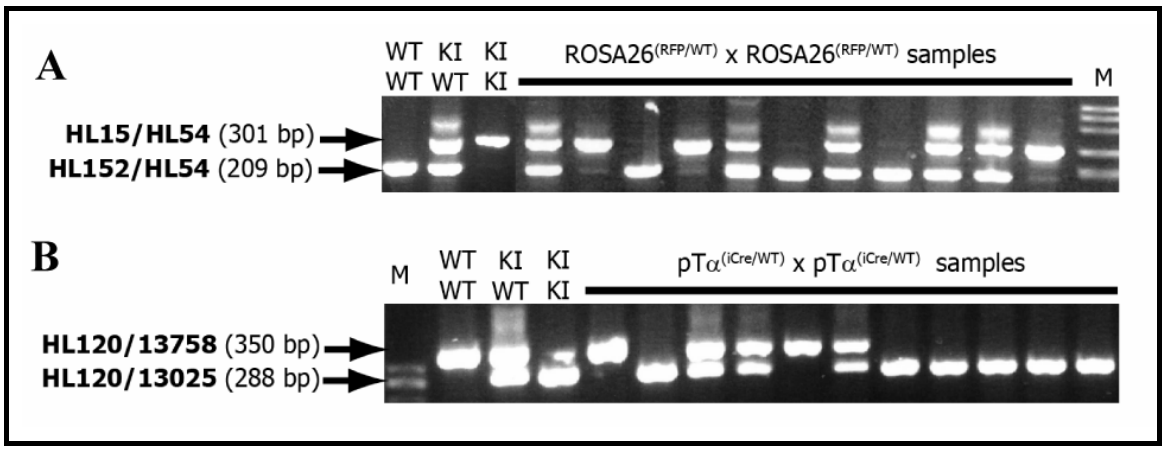

Figure 15: PCR genotyping of ROSA26-RFP (**A**) and pTα-iCre (**B**) mice. WT: wild type, KI: knock-in, M: Molecular weight marker.

17.2.4. PCR genotyping of other mouse lines:

To identify mice bearing CMV-Cre and Lck-Cre transgenes, primers VM57 and VM58 specific for unmodified, wildtype Cre were used to amplify a diagnostic 500-bp fragment. $EGFP^+$ and $EYFP^+$ mice were identified using a pair of internal primers (292 and 293) yielding a band of 300-bp after PCR amplification. Heterozygosity and homozygosity of the nude point mutation at the FoxN1 locus was investigated exploiting an amplified fragment length polymorphism (AFLP) between wildtype and mutant alleles that can be visualized by PCR-amplification of

genomic DNA with primer pair HL158/HL159 and subsequent *Eco*47III digestion of the PCR product as described by Hirasawa *et al.*[124].

18. IMMUNOLOGICAL METHODS

18.1. Hematopoietic cell isolation from mouse tissues

A suspension of single cells was obtained from thymus, lymph nodes (mesenteric, axillary and inguinal lymph nodes) and Peyer's Patches by forcing the organs through a mesh screen with holes of 70-μm in diameter in PBS/5% (v/v) FCS. Splenocytes were obtained by mechanical dissociation of the organ between two glass slides in PBS containing 5% (v/v) FCS. To collect bone marrow (BM) cells, the central cavity of two femur and tibia bones were flushed with 2-mL PBS/5% (v/v) FCS per bone.

18.1.1. Enrichment of PBL leukocytes by fractionation on a Ficoll gradient

Peripheral blood samples (5-10 drops) were collected in micro-tubes supplemented with 20 mmol/L EDTA (Sarstedt, #41-1504-005). Using a long Pasteur pipette, blood samples were underlayed with 500-µL of Ficoll-Paque (Pharmacia, d=1.077). After 15 min of centrifugation at 1500 rpm at RT in an Eppendorf centrifuge 5417R, cells were collected at the Ficoll/PBS interphase and washed with 10-mL PBS/5% (v/v) FCS. Cells were then resuspended in 100-µL PBS/ 5 %(v/v) FSC.

18.1.2. Erythrocyte lysis

Total splenocytes and bone marrow cells were centrifuged for 3 min at 2500 rpm, 4°C, soft acceleration in an Eppendorf centrifuge 5417R and resuspended in 350 μL erythrocyte lysis buffer. After 5 min incubation at RT, the lysis reaction was stopped by adding 1.7-mL of cold PBS/5% (v/v) FCS, followed by two further washes of the cells to remove all traces of lysis buffer. Viability of the cell suspension was determined by trypan blue exclusion staining.

18.1.3. Bead depletion of mature cell lineages from the bone marrow

To block Fc receptors, BM cells were incubated for 15 min at 4°C in 300-uL PBS/FCS with antibody 2.4G2 directed against CD16 and CD32. Total BM cells were then stained for 30 min at 4°C in 200-uL PBS-FCS containing the following mix of FITC-conjugated rat-anti mouse antibodies: CD3 (#17A2) CD11b, CD19, CD161, CD97, Ter119. Cells were washed once with 1-mL PBS-FCS to remove unbound antibodies and mixed with anti-rat magnetic beads (Dynal) at a ratio of 3 beads per cell in the suspension. After 30-min incubation at 4°C on a rotating wheel, beads were cleared from samples with a magnet and the supernatant was collected for further staining.

18.1.4. Enrichment of immature thymocytes *via* complement kill

Thymocyte suspensions prepared at a density of $20x10^6$ cells/mL in DMEM medium without FCS were incubated for 10 min at 37°C with a hybridoma supernatant containing rat immunoglobulin M directed against mouse CD8 (#3.168.8.1), followed by the addition of a 1:10 dilution of Low-Tox rabbit complement (Cedarlane Laboratories). After 30 min incubation at 37°C with frequent gentle mixing, viable DN cells were recovered after centrifugation at 20°C over Ficoll-Paque (Pharmacia, d=1.077).

18.1.5. Dendritic epidermal T cell (DETC) preparation

Mouse ears were split into 2 halves using forceps and further cut into small pieces (1-cm^2). The biopsies were then digested with 1-mL protease mix for 15 min at 37°C, low shaking (800 rpm) in thermomixer (Eppendorf). Cell floating in the supernatant were collected in a 15-mL Falcon tube and kept on ice. The rest of the tissue was further digested with 1-mL of fresh protease mix for 15 min at 37°C. Harvested cells were pooled in the 15-mL Falcon tube. Cell extracts were supplemented with 10 µL of EDTA (0,5 mol/L) to avoid cell aggregation, incubated 5 min at 4°C and filtered through polypropylene Filters (105 µm) to remove debris of tissues. Cells were washed with 9-mL PBS/5% (v/v) FCS, spun and resuspended in 250-µL PBS/5% (v/v) FCS for immunostaining.

18.2. Immunostaining, Flow Cytometry and Cell Sorting

Before staining, cells were routinely incubated for 15 min on ice with purified monoclonal antibody 2.4G2 to block Fc receptors. All stainings were performed using 10^6 cells in 50 μL PBS/5% FCS for 30 min on ice with light protection. Single-cell suspensions were stained with anti-mouse antibodies conjugated to fluorescein (FITC), phycoerythrin-Cy5.5 (PE-Cy5.5), phycoerythrin-Cy7 (PE-Cy7), allophycocyanin (APC), allophycocyanin-Cy7 (APC-Cy7) or biotin (see Materials, section 12). Biotinylated antibodies were detected using streptavidin conjugated to different second step reagents (see Materials, section 12). Samples were depleted of mature cell lineages by incubation with a "coktail" of biotinylated or FITC-labeled antibodies to mature murine blood cells: CD3, CD4, CD8, CD11b, CD11c, CD19, CD97, CD161, Ter119 (see Materials, section 12). Stained cells were filtered by gravity through a sterile sorter mesh to remove large cell aggregates. To exclude dead cells from the analysis, in some experiments samples were stained for 5 min at RT with a 1/20000 dilution of SYTOX Blue stock solution (Molecular Probes, #S34857), a vital fluorescent dye emitting in the UV range (Excitation: 444 nm, Emission: 480 nm). For 4-color stainings, samples were analysed on a FACS Calibur cytometer (Becton Dickinson) equipped with a band pass filter (HQ780/60, i.e., 780 ± 30 nm; AF Analysentechnik, Tübingen, Germany) in the FL-3 channel to allow simultaneous detection of PE-Cy5.5/PE-Cy7 and tdRFP. When more than 4 colours were needed, cells were acquired on a BD Aria cell sorter. FACS assisted cell sorting was performed in the flow cytometry facility of the institute using a FACS-Star or a FACS ARIA cell sorter (Becton Dickinson).

18.3. 5-fluorouracyl (5-FU) injection in mouse

For *in vivo* depletion of proliferating BM cells, 400-µL of 5-FU (10 mg/mL) or PBS as control were injected intraperitoneally. 4 days later, tibia and femurs of the injected mice were collected, BM cells harvested (18.1) and analyzed on a FACS Calibur to determine the level of red fluorescence in resting cells.

18.4. Immuno-histochemistry (IHC)

Organs were dissected and fixed by immersion in 25 mL PBS/ 4% (w/v) paraformaldehyde, pH 7.4 for 2-hrs at room temperature on a rotary wheel. Spleens were cut in half for better penetration of the fixative agent. Tissues were extensively washed in PBS to remove excess of paraformaldehyde by four successive changes of washing solution and a final overnight step on a rotary wheel at room temperature. Fixed tissues were dried briefly with tissue paper and frozen directly in Tissue-Tec OCT (Fisher; Pittsburgh, PA) above dry ice. Frozen tissue blocks were brought to –20°C, and 5-μm sections were cut using a cryostat. Sections were transferred onto pre-cleaned glass slides (Superfrost/Plus, Fisher Scientific), which were dried at room temperature for 30 min, and then either probed with antibodies or stored at –70°C. For antibody staining, slides were placed in PBS/1% (v/v) BSA for 5 min to remove the OCT. All slides were blocked with anti-CD16/CD32 (2.4G2) antibodies in PBS/1% (v/v) BSA for 15 min in a humidified chamber. Slides were washed once for 5 min in PBS/1% (v/v) BSA before being probed with the antibodies anti-CD45R-APC (RA3–6B2) and/or anti-CD3-FITC (17A2) for 1 h in a humidified chamber. Cryo-sections were then washed three times for 5 min in PBS/1% BSA, mounted in Fluoromount (Southern Biotech) and dried for 30 min at room temperature. Images were taken on a Zeiss Axioskop with the ORCA ER camera (Hamamatsu) and processed using Openlab software (Improvision).

19. IMAGING PROCEDURES

19.1. Fluorescence Stereomicroscopy

Before and after *in vitro* deletion of the NeoR-transcritpional stopper, fluorescence of multiple ROSA26 targeted clones was assayed on a fluorescence inverted microscope (Axiovert 25, Zeiss) equipped with optimal filters for the detection of EGFP (Band Pass for Excitation [BP Ex]: 470 ± 20 nm, Band Pass for Emission [BP Em]: 525 ± 25 nm) and DsRed (BP Ex: 465 ± 20 nm, BP Em: 620 ± 30 nm). Unless otherwise stated, pictures were exposed for 34-ms (bright field) or 1 to 3-s (epifluorescence), captured with a ORCA ER camera (Hamamatsu) and processed using Openlab software (Improvision)

19.2. Fluorescence Stereoscopy

Fluorescent imaging of newborn (2-day-old) animals was performed with a fluorescence stereoscope (Leica MZ16FA) equipped with an external light source and appropriate filter sets (excitation: 545 c 15-nm band pass filter; emission: 620 ± 30-nm band pass filter, Leica, Heerbrugg, Switzerland). Pictures were exposed for 34-ms (bright field) or 1 to 3-s (epifluorescence), captured with a ORCA ER camera (Hamamatsu) and processed using Openlab software (Improvision). For direct comparison of the level of red fluorescence in ROSA26-**RFP** and C57BL/6 animals (Fig. 3B), organs from 5- to 6-week-old mice were dissected and stored at 4°C in PBS/5% (v/v) FCS. Organs of the control mouse were placed side by side to their ROSA26-**RFP** counterparts and simultaneously observed. Except for the pancreas (300 ms) exhibiting very strong red fluorescence in ROSA26-**RFP** animal, all pictures were exposed for 34-ms (bright field) or 1-s (epifluorescence) on a Leica DFC480 digital camera. Details of lymphoid organs from a pTα-iCre x ROSA26-**RFP** mouse and a C57BL/6 control were observed using the same live imaging system at a higher magnification and an optimized exposure time depending on the level of fluorescence emitted: thymi (1x, 1-s), detail of spleens (3.4x, 3 s), kidney (2x, 300-ms), Peyer's patches (4.2x, 3-s), and inguinal (3.2x, 3-s) and mesenteric (2.5x, 400-ms) lymph nodes.

19.3. Whole body fluorescence imaging

ROSA26-**RFP**, ROSA26-**RFP** and pTα-iCre x ROSA26-**RFP** mice were euthanized by cervical dislocation and placed in a dark box system for imaging of fluorescence macroscopy (Hamamatsu, AEQUORIA^{TM}). Whole body fluorescence pictures were taken at optimal exposure time (3-s) and fluorescence intensity was normalized to the ROSA26-**RFP** control mouse.

19.4. Confocal Microscopy

For confocal microscopy, stained histological sections previously used in immuno-histochemistry were observed on a LSM 510 (Zeiss). Images were processed using LSM Images Browser Software (Zeiss).

RESULTS

20. GENERATION OF A REPORTER MICE WITH CRE INDUCIBLE RFP EXPRESSION

20.1. DsRed2 "knock-in" in the ROSA26 locus

20.1.1. Strategy for Cre-inducible DsRed2 reporter expression

At the time the project was initiated, only two RFP variants were available from Clontech: DsRed1 and DsRed2, from the reef coral *Discosoma sp*. In order to engineer Cre-inducible reporter cassette, DsRed1 and 2 targeting vectors were engineered following the strategy which has already been applied succesfully to EGFP, EYFP and ECFP reporters[71, 85]. Briefly, the RFP cDNA was fused to a SV40 poly-A signal (p(A)n) and cloned behind a neomycine resistance (NeoR) gene terminated by three successive p(A)n from the bovine growth hormone (BGH). This "stopper" module has been shown to promote an efficient termination of the transcription after the NeoR casette[125]. The NeoR-stopper was flanked by loxP sites in the same orientation (or "floxed") for Cre-inducible removal. The resulting expression cassette was fused to an adenoviral splice acceptor to trap the endogenous ROSA26 transcripts as described by Soriano *et al.*[81]. Two sets of targeting constructs were generated with either a NeoR cassette driven by the Thymidine kinase (TK) promoter (pHL-BP) or an IRES-NeoR cassette (pHL-BS) to positively select recombinant clones. In order to screen for targeted insertion events, a similar plasmid (pHL-BO) with an extended 5' sequence of homology (control arm) was generated by PCR amplification from E14.1 genomic DNA, cloned in place of the short arm of homology and electroporated in E14.1 ES cells after linearisation. 10 neomycin resistant clones were picked, expanded and genomic DNA (gDNA) was prepared to set up the screening PCR. Using a forward primer (HL16) outside of the targeting construct and a reverse primer (HL15) in the splice acceptor of the expression cassette (Fig. 17A), a 1.3 kb recombinant PCR product was amplified. In order to optimize the PCR conditions, gDNA of the clone yielding the weakest signal, as revealed by fluorescence intensity of the amplicon upon ethidium bromide staining[116], was serialy diluted in 1 µg/mL E14.1 gDNA as illustrated in figure 16.

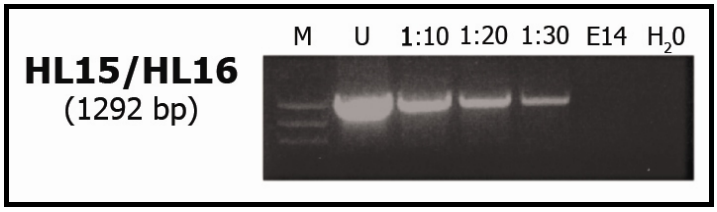

Figure 16: PCR screen for ROSA26 targeted clones (M: Marker, U: undiluted control genomic DNA of ES cells electroporated with pHL-BO control construct, 1:10 to 1:30: serial dilutions of control DNA in 1 µg/µL E14.1 gDNA).

pHL-BP and BS-DTa were linearised using *Sac* II restriction digest and electroporated into E14.1 ES cells. After 9 days of selection using 250 µg/mL G418, the number of recombinant colonies were scored. As expected, pHL-BP-DTa targeting construct yielded more colonies (n=104 in 1 electroporation) than pHL-BS-DTa (n=4 in 3 electroporations). Small number of colonies were obtained using pHL-BS-DTa construct in contrast to previously reported gene trapping of the ROSA26 locus (n=23 for one electroporation[81]). BS-DTa clones showed a severe growth retardation in comparison to their BP-DTa counterparts, supporting the idea that NeoR expression from a bi-cistronic transcript is really weak in recombinant ES clones. Attal *et al*[126] reported that IRES-dependent translation is generally less efficient than cap-dependent translation. 96 BP-DTa clones were picked, and finally screened by PCR as pool of 16 clones. BS-DTa clones were picked and screened as individual clones (Fig. 17B). Only BS-DTa#1 clone yielded a PCR fragment of expected size (1.29 kb). This clone is further referred to as E14-BS. To characterize the targeting event in E14-BS clones, the integrity of the ROSA26 locus was analysed by Southern blotting using a probe external to the targeting construct (Fig. 17A and C). E14-BS clone showed an additional band of expected size as compared to the parental E14.1 ES cell (Fig. 17C, right panel).

20.1.2. *In vitro* Cre-excision of the floxed stopper sequence

To test whether the Cre recombinase could activate the expression of DsRed2 at the ROSA26 locus, E14-BS#1 clone was transiently transfected with pCre-AC; Cre expressing cells were sorted (Fig. 18A) and grown for 6 days. Sub-clones were picked and tested for their sensitivity to 250 µg/mL G418. 5 neomycin-sensitive (NeoS) clones were expanded and gDNA was prepared. All NeoS clones retained the KI allele as detected by PCR (data not shown). Correct deletion of the IRES-NeoR-Stopper cassette was investigated in E14-BSdNeo#1 by Southern hybridization using NeoR as a probe. As expected, no signal was

detected in E14.1 cells (Fig. 17C, Lane 1). A 2.3 kb band observed in E14-BS#1 (Fig. 17C, Lane 2) corresponding to the floxed NeoR-stopper cassette was lost in E14-BSdNeo clone (Fig. 17C, Lane 3), confirming the Cre-mediated excision of NeoR cassette. An additional band of larger size (over 6 kb) was detected in E14-BS#1 as well as in E14-BSdNeo#1 (Fig. 17C, Lane 2 and 3), suggesting an additional off target integration site of the IRES-NeoR cassette. The absence of size variation for this additional fragment could be explained by the loss of one loxP site flanking the IRES-NeoR-stopper cassette after random integration. Southern blotting analysis using DsRed2 as a probe (Fig. 17C, left panel) further confirmed this hypothesis. Only one fragment of 3.96kb was detected in E14-BS (Fig. 17C, lane 2) which uniformely decreased in size after NeoR deletion (Fig. 17C, lane 3).

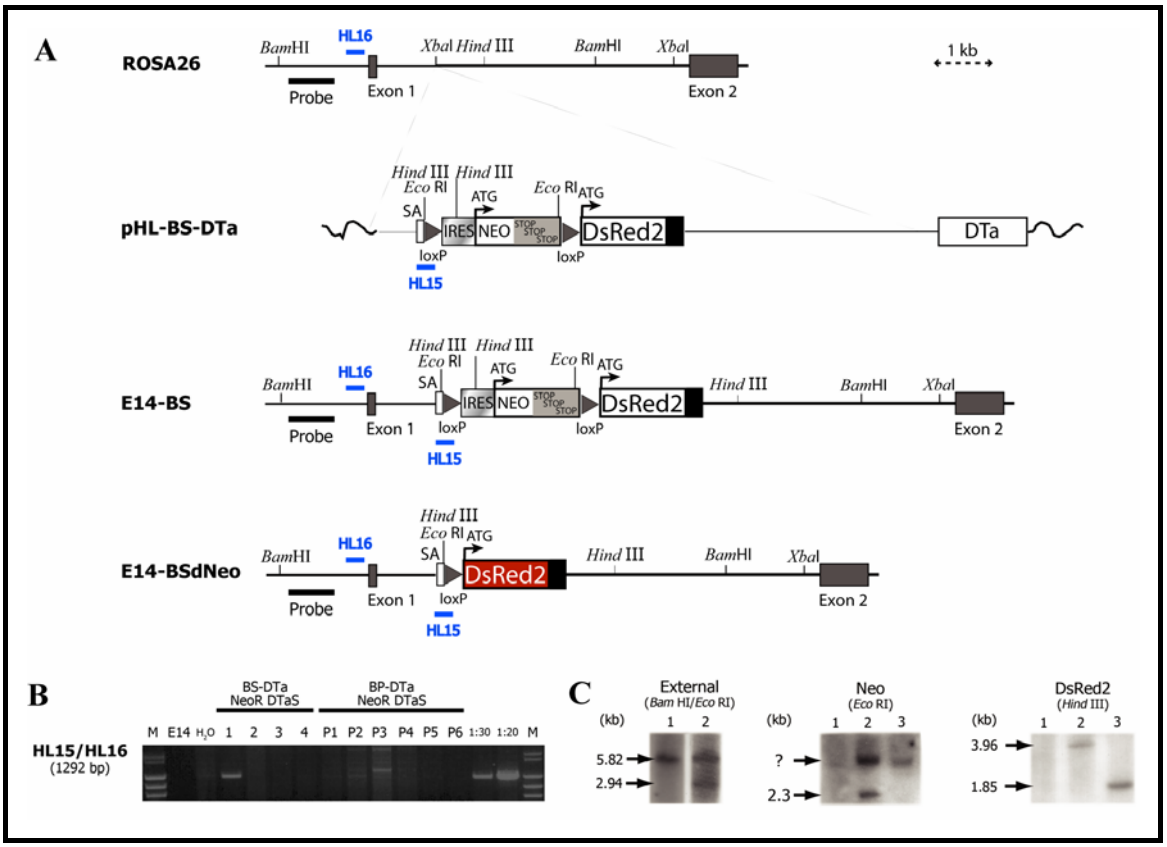

Figure 17: Targeting of DsRed2 into the ROSA26 locus. **A.** Schematic representation of DsRed2 targeted alleles. Oligonucleotide binding sites used in PCR screen as well as restriction sites of relevant enzymes used for the characterization of targeted events are given. **B**. Screen of targeted clone by PCR (M: Marker, 1 to 4: individual clones, P1 to P6: pools of clones, 1:20 to 1:30: dilutions of control DNA). **C.** Southern blot analysis using one probe external to the targeting construct and two internal probes, Neo and DsRed2. Restriction digest for each Southern hybridization are given. Size of resulting specific fragments are indicated with arrowheads. 1: E14 WT, 2: E14-BS, 3: E14-BSΔNeo, ?: unexpected additional fragment.

The selection for an additional intregration site exclusively for the IRES-NeoR cassette is another strong indication that a single IRES-NeoR integration is insufficient to provide G418 resistance for appropriate positive selection in this experiment.

20.1.3. Activation of DsRed2 expression, lack of fluorescence emission

As documented in figure 18A, DsRed2 was not expressed in sorted EGFP^{+} E14-BS#1 cells 18 hrs after transient transfection with pCre-AC. Fluorescent aggregates could be specifically detected in constitutively activated ROSA26-DsRed2 colonies (E14-BSΔNeo#1) in contrast to WT ES cells (Fig. 18B). One possible explanation for the abence of apparent red fluorescence in E14-BSΔNeo#1 by FACS (data not shown) could be the lack of recombinant transcript expression. To adress this question, RNA from E14.1, Cre-activated ROSA26-DsRed2 and ROSA26-**EGFP**[71] was extracted and analyzed by semi-quantitative RT-PCR (Fig. 18C). Recombinant cDNA was not detected in E14.1 ES cells but was specifically amplified in ROSA26-DsRed2 as well as ROSA26-**EGFP** cells. The unspliced form of the recombinant transcript could not be amplified from any of the samples analyzed even when 3 min of extension were used (Fig. 18C) indicating that splicing of ROSA26 transcripts to the adenoviral splice acceptor was correctly processed by the spliceosome.

Semi-quantitative RT-PCR analysis showed that the DsRed2 recombinant transcript was 10-times less expressed than EGFP from Cre-activated ROSA26 locus (Fig. 18C). This relative under-representation might be due to the presence of an endogenous start codon[80] in a weak Kozak concensus context[80, 127] in the first exon of ROSA26 transcripts. The endogenous ATG is maitained in the recombinant transcript (Fig. 18D) and can initiate the translation of a short peptide (n=15). This 5' upstream ORF (uORF) can have a strong incidence on the expression of genes inserted in the ROSA26 locus at the translational level. Empirical evidence shows that uORFs usually diminish translation of the main ORF by reducing the number of ribosomes reaching and initiating at the main AUG start codons[16]. A minority of ribosomes reaches the main initiation codon either by leaky scanning or by translation reinitiation mechanism[128]. After translation

termination, ribosomes can start translation at a second Kozak ATG when found in the vincinity of the stop codon. Translation reinitiation has been shown to be one important way to regulate the level of protein expression[129] as it is overall 50 to 70% less efficient than cap-dependent translation intiation. Efficiency of reinitiation is partly depending on the length of the intercistronic sequence[127]: a short (<50 nucleotides) or too long (>130 nucleotides) intercistronic sequence strongly decreased the amount of expressed protein from the second ORF[127, 130]. The loxP site 5' of DsRed2 was introduced in the pHL-BS-DTa targeting vector using a 121 bp *Xho* I/*Sal* I fragment from pL2Neo plasmid.

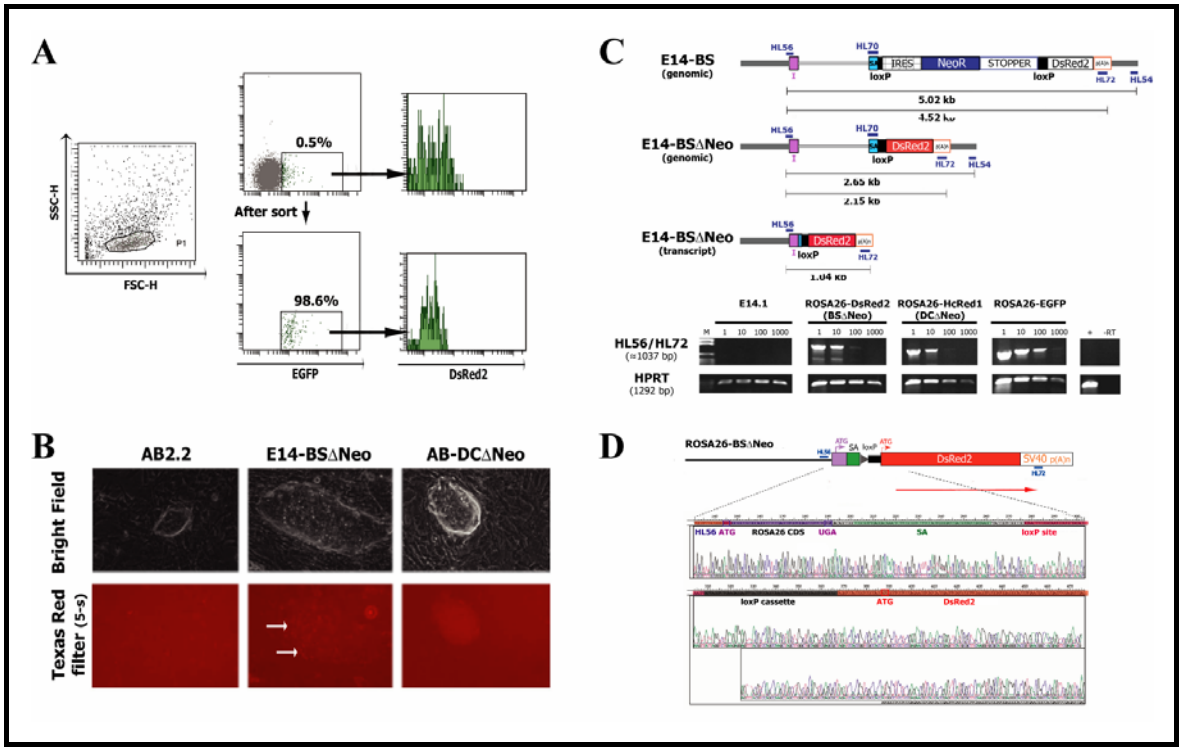

Figure 18: Analysis of E14-BS ES cells after Cre-mediated removal of IRES-NeoR. **A.** FACS analysis of E14-BS ES cells electroporated with pCRE-AC before and after sort of Cre-expressing EGFP$^+$ cells. **B.** Red fluorescence emission in ROSA26 targeted ES cells after NeoR excision. DsRed2 expression (E14-BSΔNeo) was specifically detected in small aggregates (pointing arrows) whereas HcRed1 fluorescence was homogeneous within AB-DCΔNeo colony as compared to wild-type AB2.2 control. **C.** Schematic representation of DsRed2 recombinant transcripts (1. E14-BS, 2: E14-BSΔNeo without intron splicing, 3: E14-BSΔNeo after correct splicing) and expression analysis by RT-PCR. **D.** DNA sequence of recombinant ROSA26-DsRed2 transcript. Start (ATG) and stop (UGA) codons are indicated. CDS: Coding sequence, SA: splice acceptor cassette. Oreintation of DsRed2 CDS is shown by an arrow.

After Cre-mediated recombination of the ROSA26 locus in E14-BS, it resulted in the addition of 58 nucleotides 3' of the 34-bp loxP site in ROSA26-DsRed2 recombinant transcript (Fig. 18D). This additional sequence absent in ROSA26-**EGFP**[71] might negatively effect ROSA26-DsRed2 transcript stability by lowering the efficiency of translation reinitiation. Less protected by polysomes, ROSA26-DsRed2 transcript might then be more accessible for RNA

degradation. Whether other mechanisms at the transcriptional, translational or post-translational level are responsible for the lack of red fluorescence in constitutively expressing DsRed2 E14 ES cells, has not been investigated in this work. However, the presence of fluorescent aggregates in Cre-activated ROSA26-DsRed2 colonies could indicate a problem of correct maturation or folding of DsRed2 protein in ES cells. This hypothesis is strengthend by reports from others of a similar punctuated staining in a perinuclear region when DsRed2 expression in ES cells was driven from other promoters[72, 109, 131, 132].

20.1.4. Impaired DsRed2 expression in ES cells

To test whether constitutive expression of DsRed variants was toxic for ES cells, vectors with either EGFP (EGFP.C1), DsRed1 (pDsRed1.C1) or DsRed2 (pDsRed2.C1) expressed from a CMV promoter were linearized and electroporated in E14.1 ES cells. 18 hours post transfection, DsRed1$^+$ cells were not detected (0%), very few were DsRed2$^+$ (0.3%) whereas 8.3% of cells were EGFP$^+$ (Fig.19A). After G418 selection, no stable ES clone expressing any of the DsRed variant could be derived. In contrast, 3 EGFP$^+$ clones showing a strong and homogeneous fluorescence were isolated as observed by fluorescence microscopy (Fig. 19B) and flow cytometry (Fig. 19C).

The apparent incapacity of ES cells to express transiently (Fig. 19A) and in a sustained manner (Fig. 18B) DsRed variants could be a sign of their relative cell toxicity, although the true absence of DsRed protein should be correlated with a lack of immunostaining using anti-DsRed antibody. Nevertheless, our observations and reports from others[72, 108] infer that DsRed variants are not developmentally neutral. DsRed1 and 2 apparent toxicity might be a consequence of their obligate tetramerization *in vivo* and their tendency to form aggregates[97].

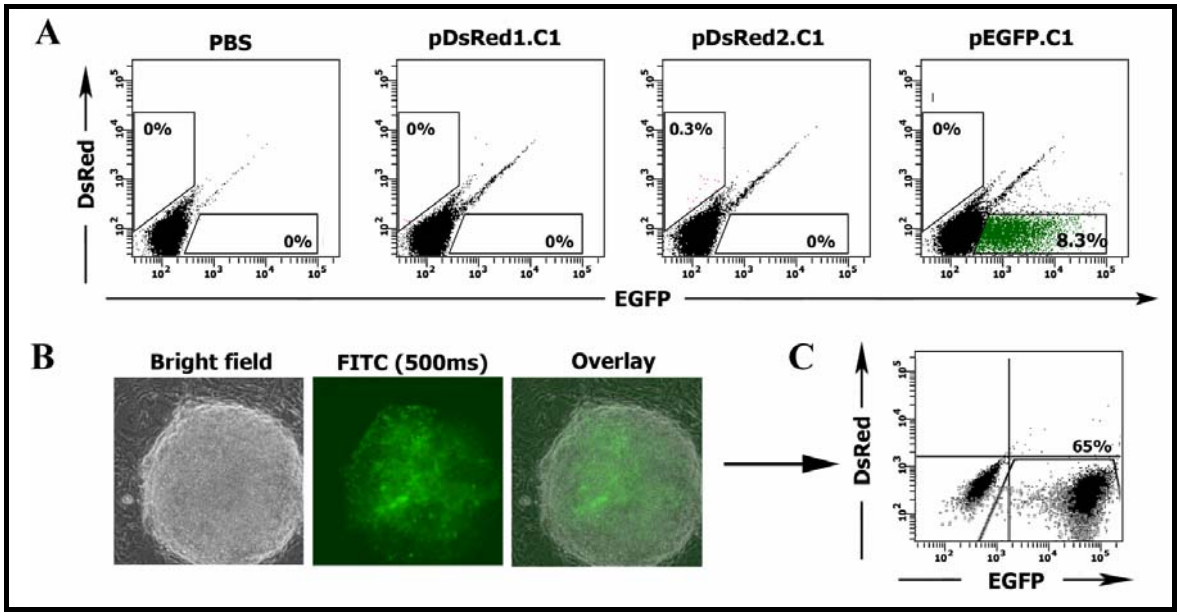

Figure 19: A. Transient expression of DsRed1, DsRed2 and EGFP fluorescent proteins in E14.1 ES cells. Only stable clones expressing EGFP could be maintained. EGFP fluorescence (**B**) and FACS profile (**C**) from one stable clone obtained after random integration of pEGFP.C1. Heterogenous EGFP fluorescence was observed in all ES cells of the colony.

20.2. Use of HcRed1, a far-red fluorescent reporter

Our inability to derive ES cells expressing tetramers of DsRed2 from the ROSA26 locus prompted us to test other red fluorescent proteins with a lower oligomerization state. HcRed1 (Clontech) is a far-red fluorescent reporter derived from a non-fluorescent chromoprotein found in the reef coral *Heteractis crispa*. HcRed1 was generated using random and site-directed mutagenesis[133]. This dimer emits fluorescence at 645-nm and has a codon-optimized sequence for enhanced expression in mammalian cells.

20.2.1. HcRed1 gene targeting into the ROSA26 locus

To target HcRed1 in the ROSA26 locus, DsRed2 was exchanged to HcRed1 in pHL-BS-DTa. The resulting targeting construct (pHL-DC) was linearised with *Sfi* I and electroporated in AB2.2, another ES cell line as we had just tested AB2.2 for germline transmission. In parallel, the Cre-inducible HcRed1 cassette was subcloned in an expression vector (pHL-DD) and electroporated in AB2.2. pHL-DD was used as positive control to optimize HcRed1 detection in our flow cytometry setup. Upon random integration, HcRed1 will be expressed as a transgene from the pCAGGS promoter, a synthetic promoter driving high level of gene expression in ES cells independently of the chromosomal insertion site[72, 108].

A somewhat lower G418 concentration (220 µg/mL) was used for the selection of recombinant clones. 9 days after selection, 8 clones were picked, propagated and screened by PCR for the presence of a targeted recombination event. The ROSA26 locus in clone AB-DC#1 was correctly targeted (Fig. 20A). An other positive clone (AB-DC#2) out of 5 additional recombinant colonies was obtained from an independent targeting experiment (data not shown).

20.2.2. *In vitro* Cre-activation of ROSA26-HcRed1 reporter locus

The IRES-NeoR cassette of AB-DC#1 and one transgenic AB-DD clone was removed by *in vitro* Cre-mediated excision. PCR amplification of the KI allele in AB-DC#1 and neomycin sensitive (NeoS) AB-DCΔNeo clone confirmed that the maintenance of the targeted allele after Cre-mediated excision (Fig. 20B). The stopper cassette was properly removed in neomycin-sensitive targeted clones as revealed by PCR analysis: using HL70/HL54 primers flanking the HcRed1 expression cassette (Fig. 20D), a 1.3 kb product could only be amplified from genomic DNA of HcRed1 targeted clones after NeoR excision (Fig. 20B). Southern blot analysis using an internal NeoR probe revealed a single band in AB-DC targeted clone. Loss of detection of the 2.4 kb band in neomycin-sensitive clones documented further the correct excision of IRES-NeoR (Fig. 20C).

20.2.3. Weak fluorescence emission in HcRed1 expressing cells

After Cre-activation, a similar amount of recombinant transcript was expressed from ROSA26-HcRed1 as compared to DsRed2 by semi-quantitative RT-PCR (Fig. 18C). However, in contrast to ROSA26-DsRed2 clones, red fluorescence could be detected on a epifluorescence inverted microscope. (Fig. 18D). Direct comparison of HcRed1 targeted clones by flow cytometry demonstrated the successful Cre-mediated induction of reporter expression (Fig. 20E): AB-DCΔNeo but not AB-DC ES cells emitted red fluorescence. Although homogeneous within ES cell colonies (Fig. 18B), the intensity of fluorescence was weak when expressed from the ROSA26 locus (Fig. 20E, histograms). Constitutive expression of HcRed1 from the strong pCAGGS promoter resulted in a brighter signal (Fig. 20D) but still sub-optimal for a truly complete separation of HcRed1 expressing from non-expressing cell populations (Fig. 20E, histograms). Moreover, constitutive expression of HcRed1 presented some side effects on ES cell morphology, which

could be a sign for cell toxicity. Cell size (FSC-H) and granularity (SSC-H) were dramatically increased in AB-DCΔNeo as compared to unactivated AB-DC cells (Fig. 20E, dotplot), probably due to the formation of protein aggregates.

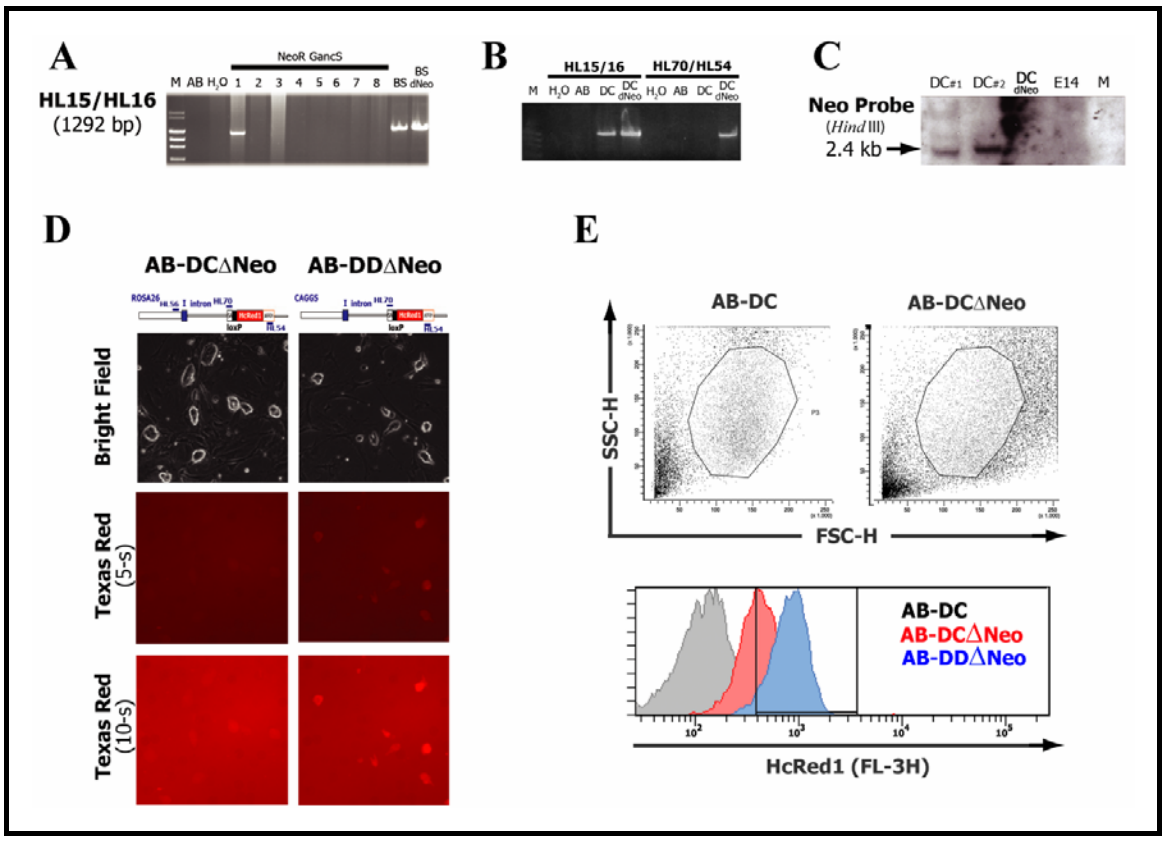

Figure 20: HcRed1 targeting into the ROSA26 locus. **A.** PCR screen of HcRed1 targeted ES pools (1 to 8). DsRed2 targeted clones before (BS) and after NeoR excision (BSΔNeo) were used as control for the amplifcation of recombinant PCR fragment. **B.** Characterization of Cre-induced HcRed1 reporter activation by PCR: targeted alleles were amplified in AB-DC clones before (DC) and after Neo excision (DCΔdNeo) using HL15/HL16 primers. Specific amplification in DCΔNeo using HL70/HL54 primers confirmed NeoR removal. **C.** Southern blot hybridization using NeoR probe. HcRed1 targeted clones before (DC#1 and #2) and after NeoR deletion (DCΔNeo), M: Marker. HcRed1 fluorescence expression in ROSA26 targeted and random inserted clones (AB-DCΔNeo and AB-DDΔNeo respectively) as detected by epifluorescence microscopy (**D**) and FACS analysis (**E**).

20.3. tdRFP, the optimal RFP reporter for lineage tracing experiment

DsRed2-obligate tetramerization to emit fluorescence, slow maturation time and potential toxicity prevented its application as a fluorescent reporter in mouse. Tsien *et al.*[110] reported the generation of DsRed variants with improved properties, namely a reduced oligomerization state and a faster maturation time. The monomer mRFP1 (t½< 1 hr) and the concatemerized tandem-dimer tdimer2(12) or tdRFP (t½: 2 hrs) were suitable for expression in mammalian cells[110]. We therefore tested these new DsRed variants to identify the best fluorescent reporter for gene targeting in ES cells.

20.3.1. tdRFP: a very bright RFP variant for expression in mamalian cells

To compare these new variants with all the fluorescent reporters tested so far, mRFP1 and tdRFP were cloned in an expression vector derived from pEGFP.C1 (Clontech). [Reporter expression will be driven by the same pair of promoter (CMV)/polyadenylation signal (SV40) transcriptional elements for all variants]. The level of fluorescence intensity and the frequency of labeled cells observed in transient transfection should give some qualitative information on the relative maturation time and brightness of a given fluorescent protein. BHK cells were transfected with circular forms of pEGFP.C1, pDsRed1.C1, pDsRed2.C1, pHcRed1.C1, pHL-FA and pHL-FB expression vectors. 18 hours later, microphotograph of cells were taken on an epifluorescence inverted microscope, and the emission of fluorescence was analysed by flow cytometry. With 90% of BHK cells emitting red fluorescence shortly after transfection, mRFP1 was expressed as efficiently as EGFP, illustrating the fast maturation and biocompatibility of this reporter. tdRFP was the second most expressed red fluorescent variant (80%), followed by DsRed2 (64%), DsRed1 (38%) and HcRed (34%). Consistent with their spectral properties (See introduction, Table 2), reporters could be arranged according to their fluorescent intensities. Of all variants tested in this experiment, EGFP exhibited the brightest fluorescence followed by the DsRed variants tdRFP > DsRed2 > DsRed1 > mRFP1 (Fig. 21A). Fluorescence intensity of HcRed1 was the lowest of all.

Ideally, the emission spectrum of a red fluorescent reporter should be distinct from EGFP to allow a combined use in multicolor lineage tracing experiments. As wild-type DsRed fluorophore matures through green fluorescent intermediates[97], we asked whether cells expressing a red fluorescent variant could be separated from $EGFP^+$ cells. Green fluorescence was only detected in EGFP transfected cells by epifluorecence microscopy (Fig. 21B). None of the RFP variants showed detectable level of green intermediate in our optical setup. However, DsRed1 and DsRed2 showed a substantial proportion of RFP^+ cells by flow cytometry with green fluorescence that could not be adjusted by compensation (Fig. 21C). We found that mRFP1 and tdRFP could be distinctively

detected from EGFP by flow cytometry, being therefore both suitable for gene targeting experiment. However, tdRFP showed a superior brightness compared to mRFP1, we decided to target this particular reporter to the ROSA26 locus.

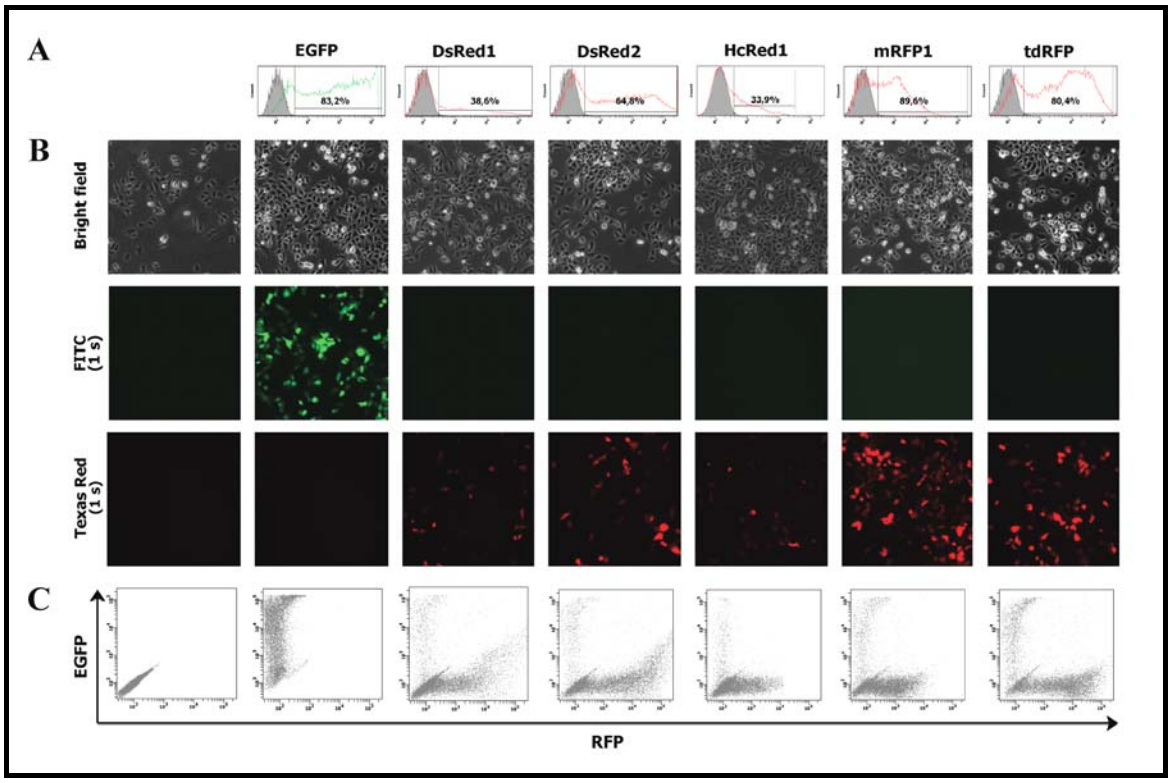

Figure 21: Transient expression of RFP variants in BHK cells. **A.** Fluorescence intensity profile of BHK cells expressing EGFP (green curve) and multiple RFP variants (red curve) 18 hrs after transfection. Relative fluorescence background of untransfected BHK cells are shown as gray filled histograms. **B.** Brightfield and epifluorescence pictures of BHK cells transfected with multiple fluorescent variants using FITC and Texas Red filters. **C.** Separation of EGFP expressing cells from multiple RFP variants by flow cytometry.

20.3.2. tdRFP targeting into the ROSA26 locus

tdRFP was subcloned into pHL-FH, a targeting vector similar to pHL-BS-DTa. Vector linearization, electroporation and selection were as in HcRed1 gene targeting experiment. ES cells used were AB2.2. 21 NeoR DTaS clones were recovered, among which 3 clones were correctly targeted as identified by PCR screen (Fig. 22A). Southern blot analysis using an internal probe specific to the neomycin sequence revealed a single integration of the IRES-NeoR cassette in all targeted clones (Fig. 22B and data not shown). Transient transfection of Cre recombinase in each AB-FH targeted clones yielded neomycin-sensitive colonies with a correct excision of the transcriptional stopper cassette (Fig. 22B). However, fluorescence emission profile of AB-FH clones before and after Cre activation revealed the expression of tdRFP before stopper excision (Fig. 22D). This

unexpected observation could be a sign of read-through across our transcriptional stopper resulting in background tdRFP fluorescence of unacceptable intensity.

Constitutive expression of tdRFP from the ROSA26 locus was well tolerated in ES cells. The fluorescence was evenly distributed throughout the nucleus and cytoplasm (data not shown). tdRFP fluorescence was homogeneous within an ES cell colony as observed by epifluorescence microscopy (Fig. 22C). Most probably, the artificial dimer tdRFP is well tolerated in ES cells as it cannot form multimers of higher order interfering with cellular proteins and their functions.

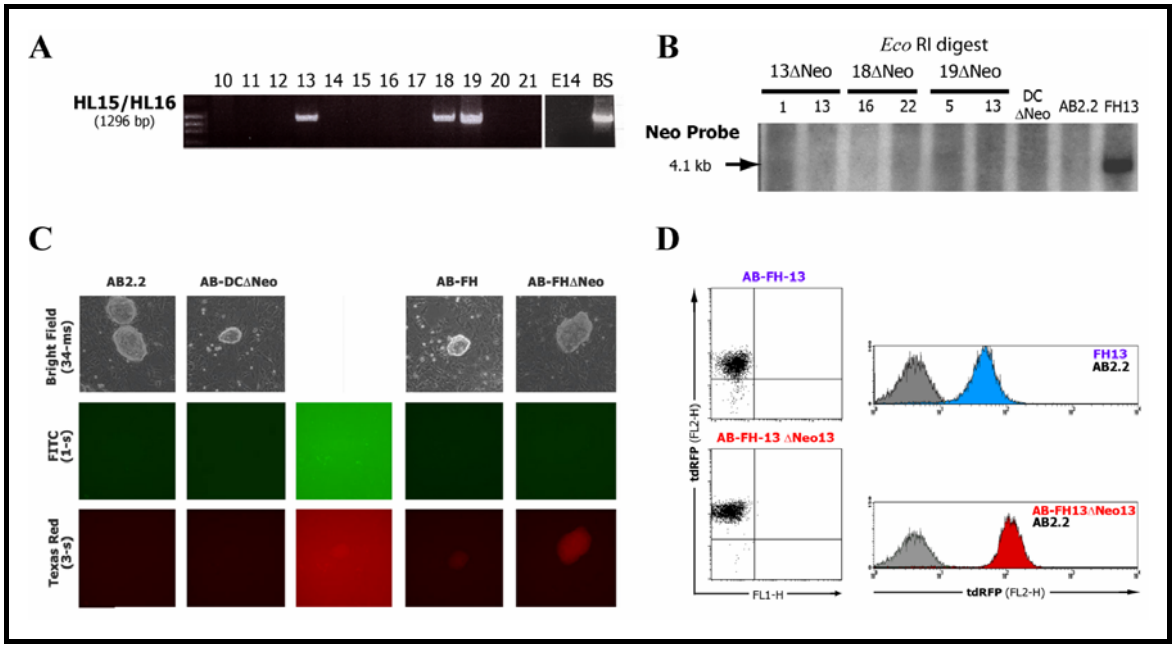

Figure 22: tdRFP targeting to ROSA26 locus yields high intensity fluorescence, even before Cre-activation of the reporter locus. **A.** PCR screen of tdRFP targeted event in individual AB2.2 ES clones (BS: DsRed2 targeted clone). **B.** Southern blot hybridization of tdRFP targeted clones after Neo deletion using NeoR probe. **C.** tdRFP fluorescence emission in targeted clones before (AB-FH) and after reporter activation (AB-FHΔNeo) detected by epifluorescence spectromicroscopy. Pictures of HcRed1 expressing AB-DCΔNeo targeted clone (3-s and 5-s exposure time) are shown to illustrate the higher brightness of tdRFP expressed from ROSA26 locus. **D.** Flow cytometry analysis of tdRFP targeted clone before and after reporter activation. AB-FH13: tdRFP targeted clone before Neo deletion (blue filled histogram), AB-FH13ΔNeo: after Neo deletion (red filled), AB2.2: wildtype parental ES cell line (gray filled).

Expression of tdRFP from the ROSA26 locus yielded a fluorescence of high intensity as opposed to HcRed1 targeted clones (Fig. 22C). Fluorescence in AB-FHΔNeo clones was dramatically increased (≈1 log) when compared to the parental AB2.2 ES cell line, giving an optimal separation of $tdRFP^+$ cells from $tdRFP^-$ cells (Fig. 22D). We therefore kept tdRFP as fluorescent reporter and designed an alternative strategy to prevent any spurious reporter expression before Cre activation of the ROSA26 locus.

20.3.3. Targeting of an inverted tdRFP to the ROSA26 locus

We constructed pHL-HH targeting vector, in which the tdRFP-encoding cDNA was located in reverse orientation relative to ROSA26 promoter (Fig. 24A). This approach was possible by combining WT loxP sites with mutant lox2372 sites, in which two nucleotides of the wild-type spacer sequence GCATACAT had been exchanged to GGATACCT[64, 134]. In order to minimize the impact of transcription reinitiation failure on the overall expression of ROSA26 recombinant transcripts, all loxP and lox2372 sites were introduced *via* linker cloning to reduce the distance between the endogenous ROSA26 stop codon and NeoR/tdRFP initiation codon. To ensure a more efficient positive selection, the IRES sequence was removed to directly fuse Neo with the ROSA26 transcripts. Due to the specific position and orientation of pairs of WT (black triangles) and lox2372 mutant sites (green triangles), Cre-mediated recombination would first induce inversion of the sequences either flanked with loxP or lox2372 sites, followed by irreversible excision of the neomycin stopper cassette along with its neighboring loxP or lox2372 site, respectively (Fig. 24A).

pHL-HH targeting vector was linearized using *Xho* I restriction digest and electroporated in BRUCE4 ES cells, which are derived from mice of the widely used inbred C57BL/6 strain. Positive selection with 220 µg/mL G418 yielded 152 clones in one electroporation. This high number of clones recovered after selection indicates that gene trapping was more efficient than when IRES-NeoR was used. All pools (n=8) of 16 clones had a correctly targeted clone as detected by PCR (Fig. 23A). The Cre-inducible tdRFP cassette was successfully targeted into the ROSA26 locus of 23 individual BRUCE4 ES clones (Fig. 23B and data not shown). Whithout Cre-activation, tdRFP fluorescence was not detected in BRUCE4-HH targeted clones (Fig. 23C) confirming the "leak-proof" property of our system. The targeted locus of one recombinant clone was characterized by Southern blotting using an external probe (Fig. 23D). The pattern of fragments observed was as expected (Fig. 12A).

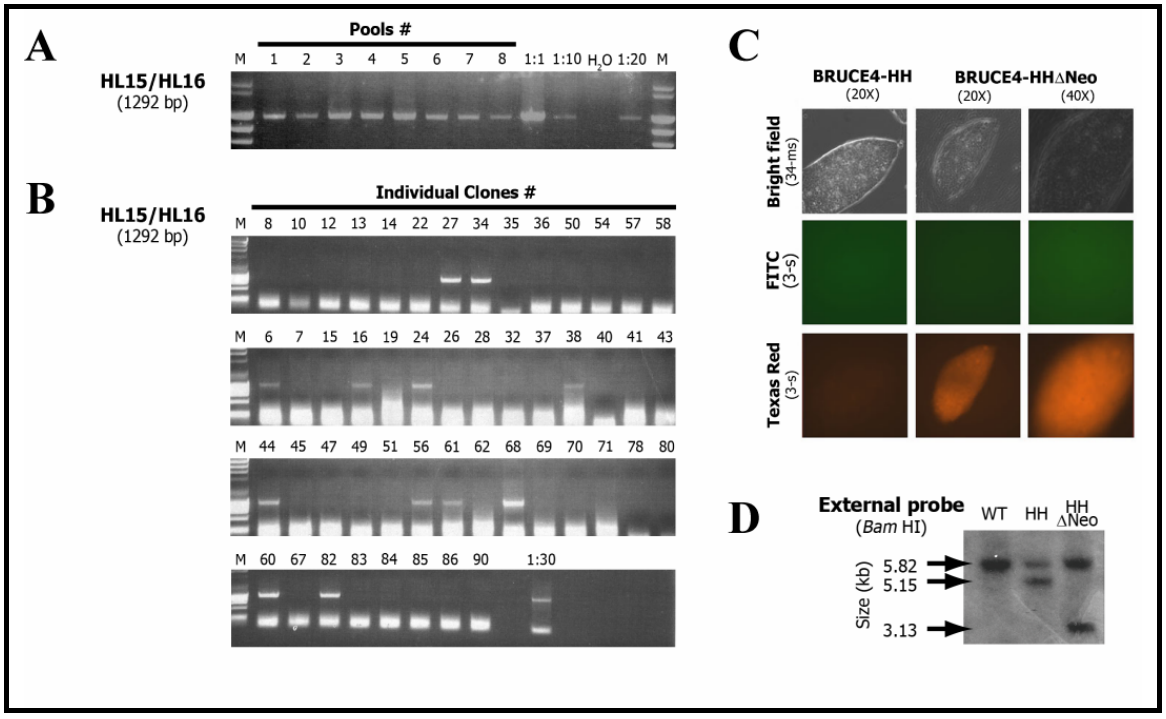

Figure 23: Targeting of tdRFP to the ROSA26 locus and succesful Cre-induction of reporter expression. Targeted events in pools (**A**) and individual clones (**B**) of recombinant BRUCE4 ES clones were screened by PCR using HL15/HL16 primer pair. M: Marker, 1:1 to 1:20 serial dilution of positive control DNA, H_2O: negative control. **C.** tdRFP fluorescence emission in targeted clones before (BRUCE4-HH) and after reporter activation (BRUCE4-HHΔNeo) as detected by epifluorescence stereomicroscopy. **D.** Southern blot analysis of wildtype and recombinant ROSA26 locus using a probe external to pHL-HH targeting construct. Size of respective fragments is given.

We assessed the ability to induce expression of our reporter *in vitro* by transient expression of Cre. HHΔNeo clones were deleted for the transcriptional stopper (Fig. 23D, third lane) and showed strong red fluorescence (Fig. 23C). No adverse effects of tdRFP expression on ES cell growth or morphology were noticeable.

20.3.4. Rapid induction of tdRFP expression upon Cre-mediated reporter inversion and stopper excision

To achieve a complete and irreversible reporter activation at the Cre-inducible ROSA26-**RFP** reporter locus (Fig. 24A, top), Cre recombinase should mediate at least two successive recombination reactions. The reversible Cre-mediated inversion at the loxP or lox2372 sites generates two alternative recombination intermediates (Fig. 24A, middle). In each case, the recombination reaction bring one of the non-intervening lox sites in the same orientation as its respective counterpart. Subsequently, the Cre recombinase can catalyze an irreversible excision reaction, using either the mutant lox2372 (Fig. 24A, left panel) or the original loxP sites (Fig. 24A, right panel). The final recombination

reaction place tdRFP under the full transcriptional control of the ROSA26 locus (Fig. 24A, bottom). Because the two remaining lox sites are incompatible with one another, no further recombination reaction can occur.

To investigate whether this Cre-mediated reporter activation was a rapid and complete process, we followed the onset of tdRFP by flow cytometry in a bulk of sorted $EGFP^+$ BRUCE4-HH ES cells expressing Cre/GFP after transient transfection with pCre-AC. At the peak of Cre expression 18 hours post-transfection, very few cells were expressing tdRFP (≈0.16%, data not shown) whereas another 18 hours later, 1% of cells were readily $tdRFP^+$ (Fig. 24B, top panel). 24 hours later, the majority of ES cells were expressing tdRFP (69%). The mean fluorescence intensity of tdRFP increased over time starting from $3.5x10^1$ 36 hrs post Cre-induction to almost double 24 hours later ($6x10^1$). The level of tdRFP accumulated within activated cells reached a maximum 60 hours after Cre-induction (Fig. 24B). One can infer from this experiment that Cre-induction of tdRFP expression is a rather fast reaction (18 hrs) and yields a maximum of fluorescence 60 hours after Cre-activation.

We then tried to isolate the intermediate products of the Cre-mediated reporter activation reaction (Fig. 24A, middle) to ask whether the constitutively activated ROSA26-tdRFP allele was indeed the main final recombination product in our system. After transient transfection of BRUCE4-HH cells with pCre-AC, Cre expressing cells ($EGFP^+$) were sorted and single-cell deposited in a 96-well cluster. 6 days later, 25 colonies were analysed by FACS (Fig. 24C) and were separated in 3 groups according to their fluorescence profile. 20% (n= 5) of the colonies were $tdRFP^-$, 13% $tdRFP^{int}$ and 68% $tdRFP^{high}$. The genomic DNA of one clone per group was prepared and charaterized at the molecular level using a combination of primer pairs to detect the 5' and 3' end of all possible recombination products (Fig. 24A). The $tdRFP^{high}$ clone (#1) was only found in activated configuration whereas the intermediate stages of recombination were detected in the two other groups. The HL54/HL160 PCR product, diagnostic for the inversion between the loxP sites (Fig. 24A, right panel), was only amplified in the $tdRFP^{int}$ clone #2. The other intermediate form was detected in the $tdRFP^-$ clone (#4) as revealed by

HL154/HL54 PCR. Other products were amplified from tdRFP^{int} and tdRFP^{-} clones, which indicates that these populations were actually mixtures of germline and recombinated forms.

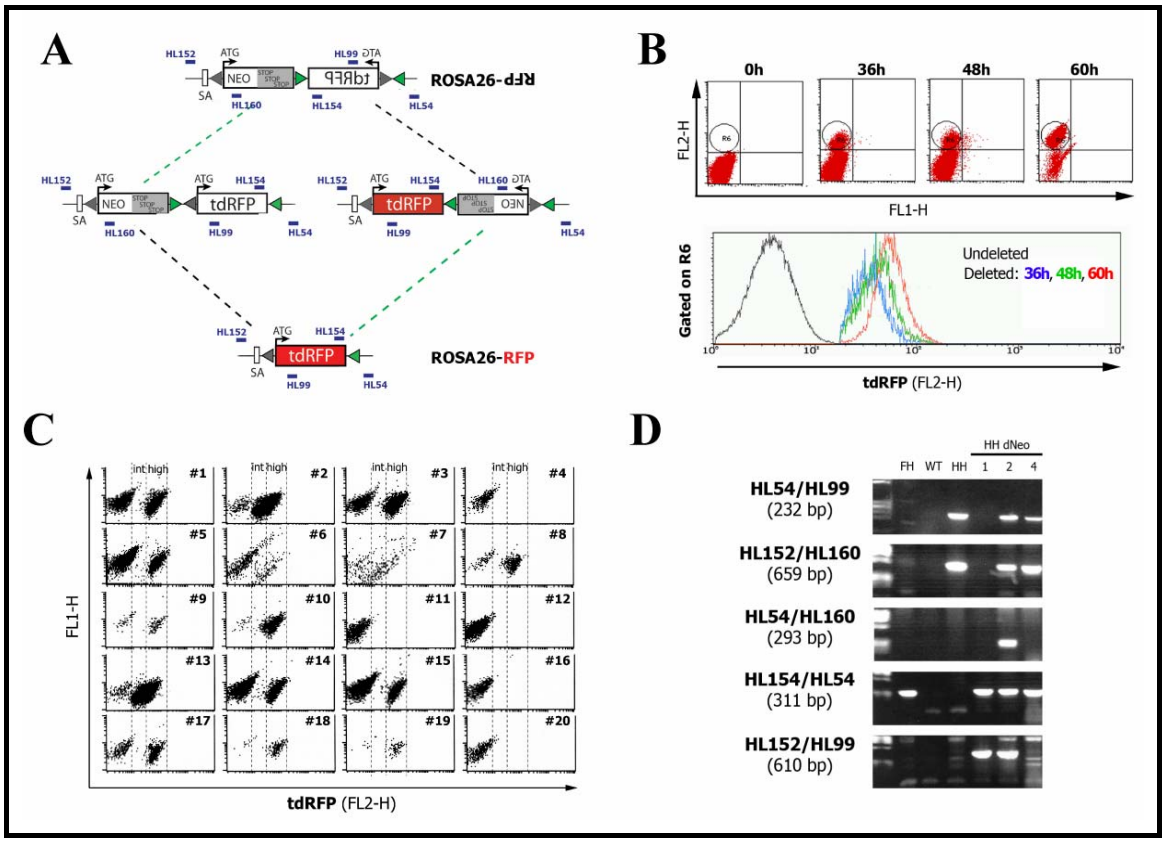

Figure 24: Efficiency of reporter activation upon Cre-mediated recombination reactions. **A.** Schematic representation of ROSA26-**RFP**, intermediates of Cre-mediated recombination and Cre-activated ROSA26-**RFP** locus. LoxP and lox2372 sites are depicted using black and green filled triangular respectively. Annealing site of primers used for PCR analysis (IV) are shown. ATG: start codon, SA: splice acceptor, Neo-Stop : transcriptional stopper. **B.** Time course of fluorescence emission upon Cre-mediated reporter activation in Cre/EGFP^{+} sorted BRUCE4-HH ES cells. **C.** Flow cytometry analysis of tdRFP fluorescence emission in individual BRUCE4-HHΔNeo colonies obtained after single cell sorting of Cre-expressing BRUCE4-HH ES cells. **D.** PCR analysis of ROSA26 locus in BRUCE4-HH ES cells and three BRUCE4-HHΔNeo subclones after NeoR excision.

Thus, Cre-mediated induction of the reporter expression is a really efficient reaction as a majority (2/3) of BRUCE4-HH cells showed an activated locus after a brief expression of Cre recombinase. Expression of Cre in a more sustained manner should yield really high level of reporter activation. As no detrimental effect of tdRFP expression was observed on ES cells, the targeted BRUCE4-HH clone #11 was used to generate inbred C57BL/6 reporter mice following standard methodology.

21. GENERATION OF A T-CELL SPECIFIC DELETER LINE : THE PTα-ICRE KNOCK-IN MOUSE

The succesful knock-in of iCre into the pTα locus required many gene targeting attempts. The several targeting strategies performed in this work are presented in the following section.

21.1. hCre targeting in the pTα locus of E14.1 ES cells

In a former gene targeting experiment, an intronless hCD4 minigene was targeted into the first exon of the pTα gene of 129/Sv-derived RW4 ES cells. The resulting pTα-hCD4 knock-in mice could not be used for the study of immature thymocyte development as the hCD4 expression was too low, most probably due to the the absence of an intron in the expression cassette[135-137] (see introduction, 3.2). To ensure an optimal expression of the Cre recombinase from the pTα locus, we fused a human codon-optimized Cre recombinase with an intronic sequence and splicing signals of the rabbit β-globin. This cassette has been readily used for robust expression of exogenous cDNA in transgenic mice[113]. We fused this expression cassette with the long and short sequences of homology taken from pKAW, the hCD4 targeting construct. A "flipped" Tk-NeoR cassette flanked by FRT sites was cloned 3' of hCre polyadenylation signal for positive selection (Fig. 25A) and subsequent FlpE-mediated NeoR excision. The PCR screen was established using dilutions of genomic DNA of ES cells in which a control arm plasmid was randomly integrated. PCR amplification using 13024/HL14 primer pair yielded a specific 1,4 kb amplicon, absent in WT E14 ES cells (Fig. 25B). pHL-AI was linearized with *Spe* I, electroporated in E14 ES cells and positively selected with 250 µg/mL G418. Random integrants were killed using 2 µmol/L Gancyclovir. Using this targeting construct, more than 3000 clones were screened and no correctly targeted clone could be identified (Fig. 25C and data not shown).

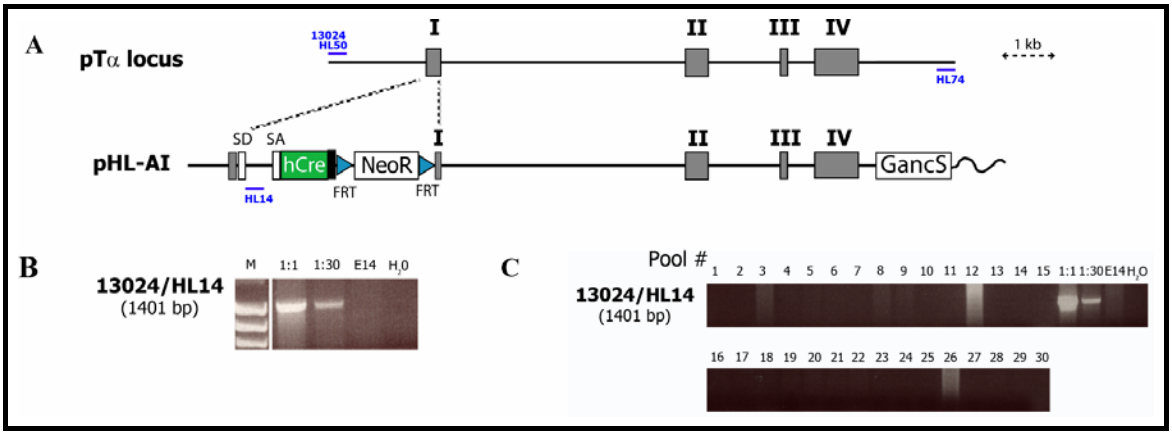

Figure 25: hCre targeting in the pTα locus. **A.** Schematic representation of pTα locus and pHL-AI targeting construct. pTα exons (roman numerals) and primers used for PCR screen are depicted. FRT site (blue filled triangular), SD: splice donor, SA: splice acceptor. **B.** Sensitivity of PCR screen using 13024/HL14 primer pair established on dilutions of positive control gDNA. **C.** PCR screen of pools of recombinant clones resulting from pHL-AI gene targeting experiment in E14.1 ES cells.

Exchanging the TK negative selection cassette to DTa in the targeting vector (pHL-AP) did neither yield a positive clone (n=400). Therefore, we decided to change the region of hCre targeting into the pTα locus.

21.2. iCre targeting into 5' UTR of pTα gene

As we failed to target the hCre recombinase in the first exon of pTα, we tried to target Cre into the 5' UTR of pTα. Cre cDNA was fused with pTα transcript by targeting an IRES-Cre-p(A)n cassette between pTα stop codon and polyadenylation signal (Fig. 26A) as previously described for other loci[138-140]. As we were concerned that hCre GC-rich sequence could be subject to gene silencing *via* CpG methylation[141], we used another codon-optimized Cre recombinase (iCre) described by Shimshek *et al.*[114], which is well expressed and highly active in transgenic mice. The long and short strings of homology were PCR amplified on AB2.2 genomic DNA. pHL-CI was linearized with *Not* I, electroporated in AB2.2 ES cells and positively selected with 250 µg/mL G418. Random integrants were killed using 2 µmol/L Gancyclovir. Although a very robust PCR screen was established using the primer pair 8361/HL74 (Fig. 26B), no targeted event could be identified among 576 clones analysed (Fig. 26C).

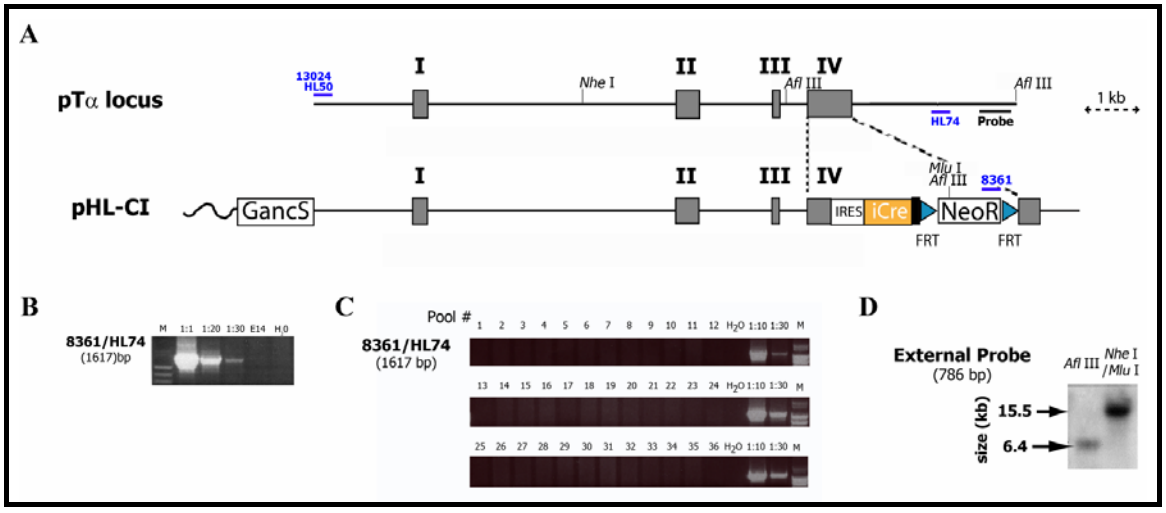

Figure 26: IRES-iCre targeting into 5' untranslated region (UTR) of pTα locus. **A.** Schematic representation of pTα locus and pHL-CI targeting construct. pTα exons (roman numerals) and primers used for PCR screen are depicted. FRT site (blue filled triangular), SD: splice donor, SA: splice acceptor, IRES: Internal Ribosome Entry Site. **B.** Sensitivity of PCR screen using 8361/HL74 primer pair established on dilutions of positive control gDNA (1:1 to 1:30). **C.** PCR screen of pools of recombinant clones resulting from pHL-CI gene targeting experiment in AB2.2 ES cells. M: Marker of molecular weight. **D.** Detection of wild-type pTα locus by Southern blot hybridization using a probe external to the targeting construct. DNA fragments resulting from two restriction digest are shown and corresponding size is given.

Alternatively, the strong and specific signal observed by Southern blotting analysis using a probe external to the targeting construct (Fig. 26D) would have enabled us to screen more clones by Southern blotting. However, the success in identifying a pTα targeted clone in another gene targeting experiment (see 21.3) led us to discontinue this approach.

21.3. iCre targeting into the first exon of pTα

Sequence comparison of the pTα locus from C57BL/6 (Ensembl website), 129/Ola (Celera) and 129/Sv (our laboratory) showed that the sequence used in our targeting vector was highly polymorphic, especially in a region 3' of exon I (data not shown). A 250 bp sequence present in 129/Sv genomic DNA was deleted in the 129/Ola genome. This polymorphism could be a possible explanation for our inability to target efficiently the pTα locus. Previous targeting of E14.1 (129/Ola derived) with pHL-AI, a targeting vector with 129/Sv-derived sequences of homology, could result in a drop of targeting efficiency limiting homologous recombination reactions[142]. Gene targeting of ES cells derived from 129/Sv mouse strain like AB2.2 should help us to increase pTα targeting efficiciency.

21.3.1. pHL-IE targeting construct and gene targeting experiment in AB2.2

We improved former pHL-AI targeting construct in replacing hCre cDNA by iCre. For positive selection of the recombinant clones, a fliped NeoR cassette was inserted in reverse orientation to the pTα promoter. The resulting targeting construct (pHL-IE, Fig. 28F) was linearized with *Not* I, electroporated in AB2.2 ES cells and colonies were screened using a new PCR screen, which was more sensitive than the one previously described (Fig. 27).

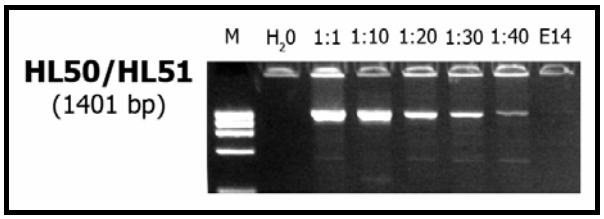

Figure 27: New PCR screen (M: Marker, 1:1: undiluted control genomic DNA of ES cells electroporated with pHL-AL#inv control construct, 1:10 to 1:40: serial dilutions of control DNA in 1 µg/µL E14.1 gDNA) for iCre targeting into the first exon of pTα

204 colonies were individually screened this time by single clone PCR (Fig. 28A). As the quality of genomic DNA preparations is crucial for the detection of a targeted event, the A260/A280 spectrophotometric ratio was measured for each individual clones. In most of the samples, A260/A280 ratios were normal ranging from 1,7 to 1,9 (data not shown). PCR amplification of a 600-bp diagnostic fragment using gp120 specific primer pair HL36/HL37 (Fig. 28B) further confirmed the high-quality of genomic DNA preparation. One positive clone (#44) was identified by HL50/HL51 PCR screen (Fig. 28A). The correct targeting event was confirmed on a second DNA preparation using the HL50/HL51 screening PCR (Fig. 28C) and hCD4 screening PCR (Fig. 28D).

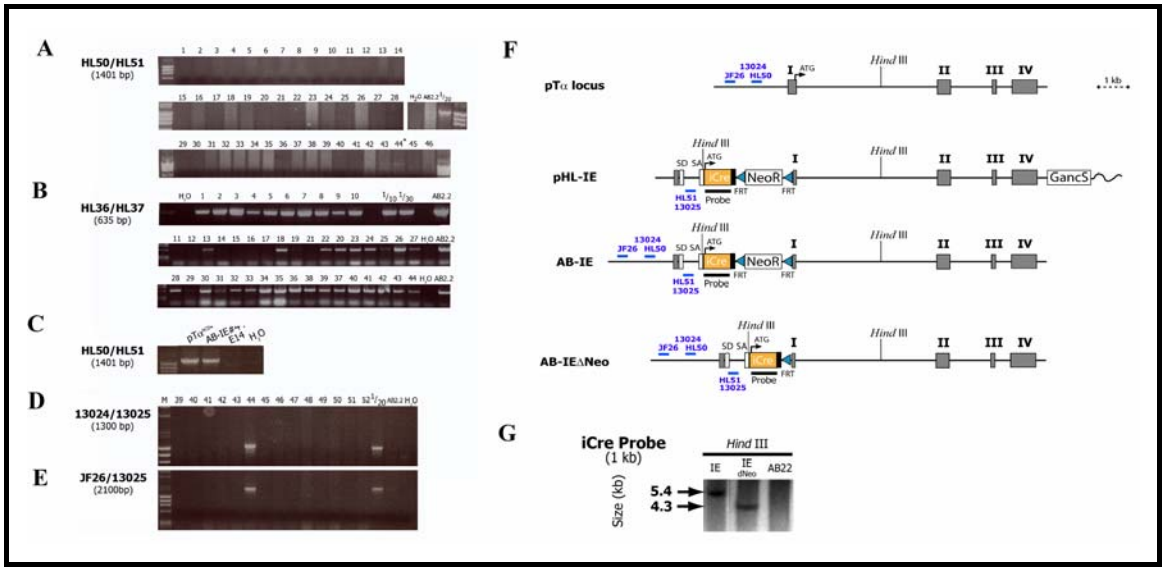

Figure 28: Identification and characterization of pTα-iCre targeted clone. **A.** PCR screen of individual clones for iCre targeting into pTα locus. Clone #44 was identified as positive. **B.** Assay of genomic DNA quality for each DNA preparation from individual clone by PCR amplification of gp120 as previously described in section 16.7. **C.** Confirmation of the targeted event by PCR on an independent gDNA preparation. ´Genomic DNA of a pTα-hCD4 targeted clone was used as positive control. Targeted event was further confirmed by PCR using an alternative primer pair for PCR screen (**D**) and an additional primer combination with JF26 (**E**) located 5' of the external Southern probe. **F.** Schematic representation of pTα locus, pHL-IE targeting construct and resulting recombinant pTα-iCre locus before and after FlpE-mediated NeoR excision. Primer location and restriction sites used in the characterization of the targeting event are shown. **G.** Southern blot hybridization of pTα-iCre targeted clone before (AB-IE) and after FlpE-mediated NeoR excision (AB-IEΔNeo) using an internal iCre probe. Size of specifc DNA fragments are given.

We failed to establish a sensitive Southern blot analysis using a probe external to the targeting construct (data not shown), mostly due to the presence of multiple repetitive sequences in the pTα locus[47]. Therefore, another PCR analysis was performed with a forward primer lying further upstream of the short sequence of homology used in the targeting construct (Fig. 28E). Together with a Southern blot analysis using iCre as a probe (Fig. 28G), the integrity of the targeted locus was confirmed. An additional targeted clone (AB-IE#281) out of 300 recombinant colonies was otained from an independent targeting experiment in AB2.2 ES cells and characterized following the same strategy (data not shown). In both targeted clones, the FRT flanked NeoR cassette was removed *in vitro* by transient transfection with a FlpE-expressing plasmid (data not shown). One NeoS subclone *per* targeted line was injected into C57BL/6 blastocyst following standard methodology[58].

21.3.2. pTα-iCre x ROSA26-tdRFP double KI ES cells and chimera analysis

The succesfull excision of the NeoR selection cassette in pTα-iCre targeted clone allowed for re-targeting of AB-IE#44ΔNeo cells with constructs using NeoR as positive selection cassette. Knowing the high targeting efficiency of ROSA26 locus, we could easily generate double targeted ES cells (Fig. 29). Out of 10 pools of 16 clones, 3 pools showed a homologous recombination event as identified by PCR (Fig. 29A, top). 3 individual clones were correctly targeted to the ROSA26 locus (Fig. 29A, middle and data not shown) and conserved the pTα-iCre allele (Fig. 29A HL50/HL51). Each targeted clone was confirmed twice by PCR on independent DNA preparation (Fig. 29A, bottom and data not shown). 2 double targeted clones (#3 and #74) were injected into C57BL/6 blastocysts. Although 50% of these blastocysts gave rise to chimeras (Fig. 29B), the contribution of targeted ES cells to the chimeras was low (10 to 30%). Intercross of chimeric males with C57BL/6 female never gave transmission of the targeted alleles to the germline (Fig. 29B). Similar results were obtained with the parental pTα-iCre AB-IE ES cell line (Fig. 29B). Despite the fact that untargeted AB2.2 ES cells had been tested before hand and showed germline transmission (data not shown), our negative results and reports from others (Madan, our laboratory) indicate that the AB2.2 ES cells used in our gene targeting experiments have lost their pluripotency, possibly during a round of ES cell expansion.

We took advantage of the chimeras to test whether our pTα-iCre deleter allele could activate the ROSA26 reporter locus in a specific manner. The ES cell contribution to the hematopoietic system of the chimeras we analysed (n=3) was really low (0.10 to 1%) as indicated by the expression of Ly9.1, a congenic marker specifically expressed on lymphocytes of the 129 mouse strains (Fig. 29C and E). $tdRFP^+$ cells were found in the thymus (Fig. 29C and D) and in peripheral organs such as spleen (Fig. 29E) and lymph nodes (data not shown). All $tdRFP^+$ thymocytes were $CD3^+$ in the thymus (Fig. 29C). Although some immature double positive $CD4^+CD8^+$ thymocyte as well as single positive $CD4^+$ were labeled in the chimeric mouse we analysed, the main population of $tdRFP^+$ cells was $CD8^+$ (Fig.

29D). Due to the limited number of chimeras generated from double targeted ES cell injections, we could not investigate whether this developmental bias to the CD8 subset was statistically relevant or was a chimera artefact. Analysis of splenocytes in chimeric animals reproducibly showed that ES-derived $CD19^+$ cells were never $tdRFP^+$ (Fig. 29E). In contrast, all $tdRFP^+$ splenocytes were $CD3^+$ (data not shown) illustrating the T-lineage specificity of reporter induction.

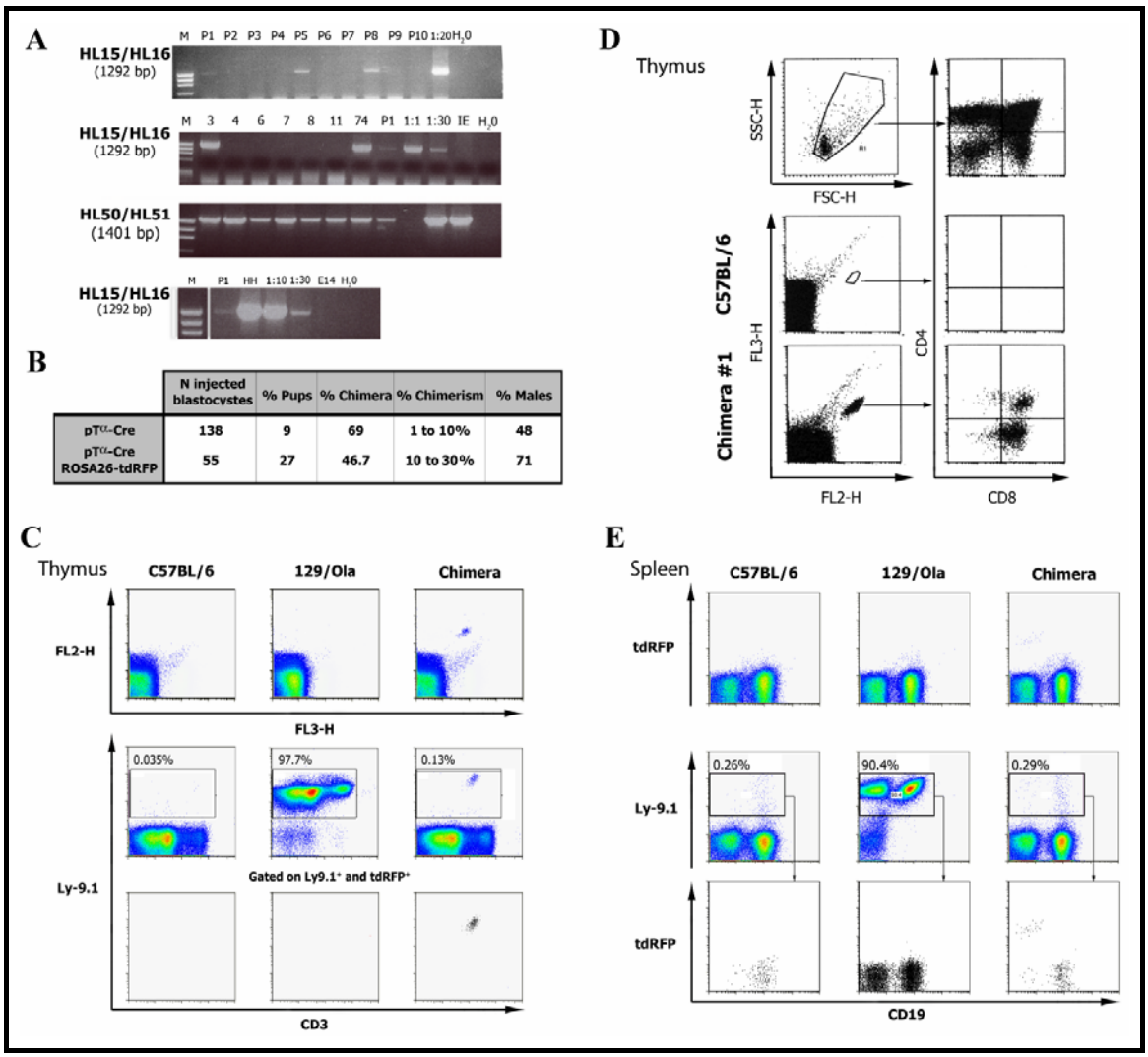

Figure 29: tdRFP targeting to the ROSA26 locus in pTα-iCre ES cells and analysis of double KI chimeras. **A.** PCR screen of pools (top) and individual clones (middle top) of AB-IE44ΔNeo ES cells targeted with pHL-HH. Maintenance of pTα-iCre allele in ROSA26-**RFP** targeted clones was confirmed by PCR (middle bottom). Targeted event was confirmed on an independent gDNA preparation (bottom) using ROSA26 knock-in screening primer pair. M: Marker, P1-P10: Pools, 1:20 : dilution of positive control DNA, IE: parental pTα-iCre targeted clone. **B.** Statistics of transgenesis using double knock-in pTα-iCre x ROSA26-**RFP** and parental pTα-iCre#44 AB2.2 ES cells. **C.** Evaluation of the degree of ES cell contribution to the lymphoid lineage by flow cytometry using Ly9.1 donor marker. 129/Ola mice were used as postive control for the Ly9.1 staining. **D.** Developmental status of $tdRFP^+$ thymocyte in chimeric mice according to CD4/CD8 expression. **E.** FACS analysis of splenocytes in double knock-in chimera. $CD19^+$ B cells derived from the ES cell are not expressing tdRFP.

These results were very encouraging as they show that our reporter system is working in principle and can specifically label cells of the T-lineage. We therefore performed a new set of targeting experiments in other ES cell lines to

generate pTα-iCre deleter mouse.

21.3.3. iCre targeting in the pTα locus of E14.1 and BRUCE4 ES cells

To target efficiently iCre in BRUCE4 ES cells, isogenic sequences of homology were amplified by PCR and exchanged in the final targeting vector (pHL-IG). Although a good number of recombinant clones was recovered after G418 selection (n=232) with this targeting construct, we failed to identify BRUCE4 targeted clones. In parallel, we tried one more gene targeting experiment in E14.1 ES cells using non-isogenic pHL-IE targeting construct. 5 pools of 16 clones showed a PCR product using HL50/HL51 primers (Fig. 30A). Individual targeted clones were identified in every positive pools (Fig. 30B and data not shown). This relatively high targeting efficiency (1,25%) of pHL-IE in contrast to previous attempts with pHL-AI is difficult to explain. Clearly, non-isogenicity of the targeting vector was not the main obstacle for successful gene targeting experiment. The change of NeoR orientation between pHL-AI/pHL-IE targeting construct might have been beneficial. May be, the decisive change was the use of a more sensitive PCR screen to identify correct homologous recombination event. The single integration event in the ES cell genome was confirmed by Southern blot analysis using iCre as an internal probe (Fig. 30D). A PCR analysis similar to the one in figure 28E was performed and confirmed the correct targeting of iCre to the pTα locus (data not shown). In all positive clones, the neomycin cassette was succesfully removed as shown by Southern analysis (Fig. 30D). A PCR analysis using JF26/13758 primers confirmed the correct deletion of the neomycin cassette at the pTα locus (Fig. 30F). In this PCR, the forward primer JF26 outside of the targeting construct and a reverse primer (13758) located immediately after the 5' FRT site (Fig. 30E) amplified two products in E14-IEΔNeo clones which corresponds to the WT (2.6 kb) and the targeted allele of pTα (≈5.3 kb). The KI allele from NeoR E14-IE cells could not be amplified because the NeoR cassette was increasing the size of the JF26/13758 product over the limit of extension used in this PCR.

To inject a pTα-iCre KI clone with the best chance of germ line transmission, we analyzed the expression of several genes associated with the

pluripotency of ES cells[143] by semi-quantitative RT-PCR. *dppa*2, 3, 4, 5, *nanog* and *oct*3/4 were highly expressed in most of the targeted clones as in the E14.1 control except for clone E14-IE#191ΔNeo5. Expression of *pramel*4, 5, 6 and 7 genes in E14-IE#236ΔNeo3, #265ΔNeo4 and #358ΔNeo1 was ≈10 times less than in E14.1.

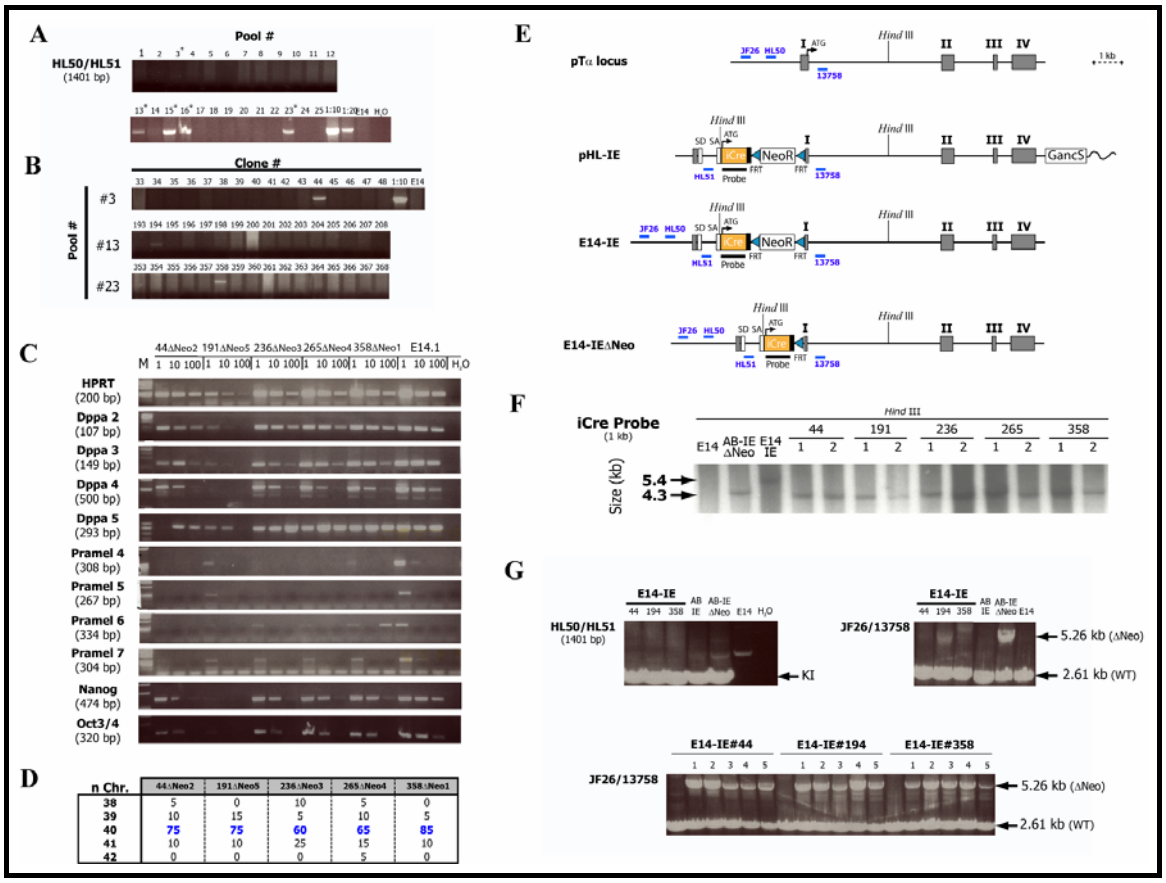

Figure 30: Screening and characterization of E14-IE targeted clones. **A.** Positive pools (*) of recombinant clones were identified by PCR screen. **B.** Individual clones with targeted event were found for each positivie pools using the same PCR screen. **C.** Expression of pluripotency associated genes in independent clones of pTα-iCre after FlpE-mediated excision as detected by RT-PCR amplification. **D.** Karyotype analysis of 5 independent pTα-iCre targeted clones after FlpE-mediated excision. Frequency of normal caryotype is highlighted in blue. **E.** Schematic representation of pTα locus, pHL-IE targeting construct and resulting recombinant pTα-iCre locus before (E14-IE) and after FlpE-mediated NeoR excision (E14-IEΔNeo). Primer location and restriction sites used for characterization of targeted event are shown. **F.** Southern blot hybridization of pTα-iCre targeted clone using an internal iCre probe. Size of specifc DNA fragments is given. AB-IEΔNeo from previous AB2.2 gene targeting experiment is used as control for NeoR deletion. **G.** Confirmation of pTα-iCre targeted locus integrity using multiple PCR amplification. PCR using primer pair HL50/HL51 was used to confirm presence of KI allele. NeoR excision was confirmed by PCR using JF26/13758 primer pair.

The lack of *pramel* gene expression in E14-IE#44ΔNeo2 could be due to the use of a lower amount of starting cDNA in this particular sample. E14-IE#191ΔNeo5 was not used for blastocyst injection as it showed a completely different transcriptome, lacking the expression of *nanog* and *oct*3/4 which are the key regulators for the maintenance of pluripotency in mouse ES cells[54]. Loss of

heterozygosity of one allele[144] or chromosome[145] is frequent in ES cells and can be associated with loss of pluripotency. Therefore, we performed a karyotype analysis of metaphasic chromosomes in pTα-iCre targeted clones (Fig. 30D). With more than 75% metaphases showing a normal set of 40 chromosomes, clones E14-IE#44ΔNeo2 and #358ΔNeo1 were selected to generate pTα-iCre deleter line. Both clones produced chimeras and E14-IE#44ΔNeo2 transmitted pTα-iCre KI allele to the offspring.

22. CRE-INDUCIBLE ROSA26-RFP MOUSE: ONE REPORTER FOR MULTIPLE APPLICATIONS

22.1. Characteristics of ROSA26-RFP mice prior Cre-activation

Un-activated ROSA26-**RFP** reporter mice were successfully derived from BRUCE4 ES cells and maintained on a pure C57BL/6 background. Inter-cross of heterozygous animals produced offspring of all genotypes as typed by PCR (Fig. 15A). The ROSA26-**RFP** allele segregated with predicted Mendeleian ratio (data not shown). Homozygous ROSA26-**RFP** animals were viable, fertile and were used to maintain the ROSA26-**RFP** line. Knock-in of one reporter allele in the ROSA26 locus did not significantly alter the normal cellularity of lymphoid organs (data not shown). Importantly, we never detected background expression of tdRFP in ROSA26-**RFP** mice (Fig. 33A, right pannel and Fig. 34A) due to the reverse orientation of the reporter to the ROSA26 promoter (Fig. 32A). These data show that introduction of the tdRFP encoding nucleotide sequence into the ROSA26 locus does not interfere with mouse development.

22.2. Germline activation of the ROSA26-RFP reporter in the mouse

To assess the efficiency of *in vivo* reporter activation and compatibility of ubiquitous tdRFP expression with normal development and postnatal life, ROSA26-**RFP** reporter mice were inter-crossed with huCMV-Cre transgenic animals for ubiquitous deletion of the loxP-flanked transcriptional stopper including germ cells. Splenocytes of resulting offspring was analyzed by FACS to monitor the induction of tdRFP expression. Unexpectedly, ROSA26-**RFP** activation was not complete in all animals, varying from 30 to 100% of total splenocytes depending on the individual analysed (Fig. 31A). The deletion was not mosaic as the degree

of tdRFP labeling was the same in multiple lymphoid organs of a given mouse (data not shown). Similar fluctuations of reporter activation were found in huCMV-Cre x ROSA-GFP reporter animals (data not shown). Therefore, the observed compound deletion cannot be explained by a technical limitation specific to our reporter locus, but most likely by the variegated expression of multi-copy huCMV-Cre transgenes[50]. tdRFP reporter expression was not altering the lineage equilibrium between T and B cells in the spleen as compared to a WT C57BL/6 mouse (Fig. 31B). Thus, reporter expression did not seem to negatively influence the development of one given lineage at the expense of another. Importantly, the T/B-cell ratio was the same in tdRFP$^+$ and tdRFP$^-$ populations of chimeric animals indicating that a normal cell homeostasis is maintained regardless of tdRFP expression.

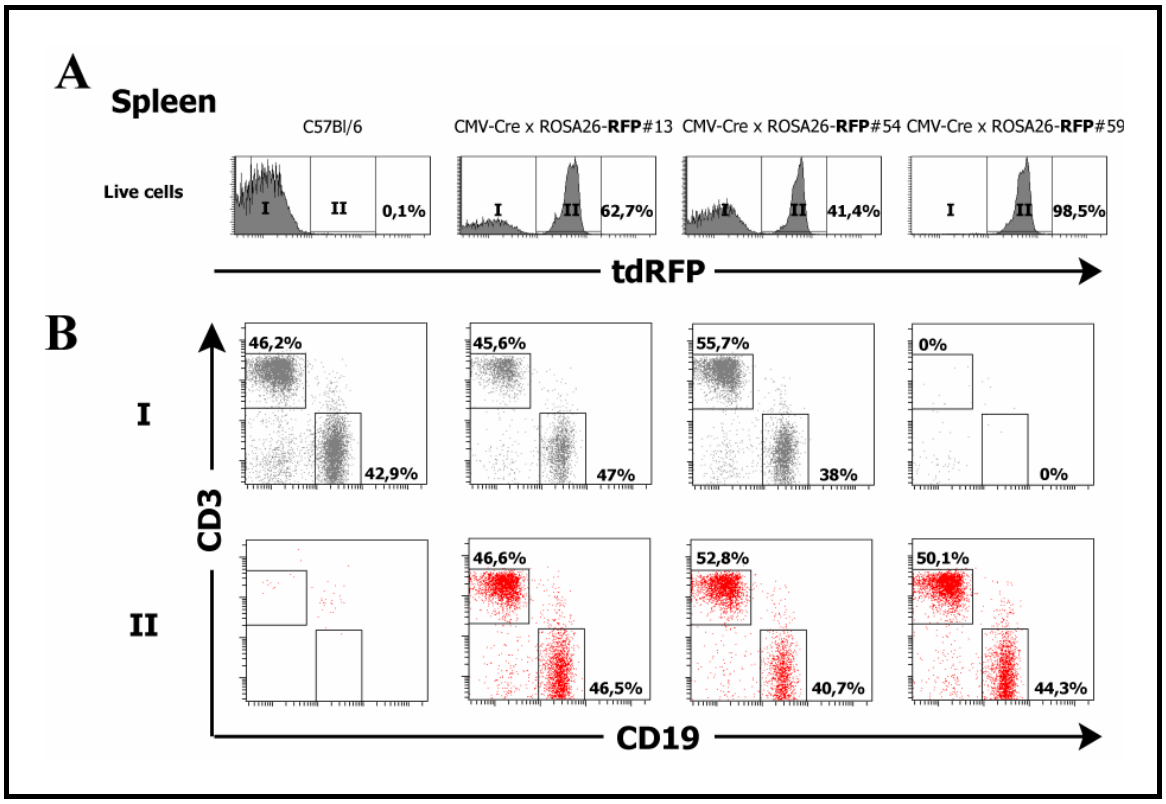

Figure 31: A. Mosaic reporter activation in huCMV-Cre x ROSA26-**RFP** animals. Histogram of tdRFP fluorescence emission in erythrocyte-depleted spenocytes from C57BL/6 and 3 huCMV-Cre x ROSA26-**RFP** animals. Percentage of tdRFP$^+$ cells is given for each mice. **B.** Expression of tdRFP in lymphocyte does not alter T/B lineage ratio of splenocytes. Proportion of CD3/CD19 splenocyte populations for each tdRFP$^-$ (black) and tdRFP$^+$ (red) splenocyte subsets as defined in A (I and II populations).

To generate a constitutively activated reporter mice, we backcrossed animal typed positive for Cre and the reporter allele onto C57BL/6. Offspring typed positive for Cre and ROSA26-**RFP** reproduced the incomplete activation phenotype, most probably because the compound deletion was also found in germ

cells. ROSA26-**RFP** (activated reporter) progeny typed negative for Cre was further backcrossed onto C57BL/6. All heterozygous offspring for the reporter locus showed a complete recombination event as shown by Southern hybridization (Fig. 32A and B, lanes **RFP**/WT). ROSA26-**RFP** animals were fertile, allowing the establishment of a mouse line constitutively expressing tdRFP as a donor marker for cell transplantation analogous to ROSA26-EGFP, EYFP and ECFP strains[71, 85, 125]. Activated reporter ROSA26-**RFP** allele was stably transmitted to the offspring at expected frequency (data not shown). ROSA26-**RFP** mice did not show any obvious phenotype.

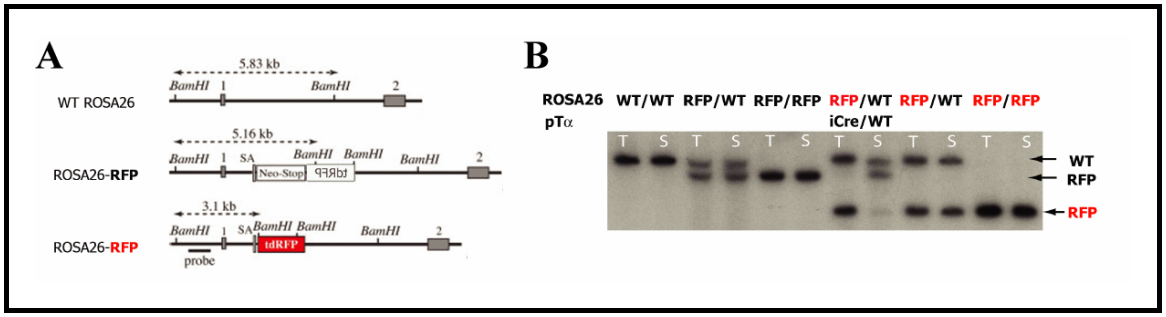

Figure 32: A. Schematic representation of wildtype, targeted (ROSA26-**RFP**) and activated (ROSA26-**RFP**) ROSA26 locus. ROSA26 exons are depicted as numerals. Location of restriction sites used for Southern hybridization and size of resulting fragments detected using an external probe are given. SA: splice acceptor, Probe: location of external probe. **B.** Southern blot hybridization of *Bam* HI digested genomic DNA from thymus (T) and spleen (S) samples using the external probe depicted in A. Genotype for ROSA26 and pTα locus of animals used in this experiment are indicated. WT: wildtype, **RFP**: floxed ROSA26-**RFP**, **RFP**: activated ROSA26-**RFP**.

Intercross of heterozygous ROSA26-**RFP** animals produced offspring of all genotypes as shown by Southern (Fig. 32B). Homozygous ROSA26-**RFP** animals were obtained at expected frequency (data not shown). These mice showed normal behavior, were viable and fertile highlighting the innocuity of constitutive RFP expression on mouse development.

22.3. Strong ubiquitous expression of tdRFP in ROSA26-RFP mice

Heterozygous ROSA26-**RFP** animal exhibited robust ubiquitous red fluorescence as seen by whole body fluorescence imaging (Fig. 33A, left panel). Tissues from the three germ-layers were labeled (Fig. 34A, right pannel). The fluorescence intensity was high, far over the background autofluorescence as shown by direct comparison of several organs of WT and ROSA26-**RFP** mice (Fig. 34B, left panel).

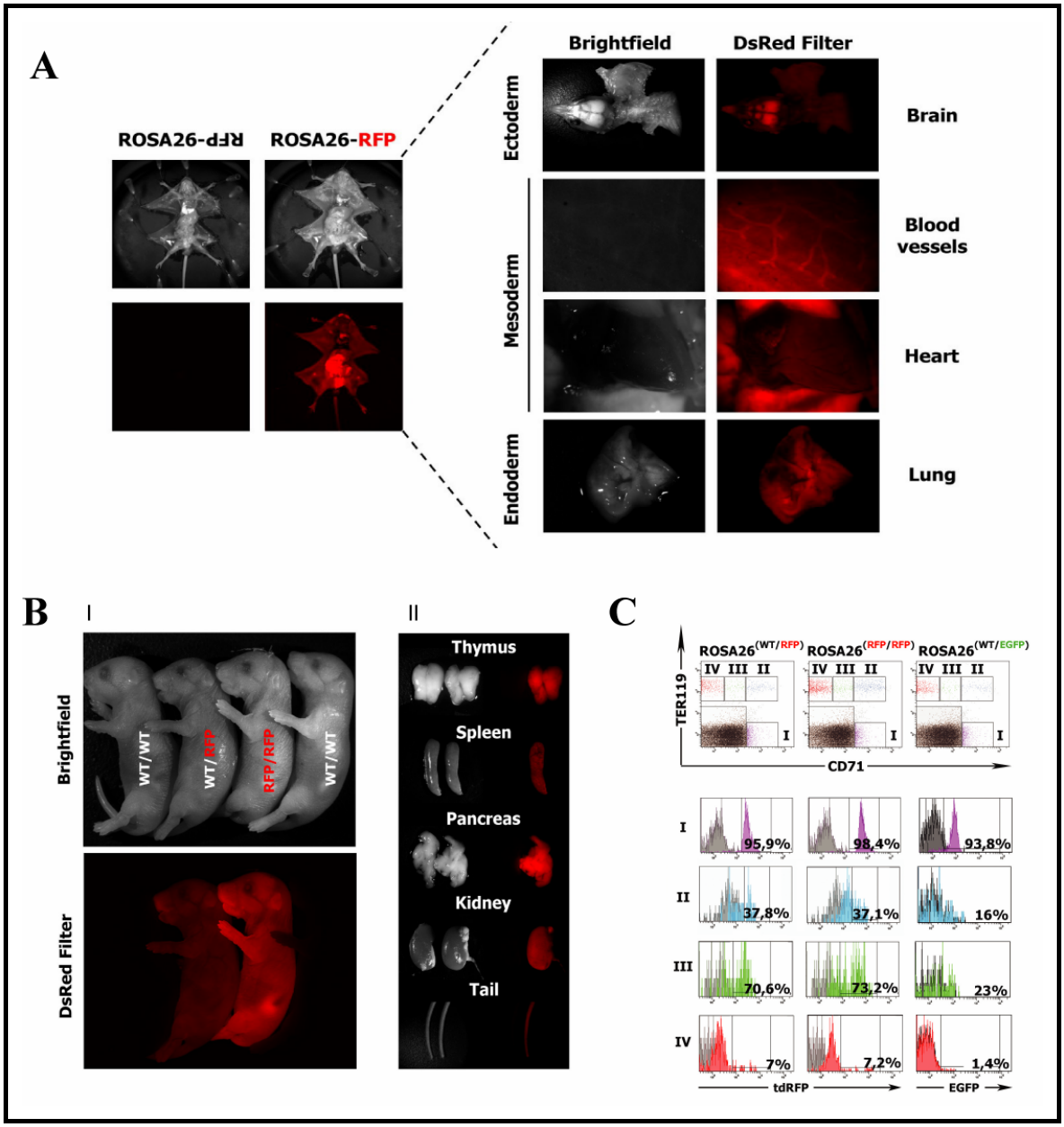

Figure 33: Fluorescence imaging of ROSA26-**RFP** and reporter activated ROSA26-**RFP** animals. **A.** Left: Whole body bright field and fluorescence imaging (34-ms and 3-s exposure time respectively). Right: Brightfield and fluorescence stereoscopy of several ROSA26-**RFP** organs and tissues: Following magnification and exposure time were used for each organ: brain (0.71x, 1s), blood vessels (10x, 5s), heart (2x, 1s), lung (0.71x, 1s). **B.** Litter of newborn pubs from an inter-cross of heterozygous ROSA26-**RFP** parents (I). Genotype for each newborn is indicated: WT: wild-type; WT/**RFP**: heterozygous ROSA26-**RFP**; **RFP** /**RFP**: homozygous ROSA26-**RFP**. (II) tdRFP expression in adult tissues of heterozygous ROSA26-**RFP** mouse; Brightfield and fluorescence imaging of organs from a C57BL/6 control animal (left) and ROSA26-**RFP** mouse (right). Following magnification and exposure time were used for fluorescence picture acquisition: thymus (1x, 1s), spleen (0.71x, 1s), pancreas (1x, 300ms), kidney (0.71x, 1s), tail (0.71x, 1s). **C.** Expression of tdRFP in different erythrocyte stages. 3-color FACS analysis of splenocytes stained with anti-TER119 and anti-CD71 (anti-transferrin receptor) antibodies. Shown are only cells electronically gated through a lymphocyte-like gate to include lymphocytes, erythrocyte progenitor stages and few mature erythrocytes. The dot plots show the gates used to discriminate erythrocyte maturation stages. Histograms of tdRFP fluorescence in the TER119/CD71 subsets defined on dotplots are shown (note corresponding color code).

Homozygous ROSA26-**RFP** animals showed an even stronger fluorescence than their heterozygous littermates (Fig. 34A, right panel). Rigorous inspection of ROSA26-**RFP** mice using fluorescence stereoscopy revealed that hairs were the only macroscopic structures devoid of tdRFP expression. Collectively, these data

document the maintenance of ubiquitous ROSA26 expression upon Cre-mediated reporter activation in the entire mouse.

22.4. 100% of cells are labeled in ROSA26-RFP mice

To evaluate the degree of labeling in activated ROSA26-**RFP** mice, the fluorescence profile of cell suspensions extracted from several lymphoid organs was analysed by FACS (Fig. 34A). Quantification of $tdRFP^+$ cell populations from heterozygous and homozygous ROSA26-**RFP** mice revealed that virtually all cells were expressing tdRFP (≈ 99%), with a notable lower labeling found in bone marrow due to contaminating mature erythrocytes. Indeed, in the hematopoietic system, late stages of adult erythrocytes were not labeled as detected by flow cytometry (Fig. 33C). Erythrocytes develop from a $TER119^-CD71^+$ (I) pro-erythroblast stage *via* $TER119^+CD71^+$ (II) and $TER119^+CD71^{int}$ (III) erythroblasts to $TER119^+CD71^-$ (IV) mature erythrocytes[146]. While proerythroblasts ($TER119^-CD71^+$) express tdRFP at essentially the same frequency and exhibit similar fluorescence intensities as other nucleated cells (e.g., $TER119^-CD71^-$ lymphocytes), tdRFP expression was lost towards more mature erythrocyte stages, in which an increasing fraction of cells had expelled the nucleus. A similar observation was made in activated ROSA26-**GFP** mice (Fig. 33C, right column) confirming previous report from others[71].

This essentially complete degree of cell labeling in ROSA26-**RFP** was observed without variance in all mice analyzed (n=12). As previously observed by fluorescence stereoscopy (Fig. 33B), homozygous ROSA26-**RFP** showed a brighter fluorescence (mean intensity: $8.5x10^2$) than heterozygous animals (mean intensity: $5x10^2$) for a given cell suspension (lymph nodes and spleen). Cells of thymus and bone marrow showed heterogeneity with respect to fluorescence intensities (Fig. 34A). This was not due to partial recombination reactions at the reporter locus as intermediate products were not detected in ROSA26-**RFP** mice by Southern blotting or PCR (data not shown).

An experiment in which 5-Fluorouracil (5-FU) was injected in the peritoneum of ROSA26-**RFP** mice gave some hints on the biological relevance of

this fluorescence heterogeneity. 5-FU is a nucleotide analogue that inhibits the activity of thymidylate synthetase which affects pyrimidine synthesis and leads to depletion of intracellular TTP pools[147]. The resulting alteration of the balance of deoxynucleotide (dNTP) pools disrupts DNA synthesis, blocking cellular proliferation and cell cycle progression. Upon 5-FU i.p. (intra-peritoneum) injection of ROSA26-**RFP** animals, all bone marrow cells became tdRFP^{hi}. This effect was specifically seen with 5-FU injected animals. Control ROSA26-**RFP** mouse only injected i.p. with PBS had a normal heterogeneous profile of fluorescence intensity. Thus, the proliferation status seems to determine the overall fluorescence intensity of a cell (Fig. 34B). Full accumulation of tdRFP was only seen in resting cells.

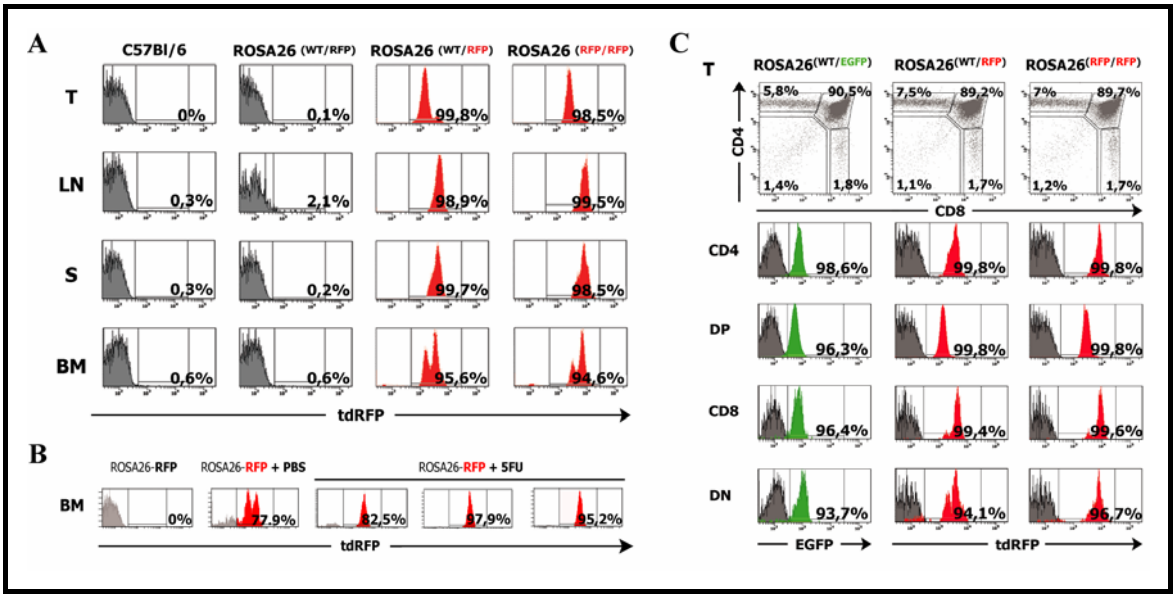

Figure 34: A. FACS analysis of erythrocyte-depleted, unfractionated hematopoietic cells from the indicated lymphoid organs of C57BL/6, floxed ROSA26-**RFP**, heterozygous and homozygous activated ROSA26-**RFP** animals. Red shaded histogram: tdRFP expressing cell; gray shaded histogram: tdRFP$^-$ controls. T: thymus, LN: lymph Nodes, S: spleen, BM: bone marrow. **B.** Flow cytometry analysis of 5-FU-treated unfractionated bone marrow cells of heterozygous ROSA26-**RFP** mice. The obvious heterogeneity with respect to fluorescence intensity is due to differences in cell cycle status of the bone marrow cells in untreated ROSA26-**RFP**. **C.** Comparison of fluorescence intensities between different thymocyte subsets of heterozygous and homozygous activated ROSA26-**RFP** mouse and a heterozygous activated ROSA26-**GFP** mouse[71]. The gates used to discriminate CD4/CD8 subpopulations are shown on each dot plots (top). The histograms show the fluorescence intensities of the different CD4/CD8 subsets. The gray shaded histograms (negative control) represent cells of the corresponding thymocyte subpopulations from a floxed ROSA26-**RFP** reporter mouse. DN: double negative, DP: double positive.

Flow cytometric analysis of the thymocyte compartments further showed that the level of red fluorescence is defined by the particular cell type and its developmental stage (Fig. 34C). Single positive CD4$^+$ and CD8$^+$ thymocytes were significantly more fluorescent double positive CD4$^+$CD8$^+$ immature thymocytes, which are highly proliferative. The double negative CD4$^-$CD8$^-$ pre-thymocytes show

an heterogenous level of fluorescence, which is expected as this subset is comprised of a mix of proliferating and resting cells. Similar heterogeneity in fluorescence intensity was observed in ROSA26-**GFP** mice (Fig. 34C, left column), confirming that this phenomenon was dependent on the biology of a cell and not associated with the mis-expression of our activated reporter. Flow cytometric analysis of thymocytes from ROSA26-**RFP** mice also showed that high level of tdRFP expression was not impairing the development of T-cells at any stage as the frequencies and absolute cell numbers of each subsets were similar to WT mice (data not shown). These data illustrate the complete absence of troublesome reporter expression variegation effects upon constitutive activation of tdRFP from the ROSA26 locus.

22.5. Inducible activation of ROSA26-RFP in T-cell specific Cre deleter mice

To test whether ROSA26-**RFP** reporter expression could be activated in a cell-type specific manner, ROSA26-**RFP** mice were inter-crossed with Lck-Cre transgenic animals[76]. The Lck-Cre deleter line is the most commonly used Cre-deleter strain for specific genomic manipulation in the T-cell compartment. Flow cytometric analysis of splenocytes from the resulting offspring revealed specific RFP expression activation in $CD3^+$ T-cells whereas $CD19^+$ B cells remained RFP^- (Fig. 35A). However, deletion patterns that were more complex than expected using transgenic Lck-Cre deleter mice, precluded a true quantification of reporter activation (presented in a later section).

To rigorously exclude any problem with lineage-specific activation of the ROSA26-**RFP** knock-in allele as explanation for the observed deletion fluctuations, we inter-crossed our reporter mice with pTα-iCre deleter mice. Progeny showed a highly specific and efficient (≈98%) labeling of T-lineage cells (see section 23.3). The high specificity and efficiency of reporter activation is illustrated in figure 35B. Upon a short para-formaldehyde fixation step, tdRFP retained its fluorescent properties and could be combined with immunohistochemistry stainings on histological sections for lineage tracing analysis. tdRFP fluorescence was exclusively found in the cytoplasm and nucleus of reporter activated cells in pTα-

iCre x ROSA26-RFP mice (Fig. 35B). In lymph nodes of such animals, virtually 100% of $CD3^+$ T lymphocytes expressed tdRFP whereas no $CD45R^+$ B-cells were labeled (Fig. 35B). Moreover, tdRFP proved sufficiently stable to support reliable detection of red fluorescence in all tdRFP-expressing cells even in fixed tissues using confocal microscopy (Fig. 35C). tdRFP reporter line is the second mouse strain expressing a Cre-inducible fluorescent protein from the ROSA26 locus that can be monitored efficiently both cytofluorometrically and histologically, adding an alternative to EYFP for multicolor lineage tracing analysis[85].

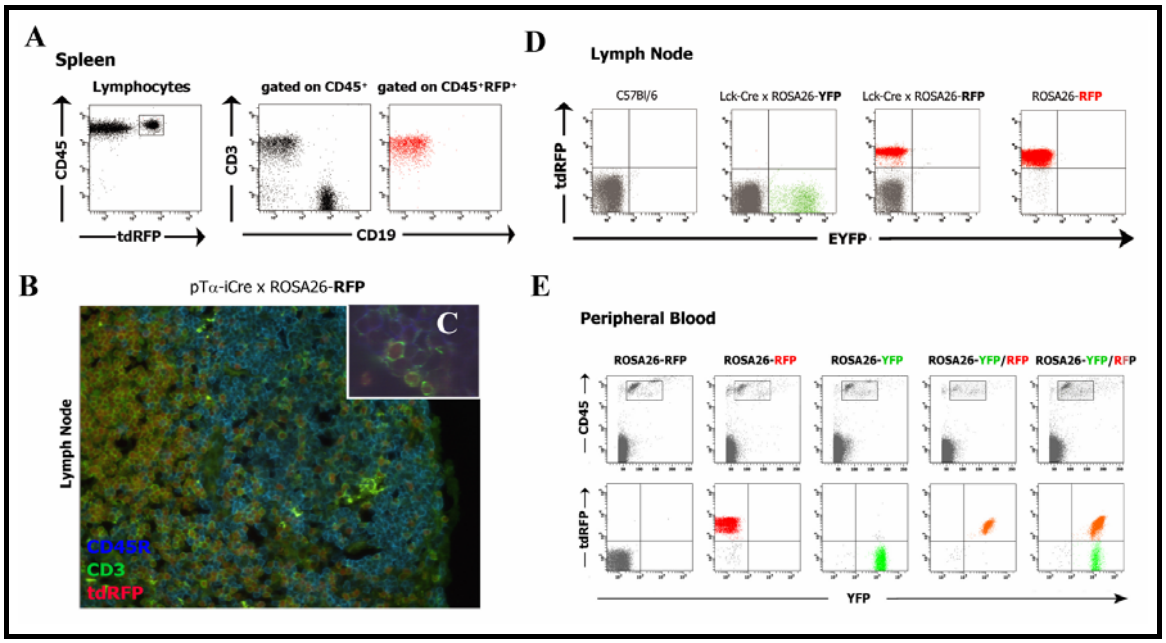

Figure 35: A. Specific activation of reporter expression in Lck-Cre x ROSA26-**RFP** mice. Dot plots of CD3/CD19 expression for total $CD45^+$ or $tdRFP^+CD45^+$ cells are shown. $CD3^+$ but not $CD19^+$ splenocytes express tdRFP, highlighting the T-cell specific induction of tdRFP expression in this T-cell specific Cre-deleter strain. **B.** Immunohistochemistry of lymph node section from a pTα–iCre x ROSA26-**RFP** mouse (magnification: 40x). Note that virtually 100% of $CD3^+$ cells (T-lymphocytes) exhibit red fluorescence. **C.** Confocal image of the section shown in B. **D.** Two-color-FACS analysis of lymph node cells of the indicated mouse strains, illustrating easy discrimination of tdRFP and YFP-expressing cells. The analysis of the individual samples was done with identical FACS Calibur instrument settings. **E.** Total peripheral blood cells were gated based on FSC/SSC and CD45 expression (not shown). Data are shown left to right from control C57BL/6 mice, mice heterozygous for a constitutively activated ROSA26 allele (either ROSA26-**RFP** or ROSA26-**YFP**), and triple-compound mice. These mice which were generated by mating an animal carrying a constitutively activated ROSA26-**YFP** allele and a ubiquitously deleting Cre transgene with a floxed ROSA26-**RFP** reporter mouse. Due to variegated expression of the Cre transgene, mice with mosaic activation of ROSA26-**RFP** allele allowed simultaneous detection and separation by FACS of RFP/YFP double positive cells from cells expressing only YFP fluorescent reporter.

These data illustrate the successful lineage-specific Cre-mediated activation of ROSA26-**RFP** reporter locus.

22.6. Full compatibility of tdRFP with EGFP and EYFP fluorescent reporter

For muticolor lineage tracing experiments, it would be useful to see whether tdRFP could be distinctly discriminated from commonly used EGFP or EYFP. We therefore analysed lymph node cells from germline activated ROSA26-**RFP** and ROSA26-**YFP** by FACS and showed that tdRFP expressing cells could be nicely separated from EYFP expressing cells using standard parameter cross-compensation (Fig. 35D). In addition, population of cells co-expressing tdRFP and EYFP could be detected and separated from single reporter expressing cells inside a same animal (Fig. 35E). To generate these mice, we took advantage of the previously described variegated Cre expression in huCMV-Cre transgenic mice (see section 22.2): we inter-crossed a mouse carrying an activated ROSA26-**YFP** allele with a floxed ROSA26-**RFP** mouse on a Cre deleter background. Resulting offspring showed occasionaly a chimeric activation of ROSA26-**RFP** reporter. Flow cytometry analysis of leukocytes from peripheral blood of heterozygous ROSA26-**RFP**, ROSA26-**YFP** or triple compound (huCMV-Cre/ROSA26-**YFP**/**RFP**) mice allowed the simultaneous visualization of single positive YFP^+, RFP^+ and double positive YFP^+RFP^+ cells. This is the first report of simultaneous detection of YFP^+ from YFP^+RFP^+ within the same animal, overcoming the technical limitation encountered when the pair of YFP/GFP reporters was combined[89] (see introduction, section 4.2).

22.7. ROSA26-RFP cells are primed for Recombinase Mediated Cassette Exchange (RMCE)

Expression of transgenes in mammalian cells or transgenic animals is difficult to control because it is markedly influenced by position effects[148]. Recombinase-mediated cassette exchange (RMCE) in ES cells should be useful to facilitate the insertion of multiple transgenes into well-characterized pre-targeted loci that imparts specific and reproducible regulation of transgenes in the mouse[149]. RMCE is a two-step procedure. First, recognition sites (loxP or Frt) for a site-specific recombinase (Cre or FlpE) are targeted to the locus of interest by homologous recombination. Second, site-specific recombination inserts a replacement sequence into this pre-tagged site[150]. Upon Cre-activation and

complete recombination reaction, the final configuration of ROSA26-**RFP** locus is RMCE primed as the tdRFP-p(A)n cassette is flanked by two incompatible lox sites (Fig. 36A). We asked whether we could use our activated reporter locus to exchange tdRFP to a floxed expression cassette at the ubiquitously expressed ROSA26 locus. *In vitro* generated ROSA26-**RFP** ES cells were transformed with an exchange vector (pX2GFP) bearing a floxed EGFP cDNA fused to BGH p(A)n sequence and a Cre-expression vector (pCre-AC). 18 hours post transfection, 200 $EGFP^{+}$ cells expressing Cre were sorted and single-cell deposited onto 96-well clusters. After 6 days of culture, the ES cell colonies were screened by eye whithout the use of a selective agent for the loss of tdRFP expression and gain EGFP fluorescence on an epifluorescence microscope.

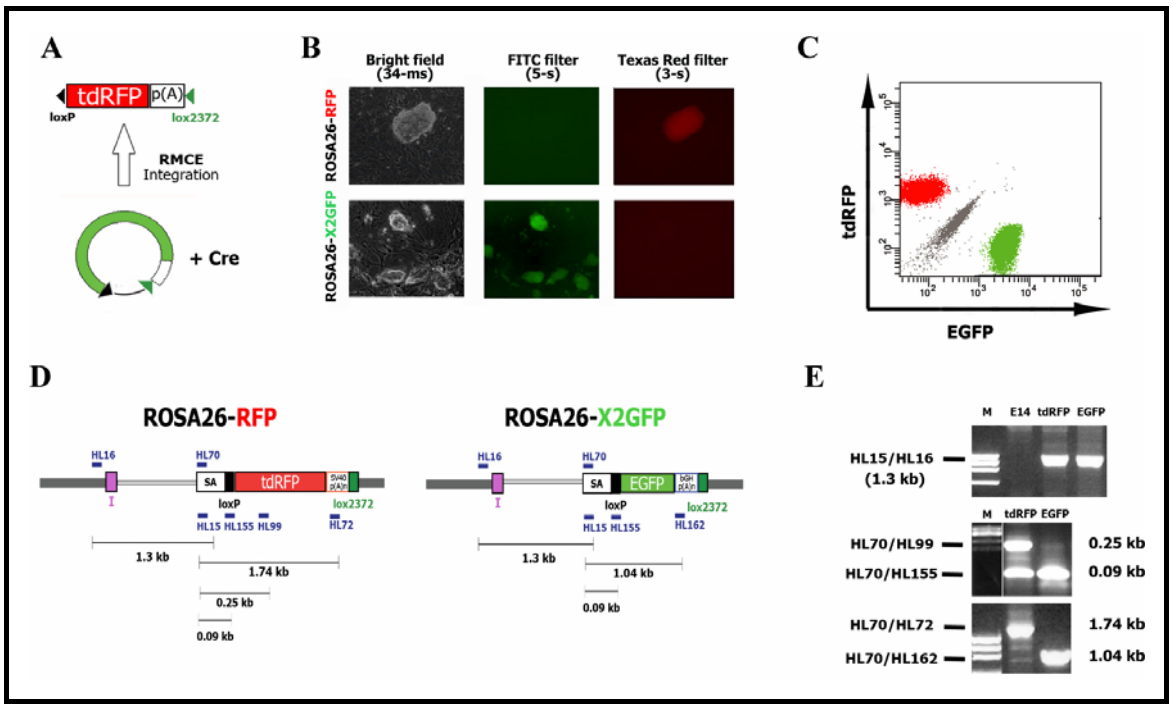

Figure 36: Recombination Mediated Cassette Exchange (RMCE) at the ROSA26 locus. **A.** Schematic representation of RMCE reaction. Cre recombinase catalyse the integration reaction of loxP/2372 flanked GFP-p(A)n cassette at the activated ROSA26-**RFP** cells. As the lox site flanking tdRFP and EGFP expression cassettes are incompatible, the integration remains stable. **B.** Fluorescence stereomicroscopy of ROSA26-**RFP** and ROSA26-**X2GFP** cells. Clones with exchanged ROSA26 locus lose tdRFP expression and display EGFP fluorescence. **C.** Concomittent detection of tdRFP and EGFP expressed from ROSA26 locus by FACS. tdRFP or EGFP-expressing cells can be separated in a mix of ROSA26-**RFP** and ROSA26-**X2GFP** ES cells. **D.** Schematic representation of activated ROSA26-**RFP** and exchanged ROSA26-**X2GFP** alleles. Primer location and size of amplified fragments used in (E) are shown. **E.** Characterization of the exchanged event by PCR. ROSA26-**RFP** and ROSA26-**X2GFP** maintained the knock-in allele (top). E14.1 genomic DNA was used as negative control. SA-loxP sequence was detected in both tdRFP and EGFP-expressing cells whereas tdRFP-specific fragment amplified using HL70/HL99 primer pair was absent in ROSA26-**X2GFP** (middle). The exchanged clone has lost tdRFP to EGFP expression cassette as observed by amplification of ROSA26-**X2GFP** but not ROSA26-**RFP** specific fragment (bottom).

Among 148 colonies recovered after the sort, 2 clones showed the expected fluorescence pattern. One of these exchanged clones (X2GFP#1) shown in figure 36B, was further characterized by PCR (Fig. 36 E). Amplification of a 1,3 kb

product using ROSA26 KI screening primers from X2GFP DNA confirmed that RMCE did not alter sequences of the ROSA26 targeted allele outside of the "floxed" fragment (Fig. 36D and E, top). No PCR product was amplified using primer pairs specific for the ROSA26-**RFP** allele [HL70/HL99 for SA-tdRFP] showing that tdRFP had been excised from the ROSA26 locus (Fig. 36E, middle). Finally, a multiplex PCR amplifying the whole reporter expression cassette in RMCE primed ROSA26-**RFP** [HL70/HL72 for SA-tdRFP-SV40 p(A)n] and in exchanged ROSA26-**X2GFP** allele [HL70/HL162 for SA-tdRFP-BGH p(A)n] proved that tdRFP had indeed been replaced to X2GFP at the ROSA26 locus (Fig. 36E, bottom). Southern blot analysis using a probe outside of the KI allele remains to be performed to unambiguously prove the exchange of tdRFP to X2GFP *via* RMCE.

Interestingly, while analysing a mixture of ROSA26-**X2GFP** and ROSA26-**RFP** cells by FACS (Fig. 36C), we noticed that ROSA26-**X2GFP** clones exhibited a much brighter fluorescence than observed in ROSA26-**GFP** KI animals (Mao *et al*[71]. and Fig. 36C) although the analysis was done with identical instrument settings. This discrepancy is of importance as ROSA26-**GFP** KI animals have been bearly used so far in lineage tracing experiments, mostly due to the really moderate fluorescence shift obtained after Cre-mediated activation of the reporter. Presence of a residual proviral sequence 5' of the reporter cassette in ROSA26-**EGFP**[71] but absent in ROSA26-**X2GFP** might explain this difference in EGFP level by negatively affecting EGFP expression. Alternatively, the EGFP-p(A)n cassette could have integrated a second time in a gene expressed in ES cells. Southern blotting analysis remains to exclude this possibility.

Taken together, these data illustrate the feasibility of selection-free RMCE to our activated ROSA26-**RFP** locus. The exchanged clones are easily detected using our screening method based on fluorescence expression. RMCE at the ROSA26 locus can allow for the rapid generation of reporter strains with enhanced detection properties to add more tint to the multicolor palette available for lineage tracing experiments.

23. THE PTα-ICRE DELETER MOUSE: A RELIABLE CRE KNOCK-IN STRAIN FOR EFFICIENT GENOME MANIPULATION IN T-LINEAGE CELLS

23.1. Non-toxicity of iCre-expression in pTα-iCre deleter mice

pTα-iCre deleter mice were successfully derived from E14.1 ES cells and backcrossed for at least 5 generations on C57BL/6 background. Heterozygous pTα-iCre mice were genotyped by multiplex PCR (Fig. 15B). These animals were fertile and had normal behavior. Cellularity of cell suspensions from several lymphoid organs was completely normal (data not shown) indicating that the level of iCre expression in these mice is well tolerated and not associated with Cre-mediated cell toxicity[151]. Inter-cross of heterozygous pTα-iCre animals produced offspring of all genotypes (data not shown). Homozygous progeny was viable and fertile. When backcrossed onto C57BL/6 background, pTα-iCre allele segregated with predicted Mendeleian ratio (data not shown). Homozygous pTα-iCre mice were used to maintain the deleter line or mated with homozygous ROSA26-**RFP** animals to generate pTα-iCre x ROSA26-**RFP** mice. Offspring were normal in regard to cellularity and proportion of all hematopoietic lineages (data not shown). These date illustrate the innocuity of pTα-iCre expression on mouse development.

23.2. Specific labelling of lymphoid organs in pTα-iCre x ROSA26-RFP mice

To assay the specificity of our pTα-iCre deleter strain, pTα-iCre x ROSA26-**RFP** reporter mice were analysed by epifluorescence stereoscopy (Fig. 37A). Whole body fluorescence intensity imaging showed bright fluorescence restricted to primary (thymus, spleen) and secondary (lymph nodes, tonsils, Peyer's patches, appendix) lymphoid organs (Fig. 37B). Reporter activation was delineating specific fluorescent zones in Peyer's patches and appendix (Fig. 37A).

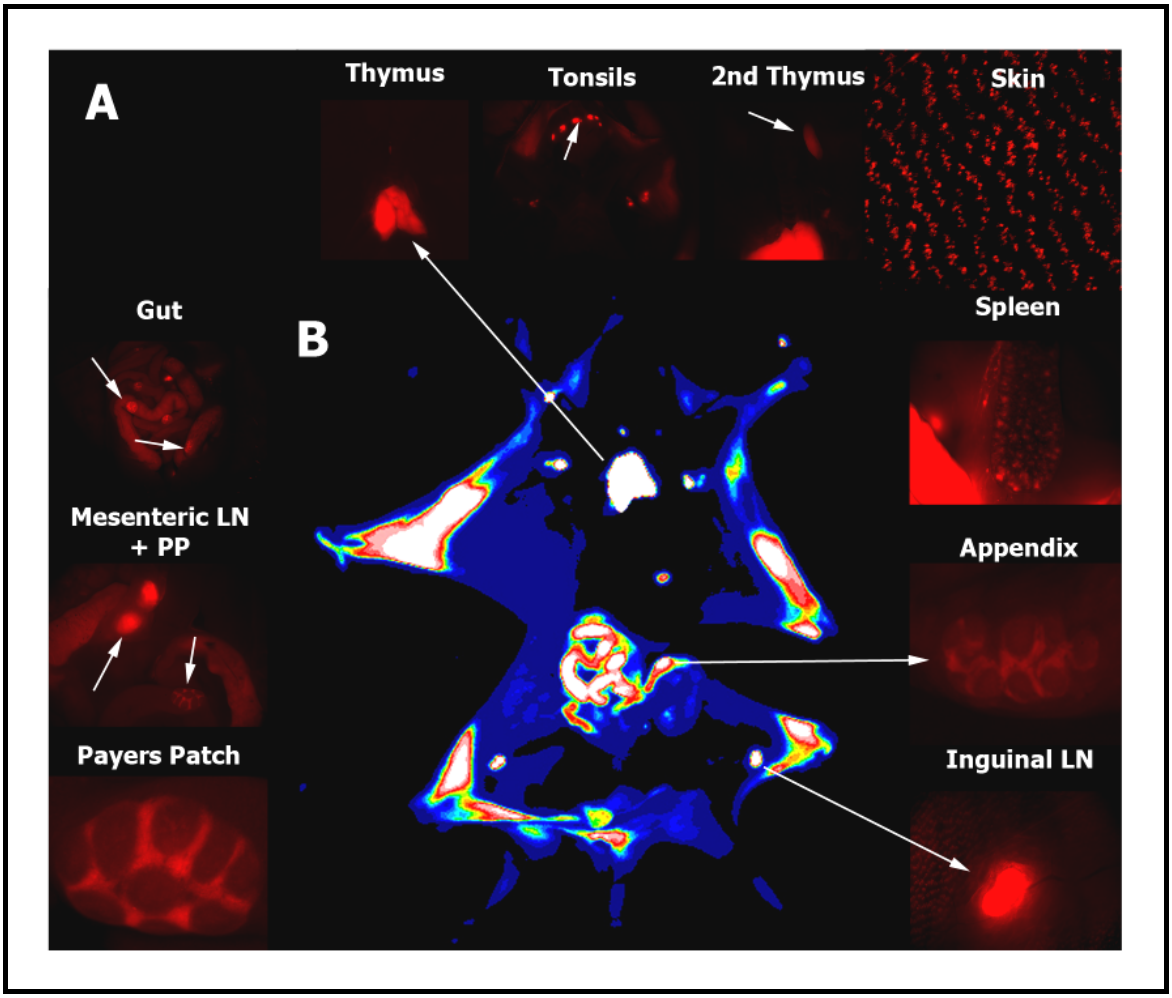

Figure 37: tdRFP expression in pTα-iCre x ROSA26-**RFP** mouse. **A.** Fluorescence spectroscopy of tissues in compound mouse confirmed presence of tdRFP-expressing cells in thymus (cervical and thoracic thymi), spleen, lymph nodes (axiliary, inguinal, mesenteric and tonsils), Peyers patches and appendix. The skin also showed a peculiar pattern of reporter activation. **B.** Intensity plot of whole-body fluorescence of a pTα-iCre x ROSA26-**RFP** mouse. Blue: low level of fluorescence expression, white: high level of fluorescence, black: no fluorescence. Area of high fluorescence intensity are restricted to lymphoid organs.

Interestingly, the skin of pTα-iCre x ROSA26-**RFP** was also labeled (Fig. 37A, top right). The discovery of this particular array of low intensity fluorescence pattern along the whole body of pTα-iCre x ROSA26-**RFP** animals is a surprising finding as the skin, beside dendritic epidermal T-cells (DETC), is not densely populated by cells of lymphoid origin.

Direct comparison of internal organs from pTα-iCre x ROSA26-**RFP** with floxed ROSA26-**RFP** and activated ROSA26-**RFP** control mice further illustrated the lymphoid specificity of reporter activation. Whereas heart, kidney and liver showed no detectable red fluorescence (Fig. 38A); thymus, spleen and lymph nodes were strongly fluorescent (Fig. 38B). The intensity of fluorescence in

pTα-iCre x ROSA26-**RFP** was lower than in ROSA26-**RFP** organs, suggesting that not all cells of lymphoid organs had activated RFP expression.

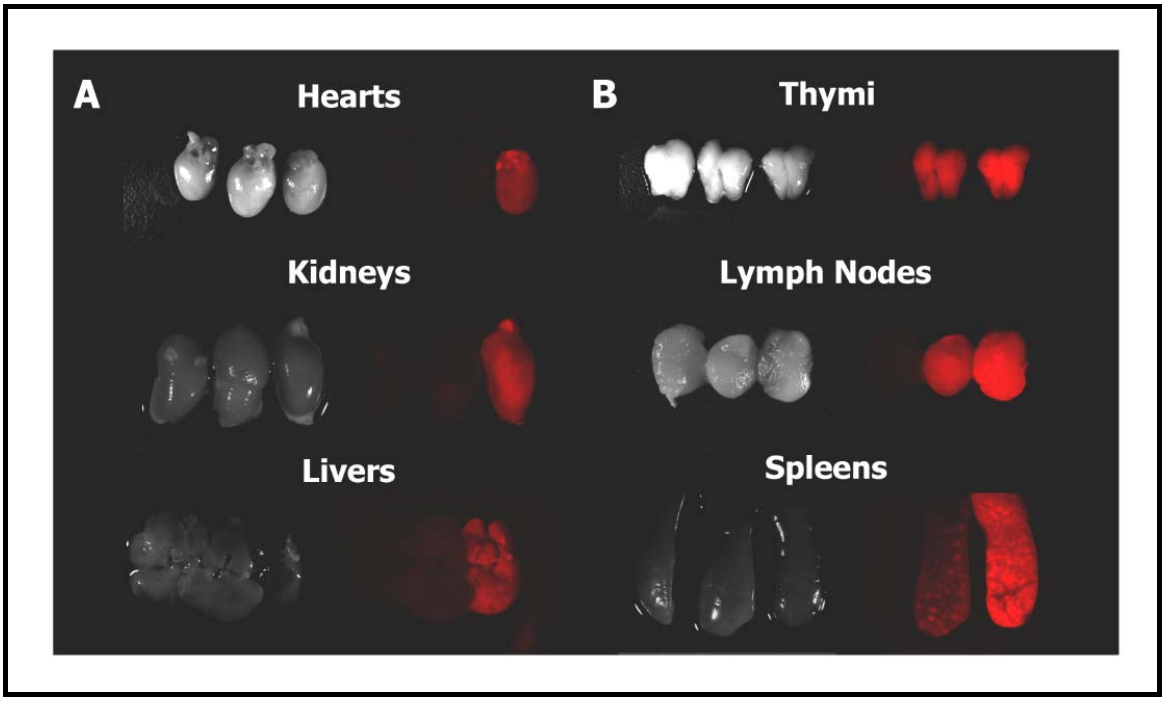

Figure 38: Comparison of fluorescence emission in adult tissues of pTα-iCre x ROSA26-**RFP** mouse (middle) with C57BL/6 negative control (left) and heterozygous ROSA26-**RFP** (right) animals. Fluorescence was not detected in heart, kindey and liver (**A**) in contrast to lymphoid organs (**B**) of pTα-iCre x ROSA26-**RFP** mouse in contrast to the ubiquitous expression observed in ROSA26-**RFP** animal. Note that fluorescence emission is restriced to areas in the spleen of pTα-iCre x ROSA26-**RFP.**

The most strinking difference was seen in the spleen (Fig. 38B, bottom). Fluorescence was specifically compartmentalized in circular areas. These peculiar fluorescent structures within the spleen were T-cell zones of the white pulp as observed by immunohistochemistry of pTα-iCre x ROSA26-**RFP** spleen sections. Specific reporter activation in $CD3^+$ T-cells was detected in zones surrounding unlabeled $CD19^+$ B-cells (Fig. 39A). Flow cytometry analysis of splenocytes allowed for the quantification of reporter activation efficiency. Virtually all (99%) of αβ-TCR^+CD3^+ T-cells were distinctly labeled in contrast to $CD3^-$ splenocytes which comprise mostly B-cells (Fig. 39B). Altogether, these data illustrate the high specificity of reporter expression in zones of lymphoid organs normally colonized by T-cells. Of note is the surprising fluorescence pattern seen in the skin which has been further addressed in section 23.4.

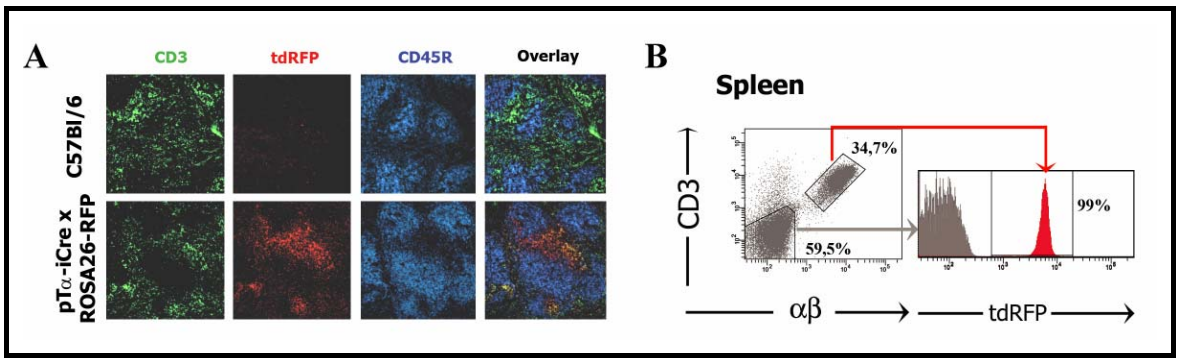

Figure 39: A. Specific localization of tdRFP expression to T cell zones in the spleen. Immunohistochemistry of spleen sections from a pTα-iCre x ROSA26-**RFP** mouse and a C57BL/6 control (magnification: 10x). $CD3^+$ splenocytes specifically express tdRFP in pTα-iCre x ROSA26-**RFP** animals. **B.** Faithful, lineage-specific induction of tdRFP expression in pTα-iCre mice. Flow cytometry analysis of splenocytes from a pTα-iCre x ROSA26-**RFP** mouse. The dot plots to the left show the position of the electronic gates for the identification of non-T lineage cells (gray) and TCRαβ-expressing T lymphocytes (red arrow). Note that virtually all αβ T-cells exhibit strong uniform red fluorescence.

23.3. Specific reporter activation in all T-related lineages of pTα-iCre x ROSA26-RFP mice

Our system allows the identification of cells that go through a pTα-expressing stage. Rigorous inspection of all lineages of the hematopoietic system by flow cytometry demonstrated a T-cell specificity of reporter activation of our pTα-iCre deleter line. Cells of myeloid and erythroid lineage (Fig. 40A) were not marked in pTα-iCre x ROSA26-**RFP** mice suggesting that pTα is not expressed in progenitors and mature cells of lineages branching off early the T-cell developmental pathway (see introduction, section 1.1). Among the lymphoid lineage, T and B-cells are developmentally linked and thought to share a common progenitor in the bone marrow (CLP)[18]. Splenic and thymic $CD19^+$ B cells were completely lacking reporter activation (Fig. 40B). In contrary, ≈ 98% of $CD3^+$ T-cells in the thymus and in the periphery had activate the reporter (Fig. 40B). Exclusive reporter activation in T but not B-cells indicates that pTα-iCre expression occurs after the T/B lineage decision. This is an interesting finding as it challenges results obtained from others in which the expression of a pTα-controlled reporter was already detected in the CLP progenitor population[22, 24]. This discrepancy will be questioned further in a next section (24.3) by delineating the expression of pTα-iCre in BM subsets.

Abolition of NK-T cell development in pTα KO mice[48] showed that NK-T cell was linked to T cell development as opposed to NK cells which were found at

normal cell number and frequencies. Not surprisingly, almost all NK-T cells were labeled (97 % in the thymus) in pTα-iCre x ROSA26-**RFP** mice (Fig. 40C) whereas NK cells did not activate the reporter locus. This result confirms that NK-T cells represent a distinct lineage of NK cells which express pTα during its development. In contrast, pTα is not expressed during NK-cell development.

αβ but not γδ-T cell development is severely impaired in pTα KO mice. This fact might infer that expression of the pre-TCR is required to direct immature thymocytes to the αβ-lineage. Normal αβ *vs* γδ lineage commitment could take place *via* stochastic expression of pre-TCR components exclusively in αβ-T cell precursors or an instructive signal driven by the pre-TCR upon productive β-chain rearrangement (see introduction, section 1.5). In order to test whether pTα expression could be used as a lineage marker for αβ-T cells, we analysed the degree of reporter activation in αβ and γδ-T cells in the thymus (Fig. 41A). The high level of tdRFP labelling found in thymic γδ-T cell of pTα-iCre x ROSA26-**RFP** animals unambiguously prove that most γδ-T cell are derived from pTα–expressing precursors at one stage of their development. This result is the first genetical evidence that pTα might be expressed in both αβ and γδ-T cell precursors. Thus, pTα-expression is not a marker for αβ *vs* γδ-T cell lineage commitment which is in itself a strong indication for the instructive role of the pre-TCR in this lineage decision.

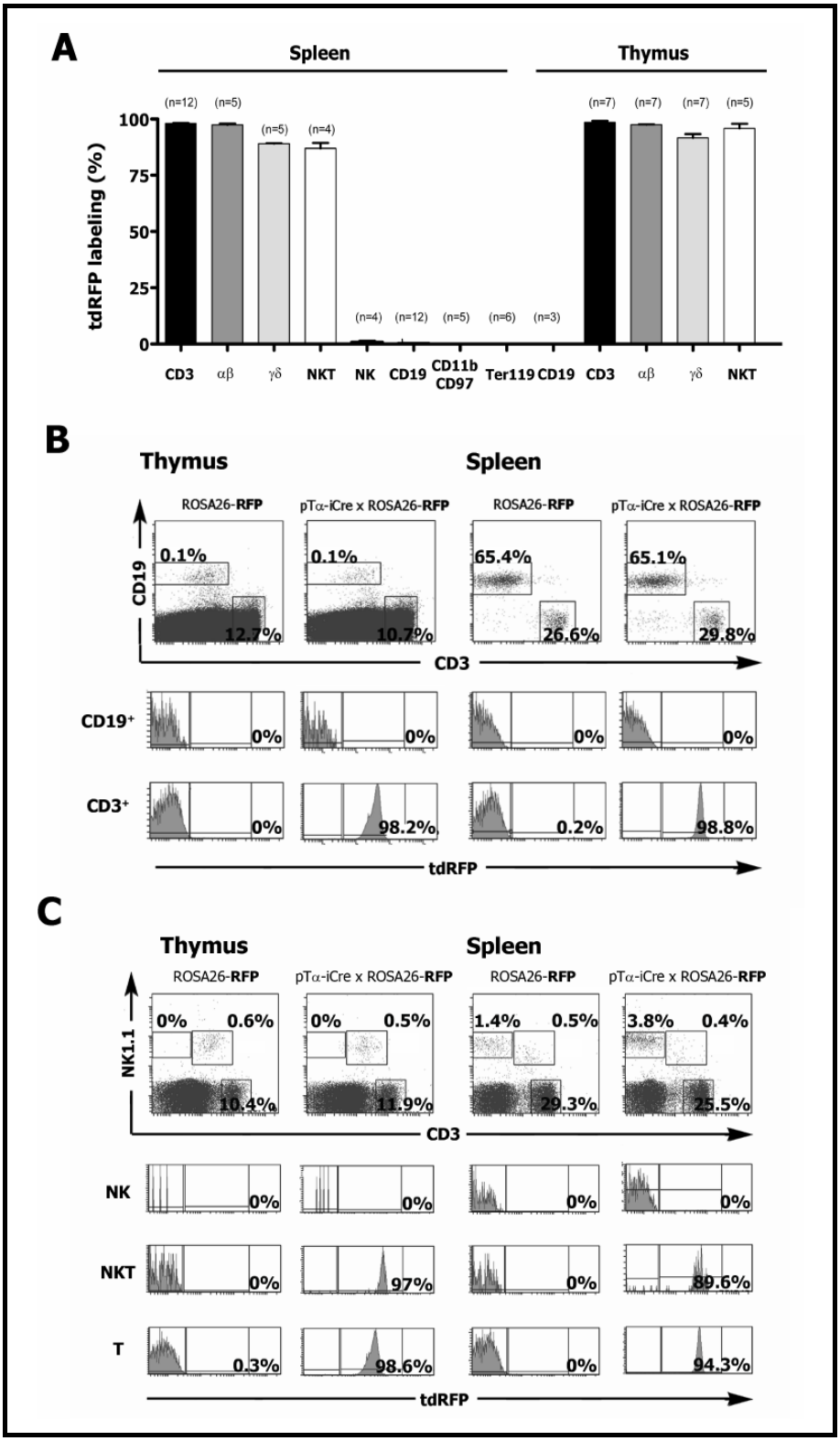

Figure 40: Reporter activation is restricted to T-cell related lineages in pTα-iCre x ROSA26-**RFP** mice. **A.** tdRFP expressing cells are only found in αβ, γδ $CD3^+$ and NKT-cells in the thymus and in the periphery (spleen). The number of animal analysed *per* lymphoid subset is indicated on top of each corresponding bar. **B.** Flow cytometry analysis of thymocytes and splenocytes from a pTα-iCre x ROSA26-**RFP** mouse and a C57BL/6 control. The dot plots (top) show the position of the electronic gates used for the identification of B-cells and CD3-expressing T lymphocytes. In both thymus and spleen, fluorescence emission was specifically detected in T-cells (≈ 98%). **C.** Similar approach was used to analyse tdRFP expression among the NK-lineage cells. The gates used to discriminate NK/NKT/T-cell subpopulations are shown on each dot plots (top). The histograms show the fluorescence intensities of the corresponding subsets.

Most of γδ-T cells express pTα during their development and activates the reporter locus. Interestingly, we reproducibly noticed a lower degree of γδ-T cell labeling compared to αβ-T cells (Fig. 41B). On average, 91.7±4.46% of γδ-T activated the reporter in the thymus as opposed to 97.5±0.62% for αβ-T cells. Efficiency of labeling was even lower in the periphery (88.1±2.52%) whereas the proportion of reporter expressing cells remained constant for αβ-T cells (97.4±0.59%). This somewhat lower level of reporter expression was not due to specific silencing of ROSA26 locus in a subset of γδ-T cells as virtually all (99%) γδ-T cells in ROSA26-**RFP** mice were tdRFP$^+$ (Fig. 41D). We hypothesized that these tdRFP$^-$ γδ-T cells might express a certain subtype of γδ-TCR at their cell surface. To see whether tdRFP$^-$ γδ-T cells express a peculiar type of Vγ chain, thymocytes from pTα-iCre x ROSA26-**RFP**, floxed ROSA26-**RFP** and constitutively activated ROSA26-**RFP** mice were stained for anti-Vγ chain antibodies, CD3 and γδ-TCR. CD3$^+$γδ-TCR$^+$ total thymocytes expressed normal frequencies for each Vγ1, 4, 5 and 7 chains (Vγ chain numbers according to Tonegawa's classification[152]) in pTα-iCre x ROSA26-**RFP** (Fig. 41C). No obvious bias of tdRFP labeling was seen in γδ-T cells expressing each type of Vγ chain (Fig. 41D) inferring that tdRFP$^-$ cells were found at similar frequencies in all Vγ-expressing γδ-thymocytes.

All together, these data illustrate that pTα-iCre deleter mice label specifically and efficiently (almost completely) all T-cell related lineages (αβ-, γδ- and NK-T cells). Our results show for the first time that most thymic γδ-T cells (≈ 95%) expressed pTα at one stage of their development which is a prerequisite for the instructive model of αβ *vs* γδ-T cell lineage commitment[153]. The somewhat lower level of RFP labeling in γδ-T cells might infer that few immature thymocytes are committed to the γδ-T cell lineage before the onset of pTα expression. We are at present performing more experiments (RT-PCR analysis on sorted tdRFP$^-$γδ-T cells, PCR amplification of β-chain rearrangements) to further characterize this interesting population of unlabeled γδ thymocytes.

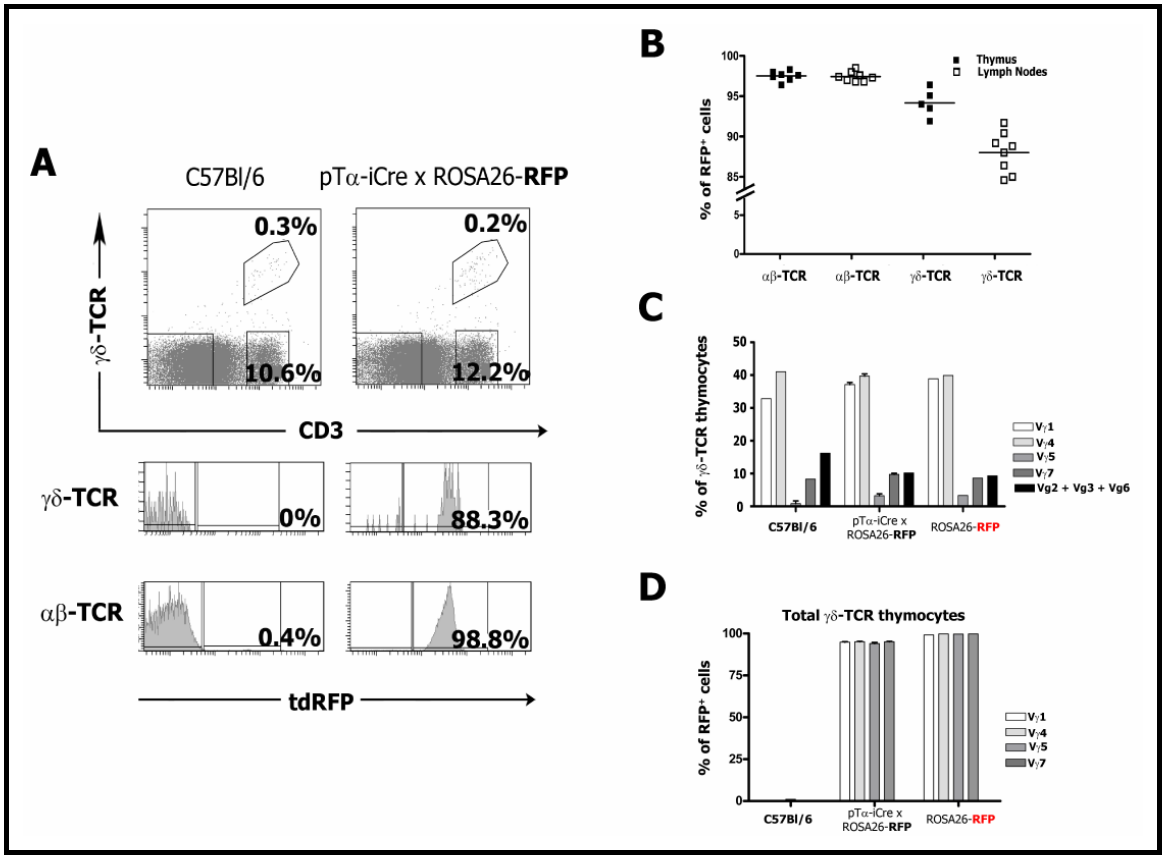

Figure 41: A. γδ-T cells are efficiently labeled in pTα-iCre x ROSA26-**RFP** mouse. Flow cytometry analysis of thymocytes from a pTα-iCre x ROSA26-**RFP** mouse and a C57BL/6 control. The dot plots (top) show the position of the electronic gates used for the identification of αβ and γδ CD3-expressing thymocytes. ≈ 90% of γδ-T cells expressed the reporter. **B.** Somewhat reproducible lower reporter activation in γδ than in αβ-T cells of thymus (■) and lymph node (□). **C.** γδ-T cells show normal Vγ-chain usage in pTα-iCre x ROSA26-**RFP** mouse as compared to C57BL/6 control. Total thymocytes were at first gated on FSC/SSC and γδ-TCR/CD3 expression (not shown). Percentage of total γδ-TCR$^+$CD3$^+$ cells expressing each Vγ chain. Data are shown left to right from control C57BL/6 mouse, pTα-iCre x ROSA26-**RFP** mouse and a constitutively activated ROSA26-**RFP** allele. **D.** No bias of reporter activation in γδ T-cell subtypes. γδ T-cells with particular Vγ-chains express similar level of tdRFP. Note the constant somewhat lower reporter activation observed in pTα-iCre x ROSA26-**RFP** mouse compared to constitutively activated ROSA26-**RFP** control.

23.4. pTα-iCre marks dendritic epidermal T-cells (DETC) in the murine skin

As previously reported, direct comparison of the skin of pTα-iCre x ROSA26-**RFP** with floxed ROSA26-**RFP** and constitutively activated ROSA26-**RFP** animals revealed a distinct and organised fluorescence pattern (Fig. 42A). To identify the nature of the cells responsible for these arrays of tdRFP fluorescence in pTα-iCre x ROSA26-**RFP** animals, we first looked at subsets of T-cells known to reside in the murine skin. The main population of T-cells in the murine epidermis are γδ-T cells expressing a distinct subtype of γδ-TCR[34]. The Vγ5/Vδ1 γδ-T cells referred to as dendritic epidermal T cells (DETC), are exclusively produced by the fetal thymus since DETC development cannot be supported by an adult thymus[34].

These cells express CD90.1, CD3 and form a continuous network among the basal layer of keratinocytes[34].

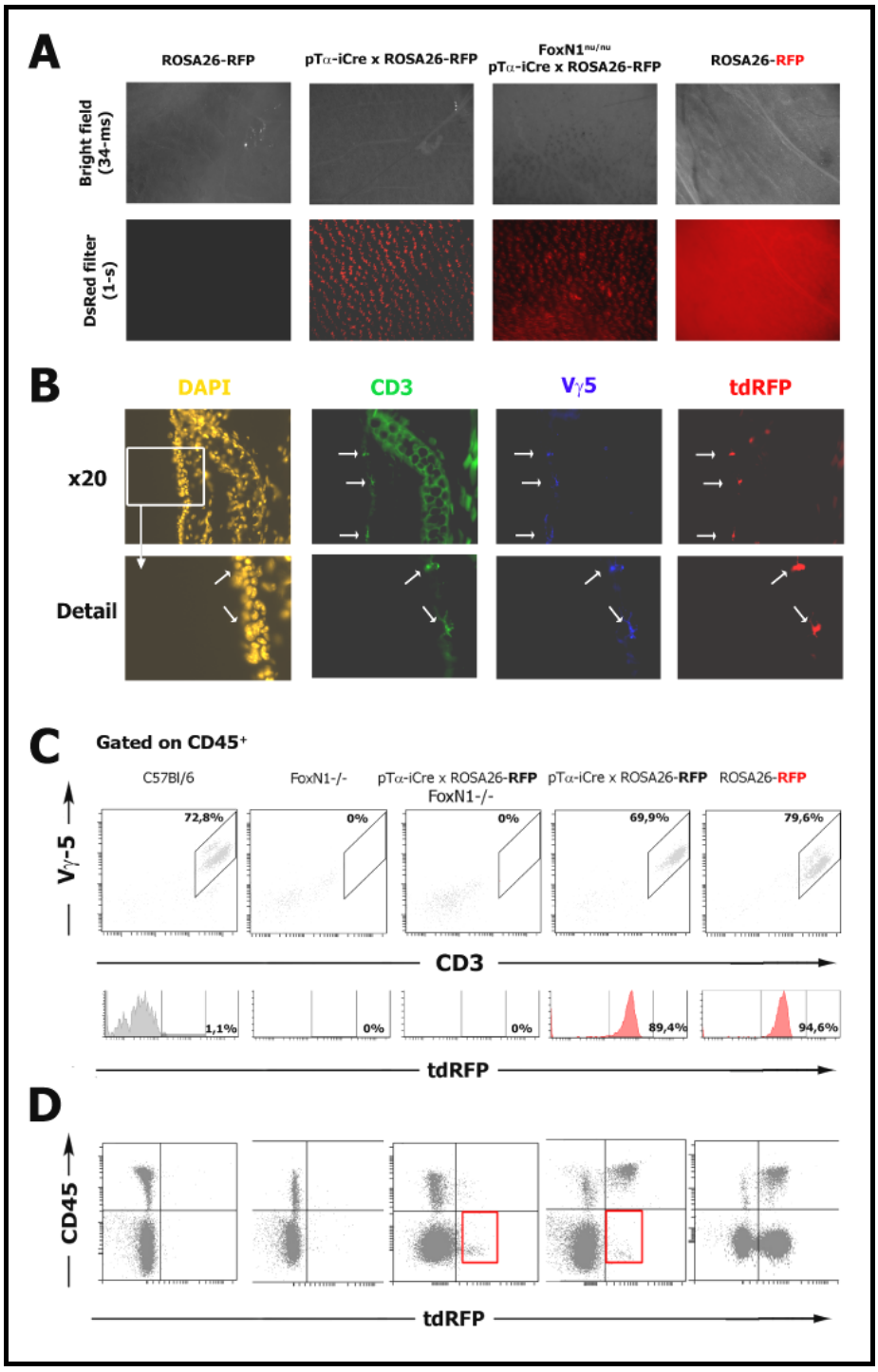

Figure 42: tdRFP expression in the skin of pTα-iCre x ROSA26-**RFP** animals. **A.** Skin details of the indicated mouse strains seen by fluorescence stereoscopy.The unusual fluorescent reporter activation pattern is specifically observed in pTα-iCre x ROSA26-**RFP** mice on WT and nude background. Green autofluorescence was substracted from the fluorescence observed in the red chanel using Openlab processing software to get a better resolution of tdRFP expressing cells (magnification: 5x, exposure time: 2s). **B.** Dendritic epidermal T-cells are labeled in pTα-iCre x ROSA26-**RFP** animals. Immunohistochemistry of an ear section from a pTα-iCre x ROSA26-**RFP** animal (magnification: 20x). $V\gamma5^{+}CD3^{+}$ DETCs are indicated with white arrowheads. **C.** Skin DETC express tdRFP. Quantitative analysis of tdRFP expression in epidermal cells of indicated mouse strains by FACS. Extracted cells were gated based on FSC/SSC and expression of the pan-hematopoietic marker CD45 (not shown). $FoxN1^{(nu/nu)}$ animals are devoid of DETC. **D.** Total cells from ear suspension were analysed for the expression of CD45 and tdRFP. Some $CD45^{-}$ cells express tdRFP in the skin of pTα-iCre x ROSA26-**RFP** on C57BL/6 and nude background (red rectangular).

Immunohistochemistry analysis of mouse ears showed specific tdRFP fluoresence emission in pTα-iCre x ROSA26-**RFP** (Fig. 42B) compared to ROSA26-**RFP** (data not shown). tdRFP$^+$ cells were stained positive for CD3 and Vγ5 cell surface antigens (Fig. 42B) and presented the characteristic dendritic shape of DETC cells (Fig. 42B).To quantify the level of DETC expressing the reporter in our deleter mice, epidermal cell suspensions of ears from several mouse strains were prepared using mild enzymatic digestion and were subsequently stained for CD3, Vγ5 and the pan-hematopoietic marker CD45. DETCs (CD45$^+$CD3$^+$Vγ5$^+$) were the main population of cells of hematopoietic origin ($\approx$ 70%) and encompassed all CD3$^+$ expressing cells in our skin preparation (Fig. 42C). As expected, no DETC of C57BL/6 control mice showed reporter activation (Fig. 42C) whereas $\approx$ 90% of DETC in pTα-iCre x ROSA26-**RFP** were expressing tdRFP [Note that the number of cells expressing the reporter might be underestimated. This preliminary experiment was done without live staining and need to be repeated for a careful evaluation of RFP$^+$ frequency in DETC cell type]. We confirmed the identity of CD45$^+$CD3$^+$Vγ5$^+$ cells by analysing epidermal cell suspensions of athymic FoxN1$^{nu/nu}$ (nude) animals in which DETCs development is abbrogated. As expected, DETC could neither be detected in nude nor in compound pTα-iCre x ROSA26-**RFP** nude animals.

Reporter activation in DETC cell-type could not solely explain the red fluorescence emitted in the skin as athymic FoxN1$^{nu/nu}$ pTα-iCre x ROSA26-**RFP** animals, devoid of DETCs (Fig. 42C), showed the same pattern of reporter expression (Fig. 42A). FACS analysis of total cell suspension from mouse ears of several strains demonstrated the presence of an additional CD45$^-$ cell population expressing the reporter specifcally in pTα-iCre x ROSA26-**RFP** animal and its nude counterpart (Fig. 42D). Immunohistochemistry of skin sections from pTα-iCre x ROSA26-**RFP** mice revealed labeling of cells located around the end of the bulb of hair follicules (Fig. 43, indicated with *). Careful examination of hair follicules in control C57BL/6 mice never showed background fluorescence at this location apart from the hair shaft which emitted strong autofluorescence both in the green and red channel (Fig. 43, top, indicated with H and pointing arrow). Interestingly, these RFP$^+$ cells were not CD3$^+$ in contrast to DETCs as detected by histology

(Fig. 43). More experiment are needed to better characterized these interesting cells and to understand why they are specifically labeled in pTα-iCre lines. Taken together, these data illustrate that pTα should be expressed really early during thymus ontogeny as the first waves of γδ-T cells produced in fetal thymus are labeled by pTα-iCre. pTα-iCre could be applied for studying fetal thymopoiesis.

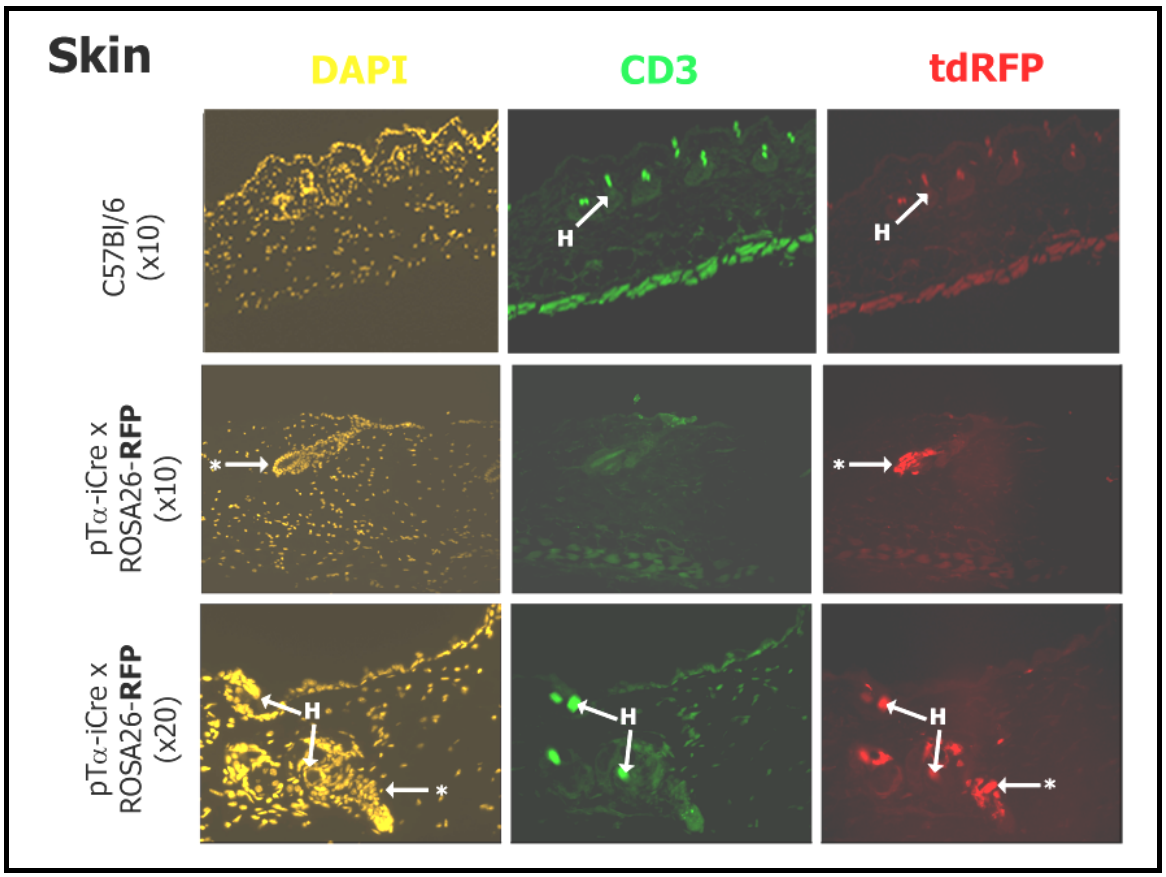

Figure 43: Immunohistochemistry of skin section from a pTα-iCre x ROSA26-**RFP** and C57BL/6 control mouse (magnification indicated). $CD3^-$ tdRFP-expressing cells were found at the bulge of hair follicules. H: hair autofluorescence, *: tdRFP labeled hair follicule.

23.5. pTα-iCre expression labels extrathymic T cell development

In the absence of a thymus, residual T lymphopoiesis occurs mainly in the mesenteric lymph node and less in the Peyer's patches[154]. Ontogenic steps of this lymphopoiesis resemble those of thymopoiesis[155], but present an apparent bias towards γδ-T cell production with a paucity of polyclonal αβ-T cells[154]. To see whether pTα was expressed in unconventional extrathymic T-cells, we analysed pTα-iCre x ROSA26-**RFP** mice on a nude background. Fluorescence stereoscopy of Peyer's Patches (PP) and inguinal lymph nodes (ILN) from euthymic and athmic mice showed specific labeling in both lymphoid organs (Fig. 44A). Fluorescence

was bearly detectable in Peyer's Patch of pTα-iCre x ROSA26-**RFP** FoxN1$^{nu/nu}$ compared to euthymic counterpart. Although of weak intensity, Peyer's Patch fluorescence was exclusively restricted to the interfollicular T-cell zone as in pTα-iCre x ROSA26-**RFP** animals. Inguinal lymph nodes of nude pTα-iCre x ROSA26-**RFP** mice were larger than in euthymic animals but exhibited less reporter activation. FACS analysis of PP cell suspension was conducted to see whether the observed low intensity of fluorescence was due to an inefficient reporter activation in T cells produced from the extrathymic pathway (Fig. 44B). Notably, B cells were not labeled in both euthymic and athymic mice. Although under-represented in the PP of athymic mice (0.4 to 4%) compared to euthymic mice (10-15%), $CD3^+$ T-cells in nude animals activated the reporter expression as efficiently as in euthymic mice (96%). More experiments are currently performed to search for the onset of reporter activation to map the early events of extrathymic development. One can already conclude from these initial experiments that alike thymopoiesis, extrathymic T-cell production necessarily goes through a pTα expressing stage. In addition, the overall fluorescence intensity of the reporter is directly correlated to the number of T-lineage cells residing in a given organ, which opens new avenues for live cell imaging and monitoring of extrathymic immune response. These preliminary data illustrate that pTα-iCre deleter mice should be extremely useful for T-cell specific deletion of genes involved in extrathymic T-cell development in athymic mice.

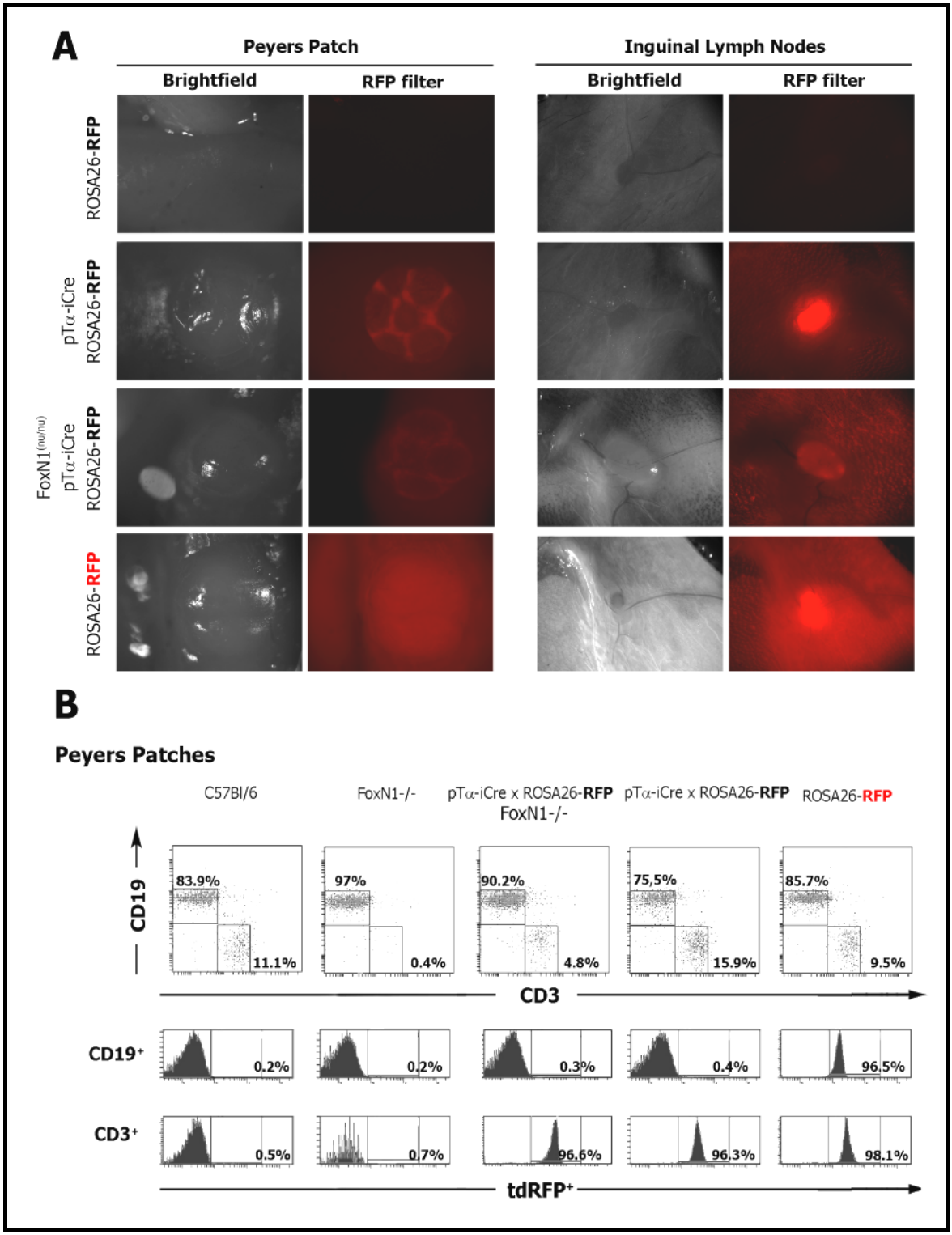

Figure 44: tdRFP expression in extrathymic T-cell development. **A.** Fluorescence spectromacroscopy of Peyers Patch and inguinal lymph nodes of the indicated mouse strains. pTα-iCre x ROSA26-**RFP** mice on C57BL/6 and nude background showed similar pattern of reporter activation in T-cell zones of Peyers Patch (magnification: 3.5x, exposure time: 2s). ILN of FoxN1$^{(nu/nu)}$ are larger and less fluorescent than euthymic counterpart (magnification: 1x, exposure time: 1s). Green autofluorescence was subtracted to the fluorescence observed in red chanel for a better resolution of tdRFP expressing cells. **B.** Quantitative analysis of tdRFP expression in T-lymphocytes of indicated mouse strains by FACS. Extracted PP cells were gated on lymphocytes based on FSC/SSC and expression of the pan-hematopoietic marker CD45 (not shown). The dot plots (top) show the position of the electronic gates used for the identification of B- and CD3-expressing T-lymphocytes. In both athymic and euthymic pTα-iCre x ROSA26-**RFP** mice, fluorescence emission was specifically detected in ≈ 96% of T-cells. The variation of CD3$^+$ cell frequency between both athymic mice is normal and often seen in nude animals.

24. pTα-iCre Marks efficiently early stages of T-cell development

T cells are generated in the thymus after colonization by bone marrow-derived progenitors *via* the peripheral blood. To investigate whether pTα expression could mark early stages of thymocyte development, we sought for the most immature T-cell subset with reporter activation.

24.1. Onset of pTα-iCre–mediated reporter activation in the thymus

The development of T lymphocytes involves multiple steps of progressive cellular differentiation that can be resolved using cell surface expression of CD4 and CD8 markers. Flow cytometry analysis of pTα-iCre x ROSA26-**RFP** thymoctes showed that essentially all single positive (SP) $CD4^+$ (99%) or $CD8^+$ (98%) naive T-cells were expressing the reporter (Fig. 45A). Double positive $CD4^+CD8^+$ immature T-cells exhibited a similarly high degree of reporter activation (98.4%). The double negative $CD4^-CD8^-$ subset, which contains the most immature thymocyte population, showed consistently a lower number of labelled cells (69.5%). The triple negative subset, defined by the absence of CD4, CD8 and CD3, can be further sub-divided into developmentaly linked subpopulations according to CD44 and CD25 cell surface expression: TN1, TN2 TN3 and TN4 (see section 1.3, introduction). Reporter activation in TN subsets of pTα-iCre x ROSA26-**RFP** animals (n=5) showed similar results without variance (Fig. 45B). 13.3±2.8% of cells in the most primitive subset (TN1) were expressing the reporter. Surprisingly, TN2, the consecutive developmental stage, entailed 10 times less $tdRFP^+$ cells (2±0.5%). To discriminate TN2 from TN3 cells, gates were carefully set according to CD117 expression. The proportion of $tdRFP^+$ cells further increased in TN3 (36,1±7.4%) to reach a maximum of labeling in the TN4 subset (91±3.5%). A similar pattern of fluorescence was observed in pTα-iCre x ROSA26-**YFP** animals (Fig. 45B): the TN2 subset contained less cells with an activated reporter (6%) than TN1 (44%); EYFP expression was massively upregulated in TN3 cells (86.9%) to reach a maximum in the TN4 subset (98.7%). In conclusion, the increase in reporter activation between TN2 and TN3 stages is observed in two independent reporter mice, thus most likely correctly reflecting the sequential activation of pTα transcription.

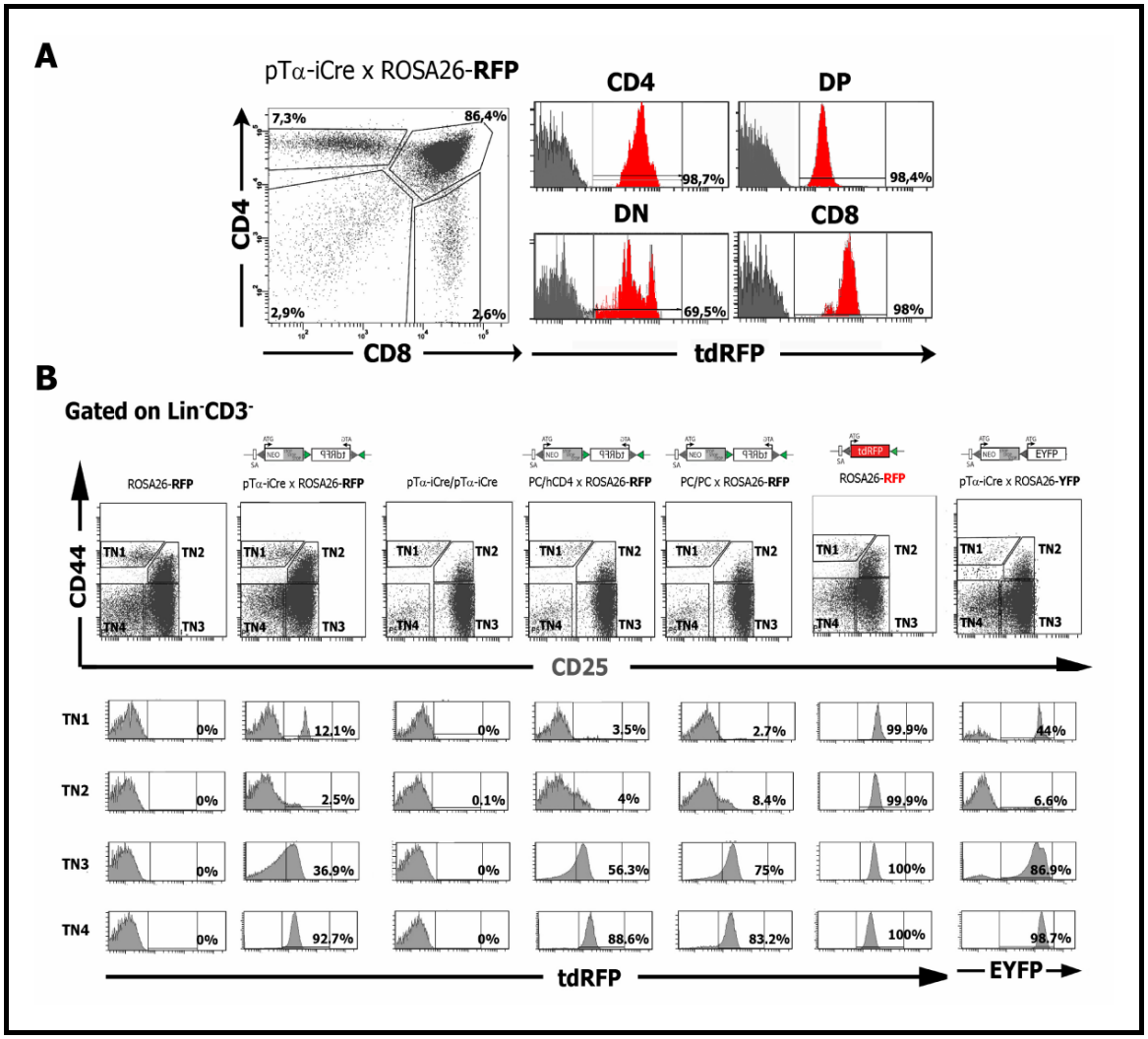

Figure 45: Quantitative analysis of tdRFP expression in thymocytes of pTα-iCre x ROSA26-**RFP** mice by FACS. **A.** Extracted thymocytes were gated on lymphocytes based on FSC/SSC (not shown). The dot plots (left) show the position of the electronic gates used for the identification of single positive CD4 and CD8, double positive (DP) and double negative (DN) subsets. The histograms (right) show the fluorescence intensities of the different CD4/CD8 subsets. The gray shaded histograms (negative control) represent cells of the corresponding thymocyte sub-populations from a floxed ROSA26-**RFP** reporter mouse. Fluorescence emission was maximal (≈ 98%) in DP, CD4 and CD8 SP. tdRFP expression was somewhat less in DN subset. **B.** Onset of tdRFP expression in TN2 subset. The dot plots (top) show the position of the electronic gates used for the identification of TN subsets. The histograms show the fluorescence intensities of the different CD44/CD25 subsets of corresponding mouse strains. PC: pTα-iCre.

The difference in proportion of TN1 and TN2 cells expressing the reporter seemed puzzeling. To understand this discrepancy, we subdivided the heterogeneous TN1 subset according to CD117 expression. Early thymic progenitors (ETP)[30] found in the CD117^{high} TN1 subset (see section 1.4, introduction) were neither labeled in pTα-iCre x ROSA26-**RFP** nor in pTα-iCre x ROSA26-**YFP** animals (Fig. 46A). Futher refinement of TN1 cells using CD24 expression according to the scheme of Petrie *et al.*[33] confirmed this observation (Fig. 46B): TN1c (8.4±4.5%), d (38.4±4.4%) and e (96.5±5.2%) but not TN1a+b which contains the ETP, had detectable reporter expression in pTα-iCre deleter mice. One possibility to explain this result is to assume that the amount of Cre

recombinase might be too low in ETP for efficient reporter activation, despite pTα-transcription. Analysis of mice (n=5) homozygous for pTα-iCre revealed a significant increase in the proportion of TN2 (6.8±3.9%) and TN3 (62.5±9.7%) cells expressing tdRFP supporting the hypothesis to some extent (Fig. 45B). This increase was not completely attributable to changes in the cellular composition in the thymus of pTα KO mice as control $pT\alpha^{(iCre/hCD4)}$ KO mice with a single pTα-iCre allele did not confer a similar level of reporter activation in TN2 (4%) and TN3 (56.3%) subsets. These results demonstrate that doubling the expression of iCre in homozygous pTα-iCre reporter mice can indeed increase the proportion of cells activating the reporter in TN2/TN3 subsets somewhat. However, $CD117^{hi}$TN1 cells remained unlabeled in these mice (Fig. 46A).

The observed lack in marker activation can be interpreted in at least two ways. The most straight-forward explanation would be that the mainstream ETP does not yet express pTα. Alternatively, cells of the ETP stage might exit this earliest maturational stage too rapidly, leaving not sufficient time for Cre-mediated recombination of the targeted ROSA26 locus and maturation of tdRFP protein. Rigorous inspection of endogenous pTα expression in TN subsets using a highly sensitive RT-PCR assay (Fig. 46C) strongly supported the first hypothesis. TN1c and d but not TN1a+b express pTα. The nature of cells expressing pTα in TN1c and d subsets is unclear and remains to be investigated. Endogenous pTα transcripts were detected at increasing levels in consecutive developmental stages. The peak of pTα expression was found at the TN3 stage, which correlates with the massive upregulation and accumulation of tdRFP in pTα-iCre x ROSA26-**RFP** mice. Taken together, these data demonstrate that the mainstream ETP is not labeled in pTα-iCre x ROSA26-**RFP** mice and that the onset of reporter activation takes place at the TN2 stage of classical thymopoiesis. More experiments are required to better characterize TN1c/d cells expressing pTα.

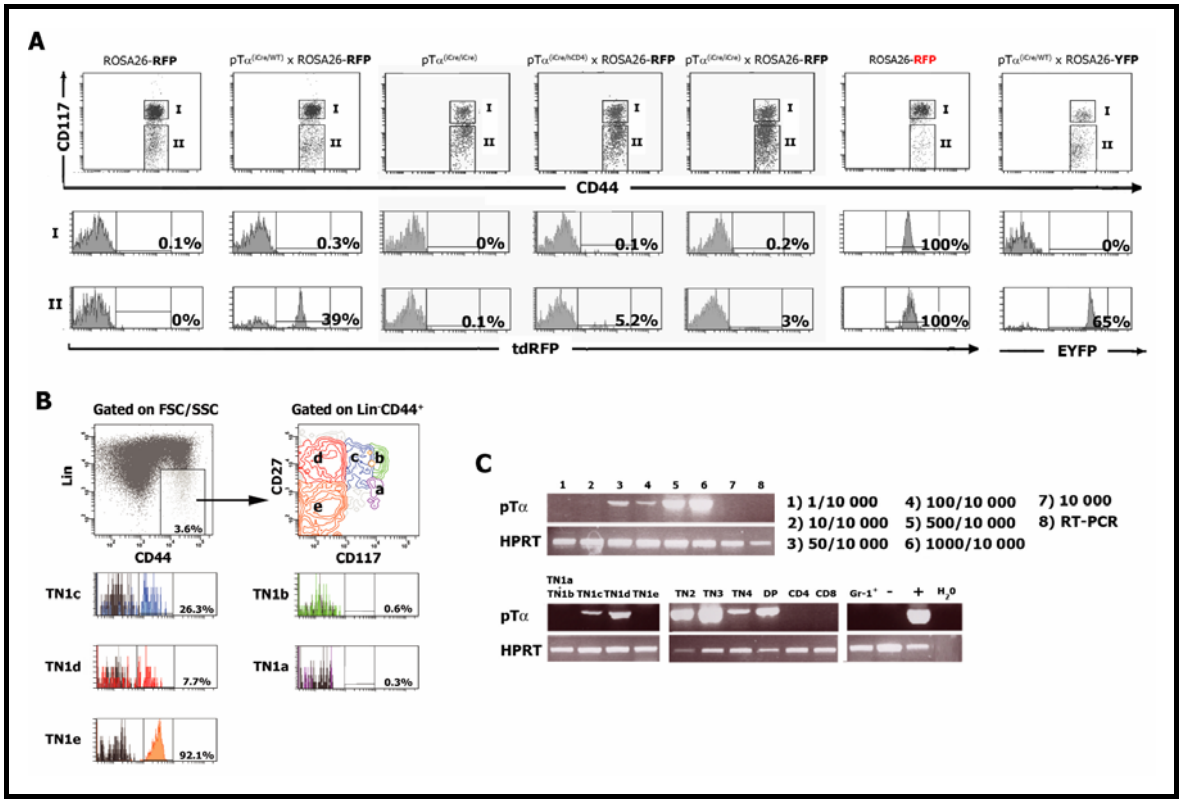

Figure 46: Quantitative analysis of tdRFP expression in TN1 thymocyte subset of the indicated mouse strains by FACS. **A.** Extracted thymocytes were gated on lymphocytes based on FSC/SSC and lineage marker negative cells (not shown). The dot plots (top) show the position of the electronic gates used for the identification of ETP (I) and $CD44^+CD117^{lo/-}$ (II) TN1 subsets. RFP fluorescence emission was detected only in $CD44^+CD117^{lo/-}$ TN1 cells. **B.** TN1a and b do not express tdRFP. The dot plots (top) show the position of the electronic gates used for the identification of TN subsets according to the scheme of Petrie *et al.*[33]. TN1c, d and e subsets express tdRFP. **C.** Sensitive RT-PCR analysis of pTα expression in thymocyte subsets. Top: Range of RT-PCR sensitivity. $CD44^+CD25^+$ TN3 cells were single cell sorted in 10 000 $CD19^+$ splenocytes according to the indicated frequency. Reliable detection of pTα transcript was observed in sample #3. Limit of detection of this assay is 0.5% of pTα expressing cells. Bottom: 10 000 cells of indicated thymocyte subsets (5000 for TN1 a+b) were sorted and prepared for mRNA extraction. cDNA preparations were adjusted according to the signal given by HPRT amplification. TN1 c and d but not a,b and e were expressing pTα. Other immature thymocyte subsets but not mature CD4 and CD8 SP expressed pTα. Negative controls: Gr-1: 10000 myeloid cells from the spleen, #8 and -: -RT controls, +: positive control (10 000 $CD44^+CD25^+$ cells).

24.2. pTα-iCre: a superior tool for Cre-mediated genomic modifications in the T-cell lineage

While using Lck-Cre deleter mice, we noticed deletion patterns that were more complex than expected. Inspection of Lck-Cre x ROSA26-**RFP** animals of the same litter under a fluorescence microscope revealed 3 kinds of reporter activation (Fig. 47A). In some animals as in mouse #248, tdRFP was specifically detected in lymphoid tissues. Using the same exposure time for video capture, it was apparent that tdRFP fluorescence was significantly less intense in Lck-Cre x ROSA26-**RFP** than in pTα-iCre compound mice (Fig. 47A, middle panel) probably indicating a lower efficiency of reporter activation when using lck-cre. In strong contrast to the fluorescence pattern regularly observed in pTα-iCre x ROSA26-**RFP** mice, mosaic and ubiquitous ROSA26-**RFP** activation in Lck-Cre x ROSA26-**RFP** animals

(Fig. 47A, left and right panel respectively) clearly demonstrate nonspecific Cre expression in cells unrelated to the T-cell lineage. FACS analysis of splenocytes from 13 Lck-Cre x ROSA26-**RFP** animals showed a majority of mice (n=10) with specific tdRFP-labeling in the T cell compartment while 3 mice also showed labeling in the B-cell lineage (Fig. 47B). Similar observations have been reported by Wilson *et al.* (see http://depts.washington.edu/immunweb/faculty/wilsonlab-reagent.html) indicating that Lck-Cre transgenic animals are not optimal for Cre-mediated genomic manipulations in the T-cell compartment. Percentage of tdRFP-positive T lymphocytes varied remarkably between individual Lck-Cre mice as opposed to pTα-iCre animals (Fig. 47B). Similar variations were found in Lck-Cre x ROSA26-**GFP** and Lck-Cre x ROSA26-**YFP** reporter animals ([71, 78, 125] and our own observations) revealing a general unreliability of Lck-Cre expression.

To further investigate the efficiency of reporter activation in both Lck-Cre and pTα-iCre deleter strains, the degree of tdRFP-labeling in each CD4/CD8 thymocyte subset was analysed by FACS (Fig. 47C). Although Lck-Cre and pTα-iCre deleter mice showed the same ratio of CD4 SP, CD8 SP, DP and DN cells (Fig. 47C, top), the percentage of tdRFP$^+$ thymocytes in all subsets varied dramatically between individual Lck-Cre mice. In sharp contrast, the same high efficiency of reporter activation was observed in all pTα-iCre animals studied so far (Fig. 47C, bottom). Inefficient and non-specific activation of a reporter locus in Lck-Cre mice has been observed by others too[78] and can be explained with position effect variegation (PEV) of multi-copy transgenes, a well known inhibitory effect of hetero-chromatin[51]. In addition, pTα-iCre was 3 times more efficient than Lck-Cre transgenic mice to activate the ROSA26-**RFP** reporter in the DN subset as shown by considerable lower mean level of tdRFP-labeled cells in Lck-Cre mice (23±17.0%) than in pTα-iCre animals (68.5±7.9%) (Fig. 47C, bottom).

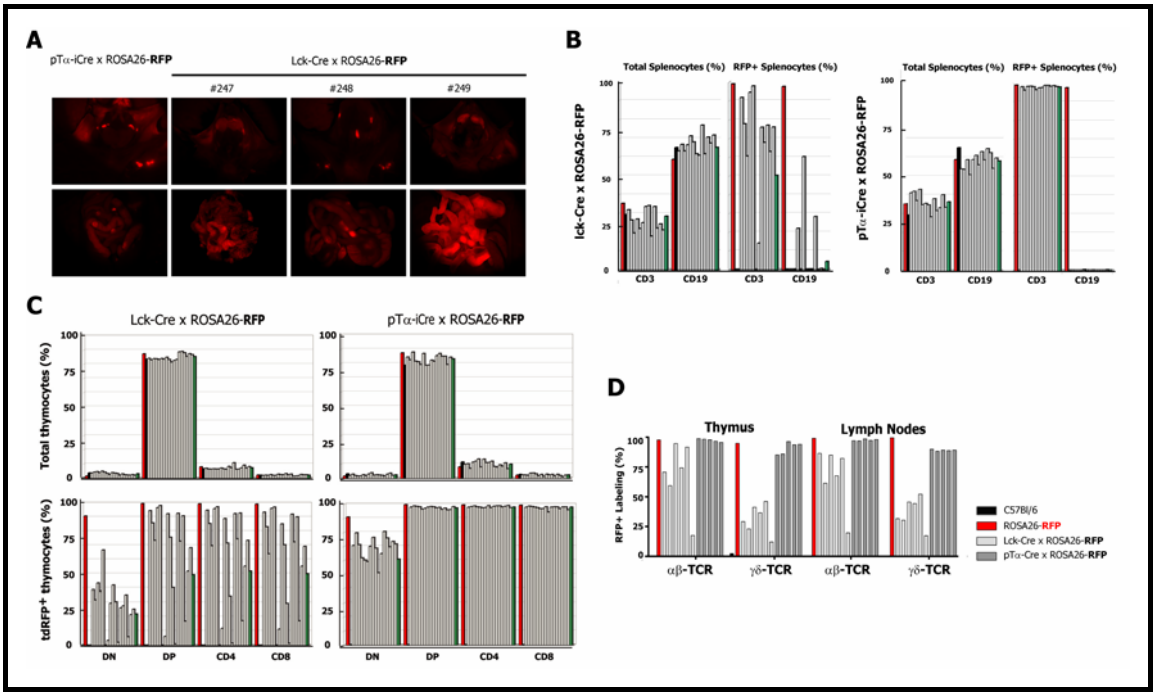

Figure 47: More specific, efficient and reliable reporter activation in the T-cell compartment of pTα-iCre knock-in mice than in Lck-Cre transgenic animals. **A.** Fluorescence stereoscopy of 3 Lck-Cre transgenic littermate. A pTα-iCre x ROSA26-**RFP** animal was used as a control for T-cell specific reporter activation. The striking great variability of reporter activation pattern seen in Lck-Cre animals as opposed to specific pTα-iCre mouse is illustrated for the head part (top) and gut (bottom). **B** and **C.** Level of reporter activation in B/T-lymphocyte (B) or CD4/CD8 thymocyte (C) subsets in corresponding mouse strains: black bar: ROSA26-**RFP**, red bar: activated ROSA26-**RFP**, gray bars: lck-Cre or pTα-iCre x ROSA26-**RFP** respectively, green bar: mean value of reporter actiation for the indicated deleter line. Each bar represents the level of reporter activation in one mouse. **D.** Labelling of αβ- and γδ-T cells in the thymus and in the periphery (LN) of Lck-Cre (light gray) and pTα-iCre (dark gray) deleter animals crossed onto ROSA26-**RFP** background. Each bar represents the level of reporter activation in one mouse of indicated strain.

Finally, although γδ T-cells are absolutely dependent on Lck for their development[156], less than 50% of γδ T-cells in the thymus and periphery were labelled in most Lck-Cre mice, (Fig. 47D) precluding the use of Lck-Cre to optimaly trace γδ T-cell development. Collectively, these results reflect the superiority of pTα-iCre deleter mice in terms of timing, efficiency and specificity of reporter activation over the most commonly used Lck-Cre transgenic line to study T-lineage cells and their development. pTα-iCre KI mice set a new standard for T-lineage specific Cre-mediated genome manipulations in mature and developing thymocytes.

24.3. Cells expressing tdRFP in the bone marrow of pTα-iCre x ROSA26-RFP mice

Although no Cre-inducible reporter activation was detected in the main ETP population of pTα-iCre x ROSA26-**RFP** mice, 0.3% bone marrow cells depleted of mature cell lineages (Lin^-) were expressing tdRFP (Fig. 48A). Lin^-tdRFP^+ cells were specifically found in the $CD117^-Sca\text{-}1^-$ (0.3%) $CD117^-Sca\text{-}1^+$ (2.1%) but not in the

$CD117^{+}Sca\text{-}1^{+}$ compartment which entails hematopoietic stem cells (HSC) and multipotent progenitors (LMPP and ELP). These data exclude HSC, LMPP and ELP from the bone marrow cell population in which Bruno *et al.*[43] described pTα expression. Reporter activation in BM subsets was correlated with endogenous expression of pTα, as assessed by sensitive RT-PCR (Fig. 48B). Resolution of BM cell populations according to cell surface expression of lineage markers, CD117 and Sca-1 showed that only $CD117^{-}Sca\text{-}1^{+}$ cells among the Lin^{-} BM fraction were expressing pTα. The apparent lack of pTα expression in $CD117^{-}Sca\text{-}1^{-}$ fraction, the main Lin^{-} subpopulation of BM cells, could be due to the detection limit of our RT-PCR assay (sensitivity of 1:200).

In order to investigate the nature of $tdRFP^{+}$ cells in the BM of pTα-iCre x ROSA26-**RFP** animals, we asked whether the CLP population defined as $Lin^{-}CD117^{int}CD127^{+}$ had detectable level of reporter activation (Fig. 48C, left panel). Interestingly, only few CLPs were expressing tdRFP (0.8%). The majority of $Lin^{-}tdRFP^{+}$ BM cells were found in a cell population homogeneous for CD127 expression (Fig. 48C, right panel). 5.4% of these $Lin^{-}CD117^{-}CD127^{+}$ cells showed an activated reporter (Fig. 48C, left panel). Using a transgenic mouse that expresses the human CD25 (hCD25) marker as a reporter driven by the pTα promoter and enhancer, Von Boehmer *et al.* [24, 157] showed recently that CLP2, another BM-resident progenitor with T/B lymphoid potential, was found in the $Lin^{-}CD117^{-}CD127^{+}CD45R^{+}$ fraction.

It remains to be elucidated whether $tdRFP^{+}Lin^{-}CD117^{-}CD127^{+}$ cells likewise express CD45R and possess T/B-cell potential upon adoptive transfer. Collectively, these data document the presence of a pTα-expressing BM progenitor with a cell surface phenotype in part similar to CLP2. We are currently performing *in vitro* clonal analyses and adoptive transfer experiments to charaterize these cells and understand their developmental potential.

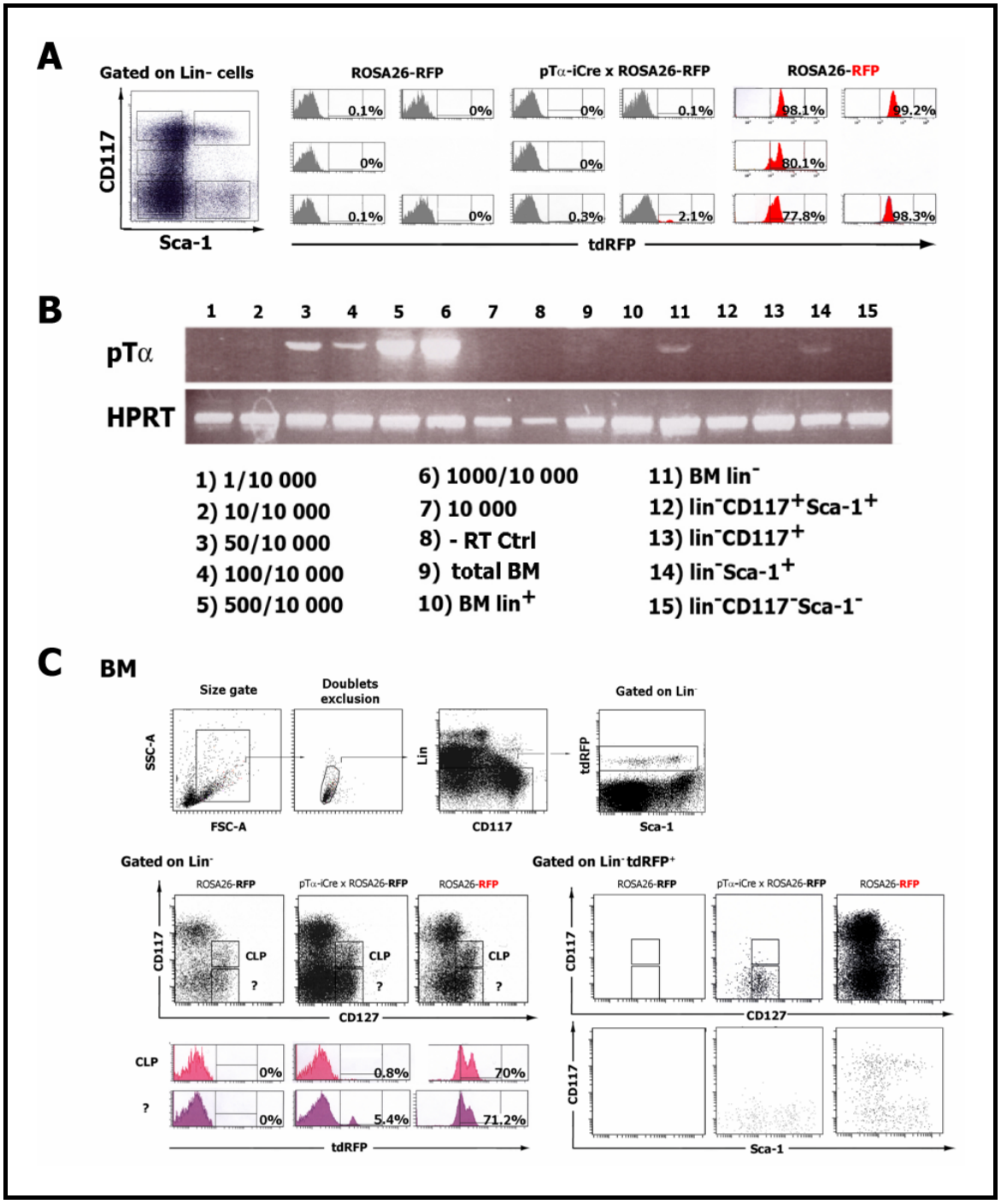

Figure 48: A. tdRFP$^+$ cells are found in the lin$^-$CD117$^-$ bone marrow fraction. Bead-depleted BM cell for lineage marker expressing cells were analysed for each indicated mouse strains.The histograms show the fluorescence intensities of the different CD117/Sca-1 subsets. **B.** RT-PCR analysis of pTα expression in indicated BM subsets. Purified mRNA from 10 000 sorted cells/BM subset were used for cDNA amplification. Each preparation was normalised according to the level of HPRT expression. Detection sensitivity was determined as in figure 46C. **C.** Lin$^-$CD117$^-$CD127$^+$ but not CLP show significant level of reporter activation (left). BM cells were depleted of cells expressing lineage marker using magnetic beads and analysed using the gating strategy indicated on top. The dot plots (top) show the position of the electronic gates used for the identification of CLP and the Lin$^-$CD117$^-$CD127$^+$ cell population. Alternative gating on Lin$^-$tdRFP$^+$ cells (right) showed that tdRFP expression was exclusively found in CD117$^-$ cells expressing heterogenous level of Sca-1 surface antigens.

DISCUSSION

25. CRE-INDUCIBLE ROSA26-RFP REPORTER STRAIN

Here, we report the modification of the ROSA26 gene locus to engineer a reporter mouse strain suitable for *in vivo* monitoring of Cre recombinase-mediated excisions in the longer wavelength range of the light spectrum. A cDNA encoding the artifically dimerized red fluorescent protein variant tandem-dimer RFP (tdRFP) was targeted to the ROSA26 locus along with a transcriptional stopper to generate a new Cre-inducible reporter line.

Our data show that the tdRFP fluorescent reporter overcomes the limitations of previously described DsRed-variants (DsRed1 and 2), which are expressed as obligate tetramers resulting in cell-toxicity in murine ES cells. Our work also demonstrates the developmental neutrality of tdRFP expression in ES cells and mice. Although two earlier reports have similarly showed non-toxicity of a RFP variant (monomer of mRFP-1) in transgenic mice[109, 111], the absence of flow cytometry data precluded any qualitative comparison of the respective red fluorescence intensity with our reporter mouse. Nevertheless, the relative brightness of the non-oligomerizing artificial dimer tdRFP is unmatched to other RFP variants such as mRFP1 (Table 2, introduction), being thus ideal for single-copy gene integrations.

Similarly to our approach, Vintersten *et al.* recently generated a Cre-inducible transgenic RFP reporter mouse by random integration of several copies of a CMV enhancer/chicken-β-actin promoter-driven DsRed.T3-transgene[108]. Although Cre-inducible expression of tetrameric DsRed.T3 illustrated the advantages of RFP reporters over fluorescent proteins with lower wavelength emissions, like increased tissue penetration and reduced background autofluorescence, the authors did not carefully examine in these mice the extent of green fluorescence emission by DsRed.T3 intermediate forms of maturation originally described by Bevis *et al.*[92]. The resulting contamination of GFP signal is a strong disadvantage for dual color experiments and could hinder correct multicolor

lineage tracing analysis. We showed that ROSA26-**RFP** mice did not present such adverse phenotype further reensuring that ROSA26-**RFP** strain is best suited for live imaging of red fluorescent cells in a genetically traceable mouse line. In addition, despite the use of a promoter that is considered to be active in many cell types, DsRed.T3-transgene expression could be variegated because of the lack of critical additional cis-regulatory elements or chromosomal positional effects, compromising the use of such reporter strain in lineage tracing studies. With our gene targeting approach, the single copy integration of Cre-inducible tdRFP into the well-characterized ROSA26 locus of inbred C57BL/6 mice get around these uncertainties. We have observed virtually complete penetrance of tdRFP expression in ROSA26-**RFP** mice with bright and widespread red fluorescence in both juvenile and adult animal tissues (Fig. 34A and -B) illustrating ubiquitous expression of the excision-activated locus.

T cell-restricted excision of floxed sequences and tdRFP expression after mating with T-cell specific Cre deleter mice provides the complementary validation of the Cre-inducibility of our reporter strain. Ubiquitous, inducible, and lineage-specific activation of tdRFP was obtained demonstrating the accessibility and functionality of the modified floxed ROSA26 locus during early embryogenesis and development of the lymphoid lineage.

If Cre is specifically expressed in one progenitor cell or a group of progenitor cells, excision activated tdRFP expression mark progeny both temporally and spatially thereafter. In cases where Cre is expressed only transiently in a group of cells in a developing embryo, progeny could be traced by the constant expression of tdRFP, even in the absence of Cre expression at later stages of development. Such approaches have been used successfully in the study of neural progenitors[158]. The ROSA26-**RFP** reporter strain (together with the YFP reporter strain currently available) will thus be very useful for monitoring the expression of Cre in living tissues, or tracing the lineage of these cells and their descendants, in cultured embryos or organs.

While tdRFP gene expression from the excision-activated ROSA26 locus mimics that of other ROSA26 knock-in lines[71, 81, 85], our reporter strain exhibited marked additional advantages. ROSA26-**RFP** provide a non-invasive marker for cell isolation because fluorescence detection does not require initial fixation or hypotonic permeabilization of cells as opposed to βgeo reporter lines. Moreover, data generated using tdRFP fluorescent protein proved to be highly reproducible in contrast to what has been reported using ROSA26-βgeo mice[54, 125], because the generation of the fluorescent signal in cells is not dependent on the variable penetration of a β-galactosidase fluorescent substrate into cells. In contrast to other fluorescent reporters (EGFP or ECFP)[71, 85], tdRFP provides sufficient signal above autofluorescence to be reliably detected by epifluoresence in fixed and sectioned tissue. In addition, the tdRFP reporter proved to be sufficiently photostable to be imaged by confocal microscopy (Fig. 36B).

tdRFP cells can easily be distinguished from cells expressing GFP/YFP spectral variants by both imaging using standard optics, and molecular analyses. We have demonstrated the concomitant detection and separation of cells expressing either one or simultaneously two fluorescent proteins cytofluorometrically without encountering problems of compensation. Our tdRFP-reporter mice can thus be used in conjunction with the many available transgenic and knock-in mouse mutants expressing GFP-based marker genes. Because of the ubiquitous expression of tdRFP in hematolymphoid cells, which can be monitored by FACS in conjunction with antibody stainings, these mice offer a powerful new tool for the study of hematolymphoid stem and/or progenitor cell populations. ROSA26-**RFP** animals represent a new resource for analyzing development in mouse embryos and adults. They can also be used as tagged populations of cells in chimeras, in addition to transplantation and cell isolation experiments.

The fact that the level of red fluorescence appears to be defined by the proliferation status of a cell provides an additional asset. 5-FU injection experiments proved that the intermediate peak of red fluorescence intensity seen in ROSA26-**RFP** mice corresponds to rapidly dividing cells which highlights the

possibility of using the level of tdRFP fluorescence emission as a qualitative marker for cell cycle progression.

One important feature of our reporter mice was its generation and further maintenance on a C57BL/6 background, the most frequently used and best characterized inbred mouse strain. As syngeneic recipients can be used, the genetically defined background of tdRFP reporter mice should facilitate the adoptive transfer of sorted cell populations, thus avoiding complications like graft rejection due to histoincompatibility. Such adoptive cell transfer experiments are critical in lineage-tracing studies and required to rigorously assess the developmental potential of labeled and unlabeled cell populations *in vivo*.

Finally, we have shown that the activated ROSA26-**RFP** locus was suitable for recombinase mediated cassette exchange (RMCE). Fidelity of tdRFP expression from the ROSA26 locus during embryogenesis and in adult life makes it an excellent choice to achieve ubiquitous expression of other genes or cDNAs. Our locus enabled selection-free targeting in ES cells to facilitate the production of new kinds of ROSA26-based reporter mice. Similarly to the RMCE-ASAP targeting methodology described by Toledo *et al* at the p53 locus[159], ROSA26-**RFP** could also be used to quickly introduce siRNA at a defined locus in somatic cells, thus accelerating phenotypic analysis in cells in which targeting point mutations by homologous recombination is extremely inefficient[62]. In addition, as disruption of the ROSA26 locus by insertion of fluorescent reporters or other cDNAs has been shown to have no obvious deleterious effect on the biology of the targeted cell, the activated ROSA26-**RFP** locus presents a clear advantage over RMCE into the p53 locus in which disruption of one p53 allele has strong effects on cell cycle progression and irradiation sensitivity.

26. THE pTα-iCRE-DELETER STRAIN AND T- LINEAGE TRACING

Specific insertion of a cell surface, fluorescent or enzymatic marker behind a well-characterized promoter should label all cells normally expressing this gene. To understand the sequence of critical differentiation events required for multipotent HSCs to give rise to T-cells and to improve our current models of T-lymphopoiesis, we tested whether pTα-expression could be a good marker for T lineage-committed precursor cells. To obtain meaningful results in lineage tracing experiments, the promoter of choice should have a narrow expression pattern, ideally only in a given lineage. This pre-requisite is however not a guaranty for success: in their attempt to label early stages of myelopoiesis using a lysozyme-Cre knock-in mouse crossed with ROSA26-**EYFP** reporter mice[85], Ye *et al.*[78] showed that the lysozyme gene was expressed at low levels in a subset of HSCs and that these cells exhibited long-term repopulation potential. The fact that a myeloid lineage affiliated gene was expressed in HSCs whithout abolishing their "stem cell-ness" stressed for a revision of the current view that lineage-specific transcription factors establish and maintain cell fate by regulating cell type-specific gene expression programs. Moreover, Hu *et al.* showed that single cells from pluripotent hematopoietic cell lines not only express a variety of lineage restricted transcription factors but also classical lineage affiliated marker genes such as β-globin and myelo-peroxidase[160]. These results seriously challenged the principle and applicability of lineage tracing methodology for mapping lineage restriction in progenitor cells. HSC could indeed express stochastically a broad range of genes which expression is normally restricted to one given lineage. In this work, we did not find any evidence for promiscous expression of pTα. In contrast, we clearly showed that the pTα promoter can be successfully used for *in vivo* lineage tracing and to map specifically T-related lineages (see section 23.3).

The pTα protein is expressed at very low amounts and does not reach the cell surface before pairing with the TCR-β chain[161]. It was therefore difficult to directly study pTα-expressing cells as they cannot easily be sorted and tested for

their developmental potential. To test whether pTα-expression could be a good marker for T lineage-committed precursor cells, we developed lineage-tracing strategies to identify intra- and extrathymic pTα-expressing cells and assess their development potential *in vivo* in a non-invasive manner. We (see section 3.2) and others[162] attempted to tag pTα-expressing cells *in vivo* with a reporter that can be used to isolate viable cells. Both the direct introduction of marker genes into the mouse *ptcra* locus using gene targeting and bacterial artificial chromosome (BAC) transgenesis[163, 164] failed to yield sufficient level of reporter expression to reliably identify pTα expressing cells, especially in the BM. To circumvent this problem, we reasoned that expression of the site-specific Cre recombinase from the pTα locus would be sufficient for conditional Cre-mediated activation of a reporter allele whose expression is otherwise blocked by a "floxed" transcriptional stopper fragment[38]. Success of Cre/lox gene modification strategies requires a sufficient amount and defined pattern of Cre expression. For rapid and efficient reporter activation, we had to develop a Cre expression cassette to ensure an optimal level of Cre protein in pTα-expressing cells and minimize the risk of transgene silencing via epigenetic mechanisms. In addition, to minimize unpredictable effects of variegated reporter expression associated with multicopy transgene insertion, we opted for a knock-in approach of the pTα locus to ensure reliable expression of the reporter. We therefore introduced an improved version of the cre recombinase gene into the first exon of the pTα gene by homologous recombination (see section 21). The functionality of pTα-iCre knock-in mice was assessed *in vivo* by intercross with the ROSA26-**RFP** reporter strain[115]. iCre expression from the pTα locus showed to be sufficient for reliable reporter activation (see section 23.2 and 23.3). Rigorous inspection of internal organs by fluorescence stereoscopy (see section 23.2) and various hematopoietic lineages by flow cytometry (see section 23.3) indicated that the minimal modifications resulting from the engineering of pTα-iCre maintained the lymphoid specificity of pTα expression. In addition, we showed that the onset of reporter activation correlated with endogenous pTα-expression in the thymus (see section 24.1) and in the bone marrow (see section 24.3) which further reensured us about the physiological relevance of the data obtained with our

pTα-iCre deleter mice. Thus, we showed that pTα-iCre "ancestry" mice can be used to detect individual cells that are either expressing pTα or that have expressed the gene earlier during their development.

A critical parameter for the success of lineage tracing experiments is the efficiency of Cre-mediated modification that a lineage-specific Cre recombinase can induce. A lack of complete penetrance of recombination is obviously a disadvantage in circumstances where a phenotype can only be revealed clearly by inducing a mutation in all T cells. Selection for or against unexcised cells may occur *in vivo* which is a serious obstacle for functional analysis of the inactivation of a given gene. In contrast to other T-cell specific deleter lines available so far[54, 73, 75, 76], the pTα-iCre line showed full penetrance of Cre-mediated recombination with virtually 100% of T-cells showing reporter activation (see section 23.3). In addition, we did not observe any variation regarding the efficiency of Cre-mediated tdRFP activation between individual mice in contrast to Lck-Cre transgenic animals. Using Lck-Cre transgenic animals, excision although substantial, was not complete among T cells (see section 24.2 and report from other studies[71, 78, 125]). Very likely this property reflects in part some variegated expression of the multicopy Lck-Cre transgene[51]. The report of Zhang *et al.*[54] that the distal part of the Lck promoter was really sensitive to regulatory influences from the site of the genome into which it integrates goes along this line. Only two lines exhibited the expected delayed reporter activation in late stage thymocytes illustrating the high sensibility of some parts of the Lck promoter to epigenetic regulations. Our results indicate that the pTα-iCre deleter mouse strain does not exhibit such detrimental effects of position effect variegation. pTα-iCre knock-in mice should thus become the standard Cre-deleter line for reliable and efficient T-cell inactivation of floxed genes to study, for example, their role in T-cell development.

We showed that reporter activation was highly specific to T-related lineages (see section 23.3): mature NK and B lymphocytes as well as myeloid and erythroid cells were not marked in pTα-iCre x ROSA26-**RFP** mice whereas mature αβ-, γδ- and NK-T lymphocyte showed virtually all reporter activation (95

to 99%). This key finding demonstrates that pTα can be used to specifically mark T-lineages *in vivo*. This is a substantial improvement over Lck-Cre transgenic mice in which significant B-cell labeling was sometimes observed in animals presenting an overall lymphoid specific reporter activation (see section 24.2). The fact that NK-T but not NK cells are labeled is an additional strong genetic evidence that NK-T cells develop independently from NK cells through a pTα-expressing precursor. Our deleter mouse could thus be used to better understand the individual contribution of each NK/NK-T lineages in the immune response by inactivating, specifically in NK-T cells, genes thought to be involved in NK-cell function.

The analysis of pTα-iCre x ROSA26-**RFP** mice enabled us to improve the currently unclear model of αβ *vs* γδ lineage commitment. γδ-T cells showed a high degree of reporter activation (see section 23.3) inferring that γδ-T cells should be derived from $pT\alpha^+$ precursors. This new information is compatible with an instructive model of αβ *vs* γδ-lineage commitment. In this model, pre-TCR expression is thought to occur in a common αβ-γδ thymic precursor and exclusively promote αβ-T-cell lineage commitment by diverting TCR-β expressing cells away from the γδ T-cell lineage whereas γδ T-cell lineage commitment would only proceed in γδ-TCR expressing cells and would result in a rapid extinction of pTα expression[161, 165]. Some of γδ-thymocyte precursors might diverge from the main thymocyte developmental pathway before the onset of pTα expression as thymic γδ-T cells appear to show consistently less reporter activation than αβ-T cells (see section 23.3). Further analysis, such as detection of TCR-β chain rearrangements in these cells, might be needed to confirm or refute this hypothesis.

Reporter activation was also efficiently detected in atypical subtypes of T-lymphocytes such as dendritic epidermal T cells (DETC) of the skin or extrathymic T-cells found in athymic mice (see section 23.4 and 23.5). γδ DETC cells develop exclusively prenatally as they depend on properties of the fetal/newborn stroma, i.e. DETC development cannot be supported by an adult thymus[34]. Considering that γδ DETC cells are the first T-cells to develop during

fetal life, it is possible that all T-lineage committed cells - even the earliest one produced during thymus ontogeny- necessarily go through a pTα-expressing stage during their development. This hypothesis goes in hand with the report from Bruno *et al.*[43] that pTα expression starts as early as d14.5 of fetal life, far before the onset of TCR-β chain rearrangements[34]. The high degree of T-cell labeling in athymic pTα-iCre x ROSA26-**RFP** nude mice further confirms that pTα-expression might be an absolute marker for all T-cell developmental pathways described so far during fetal and adult life. Tracing the onset of reporter activation in pTα-iCre x ROSA26-**RFP** nude mice could help us to unravel the true sites of extra-thymic T lymphopoiesis, which are still highly disputed so far.

The use of our pTα-iCre knock-in mouse allowed the discovery of a yet undescribed type of cells expressing or having expressed pTα which form a small rim at the margin of the hair follicle in the skin (Fig. 45). Interestingly, these reporter activated cells were localized in pTα-iCre x ROSA26-**RFP** mice of both WT and nude background (Fig. 44) demonstrating that these cells were not of DETC origin. This result could have important implications as it might help us to better characterize the immune function of hair follicles. It is conceivable that hair follicles might be a site for extrathymic T-cell development. Indeed, keratinocytes in the outer root sheath of hair follicles present some interesting characteristics. These keratinocytes produce biologically relevant amounts of IL-7[166] and could experimentally provide an adequate micro-environment to sustain T-cell development like thymic nurse cells as reported by Aiba [167] and Clark[168]. In addition, transcription factors playing a major role in thymopoiesis such as Lef-1[169], Gata-3[169] and Runx-1[170], as well as BMP2/4 morphogens[171] have been shown to be expressed in the bulge of hair follicles. Finally, multiple Notch receptors and ligands are expressed in both developing and adult epidermis and hair follicles[172]. OP9/OP9dl1 co-culture assays will help us to investigate the developmental potential of these reporter activated cells.

As pTα-iCre reporter activation was only detected in T-related lineages, pTα-iCre might be a good marker to study early steps of T-lymphopoiesis. Analysis of the onset of reporter activation amongst the subsets of immature thymocytes indeed gave us some indication on the developmental stage initiating the T-lineage specific genetic program. The first induction of reporter activation was seen in the TN2 subset of the canonical T-cell developmental pathway (see section 24.1). The absence of labeling in TN1a and b ETPs contradicts previous reports from Krueger *et al.*[28] who used a pTα transgenic line to trace T-lymphopoiesis. In these transgenic mice, a hCD25 reporter gene was placed under the control of the pTα promoter and upstream regulatory region, which contains the transcriptional enhancer of pTα gene[157]. Krueger *et al.* showed that most of the hCD25^{+} expressing cells were found in the TN1b subset. TN1d and e were completely negative and TN1c subset was not investigated. This discrepency to our results might be explained by the methodology used to trace pTα-expressing cells. Only one transgenic line with ~ 40 integrations showed sufficient amounts of transgenic marker expression with a pattern resembling that of the endogenous pTα[22]. Unexpectedly, B-cells in the bone marrow and thymic γδ-T cells also expressed the transgene in these animals despite the lack of detection of endogenous pTα transcripts[22]. The authors argued that these cells displayed hCD25 on the cell surface because they were recently derived from pTα expressing uncommitted precursors[22]. However, these surprising observations could equally be due to an experimental artefact of reporter expression variegation due to epigenetic influences. Alternatively, the time required for the expression and the synthesis of sufficient amount of iCre from one pTα-iCre knock-in allele might be too long to efficiently activate the ROSA26-**RFP** reporter in immature TN1a and b subsets as Rocha *et al.* recently pointed out[43]. Our results using homozygous pTα-iCre knock-in mice clearly demonstrate that twice as much pTα-iCre expression does not alter the phenotype of TN1a and b subsets (see section 24.1). These data were further confirmed by the absence of endogenous pTα transcript detection in TN1a+b subsets using a sensitive RT-PCR analysis (Fig. 46c).

Observations concerning Notch-deficient intratymic precursors suggest that T cell commitment in the adult mouse might occur exclusively in the thymus[172]. On the other hand, pTα mRNA is detected by RT-PCR in BM cells (see section 24.3), even in cells from thymus-deficient nude mice[43], which is consistent with the idea that commitment to the T lineage might also occur before entry of cells into the thymus. Analysis of BM subsets by flow cytometry and RT-PCR (Fig. 24-3) proved that pTα was neither expressed in HSC nor in MPP and ELP, the subsequent stages of hematopoietic development. Complete absence of labeling in mature B-cells strongly suggest that immature B-cell and previously described T/B bipotent common lymphoid progenitor (CLP) populations in the bone marrow are not expressing pTα. Prospective analysis of reporter expression in BM cell populations of pTα-iCre x ROSA26-**RFP** mice confirmed this hypothesis (see section 24.3). Bone marrow progenitor cells expressing tdRFP did not entail CLP. They formed a homogenous cell population defined as $Lin^{-}Sca\text{-}1^{lo}CD117^{-}IL7\text{-}R\alpha^{+}$. In contrast, Martin *et al.*[24] reported that 5% of CLP were expressing the pTα-hCD25 transgene. Transfer of $hCD25^{+}$ Lin^{-} BM population yielded T, B and NK cells. These data should be regarded with great caution as the authors mentioned that the reporter transgene was more highly expressed than *ptcra* in BM compared to thymus which could be due to a transgenic artefact. Thus, the physiological relevance of a $hCD25^{+}$ CLP subset in bone marrow might be questioned. In addition, the author identified CLP-2, a T-lineage specified subset in the BM defined as $Lin^{-}CD45R^{+}CD19^{-}$ which seemed to migrate efficiently into the thymus if placed in the blood[24]. We are currently evaluating the degree of overlap between our $pT\alpha^{+}$ BM population and CLP2. Martin *et al.*[24] claimed that the CLP2 phenotype was identified in the thymic DN1 compartment of pTα-transgenic reporter mice, but that this CLP2 appeared considerably less efficient than ETPs in their T lineage potential[24]. The low cloning efficiency that is seen in assays using CLP-2[24] might be explained by the fact that CLP-2 cells include $Ly6C^{+}$ cells[22] that are plasmacytoid DCs lacking lymphoid potential. Hence, it appears unlikely that ETPs are descendents of CLP2s. One implication of these findings is that the detection of a lineage potential in experimental assays does not necessarily mean that a progenitor gives rise to cells of that lineage physiologically. The high degree of labeling

specificity seen in our pTα-iCre x ROSA26-**RFP** mice and the reproducible reporter activation phenotype solve these ambiguities. It remains to be investigated whether $Lin^-Sca\text{-}1^{lo}CD117^-IL7\text{-}R\alpha^+$ pTα-expressing precursors can directly home to the thymus. Alternatively, this subset of cells could entail the resident bone marrow progenitor of an extrathymic T-lymphopoiesis pathway. Isolation of Lin^-RFP^+ cells in pTα-iCre x ROSA26-**RFP** mice and analysis of their developmental potential might help to distinguish between these possibilities.

Genes that are expressed downstream of HSCs might direct thymic homing by circulating progenitors. Candidate genes currently evaluated are encoding the chemokine receptor CCR9[173] and the cytokine receptors FLT3[174] and IL-7Rα[18]. However, other candidate genes might exist but remain to be discovered. Fate mapping of the early steps of T-cell development using transgenic reporter mice such as pTα-hCD25[22] or Lck-EGFP strains[53, 175] appear to bring more confusion than conclusive evidence with regard to issues of lineage commitment. We showed that these critical issues should be preferably addressed using a knock-in approach for rigorous and meaningful lineage tracing. Knock-in approaches and Cre/loxP conditional reporter activation should be favored to analyse the lineage of cells and create animal models of human diseases for pathogenesis and therapy.

SUMMARY

The pTα gene encodes the pre-T cell receptor alpha chain, an essential component of the pre-TCR complex. Using pTα expression as a specific marker for early T lineage cells, we developed a lineage-tracing strategy to visualize early intra- and extra-thymic T lineage-committed precursor cells and their progeny. To this end, a cDNA encoding an improved version of the Cre recombinase (iCre) was targeted into the pre-T cell receptor alpha-chain (pTα) gene locus. In parallel, we introduced a Cre-inducible expression cassette encoding for a very bright and non-toxic variant of red fluorescent protein (tandem-dimer RFP = tdRFP) into the ubiquitously expressed mouse locus ROSA26. Correctly targeted ES cells were used to generate "pTα-iCre deleter" and "ROSA26-tdRFP indicator" mouse strains, respectively. In cells bearing both "knock-in" alleles, pTα-driven iCre recombinase expression leads to permanent activation of the ROSA26-tdRFP reporter locus. As a result, pTα-expressing cells and their progeny exhibited persistent red fluorescence. Using this system, we routinely achieved strong and essentially complete labeling of peripheral T-cells (~98% RFP^+ cells by flow cytometry). Importantly, we did not observe any variation regarding the efficiency of Cre-mediated tdRFP activation between individual mice, a common problem in many other Cre-deleter/indicator strain combinations.

Red fluorescence was detected exclusively in cells considered to belong developmentally to the T-lineage (αβ, γδ, natural killer-T (NKT) cells, but not in other hematopoietic cells (myeloid, erythroid, B and NK cells), demonstrating the exquisite specificity of pTα expression. Exclusive reporter activation in T but not B-cells indicates that onset of pTα-iCre expression occurs after the T/B lineage decision and not in immature B-cell precursor populations or in the T/B bipotent common lymphoid progenitor (CLP) bone marrow subset. Most interestingly, > 95% of γδ-TCR expressing thymocytes and peripheral T cells were tdRFP-positive, demonstrating for the first time that almost all γδ-T cells develop – like TCRαβ lymphocytes - from a pTα-expressing precursor. This finding is surprising, as pTα and the pre-TCR are essential for normal αβ T lymphopoiesis, but not for the development of γδ cells. Importantly, even dendritic epidermal T-cells (DETC)

showed reporter activation, despite the fact that they are considered to develop from a separate, embryonic progenitor population in a first wave of T lymphopoiesis. Our findings provide an important piece of information with regard to current models of αβ/γδ lineage commitment. The extent of T-cell labeling in athymic pTα-iCre x ROSA26-**RFP** nude mice indicate that pTα is also expressed during extrathymic T-cell development. Analysis of the skin of pTα-iCre x ROSA26-**RFP** mice led to the discovery of a - to our knowledge – as yet undescribed cell population located in a characteristic pattern around the hair follicle, which either expresses pTα or must have developed through a pTα-expressing stage.

In the thymus, onset of reporter activation was found at the TN2 to TN3 stage but not in the thymic population considered to be the most immature (ETP). Finally, red fluorescence was detected in a minute subset of bone marrow cells depleted of mature cell lineages. pTα-iCre deleter mice should thus be useful for both efficient T-lineage-specific genome manipulations and identification of pTα-expressing T precursor cells in extra-thymic tissues, like the bone marrow.

REFERENCES

1. Schwarz, B.A. & Bhandoola, A. Trafficking from the bone marrow to the thymus: a prerequisite for thymopoiesis. *Immunol Rev* **209**, 47-57 (2006).
2. Bhandoola, A. & Sambandam, A. From stem cell to T cell: one route or many? *Nat Rev Immunol* **6**, 117-126 (2006).
3. Schwarz, B.A. & Bhandoola, A. Circulating hematopoietic progenitors with T lineage potential. *Nat Immunol* **5**, 953-960 (2004).
4. Bhandoola, A., Sambandam, A., Allman, D., Meraz, A. & Schwarz, B. Early T lineage progenitors: new insights, but old questions remain. *J Immunol* **171**, 5653-5658 (2003).
5. Allman, D., Sambandam, A., Kim, S., Miller, J.P., Pagan, A., Well, D., Meraz, A. & Bhandoola, A. Thymopoiesis independent of common lymphoid progenitors. *Nat Immunol* **4**, 168-174 (2003).
6. Weerkamp, F., Pike-Overzet, K. & Staal, F.J. T-sing progenitors to commit. *Trends Immunol* **27**, 125-131 (2006).
7. Wu, L. T lineage progenitors: the earliest steps en route to T lymphocytes. *Curr Opin Immunol* **18**, 121-126 (2006).
8. Petrie, H.T. & Kincade, P.W. Many roads, one destination for T cell progenitors. *J Exp Med* **202**, 11-13 (2005).
9. Miller, J.F. Immunological function of the thymus. *Lancet* **2**, 748-749 (1961).
10. Goldschneider, I., Komschlies, K.L. & Greiner, D.L. Studies of thymocytopoiesis in rats and mice. I. Kinetics of appearance of thymocytes using a direct intrathymic adoptive transfer assay for thymocyte precursors. *J Exp Med* **163**, 1-17 (1986).
11. Donskoy, E. & Goldschneider, I. Thymocytopoiesis is maintained by blood-borne precursors throughout postnatal life. A study in parabiotic mice. *J Immunol* **148**, 1604-1612 (1992).
12. Doria, G. & Agarossi, G. Immunologically competent thymus cells of bone marrow origin. *Nature* **221**, 871-873 (1969).
13. Zinkernagel, R.M., Ruedi, E., Althage, A., Hengartner, H. & Reimann, G. Thymic selection of H-2-incompatible bone marrow cells in SCID mice. Differences in T help for induction of B cell IgG responses versus cytotoxic T cells. *J Exp Med* **168**, 1187-1192 (1988).
14. Adolfsson, J., Borge, O.J., Bryder, D., Theilgaard-Monch, K., Astrand-Grundstrom, I., Sitnicka, E., Sasaki, Y. & Jacobsen, S.E. Upregulation of Flt3 expression within the bone marrow Lin(-)Sca1(+)c-kit(+) stem cell compartment is accompanied by loss of self-renewal capacity. *Immunity* **15**, 659-669 (2001).
15. Lai, A.Y., Lin, S.M. & Kondo, M. Heterogeneity of Flt3-expressing multipotent progenitors in mouse bone marrow. *J Immunol* **175**, 5016-5023 (2005).
16. Perry, S.S., Wang, H., Pierce, L.J., Yang, A.M., Tsai, S. & Spangrude, G.J. L-selectin defines a bone marrow analog to the thymic early T-lineage progenitor. *Blood* **103**, 2990-2996 (2004).
17. Igarashi, H., Gregory, S.C., Yokota, T., Sakaguchi, N. & Kincade, P.W. Transcription from the RAG1 locus marks the earliest lymphocyte progenitors in bone marrow. *Immunity* **17**, 117-130 (2002).
18. Kondo, M., Weissman, I.L. & Akashi, K. Identification of clonogenic common lymphoid progenitors in mouse bone marrow. *Cell* **91**, 661-672 (1997).
19. Spangrude, G.J., Heimfeld, S. & Weissman, I.L. Purification and characterization of mouse hematopoietic stem cells. *Science* **241**, 58-62 (1988).
20. Adolfsson, J., Mansson, R., Buza-Vidas, N., Hultquist, A., Liuba, K., Jensen, C.T., Bryder, D., Yang, L., Borge, O.J., Thoren, L.A., Anderson, K., Sitnicka, E., Sasaki, Y., Sigvardsson, M. & Jacobsen, S.E. Identification of Flt3+ lympho-myeloid stem cells lacking erythro-megakaryocytic potential a revised road map for adult blood lineage commitment. *Cell* **121**, 295-306 (2005).
21. Kuwata, N., Igarashi, H., Ohmura, T., Aizawa, S. & Sakaguchi, N. Cutting edge: absence of expression of RAG1 in peritoneal B-1 cells detected by knocking into RAG1 locus with green fluorescent protein gene. *J Immunol* **163**, 6355-6359 (1999).
22. Gounari, F., Aifantis, I., Martin, C., Fehling, H.J., Hoeflinger, S., Leder, P., von Boehmer, H.

& Reizis, B. Tracing lymphopoiesis with the aid of a pTalpha-controlled reporter gene. *Nat Immunol* **3**, 489-496 (2002).
23. Scimone, M.L., Aifantis, I., Apostolou, I., von Boehmer, H. & von Andrian, U.H. A multistep adhesion cascade for lymphoid progenitor cell homing to the thymus. *Proc Natl Acad Sci U S A* **103**, 7006-7011 (2006).
24. Martin, C.H., Aifantis, I., Scimone, M.L., von Andrian, U.H., Reizis, B., von Boehmer, H. & Gounari, F. Efficient thymic immigration of B220+ lymphoid-restricted bone marrow cells with T precursor potential. *Nat Immunol* **4**, 866-873 (2003).
25. Spangrude, G.J. & Scollay, R. Differentiation of hematopoietic stem cells in irradiated mouse thymic lobes. Kinetics and phenotype of progeny. *J Immunol* **145**, 3661-3668 (1990).
26. Wright, D.E., Wagers, A.J., Gulati, A.P., Johnson, F.L. & Weissman, I.L. Physiological migration of hematopoietic stem and progenitor cells. *Science* **294**, 1933-1936 (2001).
27. Foss, D.L., Donskoy, E. & Goldschneider, I. The importation of hematogenous precursors by the thymus is a gated phenomenon in normal adult mice. *J Exp Med* **193**, 365-374 (2001).
28. Krueger, A. & von Boehmer, H. Identification of a T lineage-committed progenitor in adult blood. *Immunity* **26**, 105-116 (2007).
29. Fowlkes, B.J., Edison, L., Mathieson, B.J. & Chused, T.M. Early T lymphocytes. Differentiation in vivo of adult intrathymic precursor cells. *J Exp Med* **162**, 802-822 (1985).
30. Fehling, H.J. & von Boehmer, H. Early alpha beta T cell development in the thymus of normal and genetically altered mice. *Curr Opin Immunol* **9**, 263-275 (1997).
31. Pearse, M., Wu, L., Egerton, M., Wilson, A., Shortman, K. & Scollay, R. A murine early thymocyte developmental sequence is marked by transient expression of the interleukin 2 receptor. *Proc Natl Acad Sci U S A* **86**, 1614-1618 (1989).
32. Ceredig, R. & Rolink, T. A positive look at double-negative thymocytes. *Nat Rev Immunol* **2**, 888-897 (2002).
33. Porritt, H.E., Rumfelt, L.L., Tabrizifard, S., Schmitt, T.M., Zuniga-Pflucker, J.C. & Petrie, H.T. Heterogeneity among DN1 prothymocytes reveals multiple progenitors with different capacities to generate T cell and non-T cell lineages. *Immunity* **20**, 735-745 (2004).
34. Hayday, A.C. [gamma][delta] cells: a right time and a right place for a conserved third way of protection. *Annu Rev Immunol* **18**, 975-1026 (2000).
35. Aifantis, I., Azogui, O., Feinberg, J., Saint-Ruf, C., Buer, J. & von Boehmer, H. On the role of the pre-T cell receptor in alphabeta versus gammadelta T lineage commitment. *Immunity* **9**, 649-655 (1998).
36. Fehling, H.J., Gilfillan, S. & Ceredig, R. Alpha beta/gamma delta lineage commitment in the thymus of normal and genetically manipulated mice. *Adv Immunol* **71**, 1-76 (1999).
37. Pear, W.S., Tu, L. & Stein, P.L. Lineage choices in the developing thymus: choosing the T and NKT pathways. *Curr Opin Immunol* **16**, 167-173 (2004).
38. Egawa, T., Eberl, G., Taniuchi, I., Benlagha, K., Geissmann, F., Hennighausen, L., Bendelac, A. & Littman, D.R. Genetic evidence supporting selection of the Valpha14i NKT cell lineage from double-positive thymocyte precursors. *Immunity* **22**, 705-716 (2005).
39. von Boehmer, H. & Fehling, H.J. Structure and function of the pre-T cell receptor. *Annu Rev Immunol* **15**, 433-452 (1997).
40. Carrasco, Y.R., Navarro, M.N. & Toribio, M.L. A role for the cytoplasmic tail of the pre-T cell receptor (TCR) alpha chain in promoting constitutive internalization and degradation of the pre-TCR. *J Biol Chem* **278**, 14507-14513 (2003).
41. Panigada, M., Porcellini, S., Barbier, E., Hoeflinger, S., Cazenave, P.A., Gu, H., Band, H., von Boehmer, H. & Grassi, F. Constitutive endocytosis and degradation of the pre-T cell receptor. *J Exp Med* **195**, 1585-1597 (2002).
42. Gibbons, D., Douglas, N.C., Barber, D.F., Liu, Q., Sullo, R., Geng, L., Fehling, H.J., von Boehmer, H. & Hayday, A.C. The biological activity of natural and mutant pTalpha alleles. *J Exp Med* **194**, 695-703 (2001).
43. Bruno, L., Rocha, B., Rolink, A., von Boehmer, H. & Rodewald, H.R. Intra- and extra-thymic expression of the pre-T cell receptor alpha gene. *Eur J Immunol* **25**, 1877-1882 (1995).
44. Groves, T., Parsons, M., Miyamoto, N.G. & Guidos, C.J. TCR engagement of CD4+CD8+ thymocytes in vitro induces early aspects of positive selection, but not apoptosis. *J*

Immunol **158**, 65-75 (1997).
45. Irving, B.A., Alt, F.W. & Killeen, N. Thymocyte development in the absence of pre-T cell receptor extracellular immunoglobulin domains. *Science* **280**, 905-908 (1998).
46. Talora, C., Cialfi, S., Oliviero, C., Palermo, R., Pascucci, M., Frati, L., Vacca, A., Gulino, A. & Screpanti, I. Cross talk among Notch3, pre-TCR, and Tal1 in T-cell development and leukemogenesis. *Blood* **107**, 3313-3320 (2006).
47. Fehling, H.J., Krotkova, A., Saint-Ruf, C. & von Boehmer, H. Crucial role of the pre-T-cell receptor alpha gene in development of alpha beta but not gamma delta T cells. *Nature* **375**, 795-798 (1995).
48. Eberl, G., Fehling, H.J., von Boehmer, H. & MacDonald, H.R. Absolute requirement for the pre-T cell receptor alpha chain during NK1.1+ TCRalphabeta cell development. *Eur J Immunol* **29**, 1966-1971 (1999).
49. Fontenot, J.D., Gavin, M.A. & Rudensky, A.Y. Foxp3 programs the development and function of CD4+CD25+ regulatory T cells. *Nat Immunol* **4**, 330-336 (2003).
50. Montoliu, L., Chavez, S. & Vidal, M. Variegation associated with lacZ in transgenic animals: a warning note. *Transgenic Res* **9**, 237-239 (2000).
51. Wakimoto, B.T. Beyond the nucleosome: epigenetic aspects of position-effect variegation in Drosophila. *Cell* **93**, 321-324 (1998).
52. Ebert, A., Lein, S., Schotta, G. & Reuter, G. Histone modification and the control of heterochromatic gene silencing in Drosophila. *Chromosome Res* **14**, 377-392 (2006).
53. Shimizu, C., Kawamoto, H., Yamashita, M., Kimura, M., Kondou, E., Kaneko, Y., Okada, S., Tokuhisa, T., Yokoyama, M., Taniguchi, M., Katsura, Y. & Nakayama, T. Progression of T cell lineage restriction in the earliest subpopulation of murine adult thymus visualized by the expression of lck proximal promoter activity. *Int Immunol* **13**, 105-117 (2001).
54. Zhang, D.J., Wang, Q., Wei, J., Baimukanova, G., Buchholz, F., Stewart, A.F., Mao, X. & Killeen, N. Selective expression of the Cre recombinase in late-stage thymocytes using the distal promoter of the Lck gene. *J Immunol* **174**, 6725-6731 (2005).
55. Doetschman, T., Gregg, R.G., Maeda, N., Hooper, M.L., Melton, D.W., Thompson, S. & Smithies, O. Targetted correction of a mutant HPRT gene in mouse embryonic stem cells. *Nature* **330**, 576-578 (1987).
56. Bronson, S.K. & Smithies, O. Altering mice by homologous recombination using embryonic stem cells. *J Biol Chem* **269**, 27155-27158 (1994).
57. Brault, V., Pereira, P., Duchon, A. & Herault, Y. Modeling chromosomes in mouse to explore the function of genes, genomic disorders, and chromosomal organization. *PLoS Genet* **2**, e86 (2006).
58. Thompson, S., Clarke, A.R., Pow, A.M., Hooper, M.L. & Melton, D.W. Germ line transmission and expression of a corrected HPRT gene produced by gene targeting in embryonic stem cells. *Cell* **56**, 313-321 (1989).
59. Behringer R., N.A., Gerstenstein M., Vintersten K. in Manipulating the mouse embryo: A laboratory manual, Vol. 1, Edn. 3rd 453-507 (Cold Spring Harbor Laboratory Press, 2002).
60. Prinz, I., Sansoni, A., Kissenpfennig, A., Ardouin, L., Malissen, M. & Malissen, B. Visualization of the earliest steps of gammadelta T cell development in the adult thymus. *Nat Immunol* **7**, 995-1003 (2006).
61. Sauer, B. & Henderson, N. Site-specific DNA recombination in mammalian cells by the Cre recombinase of bacteriophage P1. *Proc Natl Acad Sci U S A* **85**, 5166-5170 (1988).
62. Fukushige, S. & Sauer, B. Genomic targeting with a positive-selection lox integration vector allows highly reproducible gene expression in mammalian cells. *Proc Natl Acad Sci U S A* **89**, 7905-7909 (1992).
63. Araki, K., Araki, M. & Yamamura, K. Targeted integration of DNA using mutant lox sites in embryonic stem cells. *Nucleic Acids Res* **25**, 868-872 (1997).
64. Lee, G. & Saito, I. Role of nucleotide sequences of loxP spacer region in Cre-mediated recombination. *Gene* **216**, 55-65 (1998).
65. Hoess, R.H., Wierzbicki, A. & Abremski, K. The role of the loxP spacer region in P1 site-specific recombination. *Nucleic Acids Res* **14**, 2287-2300 (1986).
66. Feng, Y.Q., Seibler, J., Alami, R., Eisen, A., Westerman, K.A., Leboulch, P., Fiering, S. & Bouhassira, E.E. Site-specific chromosomal integration in mammalian cells: highly efficient CRE recombinase-mediated cassette exchange. *J Mol Biol* **292**, 779-785 (1999).
67. Schnutgen, F., Doerflinger, N., Calleja, C., Wendling, O., Chambon, P. & Ghyselinck, N.B. A

directional strategy for monitoring Cre-mediated recombination at the cellular level in the mouse. *Nat Biotechnol* **21**, 562-565 (2003).
68. Nagy, A. Cre recombinase: the universal reagent for genome tailoring. *Genesis* **26**, 99-109 (2000).
69. Zou, Y.-R., Sunshine, M.-J., Taniuchi, I., Hatam, F., Killeen, N. & Littman, D.R. Epigenetic silencing of CD4 in T cells committed to the cytotoxic lineage. *Nat Genet* **29**, 332-336 (2001).
70. Tsien, J.Z., Chen, D.F., Gerber, D., Tom, C., Mercer, E.H., Anderson, D.J., Mayford, M., Kandel, E.R. & Tonegawa, S. Subregion- and cell type-restricted gene knockout in mouse brain. *Cell* **87**, 1317-1326 (1996).
71. Mao, X., Fujiwara, Y., Chapdelaine, A., Yang, H. & Orkin, S.H. Activation of EGFP expression by Cre-mediated excision in a new ROSA26 reporter mouse strain. *Blood* **97**, 324-326 (2001).
72. Hadjantonakis, A.K., Macmaster, S. & Nagy, A. Embryonic stem cells and mice expressing different GFP variants for multiple non-invasive reporter usage within a single animal. *BMC Biotechnol* **2**, 11 (2002).
73. Eberl, G. & Littman, D.R. Thymic origin of intestinal alphabeta T cells revealed by fate mapping of RORgammat+ cells. *Science* **305**, 248-251 (2004).
74. Orban, P.C., Chui, D. & Marth, J.D. Tissue- and site-specific DNA recombination in transgenic mice. *Proc Natl Acad Sci U S A* **89**, 6861-6865 (1992).
75. Lee, P.P., Fitzpatrick, D.R., Beard, C., Jessup, H.K., Lehar, S., Makar, K.W., Perez-Melgosa, M., Sweetser, M.T., Schlissel, M.S., Nguyen, S., Cherry, S.R., Tsai, J.H., Tucker, S.M., Weaver, W.M., Kelso, A., Jaenisch, R. & Wilson, C.B. A critical role for Dnmt1 and DNA methylation in T cell development, function, and survival. *Immunity* **15**, 763-774 (2001).
76. Hennet, T., Hagen, F.K., Tabak, L.A. & Marth, J.D. T-cell-specific deletion of a polypeptide N-acetylgalactosaminyl-transferase gene by site-directed recombination. *Proc Natl Acad Sci U S A* **92**, 12070-12074 (1995).
77. Stadtfeld, M. & Graf, T. Assessing the role of hematopoietic plasticity for endothelial and hepatocyte development by non-invasive lineage tracing. *Development* **132**, 203-213 (2005).
78. Ye, M., Iwasaki, H., Laiosa, C.V., Stadtfeld, M., Xie, H., Heck, S., Clausen, B., Akashi, K. & Graf, T. Hematopoietic stem cells expressing the myeloid lysozyme gene retain long-term, multilineage repopulation potential. *Immunity* **19**, 689-699 (2003).
79. Friedrich, G. & Soriano, P. Promoter traps in embryonic stem cells: a genetic screen to identify and mutate developmental genes in mice. *Genes Dev* **5**, 1513-1523 (1991).
80. Zambrowicz, B.P., Imamoto, A., Fiering, S., Herzenberg, L.A., Kerr, W.G. & Soriano, P. Disruption of overlapping transcripts in the ROSA beta geo 26 gene trap strain leads to widespread expression of beta-galactosidase in mouse embryos and hematopoietic cells. *Proc Natl Acad Sci U S A* **94**, 3789-3794 (1997).
81. Soriano, P. Generalized lacZ expression with the ROSA26 Cre reporter strain. *Nat Genet* **21**, 70-71 (1999).
82. Heim, R., Prasher, D.C. & Tsien, R.Y. Wavelength mutations and posttranslational autoxidation of green fluorescent protein. *Proc Natl Acad Sci U S A* **91**, 12501-12504 (1994).
83. Okabe, M., Ikawa, M., Kominami, K., Nakanishi, T. & Nishimune, Y. 'Green mice' as a source of ubiquitous green cells. *FEBS Lett* **407**, 313-319 (1997).
84. Hadjantonakis, A.K. & Nagy, A. FACS for the isolation of individual cells from transgenic mice harboring a fluorescent protein reporter. *Genesis* **27**, 95-98 (2000).
85. Srinivas, S., Watanabe, T., Lin, C.S., William, C.M., Tanabe, Y., Jessell, T.M. & Costantini, F. Cre reporter strains produced by targeted insertion of EYFP and ECFP into the ROSA26 locus. *BMC Dev Biol* **1**, 4 (2001).
86. Ormo, M., Cubitt, A.B., Kallio, K., Gross, L.A., Tsien, R.Y. & Remington, S.J. Crystal structure of the Aequorea victoria green fluorescent protein. *Science* **273**, 1392-1395 (1996).
87. Wachter, R.M., Elsliger, M.A., Kallio, K., Hanson, G.T. & Remington, S.J. Structural basis of spectral shifts in the yellow-emission variants of green fluorescent protein. *Structure* **6**, 1267-1277 (1998).
88. Wachter, R.M., King, B.A., Heim, R., Kallio, K., Tsien, R.Y., Boxer, S.G. & Remington, S.J.

Crystal structure and photodynamic behavior of the blue emission variant Y66H/Y145F of green fluorescent protein. *Biochemistry* **36**, 9759-9765 (1997).
89. Stetson, D.B., Mohrs, M., Reinhardt, R.L., Baron, J.L., Wang, Z.E., Gapin, L., Kronenberg, M. & Locksley, R.M. Constitutive cytokine mRNAs mark natural killer (NK) and NK T cells poised for rapid effector function. *J Exp Med* **198**, 1069-1076 (2003).
90. Mohrs, M., Shinkai, K., Mohrs, K. & Locksley, R.M. Analysis of type 2 immunity in vivo with a bicistronic IL-4 reporter. *Immunity* **15**, 303-311 (2001).
91. Billinton, N. & Knight, A.W. Seeing the wood through the trees: a review of techniques for distinguishing green fluorescent protein from endogenous autofluorescence. *Anal Biochem* **291**, 175-197 (2001).
92. Bevis, B.J. & Glick, B.S. Rapidly maturing variants of the Discosoma red fluorescent protein (DsRed). *Nat Biotechnol* **20**, 83-87 (2002).
93. Shaner, N.C., Steinbach, P.A. & Tsien, R.Y. A guide to choosing fluorescent proteins. *Nat Methods* **2**, 905-909 (2005).
94. Matz, M.V., Fradkov, A.F., Labas, Y.A., Savitsky, A.P., Zaraisky, A.G., Markelov, M.L. & Lukyanov, S.A. Fluorescent proteins from nonbioluminescent Anthozoa species. *Nat Biotechnol* **17**, 969-973 (1999).
95. Hawley, T.S., Telford, W.G., Ramezani, A. & Hawley, R.G. Four-color flow cytometric detection of retrovirally expressed red, yellow, green, and cyan fluorescent proteins. *Biotechniques* **30**, 1028-1034 (2001).
96. Verkhusha, V.V., Kuznetsova, I.M., Stepanenko, O.V., Zaraisky, A.G., Shavlovsky, M.M., Turoverov, K.K. & Uversky, V.N. High stability of Discosoma DsRed as compared to Aequorea EGFP. *Biochemistry* **42**, 7879-7884 (2003).
97. Baird, G.S., Zacharias, D.A. & Tsien, R.Y. Biochemistry, mutagenesis, and oligomerization of DsRed, a red fluorescent protein from coral. *Proc Natl Acad Sci U S A* **97**, 11984-11989 (2000).
98. Garcia-Parajo, M.F., Koopman, M., van Dijk, E.M., Subramaniam, V. & van Hulst, N.F. The nature of fluorescence emission in the red fluorescent protein DsRed, revealed by single-molecule detection. *Proc Natl Acad Sci U S A* **98**, 14392-14397 (2001).
99. Cotlet, M., Hofkens, J., Habuchi, S., Dirix, G., Van Guyse, M., Michiels, J., Vanderleyden, J. & De Schryver, F.C. Identification of different emitting species in the red fluorescent protein DsRed by means of ensemble and single-molecule spectroscopy. *Proc Natl Acad Sci U S A* **98**, 14398-14403 (2001).
100. Verkhusha, V.V., Chudakov, D.M., Gurskaya, N.G., Lukyanov, S. & Lukyanov, K.A. Common pathway for the red chromophore formation in fluorescent proteins and chromoproteins. *Chem Biol* **11**, 845-854 (2004).
101. Wall, M.A., Socolich, M. & Ranganathan, R. The structural basis for red fluorescence in the tetrameric GFP homolog DsRed. *Nat Struct Biol* **7**, 1133-1138 (2000).
102. Yarbrough, D., Wachter, R.M., Kallio, K., Matz, M.V. & Remington, S.J. Refined crystal structure of DsRed, a red fluorescent protein from coral, at 2.0-A resolution. *Proc Natl Acad Sci U S A* **98**, 462-467 (2001).
103. Gross, L.A., Baird, G.S., Hoffman, R.C., Baldridge, K.K. & Tsien, R.Y. The structure of the chromophore within DsRed, a red fluorescent protein from coral. *Proc Natl Acad Sci U S A* **97**, 11990-11995 (2000).
104. Tubbs, J.L., Tainer, J.A. & Getzoff, E.D. Crystallographic structures of Discosoma red fluorescent protein with immature and mature chromophores: linking peptide bond trans-cis isomerization and acylimine formation in chromophore maturation. *Biochemistry* **44**, 9833-9840 (2005).
105. Lauf, U., Lopez, P. & Falk, M.M. Expression of fluorescently tagged connexins: a novel approach to rescue function of oligomeric DsRed-tagged proteins. *FEBS Lett* **498**, 11-15 (2001).
106. Jakobs, S., Subramaniam, V., Schonle, A., Jovin, T.M. & Hell, S.W. EFGP and DsRed expressing cultures of Escherichia coli imaged by confocal, two-photon and fluorescence lifetime microscopy. *FEBS Lett* **479**, 131-135 (2000).
107. Living ColorTM DsRed2. *CLONTECHniques* **XVI**, 2-3 (2001).
108. Vintersten, K., Monetti, C., Gertsenstein, M., Zhang, P., Laszlo, L., Biechele, S. & Nagy, A. Mouse in red: red fluorescent protein expression in mouse ES cells, embryos, and adult animals. *Genesis* **40**, 241-246 (2004).

109. Long, J.Z., Lackan, C.S. & Hadjantonakis, A.K. Genetic and spectrally distinct in vivo imaging: embryonic stem cells and mice with widespread expression of a monomeric red fluorescent protein. *BMC Biotechnol* **5**, 20 (2005).
110. Campbell, R.E., Tour, O., Palmer, A.E., Steinbach, P.A., Baird, G.S., Zacharias, D.A. & Tsien, R.Y. A monomeric red fluorescent protein. *Proc Natl Acad Sci U S A* **99**, 7877-7882 (2002).
111. Zhu, H., Wang, G., Li, G., Han, M., Xu, T., Zhuang, Y. & Wu, X. Ubiquitous expression of mRFP1 in transgenic mice. *Genesis* **42**, 86-90 (2005).
112. Schaft, J., Ashery-Padan, R., van der Hoeven, F., Gruss, P. & Stewart, A.F. Efficient FLP recombination in mouse ES cells and oocytes. *Genesis* **31**, 6-10 (2001).
113. Kouskoff, V., Fehling, H.J., Lemeur, M., Benoist, C. & Mathis, D. A vector driving the expression of foreign cDNAs in the MHC class II-positive cells of transgenic mice. *J Immunol Methods* **166**, 287-291 (1993).
114. Shimshek, D.R., Kim, J., Hubner, M.R., Spergel, D.J., Buchholz, F., Casanova, E., Stewart, A.F., Seeburg, P.H. & Sprengel, R. Codon-improved Cre recombinase (iCre) expression in the mouse. *Genesis* **32**, 19-26 (2002).
115. Irion, S., Luche, H., Gadue, P., Fehling, H.J., Kennedy, M. & Keller, G. in Nature Biotechnology (Submitted)2006).
116. Sambrook, J.R., D.W. Molecular cloning, a laboratory manual, Vol. 1, Edn. 3rd. (CSHL Press, New York; 2001).
117. Schwenk, F., Baron, U. & Rajewsky, K. A cre-transgenic mouse strain for the ubiquitous deletion of loxP-flanked gene segments including deletion in germ cells. *Nucleic Acids Res* **23**, 5080-5081 (1995).
118. Collier, R.J. Diphtheria toxin: mode of action and structure. *Bacteriol Rev* **39**, 54-85 (1975).
119. Koresawa, Y., Miyagawa, S., Ikawa, M., Matsunami, K., Yamada, M., Shirakura, R. & Okabe, M. Synthesis of a new Cre recombinase gene based on optimal codon usage for mammalian systems. *J Biochem (Tokyo)* **127**, 367-372 (2000).
120. Zheng, B., Sage, M., Sheppeard, E.A., Jurecic, V. & Bradley, A. Engineering mouse chromosomes with Cre-loxP: range, efficiency, and somatic applications. *Mol Cell Biol* **20**, 648-655 (2000).
121. Olson, E.N., Arnold, H.H., Rigby, P.W. & Wold, B.J. Know your neighbors: three phenotypes in null mutants of the myogenic bHLH gene MRF4. *Cell* **85**, 1-4 (1996).
122. Pham, C.T., MacIvor, D.M., Hug, B.A., Heusel, J.W. & Ley, T.J. Long-range disruption of gene expression by a selectable marker cassette. *Proc Natl Acad Sci U S A* **93**, 13090-13095 (1996).
123. Seidl, K.J., Manis, J.P., Bottaro, A., Zhang, J., Davidson, L., Kisselgof, A., Oettgen, H. & Alt, F.W. Position-dependent inhibition of class-switch recombination by PGK-neor cassettes inserted into the immunoglobulin heavy chain constant region locus. *Proc Natl Acad Sci U S A* **96**, 3000-3005 (1999).
124. Hirasawa, T., Yamashita, H. & Makino, S. Genetic typing of the mouse and rat nude mutations by PCR and restriction enzyme analysis. *Exp Anim* **47**, 63-67 (1998).
125. Mao, X., Fujiwara, Y. & Orkin, S.H. Improved reporter strain for monitoring Cre recombinase-mediated DNA excisions in mice. *Proc Natl Acad Sci U S A* **96**, 5037-5042 (1999).
126. Attal, J., Theron, M.C. & Houdebine, L.M. The optimal use of IRES (internal ribosome entry site) in expression vectors. *Genet Anal* **15**, 161-165 (1999).
127. Kozak, M. At least six nucleotides preceding the AUG initiator codon enhance translation in mammalian cells. *J Mol Biol* **196**, 947-950 (1987).
128. Sachs, A.B., Sarnow, P. & Hentze, M.W. Starting at the beginning, middle, and end: translation initiation in eukaryotes. *Cell* **89**, 831-838 (1997).
129. Meijer, H.A. & Thomas, A.A. Control of eukaryotic protein synthesis by upstream open reading frames in the 5'-untranslated region of an mRNA. *Biochem J* **367**, 1-11 (2002).
130. Peabody, D.S., Subramani, S. & Berg, P. Effect of upstream reading frames on translation efficiency in simian virus 40 recombinants. *Mol Cell Biol* **6**, 2704-2711 (1986).
131. Hadjantonakis, A.K. & Papaioannou, V.E. Dynamic in vivo imaging and cell tracking using a histone fluorescent protein fusion in mice. *BMC Biotechnol* **4**, 33 (2004).
132. Furuta, T., Tomioka, R., Taki, K., Nakamura, K., Tamamaki, N. & Kaneko, T. In vivo

transduction of central neurons using recombinant Sindbis virus: Golgi-like labeling of dendrites and axons with membrane-targeted fluorescent proteins. *J Histochem Cytochem* **49**, 1497-1508 (2001).
133. Gurskaya, N.G., Fradkov, A.F., Terskikh, A., Matz, M.V., Labas, Y.A., Martynov, V.I., Yanushevich, Y.G., Lukyanov, K.A. & Lukyanov, S.A. GFP-like chromoproteins as a source of far-red fluorescent proteins. *FEBS Lett* **507**, 16-20 (2001).
134. Clontech, L. in Living Colors User Manual, Vol. 2 42002).
135. Furger, A., O'Sullivan, J.M., Binnie, A., Lee, B.A. & Proudfoot, N.J. Promoter proximal splice sites enhance transcription. *Genes Dev* **16**, 2792-2799 (2002).
136. Le Hir, H., Nott, A. & Moore, M.J. How introns influence and enhance eukaryotic gene expression. *Trends Biochem Sci* **28**, 215-220 (2003).
137. Palmiter, R.D., Sandgren, E.P., Avarbock, M.R., Allen, D.D. & Brinster, R.L. Heterologous introns can enhance expression of transgenes in mice. *Proc Natl Acad Sci U S A* **88**, 478-482 (1991).
138. Vincent, S.D. & Robertson, E.J. Targeted insertion of an IRES Cre into the Hnf4alpha locus: Cre-mediated recombination in the liver, kidney, and gut epithelium. *Genesis* **39**, 206-211 (2004).
139. Stanley, E.G., Biben, C., Elefanty, A., Barnett, L., Koentgen, F., Robb, L. & Harvey, R.P. Efficient Cre-mediated deletion in cardiac progenitor cells conferred by a 3'UTR-ires-Cre allele of the homeobox gene Nkx2-5. *Int J Dev Biol* **46**, 431-439 (2002).
140. Michael, S.K., Brennan, J. & Robertson, E.J. Efficient gene-specific expression of cre recombinase in the mouse embryo by targeted insertion of a novel IRES-Cre cassette into endogenous loci. *Mech Dev* **85**, 35-47 (1999).
141. Chevalier-Mariette, C., Henry, I., Montfort, L., Capgras, S., Forlani, S., Muschler, J. & Nicolas, J.F. CpG content affects gene silencing in mice: evidence from novel transgenes. *Genome Biol* **4**, R53 (2003).
142. Joyner, A. in Gene targeting, a practical approach 21-33.
143. Bortvin, A., Eggan, K., Skaletsky, H., Akutsu, H., Berry, D.L., Yanagimachi, R., Page, D.C. & Jaenisch, R. Incomplete reactivation of Oct4-related genes in mouse embryos cloned from somatic nuclei. *Development* **130**, 1673-1680 (2003).
144. Larson, J.S., Yin, M., Fischer, J.M., Stringer, S.L. & Stringer, J.R. Expression and loss of alleles in cultured mouse embryonic fibroblasts and stem cells carrying allelic fluorescent protein genes. *BMC Mol Biol* **7**, 36 (2006).
145. Cervantes, R.B., Stringer, J.R., Shao, C., Tischfield, J.A. & Stambrook, P.J. Embryonic stem cells and somatic cells differ in mutation frequency and type. *Proc Natl Acad Sci U S A* **99**, 3586-3590 (2002).
146. Asari, S., Okada, S., Ohkubo, Y., Sakamoto, A., Arima, M., Hatano, M., Kuroda, Y. & Tokuhisa, T. Beta-galactosidase of ROSA26 mice is a useful marker for detecting the definitive erythropoiesis after stem cell transplantation. *Transplantation* **78**, 516-523 (2004).
147. Elstein, K.H., Mole, M.L., Setzer, R.W., Zucker, R.M., Kavlock, R.J., Rogers, J.M. & Lau, C. Nucleoside-mediated mitigation of 5-fluorouracil-induced toxicity in synchronized murine erythroleukemic cells. *Toxicol Appl Pharmacol* **146**, 29-39 (1997).
148. Wallace, H., Ansell, R., Clark, J. & McWhir, J. Pre-selection of integration sites imparts repeatable transgene expression. *Nucleic Acids Res* **28**, 1455-1464 (2000).
149. Wong, E.T., Kolman, J.L., Li, Y.C., Mesner, L.D., Hillen, W., Berens, C. & Wahl, G.M. Reproducible doxycycline-inducible transgene expression at specific loci generated by Cre-recombinase mediated cassette exchange. *Nucleic Acids Res* **33**, e147 (2005).
150. Lauth, M., Spreafico, F., Dethleffsen, K. & Meyer, M. Stable and efficient cassette exchange under non-selectable conditions by combined use of two site-specific recombinases. *Nucleic Acids Res* **30**, e115 (2002).
151. Loonstra, A., Vooijs, M., Beverloo, H.B., Allak, B.A., van Drunen, E., Kanaar, R., Berns, A. & Jonkers, J. Growth inhibition and DNA damage induced by Cre recombinase in mammalian cells. *Proc Natl Acad Sci U S A* **98**, 9209-9214 (2001).
152. Heilig, J.S. & Tonegawa, S. Diversity of murine gamma genes and expression in fetal and adult T lymphocytes. *Nature* **322**, 836-840 (1986).
153. Pennington, D.J., Silva-Santos, B. & Hayday, A.C. Gammadelta T cell development--having the strength to get there. *Curr Opin Immunol* **17**, 108-115 (2005).

154. Guy-Grand, D., Azogui, O., Celli, S., Darche, S., Nussenzweig, M.C., Kourilsky, P. & Vassalli, P. Extrathymic T cell lymphopoiesis: ontogeny and contribution to gut intraepithelial lymphocytes in athymic and euthymic mice. *J Exp Med* **197**, 333-341 (2003).
155. Hayday, A.C. & Pennington, D.J. Key factors in the organized chaos of early T cell development. *Nat Immunol* **8**, 137-144 (2007).
156. Penninger, J., Kishihara, K., Molina, T., Wallace, V.A., Timms, E., Hedrick, S.M. & Mak, T.W. Requirement for tyrosine kinase p56lck for thymic development of transgenic gamma delta T cells. *Science* **260**, 358-361 (1993).
157. Reizis, B. & Leder, P. Expression of the mouse pre-T cell receptor alpha gene is controlled by an upstream region containing a transcriptional enhancer. *J Exp Med* **189**, 1669-1678 (1999).
158. Dymecki, S.M. & Tomasiewicz, H. Using Flp-recombinase to characterize expansion of Wnt1-expressing neural progenitors in the mouse. *Dev Biol* **201**, 57-65 (1998).
159. Toledo, F., Liu, C.W., Lee, C.J. & Wahl, G.M. RMCE-ASAP: a gene targeting method for ES and somatic cells to accelerate phenotype analyses. *Nucleic Acids Res* **34**, e92 (2006).
160. Hu, M., Krause, D., Greaves, M., Sharkis, S., Dexter, M., Heyworth, C. & Enver, T. Multilineage gene expression precedes commitment in the hemopoietic system. *Genes Dev* **11**, 774-785 (1997).
161. von Boehmer, H. Unique features of the pre-T-cell receptor alpha-chain: not just a surrogate. *Nature Reviews Immunology* **5**, 571-577 (2005).
162. Reizis, B. & Leder, P. The upstream enhancer is necessary and sufficient for the expression of the pre-T cell receptor alpha gene in immature T lymphocytes. *J Exp Med* **194**, 979-990 (2001).
163. Giraldo, P. & Montoliu, L. Size matters: use of YACs, BACs and PACs in transgenic animals. *Transgenic Res* **10**, 83-103 (2001).
164. Ristevski, S. Making better transgenic models: conditional, temporal, and spatial approaches. *Mol Biotechnol* **29**, 153-163 (2005).
165. Lauritsen, J.P., Haks, M.C., Lefebvre, J.M., Kappes, D.J. & Wiest, D.L. Recent insights into the signals that control alphabeta/gammadelta-lineage fate. *Immunol Rev* **209**, 176-190 (2006).
166. Ono, M., Ariizumi, K., Bergstresser, P.R. & Takashima, A. IL-7 upregulates T cell receptor/CD3 expression by cultured dendritic epidermal T cells. *J Dermatol Sci* **11**, 89-96 (1996).
167. Aiba, S., Nakagawa, S., Hara, M., Tomioka, Y., Deguchi, M. & Tagami, H. Cultured murine dermal cells can function like thymic nurse cells. *J Invest Dermatol* **103**, 162-167 (1994).
168. Clark, R.A., Yamanaka, K., Bai, M., Dowgiert, R. & Kupper, T.S. Human skin cells support thymus-independent T cell development. *J Clin Invest* **115**, 3239-3249 (2005).
169. Andl, T., Ahn, K., Kairo, A., Chu, E.Y., Wine-Lee, L., Reddy, S.T., Croft, N.J., Cebra-Thomas, J.A., Metzger, D., Chambon, P., Lyons, K.M., Mishina, Y., Seykora, J.T., Crenshaw, E.B., 3rd & Millar, S.E. Epithelial Bmpr1a regulates differentiation and proliferation in postnatal hair follicles and is essential for tooth development. *Development* **131**, 2257-2268 (2004).
170. Raveh, E., Cohen, S., Levanon, D., Negreanu, V., Groner, Y. & Gat, U. Dynamic expression of Runx1 in skin affects hair structure. *Mech Dev* **123**, 842-850 (2006).
171. Ma, L., Liu, J., Wu, T., Plikus, M., Jiang, T.X., Bi, Q., Liu, Y.H., Muller-Rover, S., Peters, H., Sundberg, J.P., Maxson, R., Maas, R.L. & Chuong, C.M. 'Cyclic alopecia' in Msx2 mutants: defects in hair cycling and hair shaft differentiation. *Development* **130**, 379-389 (2003).
172. Vauclair, S., Nicolas, M., Barrandon, Y. & Radtke, F. Notch1 is essential for postnatal hair follicle development and homeostasis. *Dev Biol* **284**, 184-193 (2005).
173. Benz, C. & Bleul, C.C. A multipotent precursor in the thymus maps to the branching point of the T versus B lineage decision. *J Exp Med* **202**, 21-31 (2005).
174. Sitnicka, E., Bryder, D., Theilgaard-Monch, K., Buza-Vidas, N., Adolfsson, J. & Jacobsen, S.E. Key role of flt3 ligand in regulation of the common lymphoid progenitor but not in maintenance of the hematopoietic stem cell pool. *Immunity* **17**, 463-472 (2002).
175. Buckland, J., Pennington, D.J., Bruno, L. & Owen, M.J. Co-ordination of the expression of the protein tyrosine kinase p56(lck) with the pre-T cell receptor during thymocyte development. *Eur J Immunol* **30**, 8-18 (2000).

ACKNOWLEDGMENTS

This work is the result of many years of great pleasure spent in the laboratory, learning how to perform proper science, but also the expression of ceaseless support I received from many people in the Immunolgy Institute. Therefore, I would like first to show my gratitude to all the team of Pr. Dr. FEHLING as well as all the people who have been more or less involved in this project.

I would like to thank my supervisor Pr. Dr. Hans-Joerg FEHLING for welcoming me in his team as a PhD student and giving me the chance to work on such a challenging and exciting project. At the time we initiated the project, we set up really high goals and I am delighted to see that we could succeed in most of them thanks to his direction. I have learned to develop the most rigorous approaches to address lineage commitment issues, to design precise experiments and to stay highly critical on the quality of my own data. I will forever be grateful to him for the great opportunity he gave me to join for some time Gordon KELLER'S laboratory in NYC. All my thanks also for the wonderful support and all the advices he provided me for my post-doctoral applications.

My thanks also go to Pr. Dr. Hans-Reimer RODEWALD for guidance and great support. I highly appreciated your constructive criticism/inputs in discussions, most of the time R E A L L Y late in the day beside the cell sorter. That was great fun !! ;-).

I have now to acknowledge the "tiny" (only by size) Susan Schlenner for having shared the same lab as me for more than a year with all the implications it means: nicking reagents, momentary disappearance of some pens which translated by magic on my side of the office as well as listening to some weird french/tango/salsa music… Don't worry, the hell will soon be over ! ;-).

I would also like to thank all external collaborators for their support and discussions: Franz OSWALD (Ulm), Tilman BORGGREFE (Freiburg), Stefan IRION (Toronto) as well as Claudia WASKOW (NYC) and Cate BROWN (Brisbane).

I am also very grateful to Cedric HOBEL, Fanny COIGNARD and Celine COSTA for the discussions during my studies and my PhD thesis; Carmen BLUM, Rita MAHMOUDI, Sigrid ROCHUS (moin moin) for the day-to-day life administration issues; Uschi, Gulser and Flora for their technical assistance and their joy in life and finally to the indian connection (Vikas, Babita, Saanvi, Ragi, Devi and Rao) for their friendship and all the Massala evening we spent together.

Thanks all of you !

CURRICULUM VITAE

LUCHE Hervé

30 years old,

born the 21st december 1976

French Nationality

Married

e-mail : herve.luche@uni-ulm.de



QUALIFICATIONS

2000-2007	**PhD in Human Biology** passed with distinction *summa cum laudae* at the University of ULM, GERMANY.
1996-1999	**Bioengineer's degree in Biotechnology** (MSc equivalent) passed with merit at the "École Supérieure de Biotechnologie de STRASBOURG ".
	Degree in Molecular Biology (DEA, diploma equivalent**)** option Biotechnology passed with honours at the "Louis PASTEUR" faculty of Science, STRASBOURG, FRANCE.
1994-1996	**BTS diploma** (a two-year technical undergraduate course) **in Biotechnology** passed with merit at the "Lycée de la Vallée de Chevreuse", GIF SUR YVETTE, FRANCE.
	Majoring in Molecular and Cellular Biology, Genetic Engineering, Microbiology, Cell culture, Immunology, Enzymology, Biochemistry.
1994	**Baccalauréat Série D** (A-level) passed with merit at the "Lycée Thibault de Champagne", PROVINS (near Paris), FRANCE: Biology, Maths, Physics, German, English.

PLACEMENTS

2000-2007	PhD student in the laboratory of Molecular Immunology, ULM, GERMANY.
	Development of a lineage tracing strategy to mark early thymic immigrants *via* gene targeting. Generation of a Cre recombinase activated red fluorescent (tdRFP) reporter mouse into the ROSA26 locus. Bio-compatibility assessment of the red marker in multiple blood lineages. Optimisation of fixation conditions to allow simultaneous detection of fluorescence together with other immunohistology stainings.
	Generation of a new T-cell lineage specific Cre-deleter mouse strain by "knock-in" iCre into the pre-TCR α-chain locus. Investigation of RFP^+ cells in extra and intrathymic T-cell development and other blood lineages. Detection of RFP^+ cells in tiny cell subsets of the bone marrow and thymus. Analysis of pTα expressing cells in nude mouse. Managing a mouse colony (breedings, typings, time matings). Routine handling of mouse for bleeding, lymphoid organs extractions. Mastering DNA clonings, genomic DNA Southern, ES cell handling, FACS stainings.
	Key words: Molecular & cellular Biology, Gene Targeting, 6-colors FACS stainings, Cell sorting on ARIA and MOFLO, Immunohistology, Fluoresence Stereomicroscopy.
August 2004 - May 2005	Nine-month training period in Gordon KELLER's lab, Department of Gene and Cell Medicine, Mount Sinai, NEW-YORK, USA.
	Establishment of an *in vitro* system to efficiently differentiate murine ES cells into B or T cells using respectively the OP9/OP9dl1 co-culture system. Identification of a define progenitor population able to generate all blood lineages from ES cells. Identification of the human homologue of mouse ROSA26 locus by bioinformatic. Design of an inducible RFP reporter construct for gene targeting in human ES cells.
	Key words: ES cell differentiation into Embryoid Bodies, OP9/OP9dl1 co-culture, Methylcellullose assays, Bio-informatics.

1999	Nine-month training period in BRITISH BIOTECHNOLOGY Plc, OXFORD, UK. Identification of new antifungal and antibacterial targets by reverse genetics. Database screening using enzyme motifs. Cloning in *E. coli* of potential therapeutical targets, protein over-expression and purification. Assay development to screen a chemical library. Key words: Molecular Biology, Microbiology, and Bio-informatics.
1998	Two-month training period at UMR 7175: "Récepteurs et protéines de la membrane", CNRS, STRASBOURG, FRANCE. Construction of two chimeric tachykinin receptors fused either with EYFP or with ECFP to study their dimerisation by Fluorescence Resonance Energy Transfer (FRET). Key words: Molecular Biology, Cell culture, Fluorimetry.

PUBLICATIONS, MEETINGS

Jan 2007	Luche H., Weber O., Nageswara T.R., Blum C., Fehling H.J.: "Faithful activation of an extra-bright red fluorescent protein in "knock-in" Cre reporter mice ideally suited for lineage tracing studies" in European Journal of Immunology.
Jan. 2007 (Revision)	Irion S., Luche H., Gadue P., Kennedy M., Fehling H.J., Keller G.: "Identification and targeting of the ROSA26 locus in human embryonic stem cells." in Nature Biotechnology.
2006	Poster presentation at the 16th European Congress of Immunology, PARIS, FRANCE. "Two novel "knock-in" mouse strains for lineage tracing and efficient Cre-mediated manipulation within the T cell compartment."
2005	3rd Workshop on Innovative Mouse Models, LEYDEN, NEITHERLANDS.
2003	16th Meeting of Modern Trends in Human Leukaemia, WILSEDE, GERMANY. "Targeted insertion of a Cre-inducible Red Fluorescent Protein (RFP) into the ROSA26 gene locus of ES cells"

ADDITIONAL INFORMATIONS

Languages	
French	Mother tongue.
English	Write, speak and read fluently as a result of my training period in UK and USA.
German	Write, speak and read fluently. Since 2000, living in GERMANY.
Computer Science	Standard use of Gene Construction Kit, DNAStar, Clone Manager to design cloning strategies, identify best PCR oligonucleotide pairs and Southern probes. Regular use of Ensembl website to run bioinformatic analyses. Mastering DIVA and cell quest software for flow cytometry. Good knowledge in Adobe Photoshop, Illustrator, Excel, Word and Power Point. Work indifferently on PC or Apple computers.

REFEREES

Pr Dr. FEHLING	Professor in Immunology	joerg.fehling@uni-ulm.de	++ (49) 731 500 65210
Pr. Dr. RODEWALD	Professor in Immunology	hans-reimer.rodewald@uni-ulm.de	++ (49) 731 500 65200